In vitro Studies in Retinal Pigment Epithelium on the Role of Lysyl Oxidase and its Perspectives in Vitreoretinal Pathology

THESIS

Submitted in partial fulfillment

of the requirements for the degree of

DOCTOR OF PHILOSOPHY

By

K. CORAL MIRIAM MAGDALENE

2003PHXF030

Under the supervision of

Dr. N. ANGAYARKANNI

BIRLA INSTITUTE OF TECHNOLOGY AND SCIENCE

PILANI (RAJASTHAN) INDIA

2009

BIRLA INSTITUTE OF TECHNOLOGY & SCIENCE

PILANI - RAJASTHAN

CERTIFICATE

This is to certify that the thesis entitled **"*In vitro* Studies in Retinal Pigment Epithelium on the Role of Lysyl Oxidase and its Perspectives in Vitreoretinal Pathology"** and submitted by Ms. K. Coral Miriam Magdalene, ID. No. 2003PHXF030 for award of Ph.D. Degree of the Institute embodies original work done by her under my supervision.

Signature of the Supervisor:

Name in Block Capital letters : **Dr. N. ANGAYARKANNI**

Designation : **Reader,**
Biochemistry Research Department
Vision Research Foundation
Sankara Nethralaya, Chennai 600 006.
Tamil Nadu. India

Date:

ACKNOWLEDGEMENT

It gives me great pleasure that the pleasant time has come to express my gratitude for all of them who guided, supported and encouraged me through out my PhD tenure.

First I would like to give my heartfelt gratitude to the **Almighty God** without whom this thesis would not have been possible at all.

I would like to start expressing my sincere acknowledgement to my supervisor, **Dr. N. Angayarkani,** Reader, Biochemistry Research Department. I thank her for giving me the fellowship to work in her project. I thank her for her supervision, support and encouragement given throughout my work.

I would like to extend my heartfelt gratitude to **Prof. H.N. Madhavan,** Director of Research, Vision Research Foundation for the faith he had on me and for his continuous encouragement and opportunities given by him for my growth in career.

I would like to thank Padmabhushan **Dr.S.S. Badrinath,** Chairman Emeritus, and **Dr.S.B.Vasanthi Badrinath,** Director, Laboratory Services, Sankara Nethralaya, Chennai, India for providing me the opportunity to work in this esteemed institution and to pursue my doctoral programme. I owe a lot to them.

I thank **Dr. Lingam Gopal,** Chairman, Medical Research Foundation, **Dr. Tarun Sharma,** Honorary Secretary and Treasurer, Vision Research Foundation, **Dr. T.S Surendran,** Vice-Chairman, Medical Research Foundation for their support.

My sincere gratitude to **Vision Research Foundation,** for funding my project initially, which enabled me to begin my work.

I sincerely acknowledge the Department of Biotechnology for funding my project and granting me the fellowship for my research.

My Sincere thanks to **Dr.S.Ramakrishnan,** Professor Emeritus, Biochemistry Research department for all his support and encouragement throughout my work.

I would like to express my heartfelt thanks to **Dr.K.N.Sulochana, Professor and Head**, Biochemistry Research Department, for her guidance and support throughout my work She was a person who had inculcated the passion of research in me. Although she was placed in Singapore during my work here, she was constantly keeping in touch through email motivating and encouraging me. I am thankful for the inputs she gave me for designing certain experiments.

I would like to express my sincere thanks to **Dr. Venil Sumantran**, Reader, Biochemistry Research department, for her scientific assistance in writing papers.

I express my sincere thanks to **Prof. Jyotirmay Biswas**, Head Ocular Pathology Department, **Dr.S.Krishnakumar**, Professor, Ocular Pathology Department, for interpretation of my immunohistochemistry data., **Dr. Lily Therese,** Professor, L &T Microbiology Research Centre, **Dr. G. Kumaramanickavel,** Professor and Head ONGC Department of Genetics and Molecular Biology, **Dr. Shankar Anand,** Reader, Department of Genetics and Molecular Biology, **Dr. J. Malathi,** Reader, L&T Microbiology Research Centre, Vision Research Foundation ,**Dr. Dorain Gracious**, consultant, clinical lab for their kind words, support and encouragement during my research work.

My sincere thanks to **Prof. L.K.Maheswari** Vice Chancellor and Director, BITS, Pilani, for giving me the opportunity to do my thesis under the esteemed university. I would also like to thank **Prof. Ravi Prakash**, Dean, Research and Consultancy Division, **Dr. B.R. Natrajan**, Dean, Distance Learning Programme Division, **Dr. Sanjay D. Pohekar** and **Dr. Deshmukh**, Convener Ph.D. for their constant support and help.

I thank **Dr. Hemanth Jadav, Mr. Dinesh Kumar, Ms. Monica Sharma, Mr. Sharad Shrivastava, Mr. Gunjan Soni, Mr. Amit Kumar and Ms. Sunita Bansal**, nucleus members of RCD, BITS, Pilani, without whose cooperation and guidance it would not have been possible for me to pursue such goal oriented research during each of the past few semesters.

I also express my gratitude to the office staff of RCD whose secretarial assistance helped me in submitting the various evaluation documents in time and give pre-submission seminar smoothly.

I thank my Doctoral Advisory Committee (DAC) members, **Prof. A. K. Das**, **Prof. Suman Kapoor and Dr. Uma Dubey**, who spared their valuable time to go through my draft thesis and were audience to my pre-submission seminar in order to provide several valuable suggestions that immensely helped in improving the quality of my PhD thesis report.

My special thanks to **Dr.J.Madhavan**, Senior Scientist, Dept of Genetics and Molecular Biology for his help in performing the real time analysis for lysyl oxidase. He shared lot of his clinical knowledge, which helped me in understanding the basics in vitreoretinal diseases. I acknowledge his encouragement and support.

I would like to thank **Dr.Murthy, Scientist, NIOT**, Chennai for providing us with the facility of spectrofluorimeter during our initial standardization procedures for lysyl oxidase estimation. My sincere thanks to **Dr.S.V Ramanan,** Professor**,** Anna University, AUKBC, for his knowledgeable discussion on RPE physiology.

I would like to thank **Dr.Pukhraj Rishi, Dr.N.Kasinathan** and other vitreoretinal surgeons for providing me the clinical specimens for my research work.

I thank **Mr.Irungovel** and the entire team of Eye Bank for promptly informing the biochemistry department about the donor eyeball collection which was used in my study.

I extend my sincere thanks to **Mr.S.Narayan**, Manager, Vision Research foundation and **Mr.N.Sivakumar**, Academic Officer for their support.

I thank **Mr. Thiagarajan** HOD, Medical records Department and all his colleagues for their support in giving me patient's files.

I thank the **JKCN main lab staff** for sending the specimens collected in JKCN on time safely to the department for my study

I extend my thanks to **Ms.Vanitha and Ms.Vaijayanthi** of Histopathology department for helping me in preparing histology sections for my work.

I acknowledge the help and support given by my wonderful department colleagues who have been encouraging me through out my work. I begin with **Ms.Punitham** who has been with me for many years encouraging and giving timely advices, **Ms. Bharathi** for her kind help in my cell culture work and her efforts during my thesis preparation, **Ms.Saijothi** in helping me during my thesis corrections, **Ms.Bharath selvi** for her sincere and timely help in all possible ways and also in organizing the clinical sample collections, **Ms.Selvi** for her moral support, **Ms. K. Parvathy Devi** for her kind words and encouragement through out my work and also her tremendous help in formatting my thesis. All of them gave me the feeling of being at home at work.

I had the pleasure to supervise and work with **Mrs. Vandhana and Ms. Gomathy** MSMLT dissertation students who did their graduation work in our project and have been beneficial for the presented work in this thesis.

I wish to extend my thanks to all the colleagues from the Departments of Microbiology, Ocular Pathology, Genetics and Molecular Biology and Clinical Laboratory for their support.

My special thanks to **Mr.Pradeesh Kumar**, Lab Attender for helping me in procuring eye balls for my research work and for giving the required things for my cell culture work on time.

I extend my thanks to all my well wishers **Dr.V.L.Ramprasad**, **Dr.N.Soumittra**, **Dr. Rajesh, Dr.Uthra, Dr.Sripriya, Dr.Bagyalakshmi, Dr. Deepa, Ms.Sreedevi and Ms.Tamilselvi** for their encouragement, support , advices and kind words during research work. I express my thanks to **Ms.Seetha** for her timely help.

I am deeply indebted to my friends who are really **Gods** gift for me in this life.

I acknowledge my beloved friend **Mr.Sakthivel Murugan** for his love, encouragement, advices, moral support and for his wonderful company in my

life. He has been a great inspiration and a source of motivation throughout my study period.

I extend my heartfelt gratitude to my friends **Dr**.**B.Mahalakhmi** for her motherly support , motivation and encouragement through out my reaserch work, **Ms.U.Jayanthi** for her care and concern, **Ms. Amirthalakshmi** and **Ms. Sudha** for their encouraging words, concern and advices.

I am very grateful and thank God for my loving family members, my brother **Mr.K.Altar**, my sister in law **Mrs.Jeniffer** , my sister **Mrs.Pearly**, my brother in law **Mr. Ravindran** for all their love, support, motivation, encouragement and patience they had through out my research work. I specially thank my brother who helped me in procuring bovine eyeballs for my research work. My special love to the wonderful children in my family, **Angelus Raina, Amos, Sherine Karunya, and Aron** who were really a source of happiness to me.

I feel a deep sense of gratitude for my **late father, Dr.Z.Karunakaran,** and **my mother, Mrs.Kanaga Karunakaran,** who formed a part of my vision and taught me the good things that really matter in life. They bore me, raised me, supported me, taught me, and loved me. The happy memory of my father and mother still provides a persistent inspiration for my journey in this life**. I dedicate this thesis to them.**

.

K. CORAL

TABLE OF CONTENTS

LIST OF FIGURES

	fluorescence detector
4.1	Reaction of lysyl oxidase
4.2	Reactions of lysine and hydroxylysine in the biosynthesis of the cross-links in collagen (A) and elastin (B).
4.3	Specific activity of lysyl oxidase in ocular tissues.
4.4	LOX mRNA expression in human ocular tissues calibrated to retina.
4.5	Immunolocalisation of LOX protein in paraffin embedded section of normal human donor ocular tissue.
5.1	Fundus images of retina in normal and disease conditions
5.2	Correlation between MMP 2 levels and protein in PDR
5.3	Correlation between MMP 2 levels and protein in RRD
5.4	Correlation between MMP 9 and protein in PDR
5.5	Correlation between MMP 9 and protein in RRD
5.6	Ratios of MMP 9: 2 in vitreous samples of patients with PDR, RRD and control vitreous.
5.7	Distribution profile of vitreous hydroxyproline in PDR, RRD and donor eyeball controls.
5.8	LOX immunolocalisation in epiretinal membranes from PDR and PVR
6.1	Phase contrast micrograph of primary BRPE cells
6.2	Phase contrast micrograph of primary BRPE showing foci of cell growth
6.3	Phase contrast micrograph showing dividing epitheloid cells in 10 to 12 days culture.
6.4	Phase contrast micrograph showing confluent BRPE cells in 14-16 days culture.
6.5 A	Phase contrast micrograph of BRPE cells after 1st passage
6.5 B	Phase contrast micrograph of BRPE cells after 1st passage.
6. 6	Phase contrast micrograph of ARPE-19 culture.
6.7	Phase contrast micrograph of HRPE culture.
6.8	Immunofluorescence for cytokeratin 8.13 in BRPE cells.
6.9	Immunofluorescence for actin in BRPE cells.

6.10	Immunofluorescence for vimentin in BRPE cells.
6.11	Western blot for cytokeratin 8.13 in BRPE cell lysates.
6.12	^{3}H Thymidine depletion from the medium by BRPE cultures.
6.13	^{3}H Thymidine uptake by BRPE cultures.
7.1	MTT assay in ARPE-19 cells exposed to tBH
7.2	Phase contrast micrograph of ARPE-19 cells after 3 hours treatment with tBH
7.3	Phase contrast micrograph of ARPE-19 cells after 6 hours treatment with tBH
7.4	Specific activity of LOX in ARPE-19 cells exposed to tBH
7.5	DQ gelatinase assay in ARPE-19 cells exposed to tBH
7.6	TUNEL staining in ARPE-19 cells exposed to tBH after 6 hours
7.7	Intracellular reactive oxygen species measurement in ARPE-19 cells exposed to tBH
8.1	BrdU assay in BRPE cells exposed to mannitol
8.2	MTT assay in BRPE cells exposed to mannitol
8.3	Phase contrast images of RPE in culture after treatment with 50 mM mannitol
8.4	Phase contrast images of RPE in culture after treatment with 100 mM mannitol
8.5	Phase contrast images of ARPE in culture in 50 mM and 100 mM mannitol after 12 hours
8.6	Specific activity of Lysyl oxidase in RPE cells exposed to mannitol
8.7	Real time gene expression of ARPE-19 cells exposed to mannitol
8.8	10% SDS PAGE – gelatin zymography showing MMP
9.1	MTT assay of RPE cells exposed to different concentrations of glucose
9.2	Phase contrast micrograph of RPE cells exposed to glucsoe
9.3	BrdU assay in RPE cells exposed to different concentrations of glucose
9.4	Specific activity of LOX in conditioned media of ARPE-19 cells.
9.5	RT-PCR results of LOX in ARPE cells after exposure to glucose.
9.6	RT-PCR results of GAPDH in ARPE cells after exposure to

	glucose.
9.7	mRNA expression of LOX by quantitative real time PCR
9.8	Immunolocalization of LOX in ARPE cells exposed to glucose
9.9	DQ gelatinase activity assay in ARPE cells exposed to glucose
10.1	HPLC chromatogram of vitreous sample.
10.2	Distribution profile of vitreous homocysteine in eyes with PDR, RRD and the donor eyeball controls.
10.3	Pearson's correlation between homocysteine and LOX specific activity in vitreous of eyes with PDR.
10.4	Pearson's correlation between homocysteine and LOX specific activity in vitreous of eyes with RRD**.**
10.5	MTT assay in ARPE-19 cells exposed to DL Homocysteine
10.6	Specific activity of LOX in ARPE-19 cells exposed to DL-Homocysteine
10.7	mRNA expression of LOX in RPE cells exposed to DL-Homocysteine
11.1	mRNA expression of LOX by real time PCR in ARPE-19 cultures
11.2	Role of vitreous Homocysteine in LOX and MMP mediated changes of the ECM

LIST OF TABLES

ABBREVIATIONS

RPE	Retinal pigment epithelium
BM	Bruch's membrane
ZO	zona occludens
IPM	Interphotoreceptor matrix
CMB	Circumferential microfilament bundles
ROS	Rod outer segment
MCT	Monocarboxylate transporters
TGF-beta	Transforming growth factor beta
TNF-alpha	Tissue necrosis factor alpha
MHC	Major histocompatability
IL	Interleukin
GM-CSF	Granulocyte monocyte colony stimulating factor
MCP	Monocyte chemoattractant protein
bFGF	Basic fibroblast growth factor
aFGF	Acidic fibroblast growth factor
HGF	Hepatocyte growth factor
PDGF-A	Platelet derived growth factor A
VEGF	Vascular endothelial growth factor
ECM	Extracellular matrix
LFA/ICAM	Lymphocyte function-associated antigen/Intracellualr cell adhesion molecule
VLA-4/VCAM-1	Very Late Antigen-4/ Vascular cell adhesion molecule-1
PG	Proteoglycans
PMN	Polymorphonuclear

GAG	Glycosaminoglycans
N-CAM	Neural cell adhesion molecule
RP	Retinitis pigmentosa
CSR	Central serous retinopathy
PDR	Proliferative diabetic retinopathy
PED	Pigment epithelium detachment
CSE	Central serous edema
PVR	Proliferative vitreoretinopathy
SPARC	Secreted protein, acidic and rich in cysteine
MMP	Matrix metalloproteinases
AP-1	Transcription factor
SP-1	Human transcription factor
NF-kB	Nuclear factor kappa B
TIMP	Tissue inhibitors of metalloproteinases
AO	Amine oxidases
DAO	Diamine oxidase
SSAO	Semicarbazide sensitive amine oxidase
LOX	Lysyl oxidase
LTQ	Lysine tyrosylquinone
CRL	cytokine receptor-like
SRCR	scavenger receptor cysteine-rich
BAPN	β-aminopropionitrile
LDL	Low density lipoprotein
IRF	Interferon regulatory factor
cAMP	Cyclic AMP
ARPE - 19	Human Retinal pigment epithelium cel line
PBST	Phosphate buffered saline with tween
FITC	Fluorescein isothiocyanate

IF	Immunofluorescence
IHC	Immunohistochemistry
TBS	Tris buffered saline
MTT	[3-(4,5-dimethylthiazol-2-yl)-2,5-diphenyltetrazolium bromide]
DMSO	Dimethylsulphoside
DNA	Deoxyribonucleic acid
RNA	Ribonucleic acid
H_2O_2	Hydrogen peroxide
ELISA	Enzyme linked immunosorbent assay
HRP	Horse radish peroxidase
AR	Amplex red
BrdU	5-bromo-2'-deoxyuridine
PBS	Phosphate buffered saline
RT-PCR	Reverse transcriptase – polymerase chain reaction
GAPDH	Glyceraldehyde-3-phosphate dehydrogenase
PCR	Polymerase chain reaction
DEPC	Diethyl pyrocarbonate
dNTP	Deoxyribonucleotide triphosphate
cDNA	complementary DNA
DTT	Dithiothretol
SDS	Sodium dodecyl sulphate
Hcy	Homocysteine
DMEM/F12	Dulbecco's Modification of Eagle's Medium/Ham's F-12
M199	Medium 199
CRALBP protein	Cellular retinaldehyde-binding protein
TCA	Trichlorocaetic acid

NaOH	Sodium hydroxide
EDTA	Ethylenediaminetetraacetic acid
ATCC	American Type Culture Collection

CHAPTER 1 - INTRODUCTION AND LITERATURE REVIEW

INTRODUCTION

The eyes are undoubtedly the most sensitive and delicate organs we possess, and perhaps the most amazing. They present us with the window through which we view the world, and are responsible for four fifths of all the information our brain receives-which is probably why we rely on our eyesight more than any other sense. The human eye is like two spheres held in the orbital cavity by orbital muscles. The anterior segment is the front of the eye that includes the structures like the cornea, iris, ciliary body and lens. The posterior segment occupies five-sixths of the eye that includes the anterior hyaloid membrane and all of the optical structures behind it like the vitreous humor, retina, choroid, and optic nerve.The radii of the anterior and posterior sections are 8 mm and 12 mm, respectively. The junction point is called the limbus.

The two fluid-filled spaces in the eye are described as the anterior chamber which is between the posterior surface of the cornea (i.e. the corneal endothelium) and the iris. Aqueous humor fills these spaces and provides nutrients to the surrounding structures

The posterior chamber is between the lens and the retina, which is bounded anteriorly all sides by the lens, the ciliary body, and suspensory ligaments and posteriorly by the retina. It lets light pass through without refraction, helps to maintain the shape of the eye, and offers support to retina. **(Figure 1.1)**

Figure 1.1 : Structure of the eye

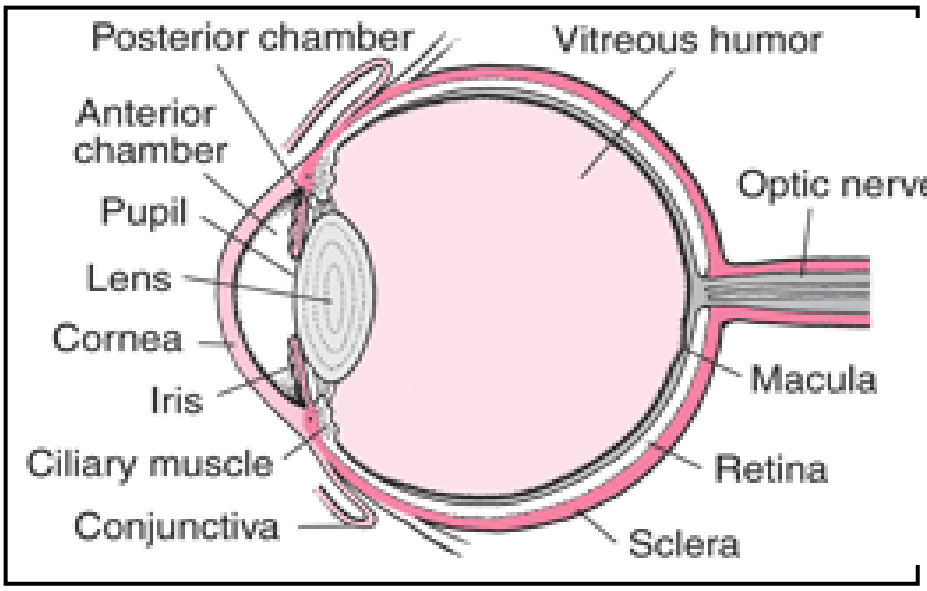

Adapted from www.google images.com

1.1. THE RETINAL PIGMENT EPITHELIUM ANATOMY AND PHYSIOLOGY

The retinal pigment epithelium is a monolayer of highly specialized pigmented cells lying between the vascular choriod and neural retina. It is derived embryologically from the same neural tube tissue that forms the sensory retina. RPE has no photoreceptive functions or neural functions, but it is necessary for the support and viability of the photoreceptors.

1.1.1 Embryology: Human eye development begins at 18th day post conception. The early optical vesicle invaginates to form a cup, the inner layer of which becomes the neurosenory retina and the outer layer becomes the RPE. The neurosensory retina differentiates into several layers, but the RPE remains as a monolayer with characteristics of a secretory epithelium. RPE differentiates at about 30 days of gestation. At the 35^{th} day melanin pigment granules are seen, which is the earliest site of pigmentation in the body. Pigmentation is completed within a week. By 6^{th} week of gestation, RPE cells synthesizes the basement

membrane material that participates in the formation of the first recognizable Bruch's membrane. At 10 weeks, RPE cells develop apical projections that extend into the subretinal space. RPE show high rates of proliferation with increased telomerase activity between 4 weeks – 6 months. Once the eye is fully grown, RPE cells are stationary, do not proliferate and undergo growth only by cell enlargement (Panda-Jonas et al., 1996; Stroeva et al, 1983).

1.1.2 Anatomic features of the RPE

The structure of the RPE is unique and is adapted to many of its complex functions. Histologically, the RPE consists of a continuous monolayer of cells beginning at the optic nerve head and extending peripherally to the ora serrata. Human adult eye has approximately 3.5 million RPE cells (Bok et al.,1993 a). Anterior to the ora serrata, the RPE continues as the ciliary pigment epithelium **(Figure 1.2).** RPE cell density decreases from the fovea centralis to the periphery (Panda-Jonas et al., 1996).

Figure 1.2: Cross section of human eye showing the anatomy of retinal pigment epithelium

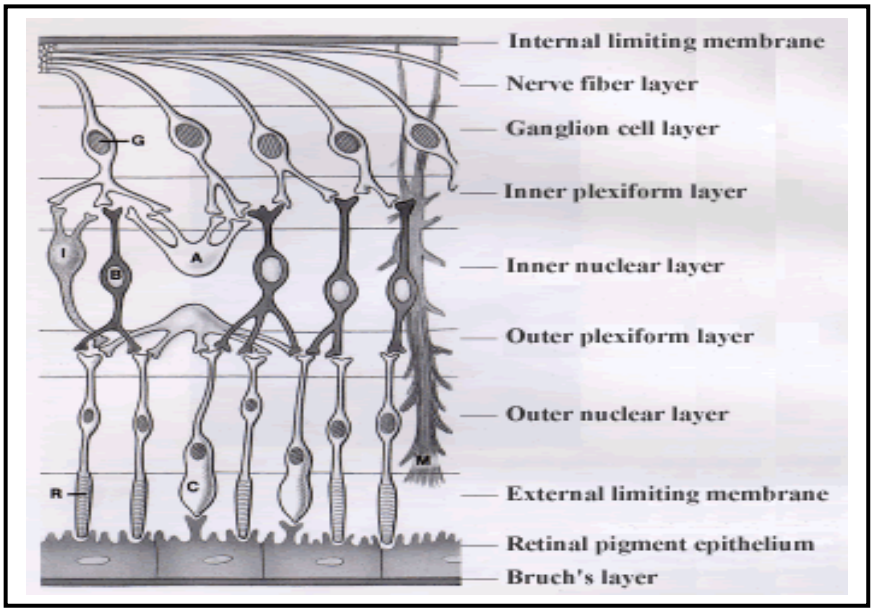

Adapted from www.googleimages.com

The apical surface of the RPE interfaces with the outer segments of the photoreceptors, while the basal domain is attached firmly to the underlying Bruch's membrane (BM). The brown colour of the RPE is imparted by its melanin granules. The highest concentration of pigment is found in the peripheral

retina and the lowest in the macula area (Weiter et al., 1986). The retina and the RPE are separated by a potential space called the subretinal space. The retina is not firmly attached to the pigment epithelium except at the optic disc and ora serrata, attachments in other places are weak and can be easily disrupted

1.1.3 General structure of the RPE

The plasma membrane and cytoplasmic contents of RPE cells are highly polarized. This polarity is essential for the many vectorial transport functions that the RPE cell carries out. The cell body of the RPE has a cuboidal configuration, when viewed in a flat preparation (Figure 1.3). *In situ* RPE cell shape varies throughout the fundus. In the macula region they are tall and narrow having 10 - 14μm diameter, whereas in the periphery they are flattened and more spread out having 60 μm diameter and are often binucleated. Each RPE is differentiated into an apical portion (facing the photoreceptor) and a basal portion (on Bruch's membrane). RPE has distinct surface domains, apical, basal and basolateral domains.

Figure 1.3: Cuboidal configuration of RPE when viewed in a flat preparation.

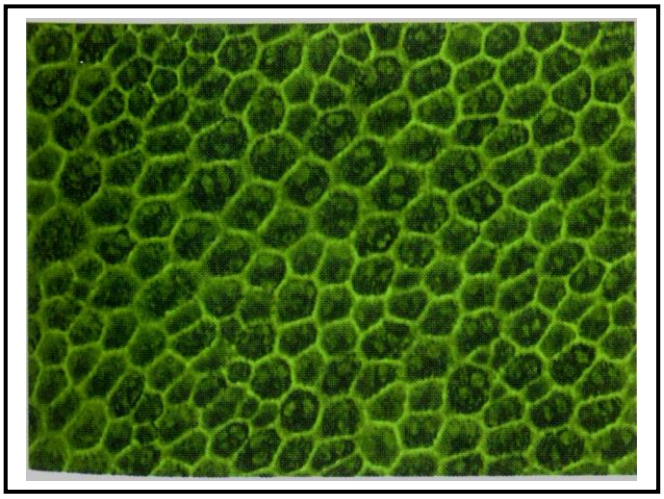

Adapted from *Thumann et al., 2001*

The apical side has numerous long microvilli (3-7μm in length) which interdigitate with the rods and cones of the retina and partially envelope them (Figure 1.4). About 30-45 photoreceptors are in contact with each RPE cell (Young et al., 1971). These interdigitations along with the extracellular matrix and neural cell adhesion molecule (N-CAM) expressed by the RPE on the apical side, allow some degree of adhesion between retina and RPE.

Figure 1.4: Apical microvilli of RPE interdigitation with rods and cones

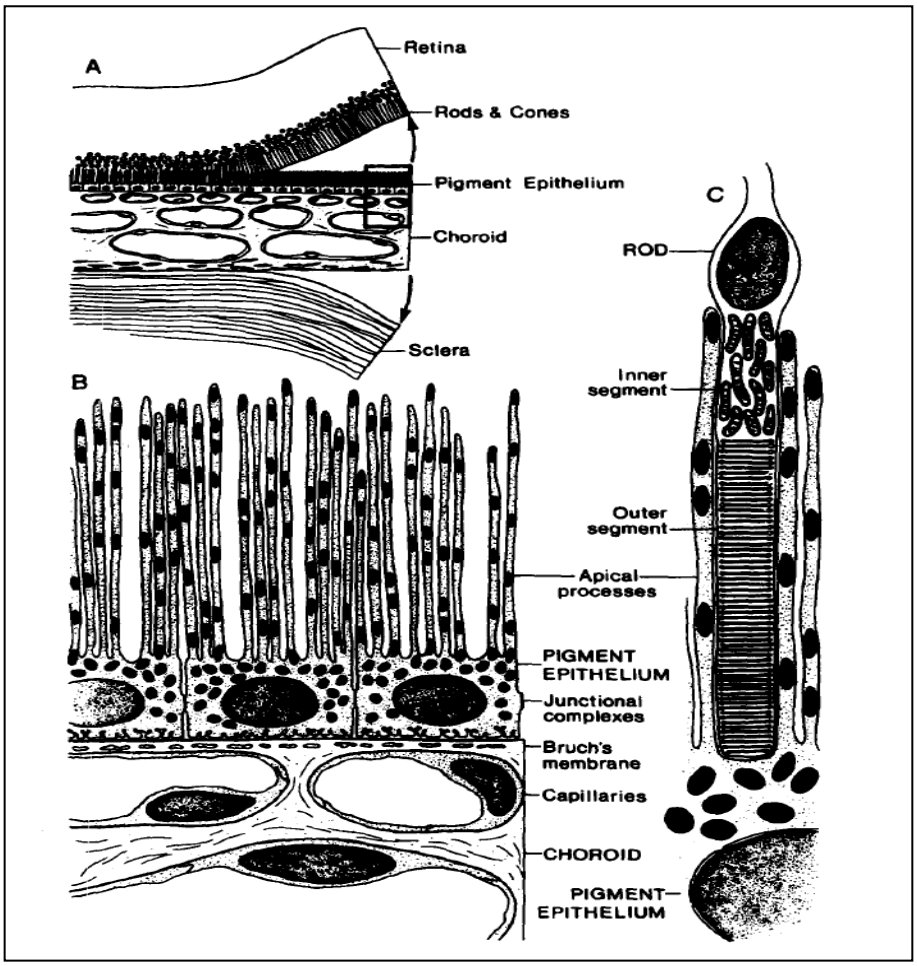

Adapted from Gallemore et al., 1997

The RPE cells are joined near the apical side by tight junctions (zonula occludens) which forms a part of the blood retinal barrier. The apical cytoplasm contains microfilaments and microtubules and also the greatest concentration of melanin granules. The basal infoldings are 1 μm and they help in the attachment of RPE to BM of choroid by expression of integrins. The small convoluted infoldings also increase the surface area for absorption and secretion. Laterally the RPE has specialized junctions called the tight junctions – zona occludens (ZO-1) and adherent junctions cadherins, connexin, desmosomes.

1.1.4 Apical plasma membrane

The apical surfaces of RPE cells face the photoreceptors, and contain both long and short microvilli (Figure 1.4). These microvillus processes interdigitate with the outer segment tips of the photoreceptor across the subretinal space. The close proximity of the large surface areas of both the photoreceptor and RPE cell plasma membranes aid in the exchange of nutrients and metabolites between these two cell types. Although there is no direct contact between the apical processes of RPE cells and the photoreceptor outer segments (Clark et al., 1986; Steinberg et al., 1985), they adhere to each other and functionally communicate across the subretinal space. The apical surface of the RPE, as well as the rod and cone outer segments are coated with an extracellular matrix called interphotoreceptor matrix (IPM) which is secreted in part, by the RPE cells (Clark et al., 1986).It is believed that the IPM may play a minor role in the adhesion of neurosensory retina to the RPE by acting as a "glue" (Marmor et al., 1989).The IPM may also serve as a medium for the exchange of metabolites between the outer segments of the photoreceptors and the RPE (Clark et al., 1986). Due to the lack of tight attachment beneath the neural retina and the RPE, the neural retina becomes detached from the RPE under certain conditions. Detachment simultaneously disrupts the photoreceptors and RPE, and can eventually lead to the loss of vision (Zayit-Soudry et al.,2007). The apical membrane of the RPE is rich in Na^+K^+ ATPase which, together with other ionic transport mechanisms, move water out of the subretinal space. The apical location of the Na^+K^+ ATPase along with the epithelium of the choroid plexus is a unique feature among epithelia, as this pump is normally located on the basal membrane (Bok et al., 1993a; Marmor et al., 1989) (Figure 1.5)

Figure 1.5: Apical location of Na^+ K^+ ATPase

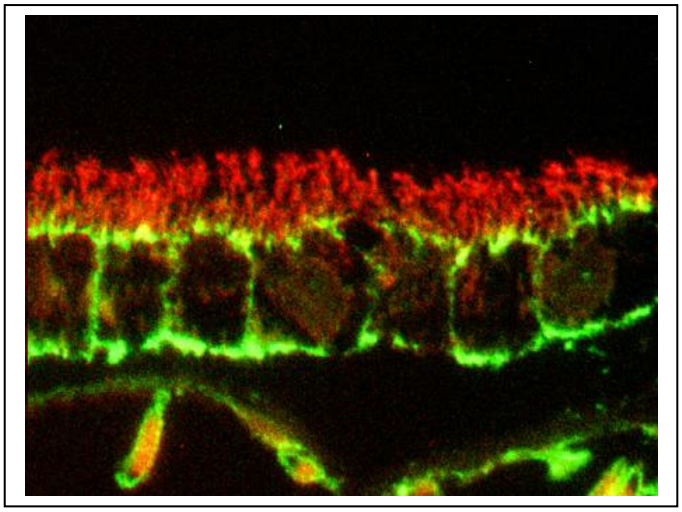

Adapted from www.googleimages.com

This apical pump is mainly responsible for absorptive fluid movement from the apical to the basal membrane of the RPE. The removal of subretinal fluid by the RPE is thought to provide the major motive force for adhesion of the neural retina to the RPE (Clark et al, 1986; Marshall , 1987). As part of the photoreceptor renewal process, the apical processes of the RPE continually phagocytize the distal portions of the outer segments of rods and cones. RPE cells ingest and degrade about 3000 million discs during a 70 year life span (Clark et al., 1986; Marshall ., 1987). Once internalized by the RPE, the phagosomes are then quickly digested by the lysosomal system in the cytoplasm of RPE cells. Each of these outer segments is renewed by new membrane assembly at the photoreceptor proximal ends. This process of shedding, phagocytosis and renewal of the photoreceptor follows a circadian rhythm (Bok et al., 1993a). It has been observed that the close approximation of the photoreceptors to the RPE is required before this process to take place.

1.1.5 Basal plasma membrane

As shown in Figure 1-4, the basal plasma membrane of the RPE cell has numerous infoldings and lies on a basement membrane which is secreted by the RPE itself (Clark et al., 1986).These infoldings are very useful for facilitating ion movement in transporting epithelia such as the RPE, as they increase the surface

area of the cell. The basal surface of the RPE express integrins α3β1, α6β1 and α5β3 and mediate attachment to BM, a fibroelastic layer which separates the photoreceptor- RPE unit from its blood supply derived from the choriocapillaris (Clark et al., 1986). BM is permeable to small molecules and some macromolecules, and is thought to contribute to the blood-retinal barrier (Pino et al., 1982; Pino et al, 1981).

1.1.6 Lateral plasma membrane

Unlike its basal and apical counterparts, the lateral plasma membrane of the RPE cell lack infoldings (Figure 1.4). The basal and lateral membranes are usually referred as a single functional unit, called as basolateral. The lateral domain of the adjacent RPE cells are connected by apical zonula occludens i.e. tight junctions and zonula adherens i.e. adherens junction (Fine , 1961). These junctions seal off the subretinal space where the exchange of macromolecules with the choriocapillaries takes place. The zonula occludens between adjacent RPE cells form a “tight” intercellular junction due to interaction between the extracellular domains of adjacent occluding molecules leading to high transepithelial resistance and an intact blood retinal barrier. Tight junctions are also responsible for the sequestration of molecules into the apical and basal plasma membrane domains.

Figure 1.6: Gap Junction and Tight Junctions in RPE

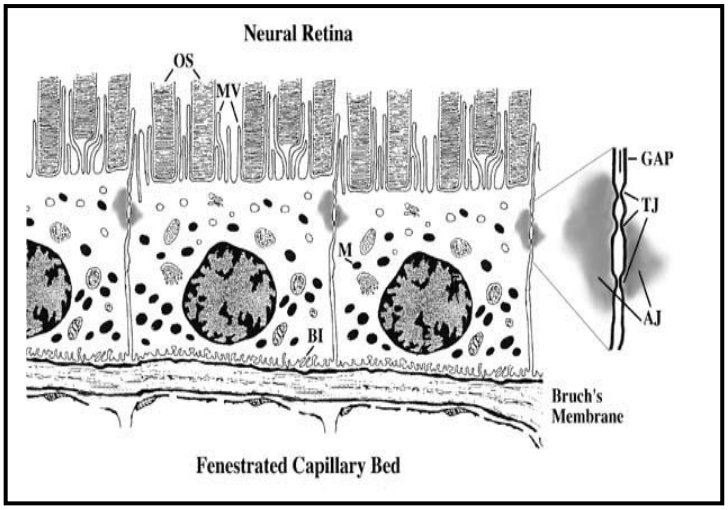

Adapted from Marmor et al., 1998

The adherens junction form a junction with a separation of 200 Å and are associated with circumferential microfilament bundles (Crawford et al., 1980).The transmembrane cadherin molecules of the adherens junction require calcium for adhesion and signalling. The cytoplasmic domain interacts with catenins, which in turn complexes with α actin and vinculin. The adherens junctions play a role in maintenance of the polygonal shape of the RPE and the organization of the cytoskeleton actin (Sandig et al., 1988).

Gap junctions are also present in the basolateral membrane called connexins which are important for the exchange of ions and metabolites between cells. (Figure 1.6) Basal membrane also expresses integrins and show focal adhesion points with the extracellular matrix (Docherty et al., 1984).

1.1.7 Cytoplasmic components of RPE: The RPE has an asymmetric distribution of cell organelles and cytoplasmic components. The nucleus is about 8-12 μm and is seen in basal part of the cell. The Mitochondria is at the basal and lateral aspect of the cell (Figure 1.7). Lysosomes are seen throughout the cell. Melanin granules which are ovoid or spherical about 1 μm diameter are localized at the apical region of the cell. The endoplasmic reticulum is located in the apical part of the cell and is involved in protein synthesis.

Figure1.7: Cytoplasmic components of the RPE

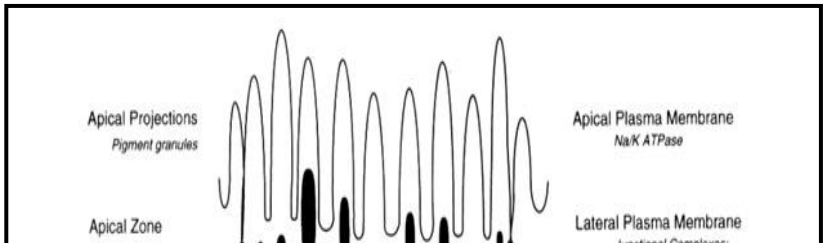

Adapted from Marmor et al., 1998

1.1.8 Cytoskeletal proteins:

The cytoskeleton is composed of three fibrous elements (actin filaments, intermediate filaments, and microtubules) and their associated proteins. Actin filaments and microtubules provide tracks for molecular motors and also provide structural support to the cell. Molecular motors are mechano-chemical engines that utilize the energy of ATP hydrolysis to perform mechanical work (Spudich et al., 1994). This work was achieved by using the conformational changes generated by ATP hydrolysis to "walk" along an actin filament or microtubule. Intermediate filaments provide mechanical strength and resistance to stretch, but do not appear to serve as tracks for molecular motors (Fuchs et al., 1994).

1.1.9 The Actin Cytoskeleton

In polarized RPE cells, actin filaments are localized to the basal infoldings, the lateral membrane skeleton, the apical projections and the dense circumferential microfilament bundles (CMBs) which encircle the cell apex and associate with the zonula adherens junctions between adjacent RPE cells. Actin filaments role in RPE functions have been demonstrated using cytochalasin. High levels of cytochalasin (5-10µm) induced gaps in well-differentiated cultured RPE cells, suggesting that actin filament disruption impaired the maintenance of epithelial integrity (Sakamoto et al., 1994). However, lower levels of cytochalasin blocked similar gap formation induced by thrombin, suggesting a role for actin assembly in producing these gaps. (**Figure 1.8)**

Figure 1.8: Actin filaments of RPE

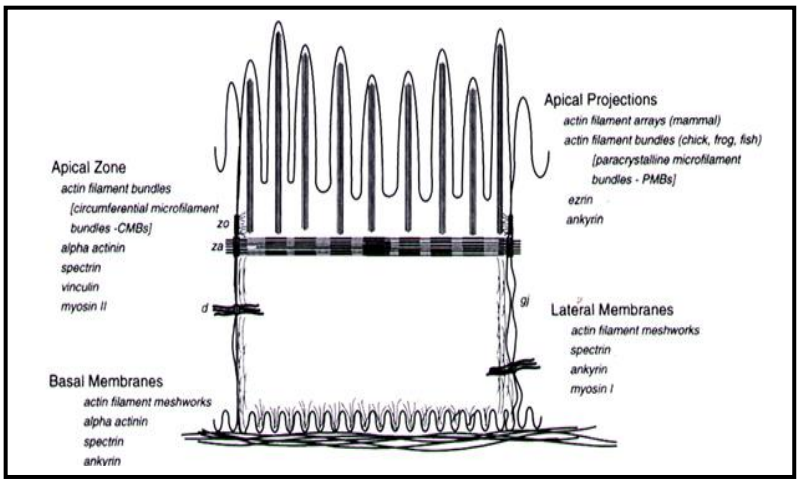

Adapted from Marmor et al., 1998

1.1.10 Intermediate Filaments

Intermediate filaments are the third fibrous component of the cytoskeleton found in the cytoplasm of most, but not all animal cells. Intermediate filaments are so named because their diameter is between that of thin actin filaments and thick myosin filaments or microtubules. Intermediate filament proteins are classified into five types based upon sequence homology, immunological cross-reactivity, and site of expression. Type I and type II intermediate filaments comprise the acidic and basic cytokeratins, respectively; both are expressed primarily in epithelial cells (Coulombe, 1993). Type III intermediate filament proteins are expressed in cells of mesenchymal origin and include vimentin, desmin, glial fibrillary acidic protein and peripherin. Type IV proteins are the low, medium, and high-molecular-weight subunits of neurofilaments (Okabe et al., 1991). Type V proteins, the lamins, are present in all nucleated cells, where they provide the structural components of the nuclear envelope (Gerace et al., 1988).

Figure 1.9: Immunoflurescence of Actin filaments

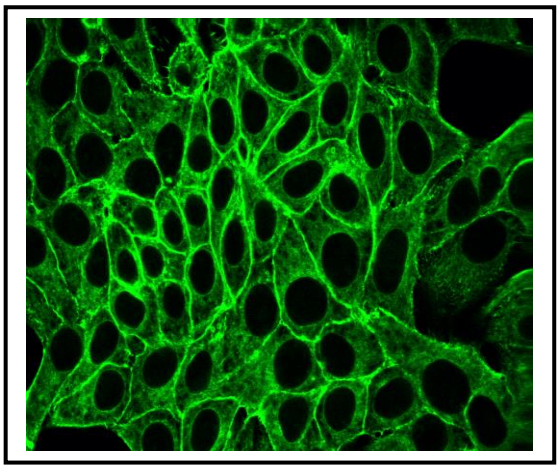

Adapted from www.googleimages.com

In epithelial cells, cytokeratin intermediate filaments are anchored at desmosomes and hemidesmosomes, where they are optimally situated to reinforce the attachment of cells to adjacent cells or to the basement lamina. The expression pattern of intermediate filament proteins in RPE cells varies with species and with culture conditions *in vitro*. Chick RPE cells are unique in that they express only vimentin intermediate filaments rather than cytokeratins (Philp et al., 1985). In the RPE of amphibian and certain mammals like rats and rabbits, only cytokeratins are expressed (Owaribe et al., 1988; Stroeva et al., 1983). In other mammals like guinea pigs, cows and humans RPE cells express both cytokeratins and vimentin or cytokeratin intermediate filaments can meet the structural needs of RPE cells. These cytokeratins are used as the cell marker of RPE when grown *in vitro.*

When RPE cells are removed from the eye and put into culture, their cytokeratin expression pattern changes (Owaribe et al., 1988). When bovine RPE cells are placed in culture, cytokeratin synthesis decreases and vimentin expression increases. (Owaribe et al., 1988). In cat RPE, when cells are sub confluent and dedifferentiated, vimentin filaments are distributed throughout the cytoplasm. When the cells become confluent and display a more differentiated phenotype, vimentin filaments are more concentrated near the cell borders (Matsumoto et al., 1990). Human RPE cells *in vivo* express cytokeratin 8 and 18 and no vimentin, but when placed in culture express cytokeratins 7, 8, 18 and 19 and vimentin (Hunt et al, 1990). Cultured human RPE cells express vimentin and much wider variety of cytokeratins than freshly isolated RPE (McKechnie et al., 1988).

The pattern of intermediate protein expression *in vitro* is influenced by culture conditions. Exposing cultured RPE cells to vitreous components decreases the proportion of cells co-expressing both cytokeratins and vimentin over time (Vinores et al., 1990). In certain pathological situations RPE cells detach from BM, migrate through the retina in epiretinal membranes. The alterations of

cytokeratin expression produced by vitreous factors may contribute to differentiated phenotypes in RPE cells.

Table 1.1: Physiological role of the RPE

Pigment functions
Light adaptation and screening
Detoxification and binding
Lipofuchscin accumulation
Antigenic properties
Outer segment phagocytosis and aging
Phagocytosis of outer segment tips
Digestion and recycling of membrane material
Aging effects; lipofuscin, drusen
Deposits and alterations in Bruch's membrane
Environment and metabolic control
Blood-retinal barrier
Transport of nutrients and ions
Dehydration of subretinal space
Synthesis of enzymes, growth factors, pigments
Interaction with endocrine, vascular and proliferative factors
Visual pigment cycle
Capture and storage of vitamin A
Isomerization of all-trans to 11-cis vitamin A
Interphotoreceptor matrix and retinal adhesion
Specialized matrix ensheathment of rods and cones
Metabolic control of adhesion
Electrical activity
Responses to light-induced ionic changes: c-wave, fast oscillation
Response to light-induced chemical signals:EOG
Nonphotic responses to chemical agents
Electrical activity Repair and reactivity
Repair and regeneration
Immunologic interactions
Scarring and pigment migration
Modulation of fibrovascular proliferation

1.1.11 Melanin pigment: The RPE is the first tissue to become pigmented (melanin) (Dorey et al., 1990), and hence it is named as pigmented epithelial cells. The ellipsoidal melanin granules called melanosomes are one of the most

conspicuous cytoplasmic components in RPE (Feeney-Burns et al., 1984). (Figure 1.10)

Figure 1.10: Melanin pigments in RPE under electron microscopy

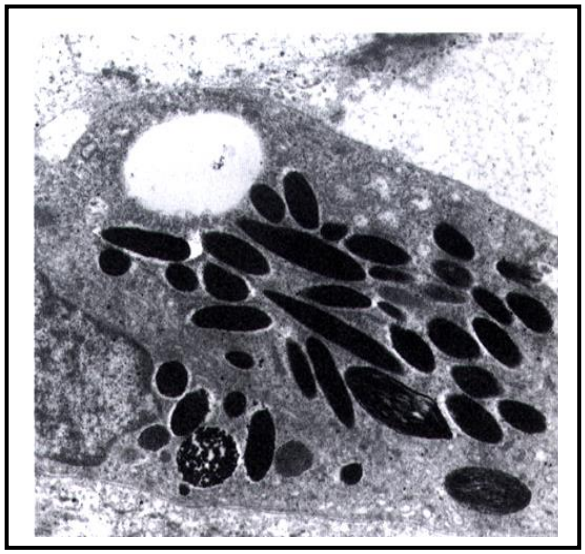

Adapted from Marmor et al., 1998

Melanosomes, the organelles responsible for the biosynthesis of melanin, appear in the development of human RPE beginning at 6 weeks of gestational age (Sarna et al., 1992). It was previously thought that melanogenesis in vertebrates was restricted to the prenatal period because of the absence of the key enzyme tyrosinase in adults (Dorey et al., 1990). Evidence is now available that melanogenesis occurs in adult RPE cells of cattle and golden hamsters (Schraermeyer et al., 1992) and adult cultured human RPE (Burridge et al., 1988). In cell culture, two different pathways have been identified in melanogenesis; melanin can be synthesized with and without formation of pre-melanosomes, the formation of melanosomes takes place within phagolysosomes and includes residue of degraded rod outer segment (ROS) (Schraermeyer et al., 1994). Within the adult RPE cell the melanin granules are located in the apical portion of the cell, adjacent to Rod Outer Segment.

Melanin granules function to reduce light scattering and block light absorption via the sclera, resulting in a better image received by the retina. Melanin also absorbs radiant energy (visible and ultraviolet spectrum) and dissipates the energy in the heat. In addition melanin can bind redox-active metal ions and

sequester them in an inactive state, thus preventing oxidative damage to the retina by these potential photosensitizing agents (Sarna et al., 1992). The absorption of light by melanin acts as an effective antioxidant to protect the RPE cells and regulate their metabolic activity; in fact, RPE cells high in melanin content exhibit significantly less formation of lipofuscin than cells low or devoid of melanin (Nilsson et al., 2003). Incase of an intense oxidative insult, structural or functional changes in RPE melanin may lead to loss of anti-oxidant capacity (Sarna et al., 1992).

The melanin in the RPE represents the single most important source for heat in thermal photocoagulation. In man, a congenital disorder associated with decrease in melanin production leads to albinism associated with decrease in vision, photophobia and nystagmus.

1.1.12 Phagocytosis of shed Rod Outer Segment.

One of the critical functions of the RPE is to phagocytose and degrade Rod Outer Segment (ROS) which is shed diurnally from the distal end of the photoreceptors. Two specific mechanism for RPE phagocytosis are proposed, a slow, non specific process and a rapid receptor mediated uptake of shed ROS. The receptor mediated uptake is a multi step process which involves recognition-attachment, internalization and degradation (Stossel et al., 1974).

Receptor ligand binding interactions between shed ROS and RPE microvilli is the first step of the phagocytic process (Bok et al., 1993a). Several studies have reported α5β5 intergin is a functional ROS receptor (Finnemann et al., 1999). Others studies suggest that it is mediated by the receptor tyrosine kinase, c-mer and its ligand Gas-6 (Hall et al., 2001).

Binding of the ROS is followed by invagination of plasma membrane around the outer segment fragment, leading to its ingestion into a phagosome. A reorganization of cytoskeletal elements particularly of microfilaments in microvilli appears to be involved in the initial stages of ingestion. An actin network forms at the site of attachment that extend into pseudopods which surrounds and engulf the fragments to form the phagosome which are transported basally (Rakoczy et al., 1994).

After this the phagosomes fuse with the lysosomes and are degraded. The lysosomal enzymes hydrolyze the sequestered outer segments into small molecules that diffuse out of the RPE and are reused within the cell. Cathepsin D is the most important enzyme that degardes rhodopsin, the major glycosylated protein present in the outer segment, another enzyme is cysteine protese cathepsin S (Rakoczy et al., 1994).

In RPE cultures the enzymatic capacity of RPE has been shown to be age independent (Rakoczy et al., 1996) but *in vivo* with age degradation of ROS appears to be diminished.

With age and pathological changes in human eye, deficient degradation of the outer segment material within the phagolysosomes may lead to the formation of lipofuchsin granules composed of ROS residue (Feeney-Burns et al., 1984). The RPE cell defends itself from the effects of reactive oxygen intermediates generated during the degradation process by a group of antioxidant enzymes (Tate Jr. et al., 1995).

1.1.13 Blood retinal barrier, transport and ionic pumps

Anatomically the outer blood retinal barrier is formed by the RPE, which controls the exchange of fluid and molecules between the fenestrated choriocapillaries and the outer retina (Figure 1.4). Two major components of RPE barrier function are the tight junctions between the RPE cells and the polarized distribution of RPE membrane proteins (Anderson et al, 1995). Since tight junction inhibit intercellular diffusion, molecular exchanges predominantly occur across the RPE cells themselves. Nevertheless, tight junctions are dynamic structures and their permeability can be modified by specific physiological conditions as well as by certain pharmacological agents (Balda et al., 1991). Further more diffusible factors secreted from the neural retina, or RPE derived growth factors (such as hepatocyte growth factor), may be involved in the regulation of the structure and function of RPE tight junctions (Balda et al., 1991; Cereijido et al., 1993). The regulation of transepithelial transport is dependent on the asymmetric distribution of cellular proteins (Drubin and Nelson et al., 1996). This polarity of the epithelial cells changes upon interaction with the environment. In RPE the Na^+, K^+ ATPase is localized at the apical cell membrane and cytoskeletal proteins like

ankyrin and fodrin known to be associated with the ATPase are localized apically, whereas in most other epithelial cells they are localized basolaterally (Gundersen et al., 1991). Important for transport functions is the presence of apical microvilli and basal plasma membrane infoldings, which increase the surface area available for the exchange of nutrients and catabolites. RPE cells have receptors in their basal and lateral membranes for nutrient that arrive through the choriocapillaries and must be transported toward the outer retina, such as retinol and its binding protein. Human RPE express two proton and coupled monocarboxylate transporters (MCT). MCT1 in the apical membrane and MCT-3 in the basolateral membrane. The coordinated activities of these two transporters could facilitate the flux of lactate and from the retina to the choroid (Robey et al., 1992).

P glycoprotein is another protein that contributes to the normal transport function of RPE cells. The protein is expressed in cultured and native human RPE cells on the apical and basolateral membrane surface (Kennedy et al., 2002). The basolateral expression of P glycoprotein serves to clear the unwanted metabolites from the subretinal space, thus serving a protective function to the neural retina.

The movement of water and catabolites from the retina toward the choriocapillaries is important for the nutrition of the retina, for maintenance of ocular pressure and possibly for maintenance of retinal attachment to the RPE. The latter effect may be generated through a “suction” mechanism that develop when RPE cells actively remove fluids from the subretinal space (Miller et al., 1982). In conjunction with passive forces, active transport of solutes across the RPE contributes to the movement of water out of the eye. Aquaporin 1 is hexahelical integral membrane protein that functions as a constitutive channel for water transport in many tissues, including the eyes. Aquaporin is expressed in human fetal and adult RPE where it facilitates water movement across the RPE monolayer (Stamer et al., 2003).

Breakdown of the blood retinal barrier has serious consequences for the health of the eye and is present in many types of retinopathies (Gariano et al., 1996). Hepatocyte growth factor is one important growth factor that regulates the barrier function of RPE cells. Adenoviral over expression of HGF in rabbit RPE induced

a chronic retinal detachment associated with separation, migration and proliferation of RPE cells and inflammation in the choroid (Jin et al., 2005).

1.1.14 Retinol Metabolism: Phototransduction begins by absorption of a photon by a highly sensitive analog of vitamin A, 11-cis-retinal that is bound to opsin proteins in the phototoreceptors. Briefly, 11- *cis*- retinal is isomerized to all- *trans*- retinal by reacting with a photon forming the photoactive visual pigment R* following the light response the photoactive pigment decays and release all- *trans*-retinal from the opsin proteins in the cytoplasm of the photoreceptors, where it is reduced to all- *trans*- retinol and transported to the RPE across the subretinal space (Hubbard et al., 1952). Provision of a continuous source of 11-*cis*-retinal is accompanied by the recycling of vitamin A analogs between the photoreceptors and the RPE. Thus the metabolism of retinol is one of the most important and highly specialized functions of the RPE. The reisomerization of all-*trans*-reitnal in the RPE is a crucial aspect of the visual cycle (Bok et al., 1990; Das et al., 1988). The cycle involves several transport mechanisms mediated by various intra and extra cellular retinoid binding proteins and enzymes, that convert retinol into its various intermediates and finally to the active 11- *cis*-retinaldehyde **(Figure 1.11)**.

Three cytosolic retinoid binding proteins that are essential for the shuttling and metabolism of retinol are present in RPE cells: cellular retinol binding protein (CRBP) for all trans retinol and cellular retinaldehyde binding protein (CRALBP) for 11 cis retinal, and RPE65, a RPE specific protein that has high affinity for all trans retinol (Lamb et al., 2004).

The interphotoreceptor matrix (IPM) juxtaposed between the RPE cell layer and the photoreceptor outer segment of the neural retina is also of importance in the visual cycle (Bok *et al*., 1993a). It is through this extracellular matrix (ECM) potentially large amount of retinoids travel in a vectorial manner back and forth between storage in the RPE and use in photoreceptor outer segment for rhodopsin synthesis. Thus in considering the role of RPE in vision it is best to consider the reactions taking place in the entire retina -IPM- RPE complex as proper processing of retinoids in all 3 compartments is important for visual functioning. It is only within the last decade that the RPE has been pinpointed as actual site of retinoid isomerization as well as uptake and storage.

Figure 1.11: Retinol metabolism

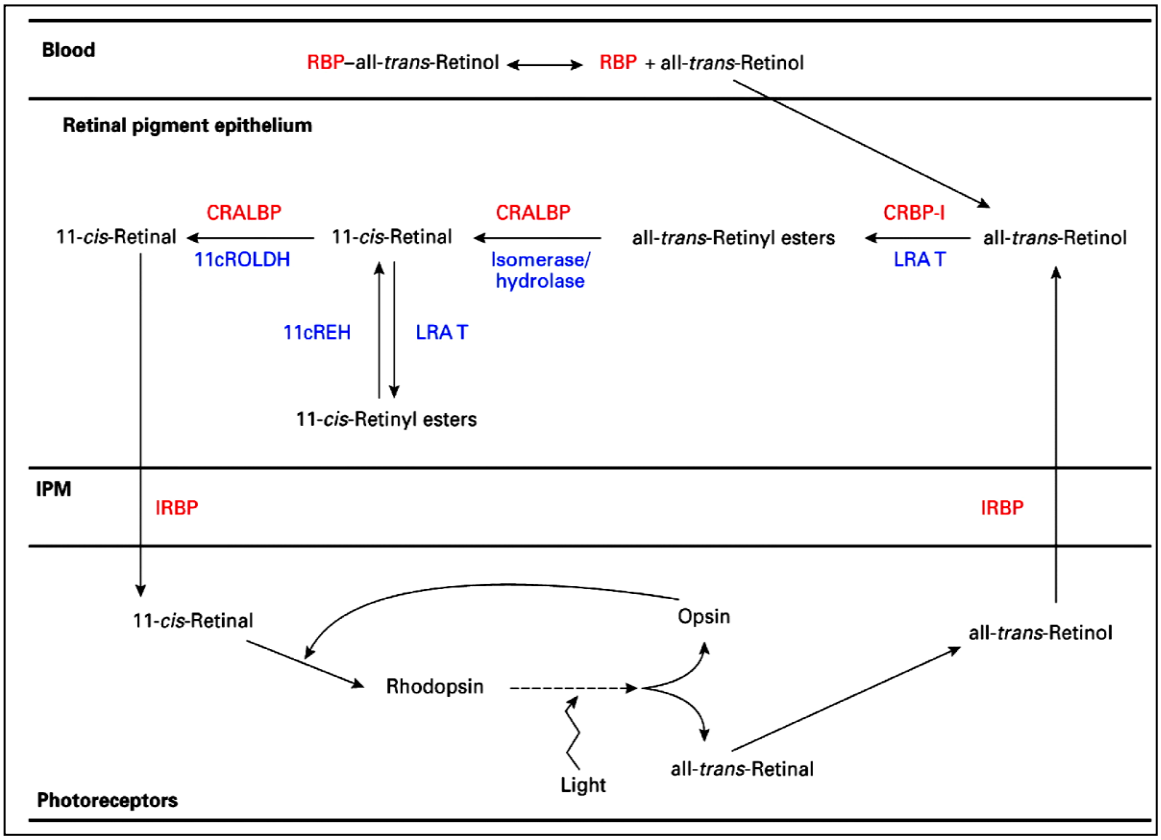

Adapted from Noy et al., 2000

Figure 1.11 shows all-*trans*-Retinol enters the eye from blood via retinal pigment epithelium cells, where it is esterified to all-*trans*-retinyl esters by LRAT (lecithin:retinol acyltransferase) leads to the formation of 11-*cis*-retinol. 11-*cis*-Retinol may either be esterified to form 11-*cis*-retinyl esters and stored, or oxidized by 11-*cis*-retinol dehydrogenase (11cROLDH) to the visual chromophore 11-*cis*-retinal. 11-*cis*-Retinal exits the pigment epithelium, and moves across the IPM (interphotoreceptor matrix) to photoreceptor cells, where it binds to opsin to form the visual pigment rhodopsin. Light absorption by rhodopsin results in isomerization of rhodopsin-bound 11-*cis*-retinal, initiating visual signalling. all-*trans*-Retinal thus formed is enzymically reduced to all-*trans*-retinol. all-*trans*-Retinol is then transported back to retinal pigment epithelium for re-isomerization and re-oxidation.

Abbreviations : CRALBP, cellular retinal-binding protein; CRBP, cellular retinol-binding protein; IRBP, interphotoreceptor retinoid-binding protein;

1.1.15 Interphotoreceptor matrix and retinal adhesion

Enzymes are synthesized for a wide range of functions including membrane transport (calcium pump, sodium-potassium pump), visual pigment metabolism (retinal binding protein, retinal ester hydrolase, isomero hydrolase-catalyses the combined isomerization and hydrolysis of all-trans retinyl ester), waste product digestion, and the elaboration of humoral and growth factors that help to respond to and/or regulate the environment of the RPE and the photoreceptors. RPE also contributes to the formation and maintenance of Interphotoreceptor matrix (IPM), which is critical for retinal adhesion.

1.1.16 Growth factors and cytokines:

RPE are known to secrete a wide variety of growth factors and cytokines under physiological and pathological conditions. While many studies have been performed delineating the regulation and effect of these factors on cultured cells in disease states, little is known about their role in the resting RPE monolayer. Secreted cytokines and growth factors in the monolayer may act in an autocrine or paracrine fashion on the cell of origin or adjacent RPE, or they may have paracrine effects on adjacent photoreceptors or choroidal cells. Chemokines and inflammatory cytokines are secreted in significant amounts only after RPE activation. *In situ* studies of the RPE monolayer reveal expression of TGF-β2, bFGF, aFGF, FGF-5, HGF and PEDF (Jin et al., 2005) and PDGF-A as well as their corresponding receptors. Local production of TGF β by the RPE monolayer could have multiple effects including maintenance of an anti inflammatory state, inhibition of cellular proliferation and stimulation of phagocytosis. FGFs typically enhance RPE cell proliferation and migration, but in the monolayer, bFGF may be acting as a survival promoting factor for RPE cells. It has been suggested that the RPE may secrete low levels of angiogenic substances in the resting state to maintain the choroidal vasculature. Vascular endothelial growth factor (VEGF) and its receptors are expressed by RPE; however, expression of VEGF in the resting monolayer appears to be very low.

Figure 1.12: Overall function of RPE in vision

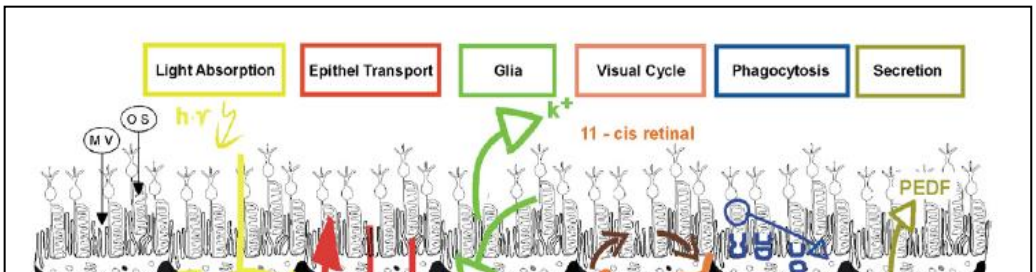

(Adapted from Wimmers S *et al* 2007)

1.2 EXTRA CELLULAR MATRIX (ECM)

In the eye the extra cellular matrix play a role in retinal adhesion and prevention of subretinal choroidal neovascular membrane formation. As the RPE resides in-between the retina and the choroid its role in the production of extra cellular matrix may have relevance in these processes. The ECM is a relatively stable substrate for cells and determines the tissue architecture and is so called the ground substance.The ECM is vital for cell's growth and development (Ramirez F et al., 2003) serving as a reservoir for growth factors (Aumailley et al., 1998).

1.2.1 Functions of extra cellular matrix

1. It holds the cells in the matrix together.
2. Provides a porous pathway for the diffusion of oxygen and nutrients to individual cells.
3. It provides a supporting scaffold for the cells.
4. It also has roles in several cellular functions differentiation, proliferation, adhesion and chemotaxis.

1.2.2 Composition of extra cellular matrix

Extra cellular matrix is composed mainly of three major classes of heterogenous molecules:

1. Structural proteins: Gives structural support to the ECM. (Collagen and Elastin)
2. Specialized proteins: Have specific functions. (fibronectin ,laminin, fibrillin and adhesion molecules) they are further classified into 3 major groups like
    1. Selectins
    2. Immunoglobulin superfamilies
    3. Integrins
3. Proteoglycans: Long chains of repeating disacchride units (GAGs) attached to a protein core.

Collagen

Collagens are most abundant proteins that makes 50% of the body protein. There are 16 types of collagen, they are predominantly synthesized by fibroblasts.

Collagens are long, helical, stiff structures. Collagens have 3 polypeptide chains two α1 (I) chains and one α2 (I) chains. Each chain has 1050 amino acids per turn, every third amino acid is glycine and the collagens are rich in proline and hydroxy proline residues. Collagen residues contribute to the structural stabilization of extra cellular matrices such as the Bruch's membrane.

Elastins

Elastins present in tissues which require the ability to deform repetitively and reversibly. Elastins are present in the core of the elastic fibres surrounded by thin beaded filaments-micro fibrils. Both collagens and elastins are synthesized as soluble monomers and are crosslinked to insoluble fibres by the activity of the enzyme lysyl oxidase (LOX) which catalyses the cross linking of these matrix macromolecules.

Fibronectin

It is an adhesive protein dimer with two large polypeptides that are joined by a pair of disulphide bonds. Contains three types of repeating motifs which are organised into seven functional domains. Functions of these domains include binding heparin, collagen, fibrin, DNA and cell surfaces. Has RGD sequence (Arg-Gly-Asp) that binds to the receptor (Ruoslahti et al., 1997).

Selectins

It is a type of adhesion molecule. Adhesion by selectins is rolling and not firm. Firm adhesion by the selectins is mediated by adhesion molecules such as LFA/ICAM 1, VLA-4/VCAM-1.It slows intravascular leukocyte transendothelial migration. E-selectin is involved in the initial PMN adhesion to endothelial cells. Selectins are also involved in angiotensin induced vascular inflammatory response.

Integrins

Integrins are transmembrane adhesion molecule which is a family-16α and 8βchains. It is activated by conformational changes in the β subunit. Its binding is influenced by divalent cations, extracellular ligands such as ICAM, fibronectin, laminin and intracellular ligands such as talin, α-actin. (Ruoslahti et al., 1997).

Cadherins

This is another widespread adhesion molecule. There are 5 different types of cadherins- N, P, R, B, E. Cadherin R is expressed in the retina**.**

Proteoglycans (PGs)

These are complex of GAGs and protein core. There are atleast 7 GAGs-which are unbranched polysacchrides made of repeating disacchrides, one component is a uronic acid (glucuronic acid or iduronic acid) and other is an amino sugar (N-acetyl glucosamine or N-acetyl galactosamine), all GAGs are sulfated giving a negative charge except hyaluronic acid. There are 2 types of PGs-1 and PGs- 2. ECM proteoglycans have different protein cores, number, length and composition of the GAG attached to each protein core. (Inatani et al., 1999)

1.2.3 Extracellular Matrix and Retinal Pigment Epithelium

RPE besement membrane has collagen types I, II, III ,IV, fibronectin, laminin (Campochiaro et al., 1986). Laminin mediates cellular adhesion with type IV collagen, and fibronectin mediates adhesion to proteoglycan components of the basement membrane. Thus these molecules mediate firm adhesion between RPE and basal lamina. RPE is involved in the synthesis of Bruch's membrane (BM) is evident from the fact that it develops from the basal lamina of the RPE extending outward one layer at a time. RPE produces many components of the Bruch's membrane's layers thus involved in its maintenance and turnover. This makes a physical barrier against the sub retinal neovascularization

Traditionally, BM is regarded as a pentalaminar structure comprising the choriocapillaris basement membrane on the outer surface of the BM, two collagenous zones divided by an elastic layer, and the RPE basement membrane on the upper surface of the BM. However, many epithelial basement membrane interfaces are characterised by hemidesmosomes within the basal aspects of the epithelia, the normal RPE is thought to lack this type of junction. The composition of BM appears to alter with age, but at any time of life the membrane contains a variety of components like proteoglycans, heparin and

chondroitin sulphate, collagens (types I and III to VI collagen) and glycoproteins (laminin and fibronectin) (Campochiaro et al., 1986; Marshall et al., 1993)However, the distribution of the individual components varies between layers of the membrane. The type I, III and V collagen are found chiefly in the inner and outer collagenous zones (Marshall et al., 1993).

The electron microscopic studies found that the immunoreactivity for type IV collagen in the RPE basement membrane is less than that of the chorcapillaris basement membrane. Although it has been suggested that this difference may reflect variation in the availability of antigenic sites between the two basement membranes, a similar labelling pattern has been observed for laminin (Marshall et al., 1992). The presence of laminin in potential adhesion plaques in the inner part of BM is consistent with the expression of cell surface receptors known as β1 integrins for which laminin isoforms are ligands on normal RPE (Matsumoto et al., 1990; Chu and Grunwald et al., 1991). Since integrins (heterodimeric receptors composed of an a and a b subunit) are major cell surface receptors which mediate adhesion interactions between b1 integrins on the RPE basal aspect and matrix components such as laminin and type IV collagen in BM play an important role in RPE adhesion to the membrane. Consistent with this theory, recent *in vitro* studies demonstrate that blocking b1 integrins with appropriate antibodies reduces the RPE attachment rate to BM. Plaque-like adhesions would not only provide attachment for RPE to BM but also could permit indirect contact between RPE and components deeper in BM (e.g., in the inner collagenous zone). These components would in turn be in a position to signal to the cells. Recent studies suggests that the integrity of BM regulates production of proteolytic enzymes and their inhibitors (Padgett et al., 1997). Although much of the proteolytic enzymes produced by RPE *in situ* probably are apically secreted toward the interphotoreceptor matrix which occupies the subretinal space between the photoreceptors and is composed of large glycoproteins and proteoglycans, it is possible that such enzymes also would allow the cells to modify their underlying matrix after synthesis and deposition.

Thus the extracellular matrix is a dynamic element with a marked influence on cell proliferation, migration, differenatitaion, attachment and remodeling. Continuous maintenance of this tissue architecture is controlled largely through

the coordinated activities enzymes such as lysyl oxidase (LOX) which crosslink collagen and elastin and matrix cleaving enzyme known as the matrix metalloproteinases (MMPs).

1.3 LYSYL OXIDASE

1.3.1 Enzyme classification of Lysyl oxidase:

Lysyl oxidase, is a copper-dependent amine oxidase that initiates the covalent cross-linking of Collagens and Elastin in extracellular matrix. The ezyme classification number is EC1.4.3.13 It belongs to the oxidoreductases class of enzymes called amine oxidases (AO). AO are divided into two groups (Figure 1.13) based on the chemical nature of the attached cofactor as

1. Flavin adenine dinucleotide (FAD) containing enzymes which includes the monoamine oxidase A (MAO-A) and monoamine oxdiase B (MAO-B) and poly amine oxidase.
2. Topo-quninone carbonyl group cofactor containing enzymes which include diamine oxidase (DAO), lysyl oxidase, plasma membrane and soluble monoamine oxidase. These enzymes are collectively called the semicarbazide sensitive amine oxidase (SSAO) due to the characteristic inhibition of the carbonyl reactive compound by semicarbazide.

The SSAO belong to a special class of ectoenzymes recognized as cell surface proteins. These molecules have the capacity to catalyse enzymatic reaction in the immediate vicinity of the cell surface or extracellularly thereby regulating the concentration and functions of the substrates and products (Jalkanen et al., 2001).

Figure 1.13: Classification of amine oxidase:

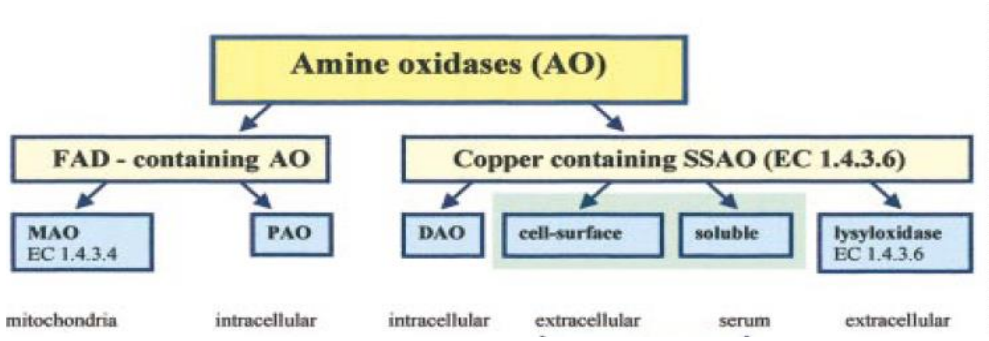

Adopted from Jalkanen et al., 2001

Lysyl oxidase belongs to SSAO that oxidizes primary amine substrates to reactive aldehydes. This enzyme is unique among the mammalian copper amine oxidases which catalyzes a critical post- translational modification essential for biogenesis of connective tissue matrices. LOX catalyses the final step of collagen and elastin cross linking by oxidative deamination of the ε - amino group of hydroxylysine and lysine residues to peptidyl α-amino adipic-δ-semialdehyde (Smith-Mungo et al., 1998). These resultant products undergo spontaneous condensations with unreacted ε-amino groups of neighbouring lysine residues or with other peptidyl aldehyde residues to generate covalent cross links required for the biosynthesis of mature functional extra cellular matrices. (Figure 1.14) The metabolism of this enzyme is as complex as the metabolism of its principle substrates, collagen and elastin.

Figure 1.14: Lysyl oxidase catalyzes the oxidative deamination of specific lysyl residues in tropocollagen and tropoelastin

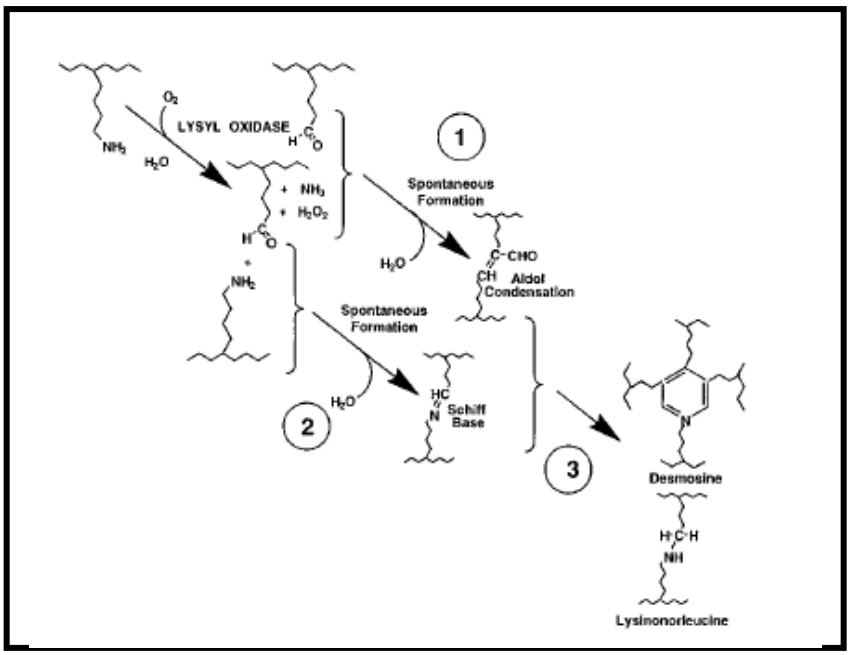

Adapted from Reiser et al., 1992

1.3.2 The Lysyl oxidase protein family

Lysyl oxidases form an enzyme family with diverse N-terminal and conserved C terminal. LOX is the first identified member of this enzyme family. Additional to LOX, four novel closely related LOX-like proteins were identified in mammals in the past decade i.e. LOXL (Kim et al., 1995), LOXL2 (Jourdan-Le et al., 1999), LOXL3 (Huang et al., 2001) and LOXL4 (Maki et al, 2001, Molnar etal.,2003). Although the LOX family members share high homology, each of the genes are located on a different chromosome: according to the human genome data at Ensembl (http://www.ensembl.org).

The C-terminal region is highly conserved in all members of the LOX enzyme family. It includes the copper-binding sites, cytokine receptor-like (CRL) domains, and lysine tyrosylquinone (LTQ) co-factor sites formed by a covalent bond between lysine 314 (K314) and tyrosine 349 (Y349) (Csiszar., 2001). The copper in LOX appears to be involved in the transfer of an electron to and from oxygen to facilitate the oxidative deamination of peptidyl lysyl substrates, and the LTQ also internally catalyzes the quinone co-factor formation (Rucker et al.,

1998). LOX contains one copper (II) cofactor per mole of the 32-kDa active enzyme. Once freed of copper, the resulting inactive apoenzyme was fully reactivated by reconstitution with copper (II) but not by divalent Ni, Cd, Zn, Co, Fe, Hg, Mg or Cd. The copper cofactor is bound in a tetragonally distorted, octahedrally coordinated ligand field (Gacheru et al., 1988; Gacheru et al., 1990). Four histidines that contribute to the formation of this field (Krebs et al., 1993) are embedded within a larger, similarly conserved domain, WEWHSCHQHYH. A database search for homology to conserved copper- binding domains revealed that this sequence element is unique to lysyl oxidase (Kosonen et al., 1997). Other copper-binding proteins have distinctly different binding domains for copper. In the other copper-containing amine oxidases, such as Diamine oxidase (DAO) and Semicarbazide sensitive amine oxidase (SSAO), the carbonyl cofactor is a peptidyl trihydroxyphenylalanine quinone. In LOX carbonyl prosthetic group is a lysyl-tyrosylquinone cofactor (Figure 1.15), unique to this group of amine oxidases, that is formed from the autocatalytic hydroxylation and oxidation of peptidyl lysyl and tyrosine residues requiring copper (Matsuzaki et al., 1998). N-terminal regions of LOX-like proteins are more variable than that of LOX. LOXL contains a proline-rich region; LOXL2, LOXL3 and LOXL4 each contain four scavenger receptor cysteine-rich (SRCR) domains at their N-terminal ends (Figure 1.16).

Figure 1.15 : Structure of the carbonyl cofactor of LOX

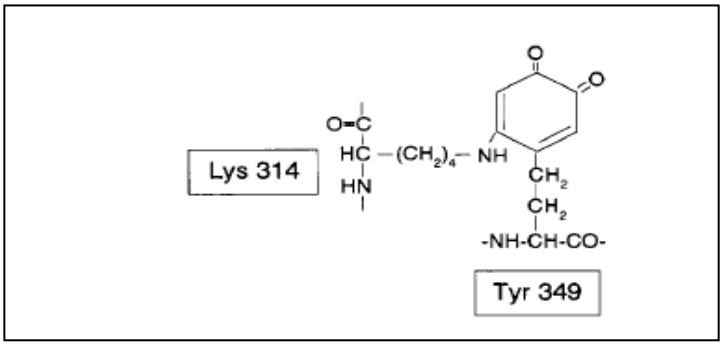

Adapted from kagan et al., 1986

Figure 1.16: The lysyl oxidase family and the domain structure of the LOX proteins.

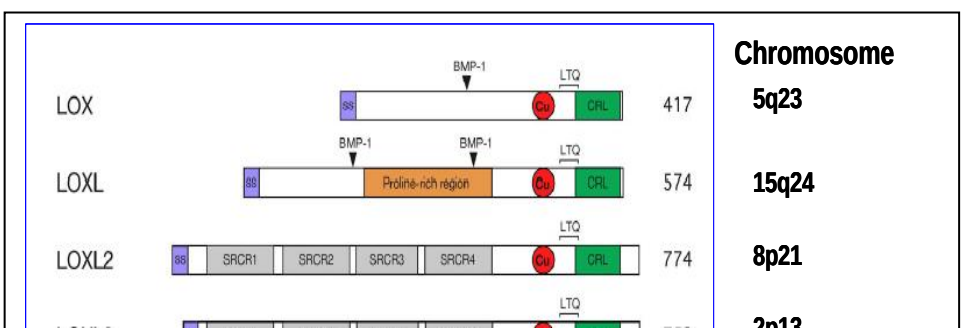

Adapted from Csizar et al., 2001

The Figure 1.16 shows predicted signal peptides represented as SS. Four scavenger receptor cysteine-rich regions (SRCR) in LOXL2, LOXL3, and LOXL4, the propeptide region in LOX, and the proline-rich region in LOXL are indicated. The highly conserved sites of the putative copper-binding region (Cu), the cytokine receptor-like domain (CRL domain) and the lysyl and tyrosyl residues forming the unique LTQ cofactor are shown. Predicted proteolytic processing sites by BMP-1 activity are indicated by arrows. The number of amino acids in each protein is found on the right and the gene location on the left.

Lysyl oxidase activity has been demonstrated for LOXL (Borel et al., 2001), LOXL2 (Vadasz et al., 2005), and LOXL4 (Ito et al., 2001), though their individual functions still have to be elucidated. The substrate or tissue specificity and biological function may vary among these family members and emerging evidence supports this possibility. The human LOX gene is located on chromosome 5q23.3-12 and encodes a 417 amino acid polypeptide, of which the first 21 residues correspond to the signal peptide. The mouse LOX gene has been mapped to chromosome 18 (Mock et al., 1992).

1.3.3 Processing of prolysyl oxidase to lysyl oxidase :

Lysyl oxidase messenger RNA is translated to produce prolysyl oxidase which gets glycosylated in the Golgi complex and is vectorally transported into vesicles for its eventual secretion. (Figure 1.17) It is synthesized as a 46 kDa preproenzyme which undergoes signal peptide cleavage and N-glycosylation to yield a 50 kDa proenzyme. At the cell surface, the prolysyl oxidase is cleaved to 32 kDa lysyl oxidase by EDTA-inhibitable metalloproteinase secreted by these cells (Trackman et al., 1992) which is important for the processing of the secreted

form of lysyl oxidase. This metalloproteinase is localized on the cell surface and appears to be the same proteinase that cleaves the c-terminal propeptide from type I-procollagen (Cronshaw et al., 1995; Panchenko et al., 1996; Trackman et al., 1992). A likely site of cleavage was first indicated by Cronshaw et al, who determined the N-terminal sequence of the mature enzyme isolated from pig aorta as between Gly-168 and Asp-169 of the precursor protein, numbered according to the human LOX sequence. Cleavage of the propeptides from procollagen by the procollagen N- and C-proteinases must precede assembly of collagen molecules into quarter-staggered fibrils, which is the form of collagen required for oxidation by LOX (Siegel et al., 1974). Thus the procollagen C-proteinase may play a dual role in collagen crosslinking by generating the LOX-susceptible collagen substrate and by converting latent proLOX to the fully functional catalyst. Copper is added at a processing step in the trans-Golgi complex. There is a relation between lysyl oxidase activity and dietary copper intake (Kosonen et al., 1997). Increase in the copper concentration in secretory vesicles are hypothesized to be important to quinine cofactor formation.

Figure 1.17: Processing of Lysyl oxidase

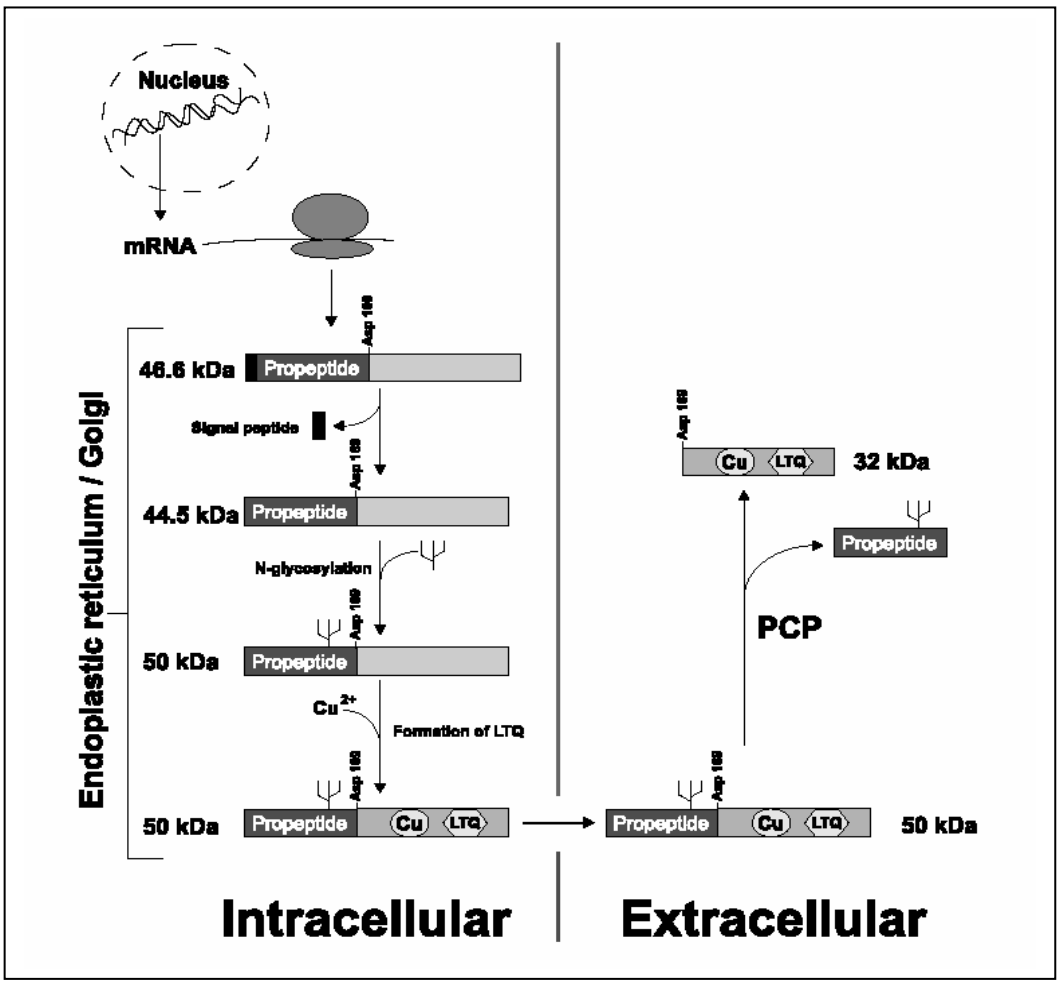

Adapted from Trackman 1990 & 1991

1.3.4 Substrate Specificity

Lysyl oxidase has the highest affinity for collagens (precipitated in the form of fibrils) and coacervated forms of elastin in the ECM. LOX oxidatively deaminates specific peptidyl lysine and hydroxylysine residues of collagen and lysine in elastin in the presence of molecular oxygen (Figure.1.18). LOX can also oxidize non-ECM, lysine-rich proteins such as histone-H1(Giampuzzi et al., 2003) as well as various lysine-rich synthetic peptides including basic fibroblast growth factor (bFGF) (Li et al., 2003).

The sequences surrounding the substrate lysine residues within elastin and collagen differ dramatically, as do their primary and three-dimensional structures, suggesting that the specificity of LOX may be flexible. Purified LOX from bovine enzyme oxidizes peptidyl lysine in a variety of basic, globular proteins,

including histone H1, although not in proteins with isoelectric points below pH 8 (Kagan et al., 1984). In view of its apparent preference for a net cationic charge in protein substrates in assays *in vitro*, it is of some interest that the oxidized lysine residues in the telopeptidyl regions of types I, II and III collagens occur within -X-GIu-Lys-Y- sequences, while that in the N-telopeptide of the type I α1 (I) collagen chain occurs in the -Tyr-Asp-Glu-Lys-Ser- sequence, thus vicinal to two sites of negative charge.

Figure 1.18: Catalytic activity of LOX

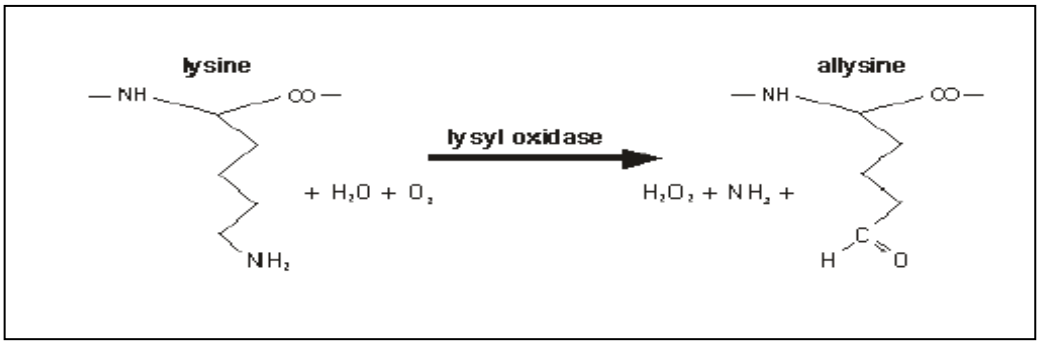

(Adapted from Kagan et al., 1986)

1.3.5 Mechanism of Action

LOX catalyses primary amine oxidation through a ping pong bi ter kinetic mechanism (Williamson et al., 1986). The first step in this reaction is the formation of a Schiff base with the lysine tyrosylquinone (LTQ) cofactor (I → II). While the LTQ is bound to the substrate, it undergoes a rate-limiting, general base-facilitated α proton abstraction . A histidine residue has been suggested to act as the general base in LOX. In the following reaction, stereospecific abstraction of the pro-S α-proton (Shah et al., 1993), takes place and the electrons migrating from the substrate carbanion reduce the LTQ cofactor (II → III). Hydrolysis of the imine intermediate releases the reactive aldehyde product, which can then react spontaneously to form lysine- or hydroxylysine derived cross-links. After the release of the aldehyde product, the reduced enzyme is reoxidized by molecular oxygen with the aid of Cu (II) to produce hydrogen peroxide and ammonia. By this way, the oxidized enzyme is regenerated and the catalytic cycle is completed

(IV → V → I) (Figure 1.19). The overall reaction is: Peptidyl-L-lysyl-peptide + O_2 + H_2O = peptidyl-allysyl-peptide + NH_3 + H_2O_2

Figure 1.19: Mechanism of action of Lysyl oxidase

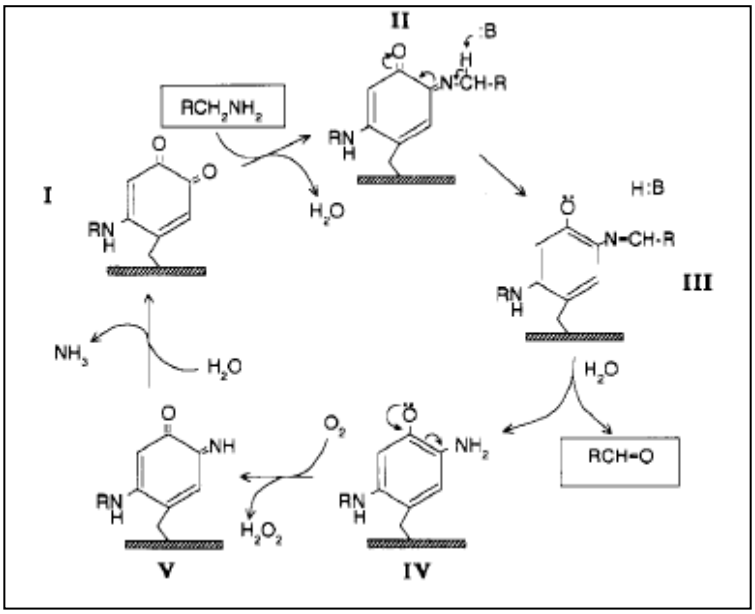

Adapted from Smith, Kagan et al., 1998

1.3.6 The catalytic activity of lysyl oxidase:

LOX oxidatively deaminates a peptidyl lysine to generate a peptidyl allysine. The reactive aldehyde of the allysine is then spontaneously able to react with another peptidyl lysine or allysine to form a covalent cross-link between proteins (Figure 1.18). The resulting peptidyl aldehydes condense spontaneously to form various bi-, tri-, and tetra functional, intra- and inter-molecular cross-links. In collagens, the lysine and hydroxylysine-derived cross-links are essential in providing the tensile strength and mechanical stability of the collagen fibrils and other supramolecular assemblies (Bailey et al., 2001). As a byproduct of the catalytic reaction, reactive aldehydes and hydrogen peroxide are generated by LOX that may contribute to some of the novel roles of LOX observed in wound healing, cell migration, motility, proliferation and differentiation (Palamakumbura et al., 2004)

1.3.7 Factors influencing lysyl oxidase activity:

Expression of the LOX mRNA, immunodetection and activity of the LOX protein have been described in various tissues in normal and pathologic processes including development, aging, wound healing, remodeling of the extracellular matrix, copper deficiency, inflammation, fibrotic disorders, tumorigenesis, and invasion. The results of these studies uncovered a series of complex transcriptional and posttranscriptional mechanisms that coordinately regulate the expression and activity of LOX. Very little is known about the tissue- and cell-specific and temporal mechanisms that regulate expression of the LOXL, LOXL2, and LOXL3 genes.

The factors that were reported to contribute to the regulation of LOX gene expression, both in normal physiologic states and in several disorders, include tissue-specific transcription factors, metal ions (Li et al., 1995), cytokines and growth factors including FGF-2, 1GF-1 (Trackman et al., 1998), and TGF-beta (Hong et al., 1999; Shibanuma et al., 1993) as given in table 1.2, hormones such as testosterone (Bronson et al., 1987), prostaglandin (Choung et al., 1998), and progestin (Langenau et al., 1999), and signaling molecules such as ras (Csiszar et al., 1996; Hajnal et al., 1993; Krzyzosiak et al., 1992), cAMP (Ravid et al., 1999), and interferon regulatory factor IRF-1 (Tan et al., 1996). Environmental conditions associated with fibrotic responses such as ozone, aerosolized cadmium result in increased lysyl oxidase activity (Kagan et al., 1994) . Reduced food intake and refeeding also can alter lysyl oxidase activity (Rucker et al., 1996). The effects and mechanism of action of these regulators have been described in diverse normal and transformed cells including lung fibroblasts (Boak et al., 1994), embryonic lung fibroblasts (Bronson et al., 1987), calf and rat aortic smooth muscle cells (Bronson et al., 1987; Contente et al., 1993), gingivial fibroblasts (Hong et al., 1999), perch ovary (Langenau et al., 1999), mesenchymal cells (Trackman et al., 1998), and osteoblastic (Pischon et al., 2004) and osteosarcoma cells (Csiszar et al., 1996).

Table 1.2: Overall view of the effect of different growth factors and cytokines on LOX expression

S.No	Growth factor studied	Cells / Tissue	Effect
1	Tumor necrosis factor α	Human umbilical vein endothelial cells (HUVEC), porcine aortic endothelial cells (PAEC) bovine aortic endothelial cells (BAEC) Osteoblast cultures	Downregulation of mRNA at low concentrations (0.1–1 ng/mL) and was maximal at 2.5 ng/mL (Rodriguez et al., 2008a) Downregulation of LOX expression and activity (Pischon et al., 2004).
2	Interleukin (IL)-1beta Interleukin-6 platelet-derived growth factor (PDGF)-BB Basic fibroblast growth factor (bFGF or FGF-2)	Human gingival fibroblast.	IL-1, IL-6, and PDGF-BB did not significantly regulate lysyl oxidase enzyme activity, 1 nM bFGF reduced lysyl oxidase and collagen mRNA (Hong et al , 2002)
3	Fibroblast growth factor	Mouse osteoblatic cells	Decreased mRNA (1-10nM) Upregulation of mRNA (0.01-0.1nM) (Feres-Filho et al., 1996)
4	Intefreon γ	Rat aortic smooth muscle cells	Downregulation of mRNA (Song et al., 2000)
5	Transforming growth factor β	Rat lung fibroblast cultures Vascular smooth muscle cells Human gingival fibroblasts	2.5-fold increases mRNA expression in fibroblasts cultures (Koslowski et al., 2003) Increased mRNA levels and enzymatic activity (Shanley et al., 1997) Increased mRNA levels and enzymatic activity (Hong et al., 1999)
6	Platelet derived growth factor	Rat vascular smooth muscle cells	Upregulation of mRNA (Koslowski et al., 2003)
7	Connective tissue growth factor	Human gingival fibroblasts	Stimulates production of lysyl oxidase enzyme activity up to 1.5-fold after 48 hours (Hong et al., 1999)

1.3.8 Inhibitors of lysyl oxidase catalytic activity:

Administration of the specific LOX inhibitor β-aminopropionitrile (BAPN) to growing animals results in a disease known as lathyrism. Lathyrism is a pathological condition known to cause increased fragility of connective tissues

and elevated solubility of collagen from tissues due to diminished cross-linking. It is known that chronic ingestion of the sweet pea (Lathyrys odoratus) results in lathyrism (Geiger et al., 1976), directly caused by the agent β-(γ-glutamyl)-aminopropionitrile present in the seed, which *in vivo* metabolized to BAPN (Gross et al., 1960). Therefore, the ability of BAPN to inhibit cross-link formation was recognized even before identification of lysyl oxidase activity *in vitro*. BAPN was found to bind covalently to the active site, as an irreversible LOX inhibitor with an inhibitory constant (Ki) of about 3 – 5 μM (Tang et al., 1983). Since then, BAPN has been used experimentally to specifically inhibit activities of all lysyl oxidase isoenzymes. At low concentrations, (10^{-4}– 10^{-6} M), it has higher affinity to bind to lysyl oxidases than to other, non-LOX amine oxidases.

Based on similarity in chemical structure, other potent LOX inhibitors are also found. Irreversible inhibitors like β-haloethylamines and β-nitroethylamine which target the active site of LOX, with inhibition constants similar to that of BAPN. Vicinal diamines like cis-1, 2- diaminocyclohexane and ethylenediamine are also potent irreversible LOX inhibitors (Gacheru et al., 1989). LOX is also inhibited by heparin (Gavriel et al., 1988), N- (5-aminopentyl) aziridine, trans-2 phenylcyclopropylamine (Nagan et al., 1998), semicarbazides, and some alkylation agents (Gavriel et al., 1988). LOX can also be inhibited by homocysteine thiolactone and its selenium and oxygen analogs in an active-site-directed and irreversible manner (Liu et al., 1997).

1.3.9 Lysyl oxidase and Metal Ion Metabolism:

Severe copper deficiency results in decreased crosslinking of connective tissue proteins, consistent with decreased function of LOX. While enzyme activity levels were decreased in the skin of weanling rats fed with a copper deficient diet, the basal, steady-state levels of LOX specific mRNA or immunodetectable LOX protein were not significantly reduced. These results suggest both that the biosynthesis of the enzyme is not markedly affected by copper deficient diets and that the increasing percentage of copper-deficient, catalytically compromised enzyme molecules which accumulate during this dietary treatment remain relatively stable. Notably, copper-deficient diets significantly reduced cardiac

LOX activity and induced cardiac pathology in male but not in female rats (Rucker et al., 1996). LOX expression, assessed at the mRNA, protein and activity levels, was markedly repressed in a population of cadmium resistant fibroblasts, compared to the cadmium-sensitive, parental population. The resistant phenotype exhibited markedly elevated levels of metallothionein and glutathione, each of which has the potential to scavenge copper.

1.3.10 Lysyl oxidase in Human Disease

Skin pathology :

Age-associated decrease in LOX mRNA was detected in rats using tail tip skin in neonatal (1.5 weeks), adult (6 months), and elderly (24 months) animals using RT-PCR. In spite of the general increase of ECM cross-linking, fewer LOX-derived crosslinks were found per collagen molecule in very old animals. LOX derived crosslinks, in addition to stabilizing ECM fibrils, appeared to protect certain lysine groups from other types of random and irreversible interactions, such as non-enzymatic glycosylation, that are known to be associated with aging and lead to loss of orderly structure and morphological changes characteristic for aging tissues. (Reiser et al., 1987).Increased amount of LOX immunoreactivity was detected in sclerodermatous skin in patients with a localized and diffuse type of systemic scleroderma compared to normal skin (Chanoki et al., 1995)

Lung fibrosis:

Lung fibrosis is a multi step process that involves both collagen accumulation and changes in the LOX that modulate the biomechanical properties of fibrils. (Tzortzaki et al., 2003) The mRNA for LOX showed a delayed increase in the lungs after bleomycin administration supporting the hypothesis that LOX modulation is evident in fibrosis of lungs.

Alzheimers disease:

Abundance of extracellular senile plaques associated with activated microglia and astrocytes in cortical and limbic brain regions are implicated in Alzheimer's disease (AD) etiology (Hardy et al., 2002). Recently, active extracellular LOX molecules, which are normally low in the rat brain and are present mainly in blood vessel walls and choroid plexus. They accumulate in a spatiotemporal

fashion within the lesion site early after brain injury (Gilad et al., 2001). This suggests that LOX is secreted by cells attracted to brain injury sites where it participates in ECM modulation.

Cutis laxa:

Cutis laxa has both autosomal dominant and recessive patterns of inheritance and is characterized by hyperextensible skin and a marked deficiency of skin elastic fibers. Deficient LOX expression has been noted in affected human skin fibroblasts derived from X-linked cases of cutis laxa which also exhibit abnormalities of copper metabolism.

1.3.11 Lysyl oxidase in diseases with defective copper metabolism:

Type IX Ehlers Danlos syndrome:

Type IX of the Ehlers-Danlos syndrome (E-D IX) is a X-linked recessively inherited disorders characterized by abnormalities in copper metabolism. These abnormalities are associated with a severe reduction in the activity of lysyl oxidase (Kuivaniemi et al.,1985 a).

Hepatic fibrosis – Wilson's disease:

Wilson's disease or hepatolenticular degeneration is an autosomal recessive genetic disorder in which copper accumulates in tissues; this manifests as neurological or psychiatric symptoms and liver disease**.** Upregulation of LOX and LOXL2 in hepatocytes of Wilson's disease and primary biliary cirrhosis (PBC) patients contribute to liver damage. The upregulation of LOX and LOXL2 in Wilson's disease could perhaps be utilized for diagnostic purposes since their expression is up-regulated in hepatocytes even before the onset of fibrosis. (Vadasz et al.,2005)

Menkes disease:

Menkes disease is an X-linked, recessively inherited disorder characterized in part by abnormal copper transport, cellular copper sequestration, and defective crosslinking of collagen and elastin. This disease appears attributable to a mutation in the gene coding for a copper transporting ATPase (Vulpe et al., 1993).

1.3.12 Lysyl oxidase in ocular diseases:

Until July 2007 there were no reports on the enzyme LOX in ocular tissues, The fisrt report was from Urban et al who found that there was a reduced number of cross-linking domains in elastin and decreased lysyl oxidase-like 2 expression leading to decreased amount of mature elastin in optic nerve heads from healthy African american individuals compared with Caucassian american donors (Urban et al.,2007). These results suggest that Elastin (ELN) and LOXL2 as candidate susceptibility genes for population specific genetic risk of primary open-angle glaucoma (POAG).

Later a genome wide association study done on Icelandic patients identified three SNPs on chromosome 15q24.1 to be significantly associated with pseduexfoliative glaucoma (PXF). The three SNPs; allele T of rs2165241, allele G of rs1048661 (R141L), allele G of rs3825942 (G135D) were in the first intron and exon one of the LOXL1 gene. This association was further confirmed in Swedish population (Hewitt et al., 2007).The pathological process of PXF is characterized by chronic accumulation of abnormal fibrillar material in the anterior segment of the eye, leading to numerous clinical complications apart from secondary glaucoma development. Thus, though the exact role of LOXL1 in the PXF is not known it could possibly contribute to the pathogenesis due to accumulation of abnormal elastin microfibrillar components. Further to these studies till date around 20 publications have been done on LOXL1 gene association with PXF. Another study by Yu et al has reported a defective elastin fibre that has been associated with increased susceptibility to laser induced choroidal neovascularization (Yu et al., 2008) in LOXL1 knockout mouse model. Thus the importance of LOX in ocular diseases is being explored recently.

1.3.13 Intracellular lysyl oxidase: In cultured fibroblasts granular LOX immunostaining was detected in the perinuclear area, which was considered to be the prepro-LOX in the ER. Strong LOX immunostaining was also found along filamentous structures in the cytoplasm of fibroblasts and cultured epithelial cell lines that prompted LOX association with cytoskeletal proteins. The processed, 32 kDa LOX was detected in the nuclei of embryonic mouse NIH3T3 fibroblasts and within the nuclei of rat vascular smooth muscle cells and LOX-related amine

oxidase activity had been detected in the nuclei of these cells (Li et al., 1997). LOX-dependent alterations in chromatin structure was seen, that may lead to the loss of positive charge in a nuclear substrate, a process analogous to acetylation of lysine residues in histones by histone deacetylase that results in changes in transcriptional rate (Wolffe et al., 1996). Although LOX is detected in the nuclei of some liver and kidney cells, the *in vivo* role of the nuclear LOX remains unclear.

1.3.14 Role of lysyl oxidase in Extracellular matrix assembly:

Lysyl oxidase play structural or other novel regulatory roles in extracellular matrix (ECM) assembly. It has been found that in cell cultures, measurable amounts of lysyl oxidase are released into the media and the expression of lysyl oxidase is most active when proliferation stops or slows, eg, at cell confluency (eg., as much as 50% of the total activity) and in tissues the bulk of the enzyme is tightly bound to its substrates within the ECM. Purification of the enzyme is difficult because of its association with ECM proteins and inactivation due to self-aggregation.

1.3.15 Lysyl oxidase in endothelial dysfunction by Hypercholesterolemia:

Hypercholesterolemia induces endothelial dysfunction, a hallmark of the atherosclerotic process, modulating the expression of key genes in vascular endothelial cells. The effect of high concentrations of native low density lipoprotein (LDL) on endothelial cell gene expression showed that the mRNA levels of lysyl oxidase (LOX), was down regulated by LDL treatment in a dose- and time-dependent manner (80% of inhibition by 180 mg/dL LDL for 24 hours). This reduction of LOX expression was associated with a decrease in LOX activity (40% and 54% of inhibition after 24 and 48 hours of LDL treatment) suggesting that LDL down regulation of LOX could contribute to the endothelial dysfunction caused by hypercholesterolemia, thus contributing to atherosclerotic plaque formation (Rodriguez et al., 2002).

1.3.16 Lysyl oxidase in endothelial dysfunction by Homocysteine:

Hyperhomocysteinemia is associated with extracellular matrix alterations including changes on the elastic properties of the vascular wall. Lysyl oxidase

(LOX) is involved in ECM maturation and play key roles in normal vascular function. Homocysteine, a well-known inducer of endothelial damage, inhibits LOX activity in vascular endothelial cells through a mechanism mediated by reactive oxygen species (ROS). Exposure of aortic endothelial cells to high Hcys concentrations (similar to those reported in severe hyper-homocysteinemia) showed a significant downregulation of LOX mRNA levels through a reduction of LOX promoter activity. LOX inhibition would reduce ECM crosslink yielding immature forms of ECM and increasing elastin and collagen solubility. The lost ECM properties associated with LOX inhibition could be related to an increase of atherosclerotic lesion vulnerability. This hypothesis was supported by a recent finding describing that LOX deficient mice show premature death, multiple aneurysms and severe alterations in vascular wall structure that compromises normal vascular functions (Raposo et al., 2004).

1.3.17 Novel roles of lysyl oxidase:

Role of LOX in retinal pigment epithelium (RPE) proliferation and migration:

Omori et al have reported that the level of lysyl oxidase mRNA in RPE cells appear to increase during cell proliferation and decrease toward differentiation (Omori et al., 2002). The level of the LOX mRNA in RPE cells grown on microporous membranes were most markedly increased by application of hyperosmotic mannitol solution on the apical side. This treatment cause the fluid transport in basal to apical direction and mimic the enhancement of fluid transport across RPE cells in the choroids to vitreous direction *in vivo*, which causes accumulation of subretinal fluid. RPE cells, may express more lysyl oxidase in response to the accumulation of subretinal fluid to enhance the interaction between RPE and its extracellular matrix. Such a response may be an important defense mechanism against cell-liberation from the RPE monolayer into subretinal space, which frequently occurs after detachment of the neural retina. The contribution of lysyl oxidase to cell migration was also observed in human peripheral blood mononuclear cells and vascular smooth muscle cells, in which hyderogen peroxide, the product of amine oxidation by this enzyme was shown to be critical to augment migration. RPE cells, in some instances, migrate onto the surface of the retina and form epiretinal membranes. Epiretinal membrane contraction exerts tractional forces on the underlying retina, causing retinal detachment leading to blindness.

1.3.18 Lysyl oxidase in tumorogenesis: It has been observed that lysyl oxidase activity and collagen synthesis are markedly reduced in malignantly transformed human cell lines. Thus, a link between lysyl oxidase activity, ECM regulation, and tumorigenesis was speculated. Asssessment of LOX expression at the protein and mRNA levels by immtinohistochemistry and in situ hybridization, respectively, in breast carcinoma tissue revealed that maximal expression of LOX and its type I collagen substrate was observed in myofibroblasts and myoepithelial cells around in situ tumors and in the fibrotic deposits facing the invasion front of infiltrating tumors

Studies have previously demonstrated that LOX mRNA is highly upregulated in invasive breast cancer cells compared to poorly invasive cells. It is also shown

that LOX activity facilitates breast cancer cell invasion. Recently, Payne et al., 2005 reported that LOX regulates breast cancer cell motility/migration through changes in cell-matrix adhesion formation. These changes are the result of a hydrogen peroxide mediated mechanism involving the FAK/Src signaling pathway (Payne et al., 2005).

Studies revealed that inhibition of LOX activity in invasive breast cancer cells leads to a corresponding increase in actin stress fiber formation as visualized using a phalloidin stain. LOX activity led to an increase in Rac and Cdc42 activity and a decrease in Rho activity. These changes correspond to a motile phenotype in the presence of LOX activity which is activated by Rac through the p130Cas/Crk/ DOCK180 signaling complex. Thus LOX functions through novel intracellular signaling pathway to regulate cell motility and migration through changes in actin filament formation. Understanding the molecular mechanisms by which LOX functions to regulate breast cancer cell motility/ migration can contribute to novel anti-cancer treatment modalities (Payne et al., 2006).

1.3.19 Assay methods for LOX estimation:

LOX can be detected at the level of mRNA expression and protein. The enzyme can be localized and also its enzyme activity can be detected. There are different methods to measure the specific activity of LOX namely.

1. Tritium release assay
2. Homovallinate coupled peroxidase method
3. Amplex red coupled peroxidase method

Assay of lysyl oxidase activity by the tritium release method :

This is the most sensitive and reliable assay which utilizes tritiated recombinant human tropoelastin substrates expressed in Escherichia coli or tritiated elastin and collagen substrates derived from aorta or calvaria organ cultures as substrates (Bedell-Hogan et al., 1993). These substrates contain [4,5-3H] lysine residues. Oxidative deamination of tritiated lysine residues releases tritium ions that exchange with the aqueous solvent. The resultant tritiated water is distilled under vacuum and quantitated using liquid scintillation system.

The major disadvantage of this methodology is that this assay is discontinuous end-point assay, and the vacuum distillation is laborious and requires dedicated custom-made equipment. But still this is the primary method used to determine lysyl oxidase enzyme activity in cell culture experiments and in other biological samples (Feres-Filho et al., 1996). It has been reported that ultrafiltration using microconcentrators can be used to separate the tritiated water, instead of vacuum distillation. However, unlike distillation, ultrafiltration runs the risk of measuring confounding enzyme activities that produce low-molecular-weight tritiated products unrelated to lysyl oxidase such as catabolic protease activity. In contrast, the vacuum distillation separates only volatile tritiated water more specifically produced by the lysyl oxidase reaction from [4,5-3H] lysine-labeled collagen and elastin substrates, hence producing low background values and more accurate results. But the major advantage of this method is its high sensitivity and specificity.

Flourimetry method :

There are two methods based on fluorimetry.

- Homovallinate coupled peroxidase method
- Amplex red coupled peroxidase method

In these two flourimetric method Lysyl oxidase oxidatively deaminates alkyl monoamines and diamines and the resultant H_2O_2 produced is detected by peroxidase coupled homovallinate or amplex red fluorescence reaction

$$RCH_2NH_2 + O_2 + H_2O \Longrightarrow RCHO + NH_3 + H_2O_2.$$

A Homovallinate coupled peroxidase method. This assay is based on a peroxidase-coupled reaction using sodium homovanillate. In the presence of horseradish peroxidase, hydrogen peroxide oxidizes homovanillate to give a fluorescent product with an excitation maximum at 315 nm and an emission maximum at 425 nm. This method is used to monitor the enzyme activity continuously and is sensitive to about 300 ng of purified lysyl oxidase when performed at 55°C. However, due to the usage of wavelengths in the ultraviolet spectrum, this method cannot be used to detect lysyl oxidase in crude biological

samples, such as cell culture medium or tissue extracts. In addition, the fluorescent product formed is unstable to the high-energy output of some

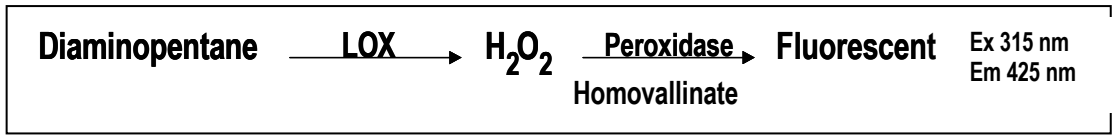

fluorometers that lack the ability to adjust the excitation slit width. This limits the universal utility of this method. The homovanillate-based assay has, however, found great utility in substrate specificity studies and in inhibition and enzyme kinetics studies of highly purified lysyl oxidase (Williamson et al., 1986).

Amplex red coupled peroxidase method: N-Acetyl-3,7-dihydroxyphenoxazine (Amplex red) is more recently used for the fluorometric measurement of hydrogen peroxide with higher sensitivity (50 nM) (Zhou et al., 1997).
Horseradish peroxidase-catalyzed oxidation of Amplex red by hydrogen peroxide

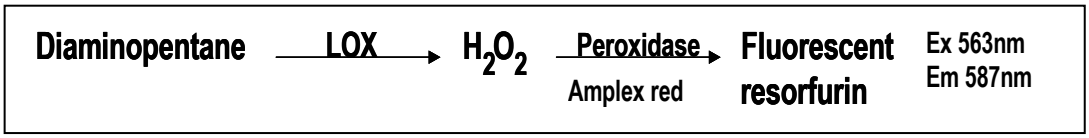

produces fluorescent resorufin with an excitation maximum at 563 nm and an emission maximum at 587 nm. Due to the higher sensitivity and the usage of higher wavelengths that reduce background fluorescence and quenching of most biological samples, this Amplex red-based method is potentially used as a more sensitive and more practical method for measuring lysyl oxidase activity. Amplex red method has not been previously applied to the assay of lysyl oxidase enzyme activity due to its unique and stringent requirements of urea containing buffers, high pH, and low ionic strength. But now a days this is the common method used for measuring LOX activity in cell cultures and biological samples.

Michaelis–Menten constant: The rate of lysyl oxidase activity measured as a function of substrate concentration was determined using 1,5-diaminopentane (0.1–6 mM) by the Amplex red-based assay method and an apparent Km value was found to be 0.3 mM This was consistent with the published Km value of 0.5 mM for 1,5-diaminopentane using homovanillate-based assay thus proving the sensitivity of Amplex red method (Trackman et al., 1981).

The advantages of Amplex red method is:

- This method is continuous and does not use protein substrates that require lengthy preparation.
- The high sensitivity of Amplex red allows the detection of lysyl oxidase as low as 40 ng per 2 ml reaction, using discontinuous assay and 200 ng per reaction using the continuous assay. This is 7.5 to 10 fold more sensitive than the homovallinate method for lysyl oxidase.
- This method does not have to be carried out at high temperatures to achieve high sensitivity as with the homovanillate based assay method.
- The linearity of fluorescence intensity with increasing concentration of enzyme shows the validity of this method to detect low amounts of lysyl oxidase.
- The advantages of using Amplex red are its very low background that changes little with time, the stability, and the high fluorescent yield of the oxidized product, all resulting in increased sensitivity for the detection of hydrogen peroxide.
- Oxidation of Amplex red produces a fluorescent resorufin which has an excitation maximum at 563 nm and emission maximum at 587 nm compared to those of the oxidation product of homovanillate at 315 and 425 nm. These spectral properties are important for avoiding interference from autofluorescence in assays involving biological samples such as cell culture medium.
- The concentration of Amplex red also plays an important role in detection of hydrogen peroxide. The use of 10 mM Amplex red results in minimum background and facilitates the detection of as low as 20 nM hydrogen peroxide.

Amplex red reacts with hydrogen peroxide at a stoichiometry of 1:1 and the oxidation product, resorufin, can be further oxidized to a nonfluorescent compound. Therefore, the proper condition for the maximum sensitivity includes an excess of Amplex red in the reaction medium to prevent further oxidation of resorufin.

Amplex red-based assay can be successfully used to measure the activity of lysyl oxidase in various samples with high sensitivity. This simple and sensitive method facilitates the detection of low levels of lysyl oxidase activity and may

permit obtaining a greater understanding of its role in regulation of extracellular matrix formation and tumor suppression.

1.4 MATRIX METALLOPROTEASES IN RETINAL PIGMENT EPITHELIUM

1.4.1 Introduction :

The matrix metalloproteinases (MMPs) family of enzymes was discovered in 1962 by Gross and Lapiere where they demonstrated a neutral collagenolytic activity elaborated by tissues from the resorbing tails of metamorphic tadpoles (Gross et al., 1962). MMPs are zinc dependent endopeptidases, secreted as pro-enzymes that are activated in the extracellular environment. They are defined by three criteria as MMPs.

1. The requirement of zinc in the active site.
2. The capacity to be inhibited by endogenous tissue inhibitors of metalloproteinases (TIMPs).
3. Evolutionary relationship to vertebrate collagenase.

MMPs are capable of degrading all components of the ECM and basement membrane. Remodelling of the ECM occurs during normal development, morphogenesis, homeostasis, and tissue repair (Moses et al., 1996). Many new proteolytic functions are also defined for these enzymes, which include the degradation of non-matrix macromolecules such as myelin basic protein, inactivation of α1 antitrypsin, release of sequestered growth factors from ECM, and cleavage of bioactive molecules from the cell surface (Pilcher et al., 1999).

Today there are over 26 different MMP members in vertebrates and homologues have been identified in other organisms like bacteria, yeast, fruit flies and plants. The MMPs are given an identifying number (MMP1, MMP2, etc.), but many scientists still use the common names which reflect the substrates as well as functional and sequence similarities.

1.4.2 Classification of matrix metalloproteinases :

The MMP family members are classified based on the substrate specificity, mode of secretion and organization of domain structure (Sternlicht et al., 2001).

A. Based on substrate specificity

1. Collagenases : which recognize native fibrillar collagen types I, II, and III (Eg : MMP 1, 8,13,18)
2. Gelatinases: which degrade denatured collagens (gelatins) and basement (Eg : MMP 2, 9),
3. Stromelysins : degrade type IV collagen, also active against laminin, fibronectin, and proteoglycans. (Eg : MMP 3, 10,11),
4. Matrilysins degrade proteoglycans and activate other MMPs. (MMP 7,26).

B. Based on the mode of secretion

1. Soluble type
2. Membrane associated MMPs (MT-MMP) which are cell-surface bound and are involved in a variety of pericellular activities

C. Based on domain structure of MMP

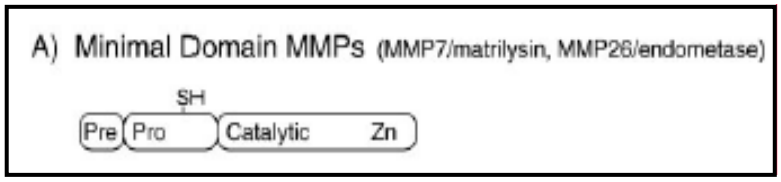

Minimal domain MMPs : The basic domain structure has a Prodomain, which is the leader sequence that targets the protein of secretion.
The Prodomain is a conserved cysteine switch motif (PRCXXPD), which maintains the proMMP in the latent form. The catalytic domain has a zinc binding motif (HEF/LGHS/ALGLXHS) that coordinates the zinc atom at the active site. It contains structural zinc and calcium ions. The cysteine switch motif maintains latency by acting as the fourth zinc binding ligand.
Apart from this basic domain structure the MMPs contain certain various small inserted domains. These smaller domains and the differences they create have resulted in an evolutionarily and functionally diverse group of enzymes with distinct yet overlapping substrates.
Eg : MMP 7, MMP 26

Simple haemopexin domain MMPs: The haemopexin domain is an ellipsoidal disc connected to the catalytic domain with hinge region rich in proline residues

which influences substrate specificity. The haemopexin-like domain has a functional role in substrate binding and interaction with the TIMPs .

Eg : MMP 1, 8, 13, 18, 2, 3, 12 and 19.

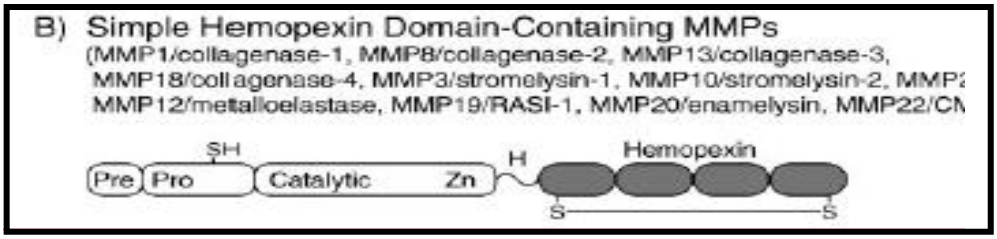

Gelatin binding MMPs : These have a 19 kDa fibronectin like insert in the catalytic domain which mimics the collagen binding motif of fibronectin needed for cleaving collagen and elastin.

Eg: MMP 2 and MMP 9.

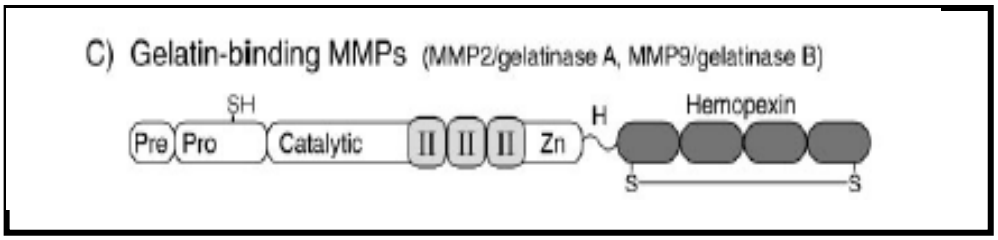

Furin activated secreted MMPs have a recognition motif for furin like serine proteinases within their catalytic domain for intracellular activation.

Eg : MMP11 and 28

Other domain variations namely Vitronectin like inserts in MMP 21, Cysteine proline rich IL1 receptor like domain inMMP 23 play essential role in proteolytic events to specific regions of the cell surface.

Transmembrane MMPs which have a transmembrane region in the C terminal needed for membrane association MMPs. Eg MT 1-MMP, MT-2 MMP, MT 3-MMP and MT5-MMP)

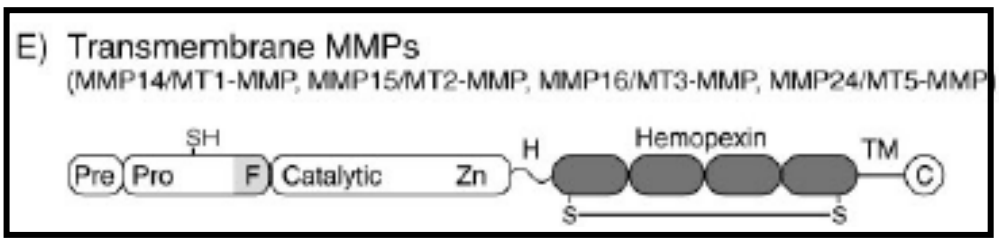

The MT4-MMP and MT 6-MMP has a glycosyl phosphatidyl inositol (GPI) link in the structures. These different domains play essential role in proteolytic events to specific regions of the cell surface.

1.4.3 Regulation of matrix metalloproteinases activity

The MMP activity must be highly regulated to avoid excessive tissue destruction, and this is achieved in three ways.

1. Transcriptional regulation (Crawford et al., 1996),
2. Proenzyme activation (Kleiner, Jr. et al., 1993),
3. Inhibition of activity by the action of the TIMPs (Murphy., 1991a).

Transcriptional regulation: Most MMPs are not constitutively expressed *in vivo* but can be rapidly induced in response to exogenous signals such as growth factors, cytokines, phorbol esters, and cell-cell or cell-ECM interactions. Exceptions to this rule is MMP-8 and MMP-9, which are stored in the secretory granules of neutrophils and eosinophils, and MMP-7, stored in secretory epithelial cells of exocrine glands (Kahari et al., 1999). Transcription can be enhanced or inhibited by association with regulatory proteins that bind to response elements in the promoters of each MMP gene. Binding sites for the transcription factor AP-1 are common to many MMP promoters and are necessary for basal gene expression. Additional regulation is provided by common inflammatory and stress associated factors, including SP-1, Ets family members, and NF-kB. It should be noted that gelatinase A is an exception to major transcriptional regulation as it is found in most tissues whether or not remodeling is occurring. This constant presence is probably possible because its post-transcriptional activation is under tighter control than the other MMPs.

Proenzyme activation: Latent MMPs are proteolytically activated in the extracellular space, with the exception of MMP-11 and MT-MMPs, which are activated before secretion by Golgi associated furin-like proteases. Plasmin is an important physiological activator of pro-MMPs and can initiate cascade of MMP activation at the cell surface (Murphy et al., 1992). For example, upon activation of MMP-9 and MMP-3, the latter can activate more MMP-9, and also MMP-1, amplifying the response. Localising this activation machinery on the cell surface, via integrin receptors and MT-MMPs, ensures that the proteolytic response is maximal in the immediate pericellular environment (Hiraoka et al., 1998). Another important, though often overlooked, activation mechanism is via reactive oxygen species released from inflammatory cells (Sorsa et al., 1999).

The tissue inhibitors of matrix metalloproteinases, or TIMPs, are physiological MMP inhibitors that bind noncovalently to the active site of MMPs at 1:1 complex and block their activation. Inactivation can also occur nonspecifically in plasma by binding to proteins such as α2 macroglobulin. The formation of such complexes determines the rate at which physiological factors can activate MMPs.

Four TIMPs have been identified in humans (Fortunato et al., 1998). They have 30–40% sequence homology at the amino acid level and have six disulphide bonds which comprise a three-loop N-terminal domain and an interacting three-loop C-subdomain. Most of the biological functions of these proteins are attributable to sequences within the N-terminal domain, although the C subdomains mediate interactions with the catalytic domains of some MMPs and with the hemopexin domains of MMP-2 and MMP-9. The TIMPs are secreted proteins of 20-29 kDa, which are variably glycosylated. They inhibit the activity of MMPs by expelling the water molecule bound to the active zinc site. They show little difference in their specificity for MMPs, with each TIMP largely capable of inhibiting most MMPs, TIMP gene expression is also regulated, which coordinate patterns of MMP/ TIMP, depending on the nature of the stimulus and the target cell (Overall et al., 1994).

Interestingly TIMP-2 is also involved in the activation of pro-MMP-2, to which it binds at the cell surface, along with MT1-MMP, facilitating proteolytic activation of pro-MMP-2 by adjacent MT1-MMP. TIMPs are expressed by a variety of cells and are present in most tissue and body fluids. TIMP-1, TIMP-2, and TIMP-4 are present in a soluble form, but TIMP-3 is insoluble and bound to the ECM (Leco et al., 1994). TIMP3 is sequestered to ECM through heparin sulfate or chondrotin sulfate proteoglycans. TIMP-3 has been found to be anti-angiogenic (Sang, 1998) and differs from other TIMPs in inhibiting tumour necrosis factor-α converting enzyme (TACE), suggesting a role in the modulation of inflammation. TIMPs have also shown to have additional biological activities independent of this primary function like cell growth, differentiation, and apoptosis (Sang, 1998).

Thus the functional proteolytic activity of MMPs in a given biological situation is thus dependent on the relative concentrations of regulatory TIMP molecules and active MMPs. Excessive MMP activity is associated with matrix degradation and a feature of destructive diseases such as rheumatoid arthritis, osteoarthritis (Cawston et al., 1996), dermal photoageing, periodontitis, and chronic ulceration(Kahari et al., 1997; Kossakowska et al., 1998; Murphy et al., 1991b; Nwomeh et al., 1999; Vaalamo et al., 1996). Aberrant regulation may also lead to excess matrix deposition, seen in chronic fibrotic disorders, and the formation of scar tissue following injury (Fukuda et al., 1998; Mattila et al., 1998; Murate et al., 1997).

1.4.4 Metalloproteinasess in the retina:

In recent years there has been a vast increase in literature concerning MMP expression in the retina. The presence of MMPs 1, 2, 3, 9, and TIMPS 1-3 have all been reported in human vitreous and interphotoreceptor matrix (Plantner et al., 1998). Gelatinase A (MMP-2) is constitutively found in normal human vitreous, where it is complexed with TIMP-2 (Brown et al., 1994).Gelatinase B (MMP- 9) is constitutively expressed in the retinal ganglion cell layer (Sivak et al., 2002). The presence of these enzymes might play a role in normal retinal matrix turn over, however clues about their physiological roles are coming from the growing list of retinal diseases with which they have been associated.

A complete list of the MMPs found to be upregulated in pathologies of the posterior segment is too long, however some of the more prominent diseases and associated MMPs are given in Table 1.3. Plantner and colleagues have demonstrated the presence of MMP-1, MMP-2, MMP-3, MMP-9 and TIMP-1, TIMP-2, and TIMP-3 in human interphotoreceptor matrix (IPM) and vitreous, using western blot analysis (Plantner et al., 1998). Increased MMPs have been observed in cases of age-related macular degeneration, proliferative diabetic retinopathy (Brown et al., 1994; Das et al., 1999), glaucomatous optic nerve head damage (Yan et al., 2000), vitreal liquefaction (Vaughan-Thomas et al., 2000) and vitreoretinopathy (Kon et al., 1998; Webster et al., 1999). The cellular source of MMPs in most of these diseases are still unknown, though their activity is likely due to combined expression from resident cells, invading vasculature, and inflammatory cells.

Table 1.3 : Different types of MMPs reported in various ocular diseases.

Ocular Diseases	Type of MMPs studied
Age related macular degeneration	**MMP 1, 3, 2, 9.**
Diabetic retinopathy	**MMP 2 and 9.**
Proliferative vitreoretinopathy	**MMP 1, 2, 3,7,9**
Pterygium	**MMP 1, 3, 2, 9 and TIMP 1,3**
Ulcerative Keratitis	**MMP 2 and MMP 9**

1.4.5 : Methods of matrix metalloproteinases estimation

MMPs can be detected by various methods.

1. Localization of MMPs by immunohistochemistry
2. Quantification – by ELISA and gelatinase assay.
3. Zymography – Detects activity by incorporation of substrate in gel
4. Western blot
5. Quantitative and semiquantitative PCR.

1.4.6 Retinal pigment epithelium and matrix metalloproteinases:

It is known that RPE in culture are capable of producing a range of MMPs (Alexander et al., 1990; Hunt et al., 1993; Sheridan et al 2001). These enzymes include matrix metalloproteinases and there is now evidence that RPE in situ also make some of these enzymes as well as tissue inhibitors of the enzymes (Padgett et al.,1997). Perhaps the balance between matrix metalloproteinases and their tissue inhibitors supports the strong adhesion that the normal RPE has for components of BM. Loss of this balance might play an important role in various vitreoretinal diseases.

1.4.7 Retinal pigment epithelium in pathology

Once differentiated, the RPE does not renew itself by cell division; it continues to carry out its versatile functions throughout the lifetime of the individual unless such processes are lost due to disease. These quiescent RPE cells in a normal eye undergo proliferation and migration or apoptosis only under pathology conditions.

Detachment of the RPE occurs between the basal lamina of the RPE cell and the inner collagenous BM. The etiology of pigment epithelium detachment (PED) can be divided into four major categories: inflammatory, ischemic, idiopathic, and degenerative. Inflammatory PED occurs when choroidal inflammation causes increased vascular permeability and breakdown of the outer blood-retinal barrier, with subsequent accumulation of fluid rich in protein under the RPE, as in Vogt-Koyanagi-Harada syndrome. In several pathologic states, such as malignant hypertension and eclampsia, ischemia of the retinal and choroidal vessel walls resulting from endovascular damage was suggested as a possible cause of breakdown of the blood ocular barrier leading to leakage and accumulation of fluid under both layers, and formation of ischemic PED. The prototype of idiopathic PED is probably central serous chorio-retinopathy, in which choroidal dysfunction resulting in multifocal hyperpermeability combined with a defect in the RPE barrier allows abnormal leakage of fluid and protein into the sub-RPE and subretinal space.

In the case of CSE, it is widely held that the pathogenesis of this disease involves a dysfunction in the ion and fluid transport activities of the RPE. This results in an accumulation of subretinal fluid between the neural retina and the RPE, thereby leading to the eventual detachment of the neural retina.

Alterations in RPE function may occur either as a result of diseases which specifically affect the RPE, such as age-related macular degeneration and central serous retinopathy (CSR) (Wang et al., 2008), or due to secondary changes resulting from many retinal diseases including retinitis pigmentosa (RP) and proliferative vitreoretinopathy (Machemer et al., 1978) and proliferative diabetic retinopathy (PDR).

The initial event of RPE dysfunction in vitreoretinal diseases is altered permeability followed by detachment, migration, proliferation and eventually membrane formation. It is evident that the epiretinal membrane in proliferative vitreoretinopathy and proliferative diabetic retinopathy has RPE cells.

The ECM is the microenvironment in which cells receive signals through integrins and cell adhesion molecules to undergo differentiated phenotype. Extensive changes take place in the ECM at the levels of matrix synthesis or breakdown during these vitreoretinal diseases associated with RPE pathology. The ECM cross linking molecule lysyl oxidase, apart from its normal function of collagen and elastin cross-linking, attributed with novel functions involved in cell proliferation and migration. With limited literature being available on LOX in ocular tissues in pathology and its novel functions being unexplored in retinal pigment epithelial cells, the work of this thesis was focused on these areas.

CHAPTER 2 : OBJECTIVES

2.1. Objectives:

Objective 1 : To Study the ocular tissue distribution of lysyl oxidase enzyme in normal and pathological conditions *in vivo*.

Objective 1.1. To study the ocular distribution of lysyl oxidase enzyme in human ocular tissues.

- To standardize LOX assay by amplex red flourimetry method
- To determine the specific activity of LOX in human ocular tissues.
- To do immunolocalization of LOX in human eye ball section
- To detect the gene expression of LOX by real time PCR in human ocular tissues.

Objective 1.2. To determine the levels of Lysyl oxidase in vitreous samples from patients with proliferative diabetic retinopathy and rhegmatogenous retinal detachment.

- To detect the specific activity of LOX in vitreous.
- To quantify MMP 2 and MMP 9 by ELISA in vitreous.
- To determine the hydroxyproline content in vitreous.
- To immunolocalize LOX in neovascular membranes.

Objective 2 : To Study the effect of *in vitro* stress conditions like oxidative stress, osmotic stress and high glucose stress on lysyl oxidase

Objective 2.1 To establish retinal pigment epithelium culture from bovine eye ball and also use human ARPE-19 cells.

- To standardize the RPE culture from bovine and human eye balls.
- To characterize them with the cell specific markers
- To study the rate of RPE cell proliferation using tritiated thymidine.
-

Objective 2.2 : To study the effect of oxidative stress on lysyl oxidase activity in RPE cells

- To see the effect of cytotoxicity of tetra butyl hydroperoxide and homocysteine by MTT assay.

- ❖ To determine the specific activity of extracelluar LOX in conditioned medium after concentration.
- ❖ To detect the levels of MMP by activity assay

Objective 2.3: To study the effect of hyperosmotic mannitol on lysyl oxidase activity and expression in RPE cells

- ❖ To see the effect of cytotoxicity of hyperosmotic mannitol by MTT assay and proliferation by BrdU labbelling assay.
- ❖ To determine the specific activity of extracelluar LOX in conditioned medium after concentration.
- ❖ To detect the levels of MMP by activity assay
- ❖ To study the gene expression of LOX by real time PCR

Objective 2.4: To study the effect of glucose on lysyl oxidase activity and expression in RPE cells.

- ❖ To see the effect of cytotoxicity of glucose by MTT assay and proliferation by BrdU labeling assay.
- ❖ To determine the specific activity of extracelluar LOX in conditioned medium after concentration.
- ❖ To detect the levels of MMP by activity assay
- ❖ To study the gene expression of LOX by real time PCR
- ❖ To do immunolocalization of LOX in RPE cells after exposure to glucose.

Objective 3: To study the modulatory role of homocysteine on the activity of lysyl oxidase; *in vivo and in vitro.*

- ❖ To detect the levels of homocysteine in vitreous samples by HPLC
- ❖ To correlate LOX with homocysteine in vitreous.
- ❖ To study the effect of homocysteine on LOX specific activity in RPE cells.

CHAPTER 3 - METHODOLOGY

3.1 MEDIA USED FOR RETINAL PIGMENT EPITHELIAL CULTURE:

The medium used for RPE cultures as given in the literature varied from DMEM-F12, Hams F12, Eagles MEM and M199 medium. We used all these media during the initial standardization process and found that Medium 199 (Table 3.1) gave a good success rate in primary culture of BRPE.

When studying the effect of glucose we have used Medium 199 media because this had 5.5 mM glucose when compared to DMEM / F12. So before experiments the cells were transiently shifted from DMEM / F12 to Medium 199. Observation under light microscope did not reveal any difference between RPE cultures grown in Medium 199 and those grown in DMEM.

Table 3.1: Comparison of Medium199 and DMEM/F12

COMPONENTS	M199 Concentration (mg/L)	DMEM/F12 Concentration (mg/L)
Amino Acids		
Glycine	50	18.75
L-Alanine	25	4.45
L-Arginine hydrochloride	70	147.5
L-Asparagine-H_2O	30	7.5
L-Aspartic acid	0.1	6.65
L-Cysteine hydrochloride-H_2O	26	17.56
L-Cystine 2HCl	75	31.29
L-Glutamic Acid	100	7.35
L-Glutamine	21.88	365
L-Histidine hydrochloride-H_2O	10	31.48
L-Isoleucine	40	54.47
L-Leucine	60	59.05
L-Lysine hydrochloride	70	91.25
L-Methionine	15	17.24
L-Phenylalanine	25	35.48
L-Proline	40	17.25
L-Serine	25	26.25

L-Threonine	**30**	**53.45**
L-Tryptophan	**10**	**9.02**
L-Tyrosine disodium salt dihydrate	**40**	**55.79**
L-Valine	**25**	**52.85**
Vitamins		
Alpha-tocopherol Phosphate	**0.01**	
Ascorbic Acid	**0.05**	
Biotin	**0.01**	**0.0035**
Choline chloride	**0.5**	**8.98**
D-Calcium pantothenate	**0.01**	**2.24**
Folic Acid	**0.01**	**2.65**
Menadione (Vitamin K3)	**0.01**	
Niacinamide	**0.025**	**2.02**
Nicotinic acid (Niacin)	**0.025**	
Para-Aminobenzoic Acid	**0.05**	
Pyridoxal hydrochloride	**0.025**	
Pyridoxine hydrochloride	**0.025**	**2.031**
Riboflavin	**0.01**	**0.219**
Thiamine hydrochloride	**0.01**	**2.17**
Vitamin A (acetate)	**0.1**	
Vitamin D_2 (Calciferol)	**0.1**	
i-Inositol	**0.05**	**12.6**
Vitamin B_{12}		**0.68**
Inorganic salts		
Calcium Chloride ($CaCl_2$) (anhyd.)	**200**	**116.6**
Cupric sulfate ($CuSO_4$-$5H_2O$)		**0.0013**
Ferric Nitrate (Fe (NO_3) -$9H_2O$)	**0.7**	**0.05**
Ferric sulfate ($FeSO_4$-$7H_2O$)		**0.417**
Magnesium Chloride (anhydrous)		**28.64**
Magnesium Sulfate ($MgSO_4$) (anhyd.)	**97.67**	**48.84**
Potassium Chloride (KCl)	**400**	**311.8**

Sodium Chloride (NaCl)	**6100**	**6995.5**
Sodium Phosphate dibasic (Na_2HPO_4) anhydrous	**140**	**71.02**
Sodium Phosphate monobasic (NaH_2PO_4-H_2O)		**62.5**
Zinc sulfate ($ZnSO_4$-$7H_2O$)		**0.432**
Sodium Bicarbonate ($NaHCO_3$)	**2200**	
Other Components		
D-Glucose (Dextrose)	**1000**	**3151**
HEPES	**5960**	**3574.5**
Hypoxanthine Na		**2.39**
Linoleic Acid		**0.042**
Lipoic Acid		**0.105**
Phenol Red	20	**8.1**
Putrescine 2HCl		**0.081**
Sodium Pyruvate		**55**
Thymidine		**0.365**
2-deoxy-D-ribose	**0.5**	
Adenine sulfate	**10**	
Adenosine 5'-phosphate	**0.2**	
Adenosine 5'-triphosphate	**1**	
Cholesterol	**0.2**	
Glutathione (reduced)	**0.05**	
Guanine hydrochloride	**0.3**	
Hypoxanthine Na	**0.4**	
Ribose	**0.5**	
Sodium Acetate	**50**	
Thymine	**0.3**	
Tween 80	**20**	
Uracil	**0.3**	
Xanthine-Na	**0.34**	

3.2 VIABILITY COUNT:

Principle: Viability assays measure the percentage of cells that are viable. This is accomplished by a dye exclusion stain, where cells with an intact membrane are able to exclude the dye while cells without an intact membrane take up the coloring agent. The dye used for exclusion stain is usually trypan blue but

erythrosin B and naphthalene black can also been used in which the dye is normally taken up by viable cells but not by the non-viable cells. The trypan blue dye exclusion is commonly used and a protocol for this procedure (Freshney et al., 2005) is as follows.

Method: The 0.4 % trypan blue dye exclusion test was carried out to find the number of viable cells in culture. A mixture of 1 volume of dye and 9 volumes of cell suspension was made in Phosphate buffered saline (pH 7.4). This was allowed to stand at room temperature for 10 minutes. Charged on to an improved neubauer chamber, the four corner 1mm sized squares were counted. Cells touching upper and left boundaries were included and those touching lower and right boundaries were excluded. Number of stained and unstained cells was separately noted. Calculations were done to express the number of viable cells as percentage. The viable cells do not take up the stain while the dead cells were stained. Cell count was carried out thrice to confirm results.

Calculation: The cell count (cells per ml) was determined as follows:

Cell count per ml = average cell count per square x dilution factor x 10^4

The cell viability (%) was determined as follows:

Cell viability (%) = cell count (viable) / total cell count (viable + non-viable) x 100

3.3 PROLIFERATION ASSAY IN RPE BY TRITIATED THYMIDINE INCORPORATION:

The most frequently used measure for cell proliferation is the thymidine incorporation assay. Cells synthesize DNA only during the S phase (DNA synthesis phase) of the cell cycle and so incorporation of the radio labelled nucleotide ^{3}H thymidine into DNA is limited to this phase. Cells that incorporate ^{3}H label can be identified by the amount ^{3}H counting in Liquid scintillation system. This measure will serve as a means of validating the proliferation of cells. (Jain et al., 1997)

3.3.1 Determining the optimum concentration of ^{3}H thymidine:

For experiments of RPE proliferation assay 0.25 and 0.5 μCi of ^{3}H thymidine was added as per earlier reports, but during the incubation period the cells were looking unhealthy and vacuolated. To evaluate if this could be due to ^{3}H toxicity, we measured the count of 0.5 and 0.25 μCi of ^{3}H added to the culture and found that the count was too high and so we diluted the ^{3}H further and the subsequent experiments were done using 30 nCi ^{3}H.

No.	Concentration of ^{3}H thymidine	Counts in DPM
1.	1.0 μCi	2700516
2.	0.5 μCi	1247679
3.	200 nCi	581342
4.	20 nCi	59596

3.4 IMMUNOFLOURESCENCE

Method: Cultured bRPE cells or ARPE cells were grown on coverslips or in chambered slides and immunofluorescence (IF) or immunohistochemistry (IHC) was done.

The entire staining procedure was done in moist chamber. For immuno-flourescnece staining, the cells were fixed with cold acetone for 30 minutes. Primary antibody (According to the dilutions standardized) was added and incubated in moist chamber for 1 hour. After which the cells were washed thrice in PBST 5 minutes each. Secondary antibody conjugated to FITC was added and incubated for 45 minutes. Washed the cells thrice in PBST, 5 minutes each. The cells were counter stained using Evan's Blue for 30 seconds. After washing in PBST it was mounted in glycerol, and viewed under Fluorescence microscope with blue filter (490 nm).

3.5 IMMUNOHISTOCHEMISTRY:

Method: The slides were placed in a immunostaining work station. The protocol was carried out with NovolinkTM Min polymer detection system. The cells grown on coverslips were fixed with 100% methanol. For paraffin sections the slides were deparaffinised and then treated with trypsin EDTA for antigen retrival and then proceeded. They were blocked for peroxidase for 10 min provided in the kit and washed with TBS. This was followed by incubation with

protein block for 30 min. After this blocking step, slides were incubated for 2 hrs with primary antibody. After washing with TBS, the slides were incubated for 45 minutes with post primary block. The slides were washed again and incubated for 45 minutes with polymer link. Finally, the slides were washed in TBS and rinsed with 0.1 M Acetate buffer pH 5.0-5.2, and stained for 20 minutes with 0.8% amino ethyl carbazone in acetate buffer (pH 5.0) or 0.3 % diaminobenzidine. The sections were counterstained with haematoxylin for 15 seconds, rinsed for 10 minutes with water, and air dried. In negative control, the primary antibodies were skipped and proceeded as above protocol.

3.6 WESTERN BLOTTING:

The first step in western blotting procedure is to separate the macromolecules using gel electrophoresis. Following electrophoresis, the separated molecules are transferred or blotted onto a second matrix, generally a nitrocellulose membrane. Next, the membrane is blocked to prevent any nonspecific binding of antibodies to the surface of the membrane. The transferred protein is complexed with an enzyme-labeled antibody as a probe. An appropriate substrate is then added to the enzyme and together they produce a detectable product such as a chromogenic or fluorogenic precipitate on the membrane for colorimetric or fluorometric detection, respectively. The most sensitive detection methods use a chemiluminescent substrate that, when combined with the enzyme, produces light as a by-product. The light output can be captured using film. Whatever substrate is used, the intensity of the signal should correlate with the abundance of the antigen on the blotting membrane.

3.6.1 Sample preparation: The cultured cells once they reach the confluence were harvested by trypsinisation and the protein was extracted using 100 µl of the HEPES buffer (pH 7.0) with protease inhibitor cocktail and sonicated for 80 cycles/min. The lysed cells were centrifuged at 10,000 rpm at 4ºC for 5 min and protein was estimated by Lowry method.

3.6.2 Protein Estimation: Protein estimation was done by conventional Lowry method. The assay was run along with a set of standard using BSA, ranging from 50 to 200 µg. The absorbance was read at 660 nm.

3.6.3 Polyacrylamide gel electrophoresis: The protein samples of RPE lysate for blotting were resolved using SDS-PAGE electrophoresis. For this purpose 10% separating gel was prepared and poured in the assembled glass plates sealed with 2% agarose gel and left it without disturbing. The separating gel was covered with saturated butanol while left for polymerization. After the separating gel was polymerized 4% stacking gel was prepared and poured above the separating gel by removing the butanol layer and the comb was placed carefully with out any air bubble and left it a side for solidification. After the gel has been solidified the comb was removed care fully.

The protein samples were mixed with 3x sample loading buffer to final volume of 50µl and incubated it at 95º C for 2 to3mins. Then the sample was loaded on the gel and run till the dye reaches the bottom of the gel. The gel was taken care fully from the glass-assembled plates. The loading order was noted by giving a small cut at one end.

3.6.4 Immunodetection: The proteins were transferred to nitrocellulose or Polyvinilidine Fluoride membrane at 100V for one hour in cold transfer buffer. Once transferred the membrane was stained with 0.5% Ponceau to the check whether the transfer was done properly. Then the blots were washed with Milli Q water and blocked with 5 % blocking solution (Skimmed milk powder). Primary antibodies were added according the standardized dilutions and incubated for 2 hours to overnight at 4°C. The blots were washed 3 times with TBST buffer 30 minutes each. The presence of the specific proteins was then shown by chemilumniscence of horse raddish peroxidase. For chemilumniscence detection Pierce western blot detection reagents were used. The blot was exposed to X-ray (Kodak X ray film) film and then the film was developed to visualize the bands.

3.7 CYTOTOXICITY ASSAY:

Principle: MTT [3-(4,5-dimethylthiazol-2-yl)-2,5-diphenyltetrazolium bromide] assay, first described by Mosmann in 1983, is based on the ability of a mitochondrial dehydrogenase enzyme from viable cells to cleave the tetrazolium rings of the pale yellow MTT and form a dark blue formazan crystals which is

largely impermeable to cell membranes, thus resulting in its accumulation within healthy cells. Solubilisation of the cells by the addition of a detergent results in the liberation of the crystals which are solubilized. The number of surviving cells is directly proportional to the level of the formazan product created. The color can then be quantified using a simple colorimetric assay. The results can be read on a multiwell scanning spectrophotometer (ELISA reader).

Protocol: The cells after exposure to experimental conditions were assayed by the following method.

The medium was carefully removed and replaced with fresh serum free media. To this MTT from (5mg/ml Stock) is added corresponding to $1/6^{th}$ volume of the medium. This is incubated for 4 hours at 37°C. After the incubation the medium was discarded and the formed crystals were solubilised in DMSO. After the crystals have dissolved (5 minutes) the plate was read at 540 nm. Results were expressed as percent viable taking the absorbance of the control cells as 100 %. (Mosmann et al.,1983)

3.8 CELL PROLIFERATION ASSAY:

Principle: During DNA synthesis (DNA replication) nucleotide analog 5-bromo-2'-deoxyuridine (BrdU) are incorporated into the genomic DNA. This nucleotide is added along with the experimental condition to the cells and incubated. Subsequently, those labeled cells are incubated with anti BrdU antibody and the labeled cells are measured using an enzyme substrate reaction as per kit protocol supplied by Roche.

Protocol: Cells are seeded in 96-well microtiter plates were allowed to grow for 48 hours. Thereafter, the cells were growth arrested in medium with 1 % serum for overnight and subsequently exposed to medium containing the agents to be tested and along with this the BrdU labeling solution is added. Subsequent steps are followed as per kit protocol from Roche.

3.9 CONCENTRATION OF CONDITIONED MEDIA USING 10 KDa CUT OFF FILTERS: Centricon YM 10 cut off filters are used for concentrating biological samples. Prior to use the filters are prerinsed with 2 ml of buffer or

deionised water and spun for 10,000 rpm for 2 minutes. Then four ml of conditioned medium is added to the centricon and centrifuged at 7500 rpm for 1 hr at 4° C. Then the filter unit is inverted to collect the retenate by spinning for 5 minutes at 7,500 rpm at 4° C. Approximately 0.5 ml retentate was obtained. The retentate is then used for lysyl oxidase specific activity assay and DQ gelatinase assay.

3.10 SPECIFIC ACTIVITY OF LYSYL OXIDASE

Principle: Enzymatic activity of lysyl oxidase is measured by determining the amount of hydrogen peroxide (H_2O_2) liberated in the reaction mixture with high sensitivity and specificity using N-Acetyl-3,7-dihydroxyphenoxazin (Amplex Red) a colourless, chemically stable, nonabsorbing, nonfluorescent derivative of dihydroresorufin. Lysyl oxidase acts on the substrate diamino pentane (DAP) to release H_2O_2. The H_2O_2 in the presence of Horse radish peroxidase (HRP) acts on the Amplex red (AR) and converts it to a strongly absorbing and fluorescing product, resorfurin that can be read at Ex- 563nm, Em- 587nm by a spectrofluorometer or fluorescence ELISA plate reader. (Palamakumbura et al., 2002)

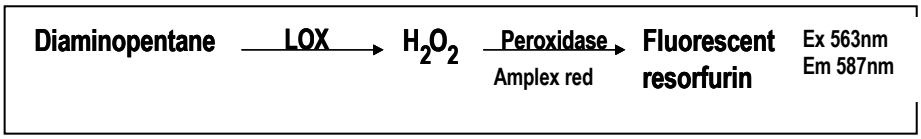

A standard graph was constructed using H_2O_2 (0.2 to 1.0 micromoles). The relative flouresecnce unit obtained in test sample was calculated based on the standard and expressed as specific activity of LOX as µm H_2O_2 /min/mg protein or nm H_2O_2 /min/mg protein.

Assay protocol: H_2O_2 standard preparation: A 20 mM stock H_2O_2 solution was prepared and diluted to 100 µM stock. From this a set of standards were prepared in the range of 0.4-2.0 µM.

Table 3.2: Protocol for hydrogen peroxide standard, for LOX assay

Sl.No.	DH_2O (µl)	100 µM H_2O_2 (µl)	*Final* Concentration (in 200 µl)
1	400	0	0 µM

2	396.8	3.2	0.4 µM
3	393.6	6.4	0.8 µM
4	390.4	9.6	1.2 µM
5	387.2	12.8	1.6 µM
6	384	16	2.0 µM

To a 96-well microplate 100 µl of the standards were added and 100 µl of conditioned medium or tissue extract supernatant was added. The assay was done in duplicates with and without 500 µM BAPN. To this 100 µl of the reaction mix containing 50 mM sodium borate pH 8.2, 1.2 M urea, 50 µM amplex red (Molecular Probes, Invitrogen) 0.1 U/ml horseradish peroxidase, 10 mM 1,5-diaminopentane substrate was added and placed in microplate reader (at 37˚C) The fluorescence was measured at excitation 560 nm and emission at 590 nm for every 5 of 10 min up to 2 hour based on the standardization. A standard graph was constructed using H_2O_2 in the concentration ranging from 0.4 to 2.0 µM (Figure 3.1).

Figure 3.1 : Standard graph of hydrogen peroxide

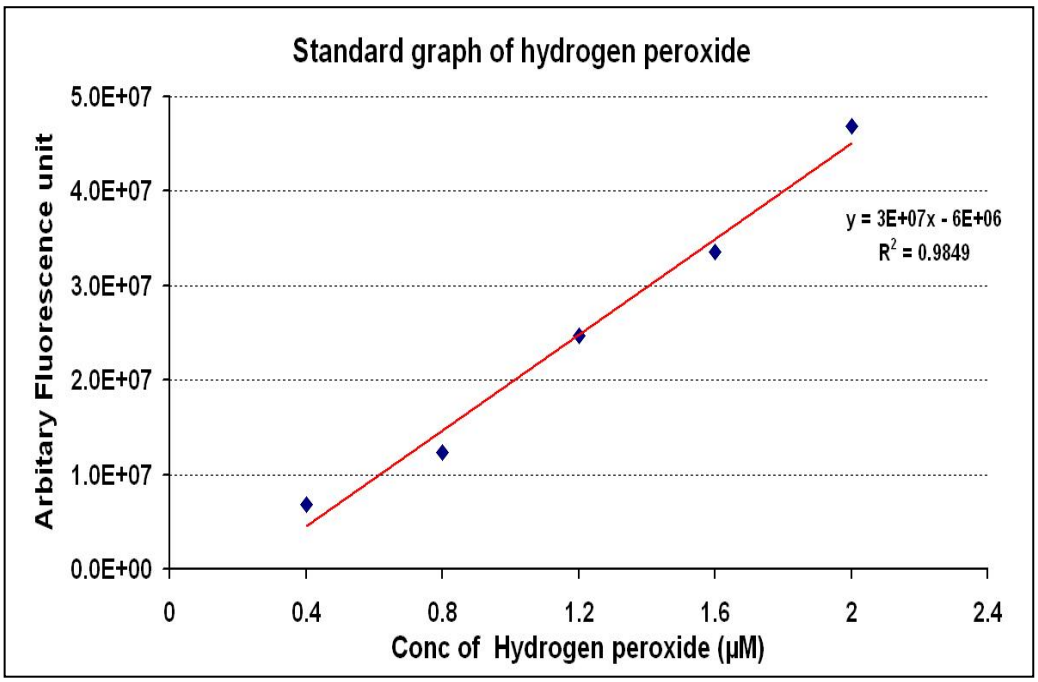

3.11 RNA ANALYSIS

3.11.1 Total RNA extraction: Cell samples were harvested and washed with PBS and the total RNA was extracted using TRI method. To the cell pellet or tissue sample 1 ml of trizol reagent (Sigma chemicals) was added and the pellet was resuspended. This was incubated for 3-5 minutes at room temperature (RT). To this 200 µl of chloroform was added and mixed well (without vortex) and kept at room temperature for 2-3 minutes. This was centrifuged at 12000 rpm for 15 minutes and the aqueous layer was carefully transferred to a new vial. To this 50 µl of isopropanol was added and incubated for 10 min at RT. After incubation it was centrifuged for 12,000 rpm for 10 min and to the pellet 1 ml of 75 % alcohol was added and centrifuged at 12,000 rpm for 5 minutes, The RNA pellet was dried and reconstituted with 20 µl of RNAse free water and stored at -80° C.

3.11.2 RNA purification

- Isolated RNA was treated by TURBO DNase (Ambion, Genetix Biotech Asia Pvt. Ltd, Chennai, India) to remove the DNA in the sample.
- 50-µl reaction containing 7.5-10.0 µgms of RNA was mixed with 1 µl of TURBO DNase 1µl (2 units) and 0.1 volume 10X TURBO DNase buffer, was incubated at 37ºC for 30 minutes.
- To the reaction mixture 0.1 volume of resuspended DNase inactivation reagent was added (5µl) and mixed repeatedly during the incubation period of 2 minutes.
- The mixture was centrifuged for 1.5 minutes at 10,000 rpm and supernatant transferred to a fresh tube.
- The TURBO DNase treated RNA was quantified before reverse transcriptase PCR.

3.11.3 Reverse transcription

- For all samples 1µg of total RNA was used to synthesize first-strand cDNA using SuperScript II® reverse transcriptase (Invitrogen, Joyvel, Chennai, India) and random primers.
- Each component was mixed and centrifuged before use.
- Following components were added according to Table 3.3.

Table 3.3: Reverse transcription cocktail protocol

Component	sample	- RT control	+ RT Control
1µg of total RNA	*n*µl	*n*µl	-
Control RNA(50ng/µl)	-	-	1µl
Random hexamers(50ng/µl)	2µl	2µl	2µl
10mM dNTP	1µl	1µl	1µl
With DEPC treated water made up to	12µl	12µl	12µl

- The sample was incubated at 65ºC for 5 minutes and then in ice for 1 minute.
- The following reaction mixture was prepared and 7µl was added to each reaction.

Component	each reaction
5X first- strand buffer	4µl
0.1M DTT	2µl
Ribonuclease Inhibitor (40 units/µl)	1µl

- Incubated at 25º C for 2 minutes.
- Superscript II reverse transcriptase 1µl (200 units/µl) was added and mixed gently.
- Incubated at 25º C for 10 minutes.
- Incubated at 42º C for 50 minutes.
- Inactivated the reaction by heating at 70ºC for 15 minutes.
- The cDNA was quantified and diluted for real time amplification or semiquantitative RT-PCR.

3.11.4 Semiqunatitative RT-PCR analysis:

Using a housekeeping gene, glyceraldehyde-3-phosphate dehydrogenase (*GAPDH*), as an internal control, the mRNA expression of LOX was analyzed by semi-quantitative RT-PCR (Czizar et al., 2001). Briefly first strand cDNA synthesis was carried and 3 µg of the TURBO DNAase treated RNA for LOX was set in the thermal cycler. PCR amplifications were performed with the specific primers designed from published human gene sequences. (Urban et al.,2007). Semi-quantitation was established by terminating reactions at appropriate intervals for each primer pair to ensure that the PCR products formed were within the linear portion of the amplification curve. PCR products were fractionated by electrophoresis using 2% agarose gel containing 0.5% Ethidium bromide with molecular marker *Hinf I* ϕ digest/100 bp ladder to confirm the size

of the resultant product. Semi-quantitative RT-PCR the bands were analyzed using Image J software.

LOX cDNA
Forward **ACGGCACTGGCTACTTCCAGTA**
Reverse **TCTGACATCTGCCCTGTATGCT**
Amplicon size- 158 bp

GAPDH cDNA
Forward **GCCAAGGTCATCCATGACAAC**
Reverse **GTCCACCACCCTGTTGCTGTA**
Amplicon size- 498 bp

RT- PCR reaction cocktail:

10 X buffer	:	5 µl
dNTPs	:	5 µl
Forward Primer	:	1 µl
Reverse Primer	:	1 µl
Taq poly	:	0.3 µl
MQ water	:	30 µl
cDNA	:	5 µl

The final reaction protocol for RT-PCR

95°C	:	15 min
95°C	:	1 min
60°C	:	1 min
72°C	:	1 min 30 sec for 45 cycles
72°C	:	10 min

3.12 ZYMOGRAPHY

Principle: Zymography is based on the principle of detection of proteolysis of their specific substrates by the matrix metallo proteases incorporated in the polyacrylamide gels. The pro forms of MMPs are activated by addition of 10% SDS without any changes in their molecular weight. After incubation in appropriate conditions the gels are stained to visualize for negative bands (Das et al., 1999).

Procedure: Gels were cast with 0.1% gelatin and the samples with the appropriate protein concentration were taken. The samples were activated with 10µl of tracking dye+10%SDS (equal volumes of 10%SDS and tracking dye) at room temperature for 1 hour. The samples were then loaded and the electrophoresis was run at 180V for approximately 2 hrs. After the run gels were washed in Triton to remove SDS. Then gels were washed with MQ water thrice 5

min each in an automatic shaker. Gels were then incubated in LSCB buffer overnight. After this the gel was washed again with MQ water twice for 5 min each. The gels were then stained with the working staining solution for 1 hour. Gels were destained with 10% acetic acid till negative bands were seen.

3.13 DQ GELATINASE ASSAY:

Principle: The substrate DQ gelatin is a fluorescein conjugate, in which the gelatin is so heavily labeled with fluorescence that it is in the quenched state. This substrate is efficiently digested by most of the gelatinases and collagenases to yield highly fluorescent peptides. The increase in the fluorescence is proportional to the proteolytic activity. The digestion product from DQ gelatin can be monitored at 495 nm excitation and 515 nm emission spectra. The background fluorescence can be corrected by subtraction the value obtained from with out enzyme control. (Notari et al., 2005).

Protocol: A 200 µl reaction was performed with 50µl of medium with and without inhibitor (1, 10- phenanthrolein). For each reaction 2.5µl of substrate DQ gelatin was added with 1X reaction buffer. A negative control of 2.5ul DQ gelatin and 1X reaction buffer was also set. 1X reaction buffer was used as blank .The fluorescent intensity of the reaction was read for every 10 min for 1hr by using the fluorescent micro plate reader equipped with standard fluorescein filters with an absorption Maxima at ~ 495nm and fluorescence emission maxima at ~515nm. Protein analysis was performed using the complete medium, filtrate and the retentate by Lowry method.

Figure 3.2: Standard graph for DQ gelatin

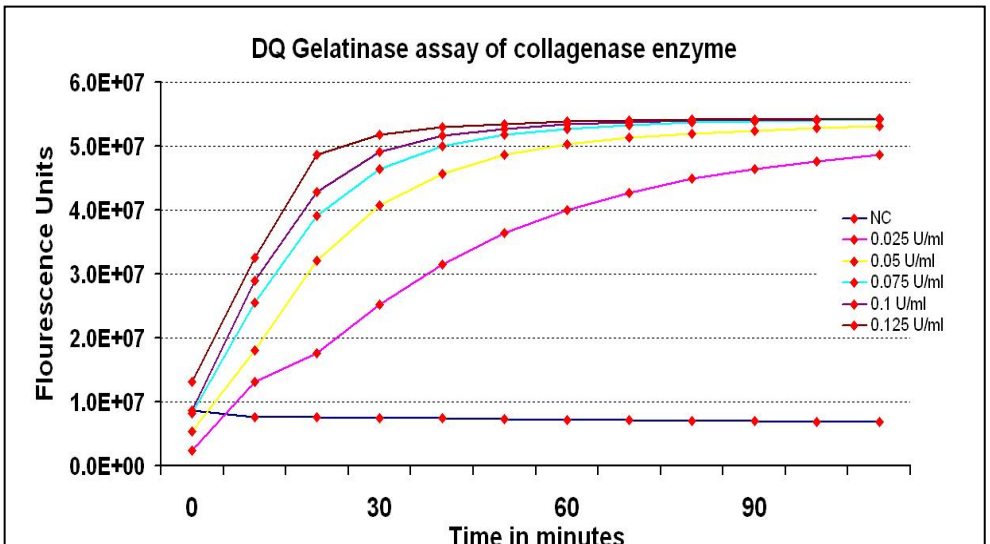

3.14 MATRIX METTALOPROTEASES 2 AND 9 BY ELISA:

The quantikine MMP 2 and MMP kit from R& D systems is a solid phase ELISA, designed to measure total MMP 2 and MMP 9. This can be used for serum, plasma and cell culture supernatants. The assay employs quantitative sand witch enzyme assay. Polyclonal antibody specific for MMP 2 and 9 have been coated on micro titer plate. Standards and samples are pipetted into the wells, which gets bound to the well by immobilized antibody. After washing unbound substances, an enzyme linked polyclonal antibody specific for MMP 2 or MMP 9 is added and then developed using an enzyme substrate reaction. The amount of colour developed is proportional to the amount of total MMPs present. Standards are run every time when assayed for samples.

Standard concentrations for MMP 2: 0.78 – 25.0 ng/mL

Standard concentrations for MMP 9: 0.312 -10.0 ng/mL

The minimum detectable dose for MMP-2 ranged from 0.03-0.40 ng/ml and for MMP-9, < 0.156 ng /ml.

Figure 3.3: Standard graph for MMP 2

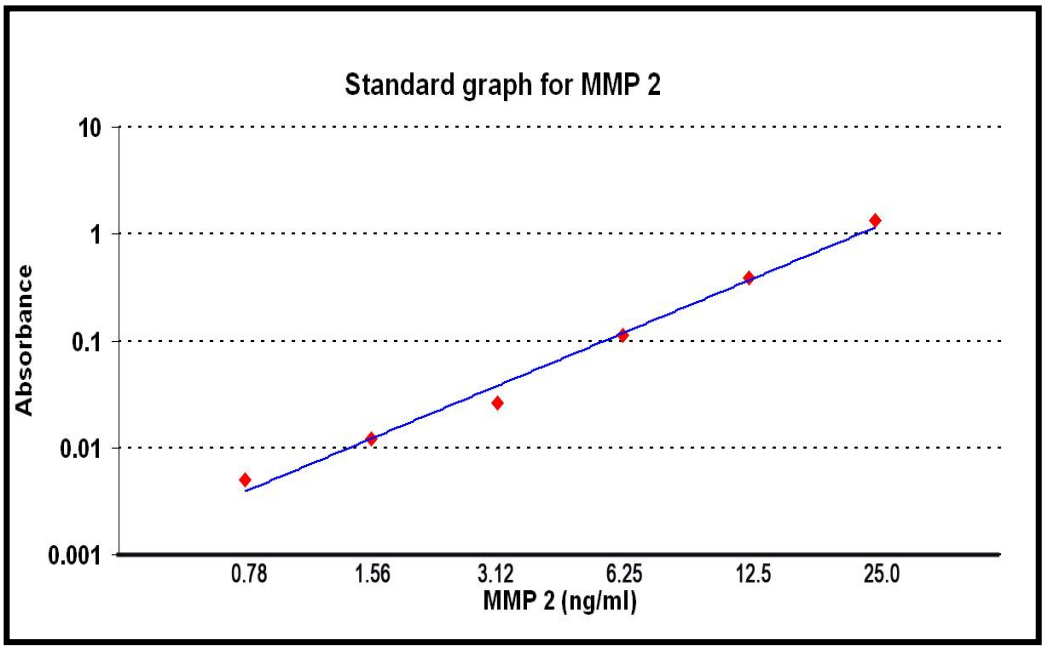

Figure 3.4: Standard graph for MMP 9

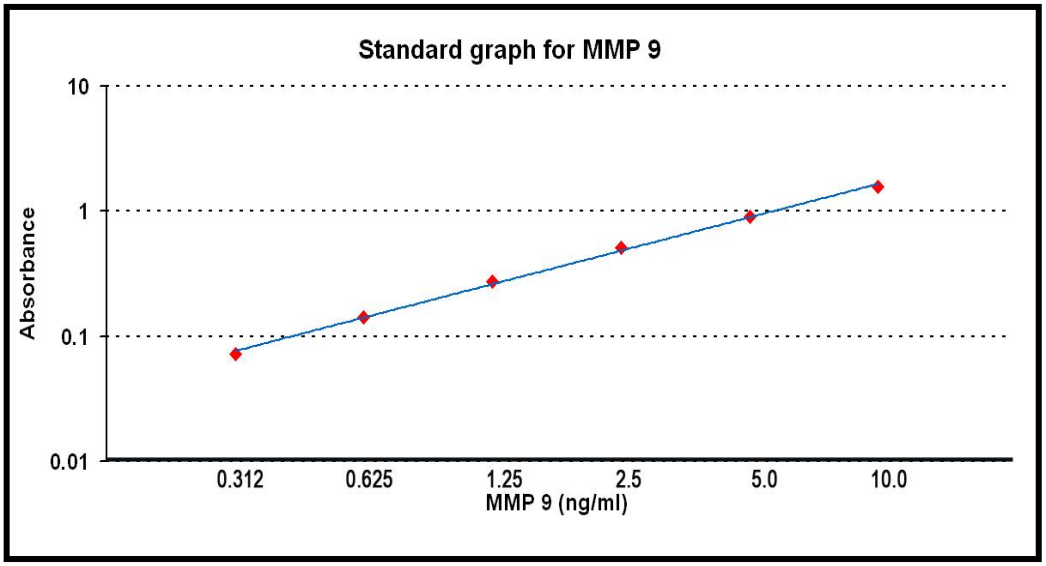

3.15 THE TUNEL ENZYMATIC-LABELING ASSAY

Extensive DNA degradation is a characteristic event which occurs in the late stages of apoptosis. Cleavage of the DNA may yield double-stranded, LMW DNA fragments (mono- and oligonucleosomes) as well as single strand breaks ("nicks") in HMW-DNA. Those DNA strand breaks can be detected by enzymatic labeling of the free 3'-OH termini with modified nucleotides (X-dUTP, X = biotin, DIG or fluorescein). Suitable labeling enzymes include DNA polymerase (nick translation) and terminal deoxynucleotidyl transferase (end labeling).

I) **Enzymatic labeling:** Cellular DNA is labeled with modified nucleotides (*e.g.*, biotin-dUTP, DIG-dUTP, fluorescein-dUTP) using exogenous enzymes (*e.g.*, terminal transferase, DNA polymerase). This labeling detects extensive DNA strand breaks.

II) **Staining with fluorochromes:** Cellular DNA is stained with fluorescent DNA-binding dyes (DNA-fluorochromes) capable of intercalating into DNA. Upon binding to DNA these dyes become highly fluorescent.

Apoptotic cells are binding less dye molecules, since they characteristically lose DNA during the staining process.

Nick translation: DNA polymerase I catalyzes the template dependent addition of nucleotides when one strand of a double-stranded DNA molecule is nicked. Theoretically, this reaction (*In Situ* Nick Translation, ISNT) should detect not only apoptotic DNA, but also the random fragmentation of DNA by multiple endonucleases occurring in cellular necrosis.

End labeling: Terminal deoxynucleotidyl transferase (TdT) is able to label blunt ends of double stranded DNA breaks independent of a template. The end-labeling method has been termed TUNEL (TdT-mediated X-dUTP nick end labeling). Cells undergoing apoptosis were preferentially labeled by the TUNEL reaction. To allow exogenous enzymes to enter the cell, the plasma membrane has to be permeabilized prior to the enzymatic reaction. To avoid loss of LMW DNA from the permeabilized cells, the cells have to be fixed with formaldehyde or glutaraldehyde before permeabilization. This fixation crosslinks LMW DNA to other cellular constituents and precludes its extraction during the permeabilization step.

Fig 3.5: End labeling of DNA fragments

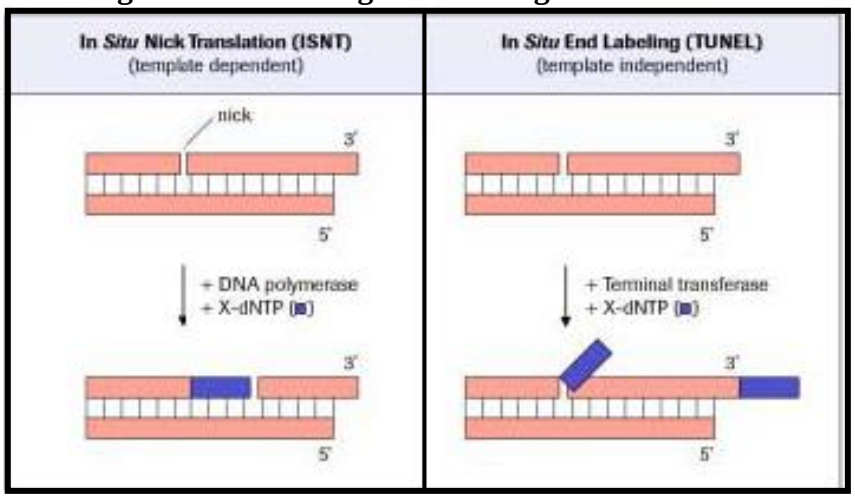

Protocol for TUNEL assay in RPE cultures:

- ❖ RPE cultures after the experimental conditions were fixed in 2% paraformaldehyde for 30 minutes.
- ❖ Cells were permeabilized with 0.1% Triton X-100 in 0.1% sodium citrate for 2 minutes at 4° C.

- ❖ They were incubated in TdT together with dUTP-FITC at 37°C for 60 minutes.
- ❖ To determine the percentage of apoptotic nuclei, TUNEL- (FITC) cells were visualized by fluorescence microscopy and counting was performed from digital images after contrast enhancement by computer.

3.16 MEASUREMENT OF INTRACELLULAR REACTIVE OXYGEN SPECIES

The extent of cellular oxidative stress was estimated by monitoring the generation of reactive oxygen species (ROS) using the fluorescent dye DCFH-DA. This technique is used for measuring 'oxidative stress' in living cells. In addition to peroxidase/H_2O_2, several species cause DCFH oxidation, including $RO_2^{\bullet}$, $RO^{\bullet}$,$OH^{\bullet}$, HOCl, and $ONOO^-$, but not $O_2^{\bullet-}$ or H_2O_2. This 'fluorescent imaging' is an assay of generalized 'oxidative stress' rather than of production of any particular oxidizing species, and it is not a direct measure of H_2O_2.

Cells were plated 24 hours before initiation of the experiment at a density of 5000 cells per well in 96-well plates. Cells were loaded with DCFH-DA at a final concentration of 50 μM for 45 minutes. After incubation, DCFH-DA was removed, and the cells were washed twice with 1X PBS (pH 7.4) and incubated with DMEM/F12 containing 1 % FBS with a bolus dose of tBH (50 and 100 μM) for 10 to 60 minutes, DCFH-DA fluorescence was determined at an excitation of 485 nm and an emission of 538 nm, by microplate-reader. Values were normalized to the percentage in untreated control groups. "DCFH-DA is taken up by cells and tissues, usually undergoing deacetylation by esterase enzymes. Oxidation of DCFH within cells leads to fluorescent dichlorofluorescein, is measured at emission 525 nm and excitation 488 nm.

3. 17 HIGH PERFORMANCE LIQUID CHROMATOGRAPHY FOR HOMOCYSTEINE

The principle of liquid chromatography is that the separation takes place in a column containing the chromatographic material in the form of small silica particles, which is referred to as stationary phase. The stationary phase used is

octadodecyl silicane (ODS). The solvent is pumped through the particle bed. By this, sample components dissolve in the mobile phase in continuous manner. A solvent delivery is connected to the column in order to feed it with fresh mobile phase. The system consists of a pump and a solvent mixing device for gradient elution. A device for applying a precise volume of sample is inserted just prior to the column via an injection loop. After passing through the column, the separated components are monitored by a detector, before ending up as separate fractions in the chromatogram.

3.17.1 Principle of Precolumn derivatization of homocysteine using OPA:

Homocysteine is treated with iodoacetic acid for alkylation of – SH group at pH 11.5 followed by reaction with OPA and β mercaptoethanol to form an isoindole derivative. This is detected using a fluorescent detector at Excitation 330nm and Emission 450nm. (Tcherkas et al., 2001).

Figure 3.6: Reaction of Hcy with Iodoacetic Acid and Ortho pthalaldehyde

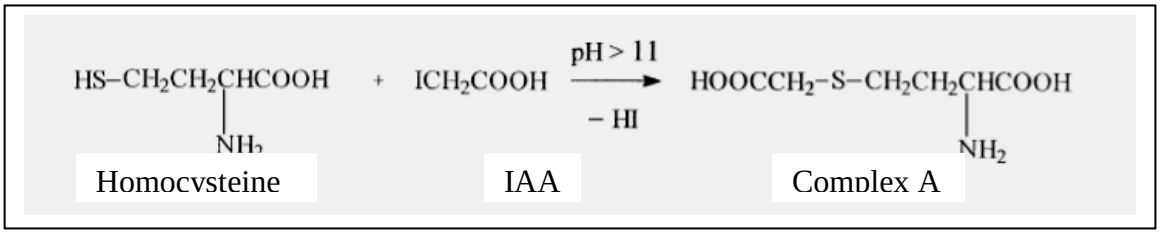

Then OPA –2 – ME was added

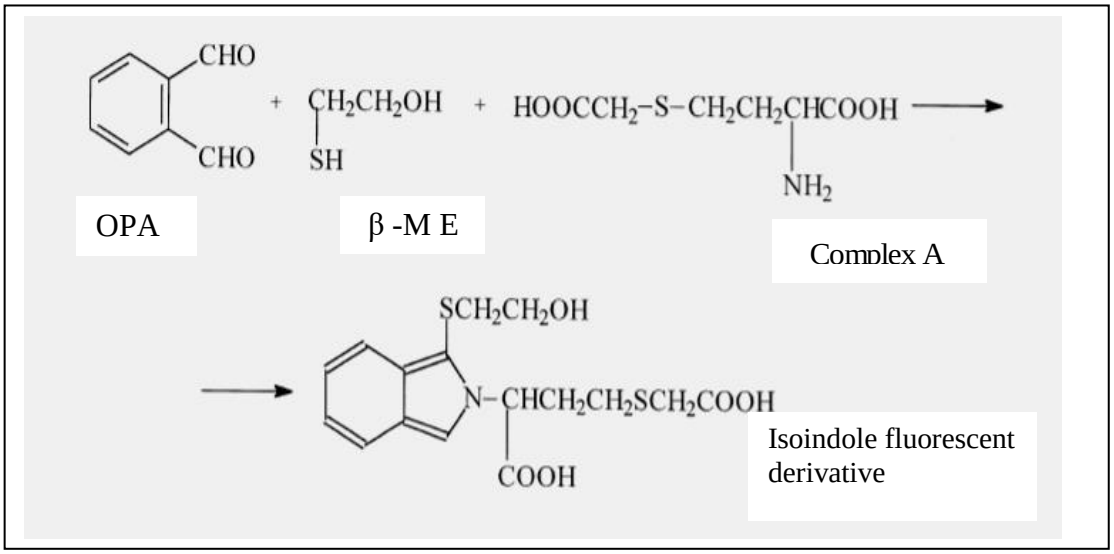

3.17.2 Processing of standard:

Working intermediate standard: From the stock standard, working intermediate standards (S1 to S4) ranging from 5-20 µg/ml was prepared as given in the flow chart below and is processed for derivatization.

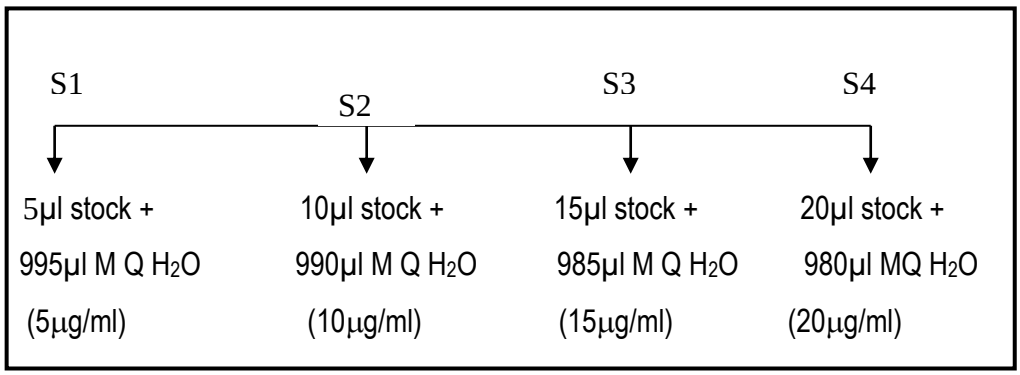

The above intermediate working standards where proceeded for derivitasation

To 20µl of intermediate standard

↓

Added 40µl IAA +120µl of borate buffer pH 11.5

↓ Mixed and Incubated at Room temperature for 1 min

Added 20µl of working OPA

↓ Mixed and Incubated at Room temperature for3min

50 µl injected is injected into HPLC which corresponds to the following concentration

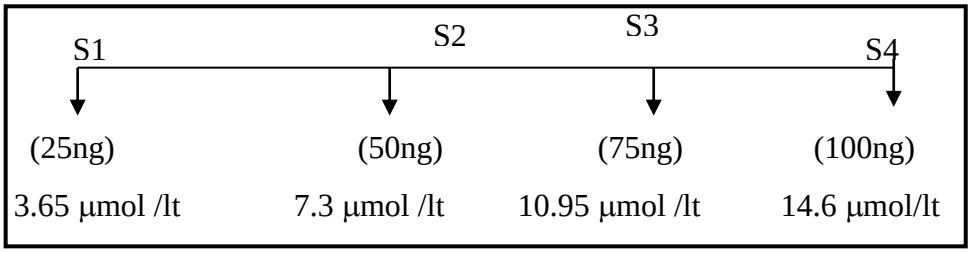

Liquid chromatography parameter:

Pressure –400 bars

Temperature - 26˚ C

Flow rate – 0.7ml / min

Detector – fluorescence

Excitation –330 nm

Emission – 450 nm

Injection volume - 50µl

Mode - isocratic

Time – 12 min

3.17.3 Processing of vitreous samples:

To 20µl of sample
↓
Added 2µl of β – mercaptoethanol
↓ Mixed and kept at RT for 30 sec
Added 40µl IAA +120µl of borate buffer pH 11.5
↓ Mixed and Incubated at Room temperature for 1 min
Added 20µl of OPA
↓ Mixed and Incubated at Room temperature for3min
50µl injected to HPLC

3.17.4 Method standardization:

Calibration: Varying concentrations of DL homocysteine standard (25-100ng) was used as calibrators.

Sensitivity - The sensitivity of the assay was based on the concentration of homocysteine detected in plasma and ocular fluid specimen.

Specificity – The specificity of the analysis was determined by spiking the sample with known concentration of standard Hcy, which results in a net increase in area proportionate to the standard concentration.

Inter-assay variations- this was done by repeating the analysis of the same standard concentration of Hcy (50ng), 'three times' in similar conditions.

Intra-assay variations – this was calculated taking the area of the Homocysteine standard (50ng) injected on different days "10 times' under different conditions.

Percentage recovery: The mean % recovery was calculated by spiking the specimen with known concentration of standard Hcy.

Figure 3.7: HPLC chromatograms of DL Homocysteine standards using Fluorescence Detector

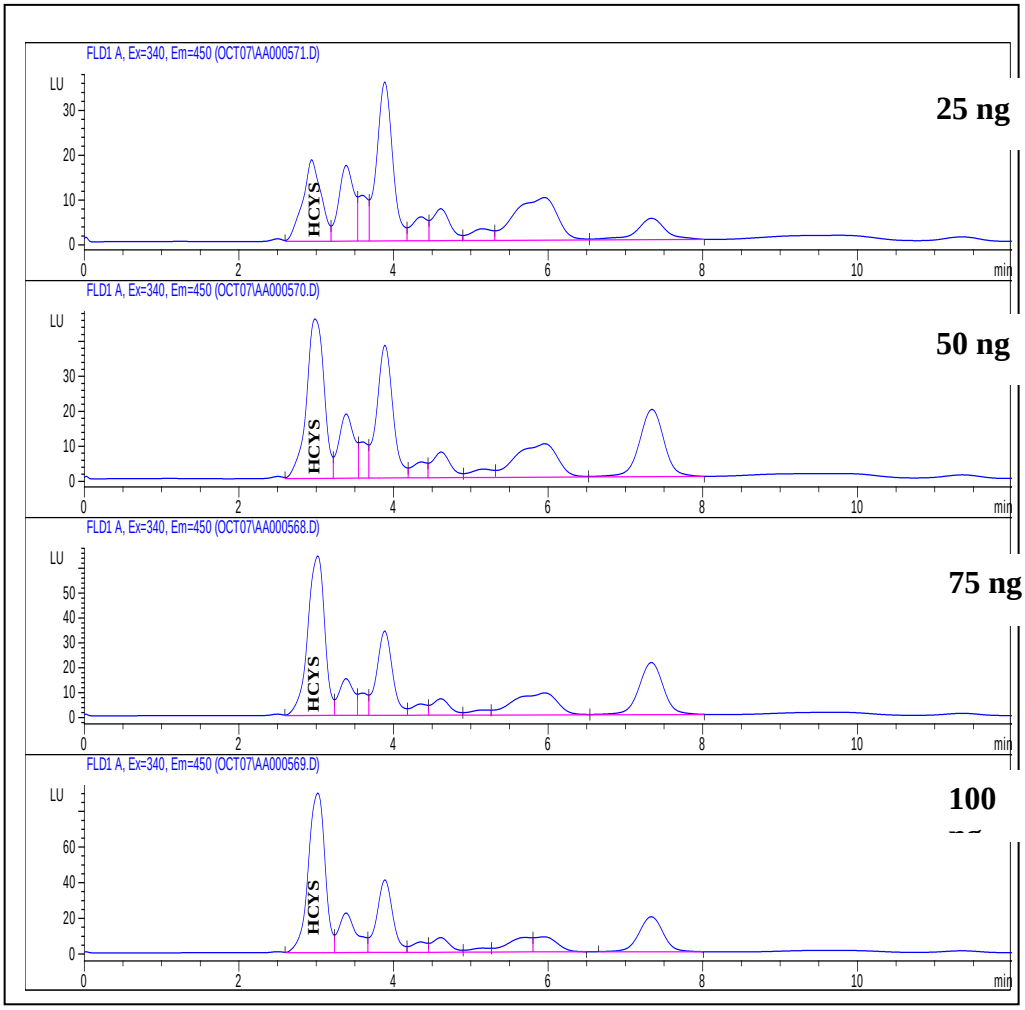

Retention time in minutes

Figure 3.8: HPLC calibration curve of DL Homocysteine standards using Fluorescence Detector

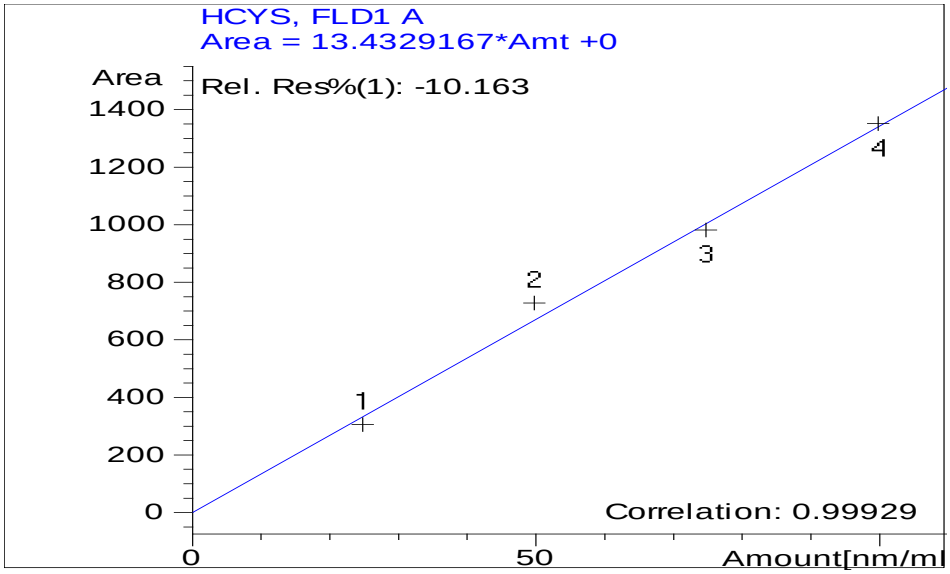

CHAPTER 4 - OCULAR TISSUE DISTRIBUTION OF LYSYL OXIDASE

4.1 INTRODUCTION

Connective tissue structures are present in all organs, and they form specialized tissues such as cartilage, bone and tendon. Connective tissues are composed of relatively few cells and an abundant extracellular matrix (ECM) (Engel et al., 1991). In most connective tissues, ECM consists of a highly regulated tissue-specific scaffold of collagens and elastin. Proteoglycans (PGs), glycoproteins and non-collagenous proteins are associated with this scaffold, building up large supramolecular structures of different combinations (Rubin et al., 1998). One of the characteristic features of ECM is that they possess a precise temporal and spatial organization relevant to the physiological function. Cells interact with ECM components and structures via specific receptors, especially integrins (Rubin et al., 1998; Heino, 2000). ECM is under constant remodeling, but the turnover rates of different components are quite divergent. In general, the half-life of collagen molecule is very long, whereas other proteins, PGs and other components turn over at a much faster rate. However, constant remodeling of ECM, i.e. simultaneous degradation and synthesis of matrix components, is an essential feature of all connective tissues

4.1.1 Collagen and Elastin: Collagens form a multigene family with at least 39 members, the genes for which are known to be dispersed throughout at least 15 chromosomes. Collagens are structural proteins of the extracellular matrix, and are the most abundant proteins in the mammalian body. Collagen molecules consist of three identical or dissimilar polypeptide chains, called α chains, and contain at least one triple-helical collagenous domain with repeating $(Gly\text{-}X\text{-}Y)_n$ sequences, i.e. a glycine residue as every third amino acid, with the frequent presence of proline and 4-hydroxyproline in the X and Y positions, respectively. In addition to the actual collagenous domains, all collagens also contain non collagenous domains. Most collagen molecules form supramolecular assemblies, and the super family can be divided into nine different families based on their

polymeric structures as : collagens that forms fibrils (types I-III, V and XI); collagens that are located on the surface of fibrils and are called fibril-associated collagens with interrupted triple helices (FACIT and structurally related collagens, types IX, XII, XIV, XVI, XIX, XX and XXI); collagens that form hexagonal networks (types VIII and X); the family of type IV collagens found in basement membranes; type VI collagen that forms beaded filaments; type VII collagen that forms anchoring fibrils for basement membranes; collagens with transmembrane domains (types XIII and XVII); and the family of type XV and XVIII collagens. (Bateman et al., 1996; Byers et al., 2001).

Biosynthesis of collagen :

The biosynthesis of the precursors of fibrillar collagens, called procollagens, involves a number of posttranslational modifications. The intracellular modifications require five specific enzymes: three collagen hydroxylases (Kivirikko et al., 1998 a) and two collagen glycosyltransferases. Once outside the cells, the procollagen molecules undergo proteolytic conversion to collagen molecules. The collagen molecules form fibrils and interact with noncollagenous and collagenous proteins, and the fibrils are stabilized by the formation of intra- and intermolecular cross-links. These extracellular modifications of collagens require two specific proteinases to cleave the N- and C - terminal propeptides and specific oxidases to convert certain lysine and hydroxylysine residues to their reactive aldehydes. (Kivirikko et al., 1989; 1998; Bateman et al., 1996: Kagan 2000).

Elastin :

Elastin is the most important component of the elastic fibres found in the extracellular matrix and provides elasticity and resilience to tissues, with the ability to deform repetitively and reversibly. Ultra structurally, elastin fibers consist of two major elements: an amorphous component made up of elastin and fibrillar component called microfibrils, which serve as a scaffold for the incorporation of elastin into the amorphous component (Cleary & Gibson 1996). Elastin is an extremely insoluble protein due to its extensive cross linking at lysine residues, and it is the most hydrophobic proteins known.

In higher vertebrates, including humans, over 30% of the amino acid residues in elastin are glycine residues and approximately 75 % of the entire sequence is made up of just four hydrophobic amino acids - glycine, valine, alanine, and proline. Tissues rich in elastin include the aorta and large blood vessels (28-32% of the dry mass), lungs (3-7%), elastic ligaments (50%), tendons (4%), and skin (2%) (Vrhovski et al., 1998).

Biosynthesis of Elastin :

Tropoelastin, the precursor of elastin, is encoded by a single gene located on chromosome 7q11 in humans and has at least 11 variants due to alternative splicing of the transcripts (Vrhovski et al., 1998). Tropoelastin undergoes only minor posttranslational modifications, and there is no evidence of glycosylation. Hydroxylation of proline residues occurs to a variable extent, 0-20%, but this hydroxylation is not necessary for the synthesis of the elastic fiber (Vrhovski et al., 1998). After translation of tropoelastin, a 67 kDa elastin-binding protein becomes bound to tropoelastin, acting as a chaperone and preventing premature intracellular aggregation of tropoelastin molecules. This association lasts until the complex has been secreted into the extracellular space, where the elastin-binding protein interacts with galactosugars of the microfibrils. At this point the affinity of the elastin-binding protein for elastin decreases dramatically, leading to the release of the tropoelastin molecule into the microfibrilar scaffold. Before tropoelastin is assembled into the amorphous component of the elastic fiber, it becomes covalently cross-linked by lysyl oxidase, which has been found to be associated with microfibrils (Kagan et al., 1986,2003).

4.1.2 Crosslink's in collagen and Elastin: In spite of the major structural differences between collagens and elastin, both proteins contain lysine or hydroxylysine derived covalent cross-links, the formation of which is catalyzed by the family of lysyl oxidase enzymes. The locations of these cross-links depend on the amino acid sequence and quaternary structural arrangements. (Siegel et al., 1974; Kagan et al. 1984; Nagan et al., 1994; Kielty et al., 1993; Smith-Mungo et al 1998). Lysyl oxidase oxidatively deaminate certain lysine and hydroxylysine residues in collagens and lysine residues in elastin to form the corresponding α-

aminoadipic-δ-semialdehydes, usually referred to by their trivial names as allysine and hydroxyallysine. (Figure 4. 1)

Figure. 4. 1. Reaction of lysyl oxidase

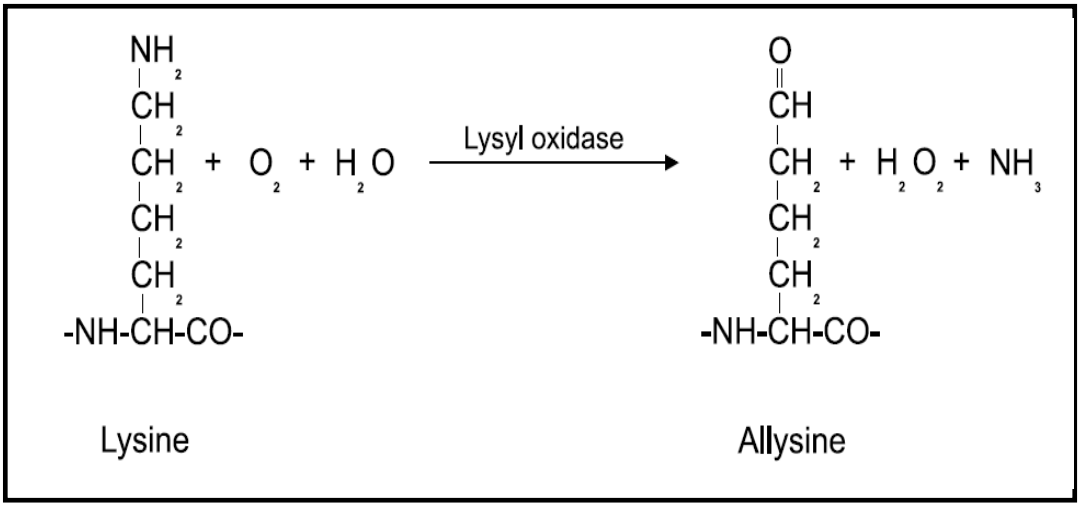

Figure 4.1 shows the reaction in which Lysyl oxidase oxidatively deaminates a peptidyl lysine to generate a peptidyl α- aminoadipic-δ-semialdehyde (allysine), which spontaneously reacts with corresponding aldehydes to form various di-, tri-, or tetrafunctional cross-links (Kagan et al., 1986).

In collagens, the lysine and hydroxylysine-derived cross-links are essential in providing the tensile strength and mechanical stability of the collagen fibrils and other supramolecular assemblies (Bateman et al., 1996; Bailey et al., 2001). Two related cross-linking pathways can be distinguished for collagens because the oxidations are restricted to two specific lysine and hydroxylysine residues, one in each of the N- and C-terminal telopeptide sequence to form allysine (aldehyde) (Eyre et al., 1984; Kagan 1986, 1994; Reiser et al., 1992; Kielty et al., 1993). The lysine aldehyde pathway occurs primarily in the adult skin, cornea, and sclera (Eyre 1987), whereas the hydroxylysine aldehyde pathway occurs primarily in the bone, cartilage, ligament, tendons, embryonic skin, and most major internal connective tissues of the body (Kielty et al. 1993). Oxidative deamination is followed by spontaneous condensation reactions that result in various bi-tri-, and tetrafunctional cross-links (Figure 4.2A). Lysine- and hydroxylysine derived aldehydes can react with corresponding aldehydes on adjacent polypeptide chains forming aldol condensation products, or with unmodified lysine and hydroxylysine residues, forming bifunctional cross-links, such as

lysinonorleucine and hydroxylysinonorleucine. The aldol condensation products can also react with a histidine residue to form aldol histidine, which may further react with an additional lysine residue to form the tetrafunctional cross-link histidinohydroxymerodesmosine (Reiser et al., 1992). In the hydroxylysine pathway, the bifunctional cross-links spontaneously undergo an Amadori rearrangement, resulting in ketoimine cross-links, which then mature further into trifunctional 3-hydroxypyridinium and lysyl pyridinium cross-links (Reiser et al., 1992, Bailey et al., 1998, Byers et al., 2001).

Figure 4.2: Reactions of lysine and hydroxylysine in the biosynthesis of the cross-links in collagen (A) and elastin (B)

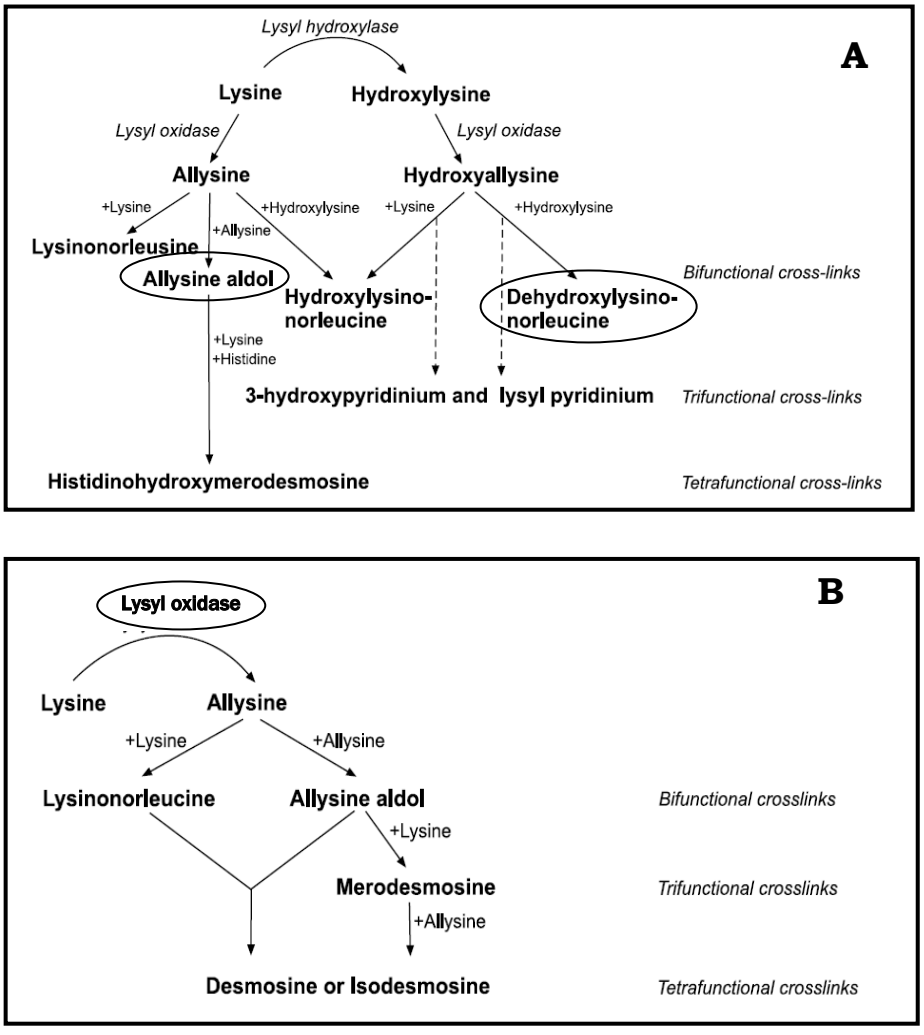

Figure 4.2: Reactions of lysine and hydroxylysine in the biosynthesis of the cross-links in collagens (A) and elastin (B). After oxidative deamination to form

reactive aldehydes, subsequent condensation reactions result in various bi-, tri-, and tetrafunctional cross-links.

The most important feature of elastin which crucial for its proper functioning of elastic fibers, is the high degree of cross-linking of the individual polypeptide chains (Kielty *et al*. 1993). Approximately 30 of the 40 lysine residues per 1000 amino acids are present in tropoelastin, are oxidated to aldehydes (Eyre *et al.* 1984, Kagan 1986, 1994, Reiser et al. 1992). Tropoelastin differs from collagens in that it has no hydroxylysine or histidine residues, and therefore only lysine-derived cross-links are found in mature elastin (Bedell-Hogan et al., 1993). In addition, certain condensation products, such as desmosines and isodesmosines, are specific for elastin and are not found in collagens (Reiser et al., 1992; Kielty et al., 1993; Bedell-Hogan et al., 1993). The cross-links in elastin are otherwise formed in a similar manner as those in collagens (Figure 4.2B). Two allysines can form an aldol condensation product, and one allysine can form lysinonorleucine with an unmodified lysine residue. Aldol condensation of the product with an unmodified lysine residue results in the trifunctional merodesmosine. Further condensation of a dehydrated aldol condensation product with dehydrolysinonorleucine, or reaction of merodesmosine with allysine results in the tetrafunctional desmosine and isodesmosine cross-links (Reiser et al., 1992; Bedell-Hogan et al., 1993). Thus LOX is a crucial enzyme for the cross linking seen in collagen and elastin. Five human LOX isoenzymes have been characterized. The contribution of each isoforms to collagen and elastin cross-linking is still unknown. The inactivation of the first described gene, LOX gene, leads to the death of homozygous mice at parturition or within the first few hours after birth (Honstra et al.,2003). Death is due to rupture of arterial aneurysms and diaphragm. Microscopic analysis of the aorta showed fragmented and disorganized elastic fibers whereas the number and diameter of collagen fibers appeared unchanged. The desmosine content of the aorta and lung was decreased by 60% and total body immature collagen cross-links (dihydroxy- and hydroxylysinonorleucine) were reduced by 40%. Thus LOX appears to play a central role in the development and function of the cardiovascular system and diaphragm. The role of the other four lysyl oxidase-like (LOXL) isoforms remains to be elucidated in cross linking.

Various disease processes, such as inflammatory reactions, neovascularisation and tumor dissemination takes place in the connective tissue. In pathological processes, balanced interactions between cells and the ECM are disturbed resulting in loss of local homeostasis (Freeman 1982; Rubin et al., 1998).

4.1.3 Ocular collagen and elastin:

The important role of ECM for the normal function of the eye is reflected by diseases in which they have been linked either to mutations in specific components of ocular ECM or to degenerative changes in ocular connective tissues (Snead et al., 1996; Bishop 2000). In human eyes, elastin is a major component of Bruch's membrane, lamina cribrosa, blood vessels, and conjunctival stroma. The normal distribution of various types of collagen in ocular tissues is given in table 4.1.

Table 4.1 : The distribution of collagen types in ocular tissues.

S.No	Ocular tissue	Type of collagen
1	Cornea Adult	III, V, VI
2	Cornea -Embryogeneis	I - IX
3	Sclera	I, III, V, VI, VIII
4	Trabecular meshwork	I, III, IV, V, VI, VIII
5	Iris	I, III, IV, VI
6	Ciliary body	I, III, IV, VI
7	Lens capsule	I, III, IV
8	Vitreous	II, IX, IV, V/XI
9	Retina	I, III, IV, V, VI
10	Choroid	I, III, IV, V, VIII
11	Optic nerve	I, III, IV, V, VIII

LOX and LOX like proteins have been co-localized in the skin, aorta, heart, lung, liver, cartilage, kidney, stomach, small intestine, colon, retina, ovary, testis and brain in mouse tissues (Hayashi et al., 2004). There are very few reports showing amine oxidase activity in bovine retina and sclera (Zuo et al., 1994), including a report on the presence of human retina specific amine oxidase in retinal ganglion cell layer (Imamura et al., 1998).With the knowledge on ocular collagen and elastin content and the pathology due to defect in these, the literature search had very little information on the LOX in human ocular tissues both in normal and pathological conditions. Hence the first objective of this thesis was to see the ocular tissue distribution of LOX in human donor eye balls.

4.2 MATERIALS AND METHODS:

4.2.1 Procurement of donor eyeball:

All experiments involving human subjects adhered to the tenets of Helsinki declaration. Human donor eye balls from CU Shah Eye bank, Sankara Nethralaya, India, was used after light microscopic examination and cornea removal (Age 65 ± 9 :M=7:F=3), for determining specific activity of LOX (n=10), real time gene expression and immunohistochemistry (n=5). Donors with

past history of diabetes, hypertension, carcinoma and sepsis were not included in the study. The donors had no history of ocular diseases.

4.2.2 Preparation of tissue extracts:

The eyeball was dissected and iris, ciliary body, vitreous, retina, choroid along with RPE were separated within 5 hours of death, The tissues were homogenized in 4M urea in 0.02M borate buffer, pH 8.0 at 4° C, whole vitreous jelly was homogenized at 4° C and all homogenate was centrifuged at 15000 g for 30 min at 4º C. The supernatants were analyzed immediately for LOX assay with and without BAPN (Kuivaniemi , 1985 b).

Activity assays for detection of LOX was performed as described in methodology chapter. Briefly 100 μg of protein was added to the final reaction mix in the presence or absence of 500 μM BAPN (Palamakumbura et al., 2002). The specific activity was calculated and expressed in terms of μmol/min/mg protein.

4.2.3 RNA extraction and reverse transcription

The eyeball was dissected and iris, ciliary body, (iris and ciliary body were processed separately unlike in activity assay) retina, choroid along with RPE were separated within 2 hours of death. Total RNA was extracted from different ocular tissues by the guanidine isothiocyanate and chloroform method. All RNA samples were treated with TURBO DNase to remove DNA contamination. For all samples 1μg of total RNA was used to synthesize first-strand cDNA using SuperScript II reverse transcriptase and random primers as given in methodology chapter.

4.2.4 Real-time PCR analyses

TaqMan gene expression assays for LOX (Hs00184706_m1) and two endogenous controls, GAPDH (Hs99999905_m1) and TBP (Hs99999910_m1), were obtained from Applied Biosystems. Quantification of gene expression was performed in a 20 μl volume in 96 well plates on an ABI prism 7300 real time PCR System, in triplicate. Each reaction included 1× TaqMan primer probe mix, 1× TaqMan Universal PCR Master Mix and 100ng of cDNA.

Cycling conditions were as follows:

2 min at 50° C, 10 min at 95° C and 40 cycles of 15s at 95° C plus 1 min at 60° C. The retina was used as the calibrator for comparison with other ocular tissues. The normalization factor for each sample was calculated by taking the geometric mean of the two housekeeping genes (GAPDH and TBP) quantities using geNorm software. Expression levels of the gene of interest (GOI) were calculated by dividing the GOI quantities for each sample by the appropriate normalization factor (Bustin et al., 2005).

4.2.5 Immunohistochemistry

Paraffin sections (5 μm) of donor eyeball were incubated with trypsin-EDTA for 30 minutes and washed with TBS. Further steps were carried out with NovolinkTM Min polymer detection system as described in methodology chapter. (Wakasaki et al.,1990).

4.3 RESULTS

4.3.1 Ocular tissue distribution

The analysis of specific activity of total LOX in the human donor eye ball was found to be the highest in vitreous 1.29 ± 0.33 μm/min/mg protein followed by iris ciliary body (ICB), 1.15 ± 0.36 μm/min/mg protein; Lens, 0.4 ± 0.07 μm/min/mg protein; Choroid with retinal pigment epithelium (CRPE), 0.35±0.06 μm/min/mg protein and retina 0.2 ± 0.03 μm/min/mg protein. (Figure 4.3)

Figure 4.3: Specific activity of lysyl oxidase in ocular tissues

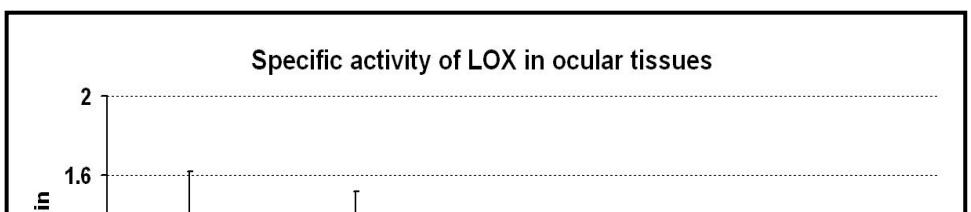

Figure 4.3: shows the specific activity of lysyl oxidase in ocular tissues (n=10).

Values are expressed as mean ± standard error mean.

ICB-Iris ciliary body, CRPE-Choroid along with retinal pigment epithelium.

4.3.2 Real time PCR analyses : mRNA quantification of LOX expression using TaqMan gene expression assay after normalizing with two endogenous controls (GAPDH and TBP) showed the least expression in retina compared to iris, choroid RPE and ciliary body. (Figure 4.4)

Figure 4.4: Lysyl oxidase mRNA expression in human ocular tissues

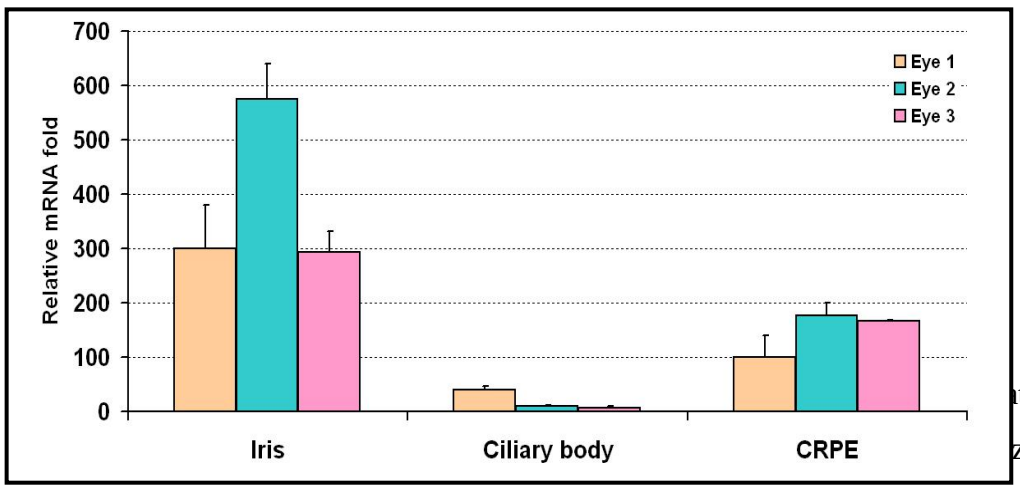

ıted

zed

against GAPDH and TBP. Each bar represents LOX expression in individual eye balls (Eye 1,2,3). CRPE-Choroid RPE.

4.3.3 Immunohistochemistry: Immunolocalisation of LOX (Figure 4.5) showed cytoplasmic and stromal positivity in cornea, iris, ciliary body, lens epithelial cells, choroid with RPE**,** optic nerve head, sclera and retinal photoreceptor cells. The negative control showed no reaction. Thus in the donor eye balls studied the specific activity, mRNA expression and localization of LOX in different ocular tissues showed a relatively similar distribution.

Figure 4.5: Immunolocalisation of LOX protein in paraffin embedded section of normal human donor ocular tissue

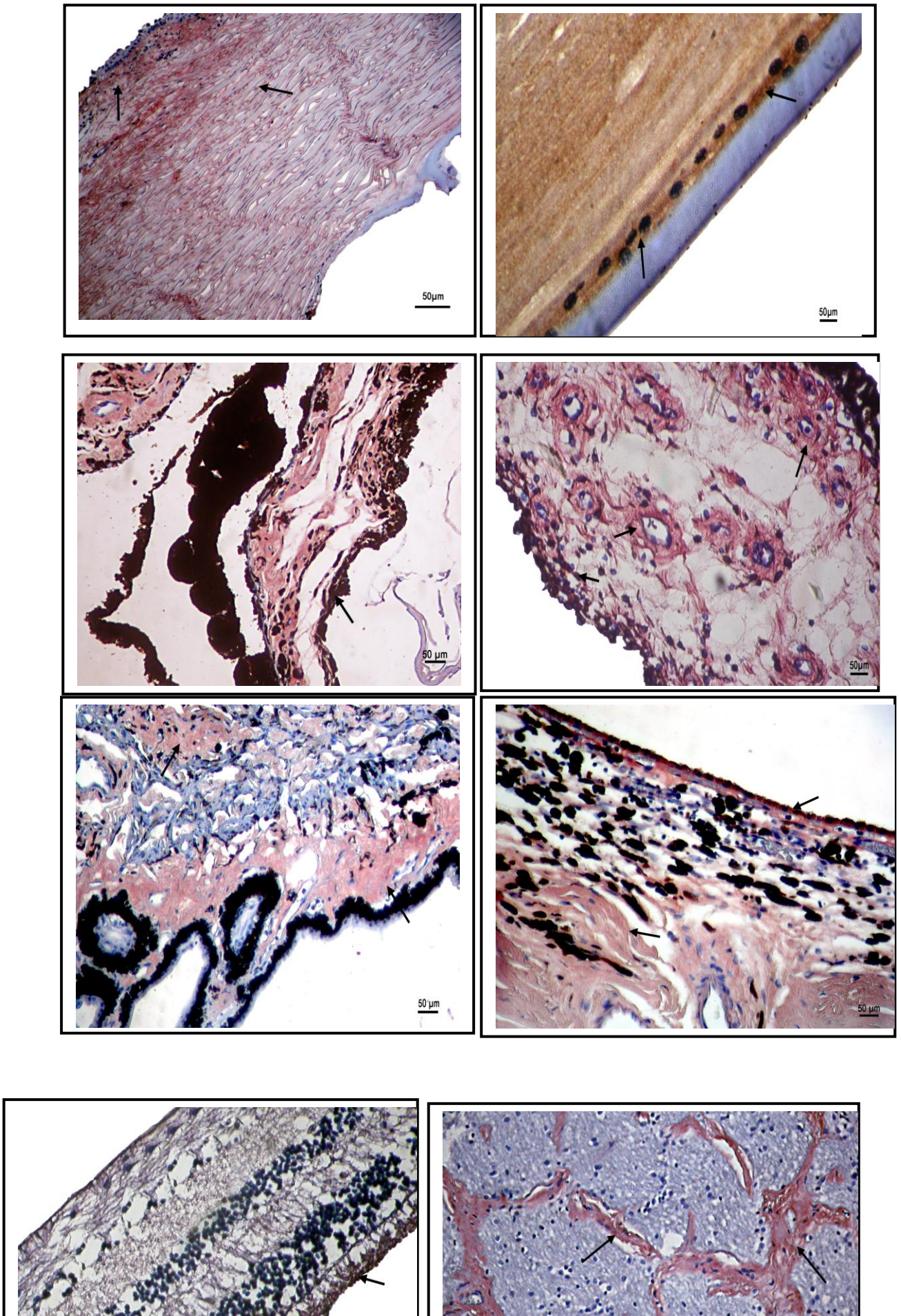

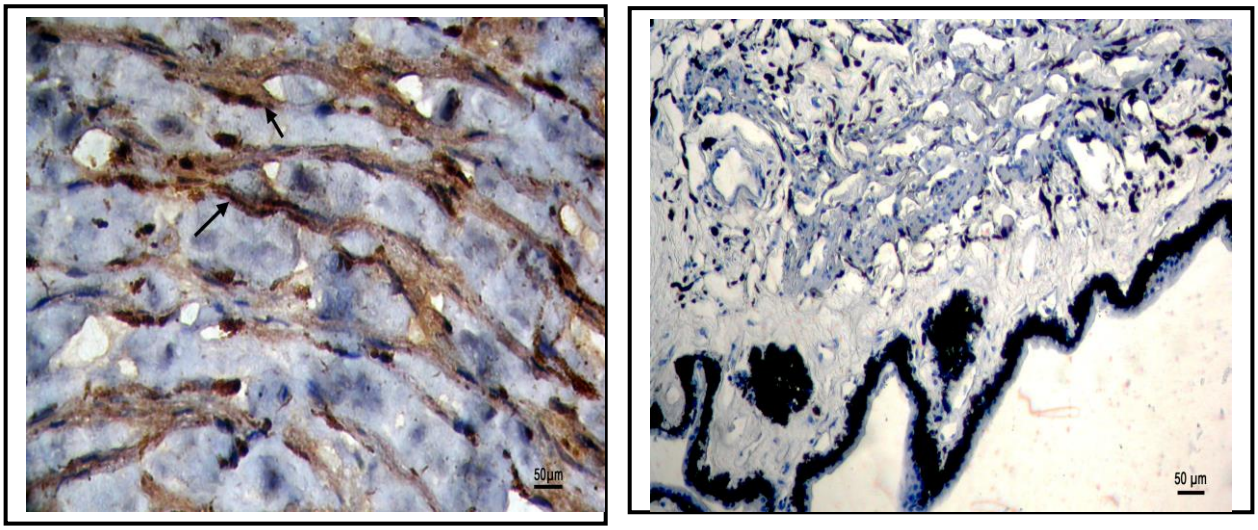

Figure 4.5: Immunolocalisation of LOX protein in paraffin embedded section of normal human donor ocular tissue by labeled streptavidin biotin method. Positive labeling seen as (reddish brown staining) is shown as arrow in cornea (1) lens (2), iris (3), ciliary body (4 and 5), choroids with RPE (6), retina (7), optic nerve head (8), sclera (9) and negative control (10) by omission of primary antibody (10). Haematoxylin was used as counter stain. Scale bar 50 µm.

4.4 CONCLUSION:

This is the first report showing LOX distribution in terms of its specifc activity and immunolocalization in ocular tissues. The variation in the specific activity of LOX in different ocular will be helpful in finding out the changes at the level of ECM in ocular pathology and therefore could be a target for intervention.

CHAPTER 5 - LYSYL OXIDASE ACTIVITY IN VITREOUS OF PROLIFERATIVE DIABETIC RETINOPATHY AND RHEGMATOGENOUS RETINAL DETACHMENT

5.1 INTRODUCTION

The extra-cellular matrix represents a heterogeneous group of macromolecules, including collagen, non-collagenous glycoproteins, elastic fibers and proteoglycans. The ECM is under constant remodeling by simultaneous degradation and synthesis of matrix components with different turnover rates. Various disease processes such as inflammatory reactions and neovascularization occur in the ECM (Rubin et al., 1998). The structural integrity of ECM depends on the collagen and elastin cross links. During the formation of inter molecular cross-links, collagen fibers become increasingly insoluble, more refractory to the action of enzymes and show a progressive increase in tensile strength (Vater et al., 1979). This is essential for normal connective tissue function, and wound healing.

In vitreoretinal diseases such as proliferative diabetic retinopathy (PDR) and rhegmatogenous retinal detachment (RRD) there is extensive ECM pathology (Sivak et al, 2002). PDR is a common complication of diabetes mellitus characterized by preretinal neovascularization and development of epiretinal fibrovascular traction and retinal detachment (Frank., 1991) PVR is an intraocular wound healing disorder characterized by a breakdown of the blood retinal barrier, cellular proliferation, and extra cellular matrix production on the retinal surface and undersurface in the subretinal space, and in the vitreous cavity that leads to formation of subretinal and epiretinal membranes (Hooymans JM., 2000). (Figure 5.1) Cell-mediated contraction of these membranes causes tangential retinal traction and fixed retinal folds. Typically, PVR occurs following surgery to repair rhegmatogenous retinal detachment (RD) or following penetrating ocular injury and associated RD. However, it may also occur in eyes with rhegmatogenous RD that have not had previous vitreoretinal surgery.

Figure 5.1: Fundus Images of Retina in Normal and Disease Conditions

Prolefartive diabetic retinopathy **Rhegmatogenous Retinal detachment**

Normal Fundus

Epiretinal membranes (ERMs) are often observed in eyes with PDR and PVR. The ERMs in PVR are composed of numerous RPE cells, macrophages or other inflammatory cells, and a variety of extracellular proteins (Hiscott et al., 2002). Several collagen subtypes, including types I to V, may be present in epiretinal membranes (Scheiffarth et al., 1988, Jerdan et al., 1989; Morino et al., 1990). The presence of collagen types in membranes which are not normally found in the vitreous implies that the cells in the membranes synthesize the collagen. In general, PVR is considered to be a proliferative vitreoretinal disorder that is not related to retinal neovascularization. However, previous studies have indicated that some PVR membranes may be accompanied by a vascular component (Asiyo-Vogel et al., 1998). ERM in PDR has also been shown to contain Types I,

II, III, IV and V collagen. There are also glial cells, pigment epithelial cells and myofibroblast present in the membrane. (Hiscott et al., 1994)

Collagen turnover in vitreous has been shown to be associated with ageing and vitreoretinal diseases, which predisposes to posterior vitreous detachment (Halfter et al.,2008, Itakura et al.,2005; Sebag 2004).Hydroxyproline levels are used to predict collagen turnover status and most of the endogenous hydroxyproline present in biologic fluids is derived from the degradation of various forms of collagen (Ozyurt et al., 2003; Simsek et al., 2004).

The matrix metalloproteinases (MMPs), a ubiquitous family of enzymes, are known to play a role in the degradation of the ECM (Sethi et al., 2000;Monica etal.,1998). MMP 2 (72-kDa gelatinase) is constitutively found in normal human vitreous, where it is complexed with TIMP-2 (Brown et al., 1994) and MMP 9 (92-kDa gelatinase) is constitutively expressed in the retinal ganglion cell layer (Sivak et al., 2002). These MMPs degrade denatured collagen (gelatin) and type IV collagen. Many MMPs have been reported in retinal pathology (Sivak et al., 2002), characteristic changes in the levels of MMP 2 and 9 activity attributing to ECM remodeling have been reported in both PDR (Jin et al., 2001; Noda et al., 2003; De La Paz et al., 1998) and RRD. (Abu El-Asrar et al., 1998; Kon et al., 1998)

Although collagen turnover in vitreous has been associated with vitreoretinal diseases and the synthesis of collagen by cells in the ERM has been reported, there are no reports on the collagen cross links in terms of lysyl oxidase activity in vitreous and epiretinal membranes in pathological conditions.

Hence in this chapter we estimated the LOX activity, hydroxyproline content, MMP 2 and 9 levels in the vitreous of PDR and RRD. Immunolocalization of LOX was also done in ERMs from PVR and PDR.

5.2 MATERIALS AND METHODS

All experiments involving human subjects adhered to the tenets of Helsinki declaration. Undiluted vitreous samples from 25 patients (Age 54 ± 10: M =21

and F=4) with PDR and 18 patients (Age 48 ± 15: M =15 and F= 3) with RRD were collected by the vitreoretinal surgeon at the time of vitreoretinal surgery. In patients with PDR the clinical ocular findings were graded at the time of vitrectomy for the presence of hemorrhage, tractional retinal detachment, and presence or absence of patent new vessels on the retina or optic disc. Patients with active PDR were graded as such on the basis of visible patent new vessels on the retina or optic disc and their absence as inactive PDR. In patients with RRD the clinical ocular findings were graded at the time of vitrectomy for the presence/absence of hemorrhage, duration of vision loss before surgery, quadrant involvement, macular status and PVR grading. Clinical details of the patients are given in Table 5.1 and 5.2 given in appendix I. The samples were transported on ice and centrifuged at 3000 rpm for 10 minutes at 4º C. The centrifuged samples were frozen at -80ºC until they were assayed with correspondingly stored control specimens. Human donor eyeballs from CU Shah Eye bank, Sankara Nethralaya, India, were used as controls after light microscopic examination and cornea removal (Age 74 ± 19: M=19:F=15). Donors with past history of diabetes, hypertension, carcinoma and sepsis were not included in the study. The donors had no history of ocular diseases. The vitreous was aspirated using a needle and syringe similar to the ones used for collecting vitreous sample. Care was taken to collect vitreous within 5 hours of death from donor specimens.

5.2.1 Specific activity of lysyl oxidase: Activity assays for detection of LOX were performed as given in methodology chapter (Palamakumbura et al, 2002). Briefly 100 μg of protein was added to the final reaction mix The fluorescence was read for every 10 min for 2 hrs at 37° C using a Dynex TRIAD multimode plate reader. Specific activity expressed as LOX as nm H_2O_2 /min/mg protein and normalized to levels of total vitreous protein in each sample.

5.2.2 Hydroxyproline estimation: Hydroxyproline was measured by the method of Wosneer *et a l* (Woessner, Jr et al., 1961), Briefly to 50 μg of vitreous, 1.0 ml of 0.05 M Chloramine T was added and incubated at room temperature for 20 minutes. Then 0.5 ml of 3.5M Perchloric acid and 0.5ml of 20% p-dimethylamino benzaldehyde solution was added to the oxidized sample and the

chromophore was developed by incubating the samples at 70°C for 30 min. The absorbance was read at 550 nm using DU 640 UV/visible Spectrophotometer (Beckman, USA). A standard graph was constructed using hydroxyproline (0.2-1.0μg; R^2=0.9853) the hydroxyproline concentration in vitreous was calculated based on the standard and expressed as μg hydroxyproline/mg protein.

5.2.3 ELISA assay for total MMP 2 and MMP 9 in vitreous: Total MMP 2 and MMP 9 protein concentrations were determined in the vitreous specimen from PDR, RRD and donor eye balls by quantitative sandwich enzyme immunoassays as given in methodology chapter. The ratio of MMP 9: 2 was determined to establish the disease background documented earlier at the level of MMPs. (El-Asrar et al., 1998)

5.2.4 Immunolocalization of Lysyl oxidase in epiretinal membrane: Paraffin sections (5 μm) of the ERMs were incubated with trypsin-EDTA for 30 minutes and washed with TBS. Further steps were carried out with NovolinkTM Min polymer detection system (Novacastra laboratories ltd, NE12 8EW, UK) as mentioned in methodology chapter. (Wakasaki et al., 1990)

5.2.5 Statistics: With SPSS software, (version:14.0) the raw data was analyzed for statistical significance using independent sample *t* test. *p* value of <0.05 was considered significant. Pearsons correlation was also done.

5.3 RESULTS:

5.3.1 Specific activity of LOX in vitreous specimens obtained from PDR and RRD: The level of total protein in the vitreous was increased 3 fold in PDR (3.82 ± 0.80mg/ml) and 7 fold in RRD (8.82 ± 2.00 mg/ml) when compared to the controls (1.12 ± 0.18 mg/ml). Which is considered as a measure of the retinal barrier permeability as observed earlier by Descamps *et al.* (Descamps et al., 2006). The specific activity of LOX with and without specific inhibitor BAPN was analyzed and expressed as nmol/min/mg protein. The mean specific activity of LOX in controls was found to be 534.8 ± 162.5 nm /min/mg protein. Relative to controls, the specific activity of LOX showed a 4 fold decrease in RRD, with a

mean of 59.1 ± 20.6 nm /min/mg protein (p= 0.006) and 3.5 fold decrease in PDR with a mean of 145.1 ± 52.3 nm /min/mg protein (p=0.028) as seen in table 5.3. In summary, the specific activity of total LOX showed a strong and statistically significant 3-4-fold decrease in PDR and RRD, relative to controls. Interestingly, in both controls and diseased vitreous the BAPN inhibited LOX activity was found to be nearly 50 % of total LOX activity in control, 43 % in PDR, and 50% in RRD **(Table 5.3)**.

Table 5.3: Comparative levels of protein, lysyl oxidase and hydroxyproline in control versus diseased vitreous

Conditions	**Protein (mg/ml)**	**LOX (nm/min/mg protein)**	**Hydroxyproline (μm / mg protein)**
Control	1.12 ± 0.18	534.8 ± 162.5 (n=34)	4.55±0.74 (n=14)
PDR	3.82 ± 0.80* (*p*=0.002)	145.1 ± 52.3 * (*p*=0.028) (n=25)	14.25 ± 4.40 * (*p*=0.049) (n=13)
RRD	8.82 ± 2.00 * (*p*=0.000)	59.1 ± 20.6 ** (*p*=0.006) (n=18)	14.93 ± 3.23 * (*p*=0.007) (n=15)

Values are expressed as Mean □ SEM.
p value : Control with PDR and RRD, respectively

5.3.2 MMP 2 and MMP 9 levels in vitreous specimens obtained from PDR and RRD: When compared with controls, the MMP 9 levels showed a highly significant increase in RRD (7 fold, p=0.039) and PDR (20 fold, p=0.001). The level of MMP 2 was increased in PDR by 1.4 fold (p= 0.076) and RRD by 1. 7 fold (p=0.036) **(Table 5.4).**

Table 5.4: Levels of MMP 2 and MMP 9 in PDR and RRD compared with controls.

Conditions	MMP 2 (ng/ml)	MMP 9 (ng/ml)
Control (n=18)	49.48 ±5.00	0.132±0.031
PDR (n=14)	69.56 ±9.55 [a]p = 0.076	2.48±0.55** [b]p = 0.001
RRD (n=10)	79.87 ±11.93** [a]p = 0.036	0.92±0.329** [b]p = 0.039

MMP 2 and MMP 9 was done and the values are expressed in ng/ml. Values are expressed as Mean □ SEM.

[a] p value : Control with PDR and RRD respectively
[b]p value : Control with PDR and RRD respectively.

Since total protein levels were elevated in PDR and RRD relative to controls, we analyzed whether there is a correlation between levels of MMP 2 and MMP 9 protein with total vitreal protein in disease versus controls. A significant positive correlation was observed between levels of MMP 2 and total vitreal protein in both PDR (p = 0.021, r = 0.608) and RRD (p = 0.041, r=0.652) **Figure 5.2 and 5.3**. The levels of MMP 9 were significantly correlated with total vitreal protein in PDR (p = 0.041, r = 0.551) but not in RRD (p = 0.358, r = 0.310) **Figure 5.4 and 5.5**

Figure 5.2 : Correlation between MMP2 levels and protein in PDR

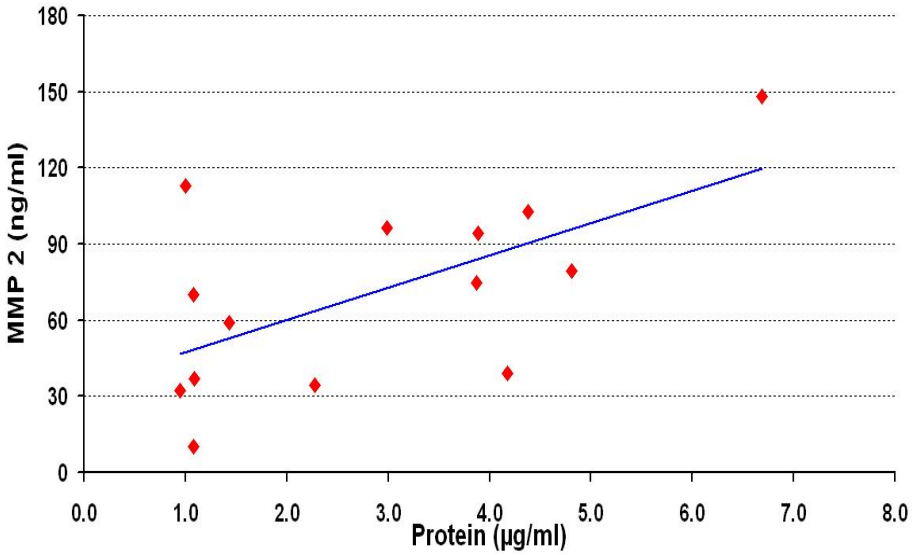

Figure 5.3: Correlation between MMP2 levels and protein in RRD

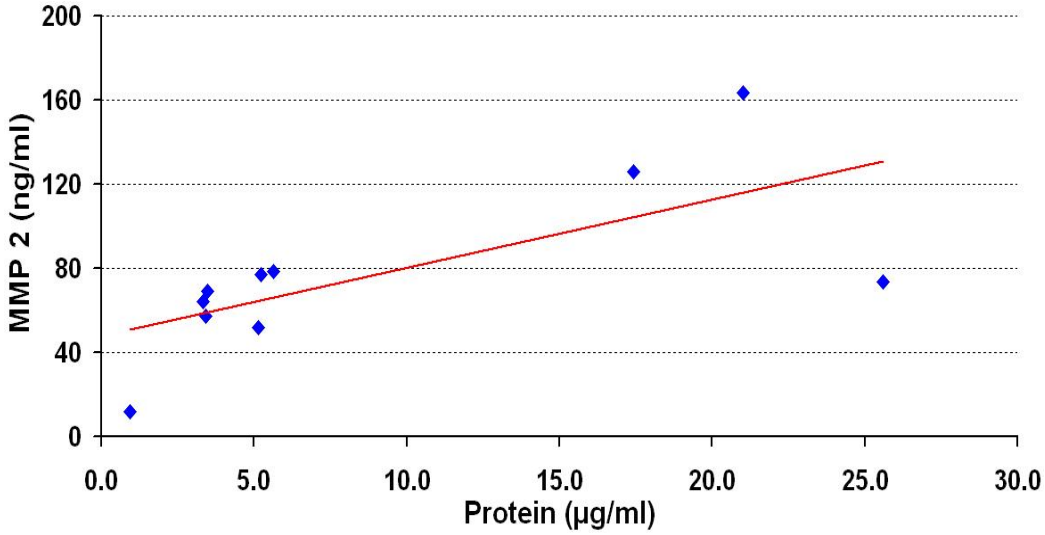

Figure 5.4: Correlation between MMP 9 and protein in PDR

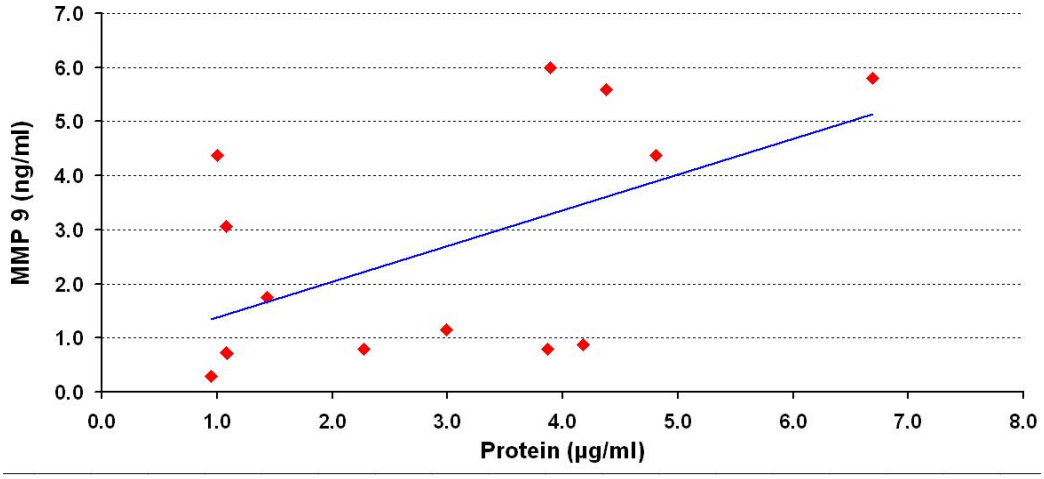

Figure 5.5: Correlation between MMP 9 and protein in RRD

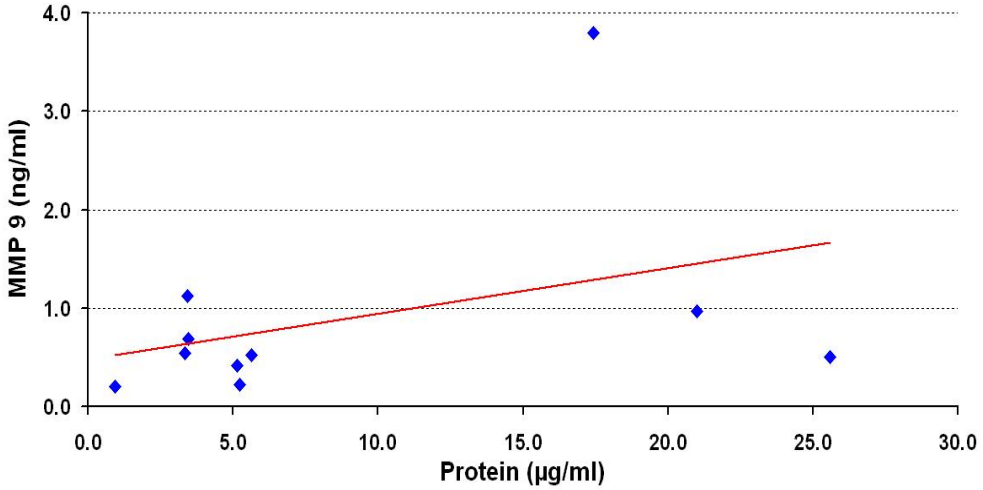

5.3.3 Ratio of MMP 9 to MMP 2 in vitreous specimens obtained from PDR and RRD: The mean MMP 9:2 ratio was highest in the vitreous samples from patients with proliferative diabetic retinopathy (0.027±0.018; p=0.000) followed by rhegmatogenous retinal detachment (0.013±0.011; p=0.004) when compared with controls (0.003±0.005). In addition, the mean MMP 9: 2 ratio from patients with proliferative diabetic retinopathy was significantly higher than in patients with rhegmatogenous retinal detachment (p = 0.035). (Figure 5.6)

Figure 5.6: Ratios of MMP 9: 2 in vitreous samples of patients with PDR, RRD and control vitreous.

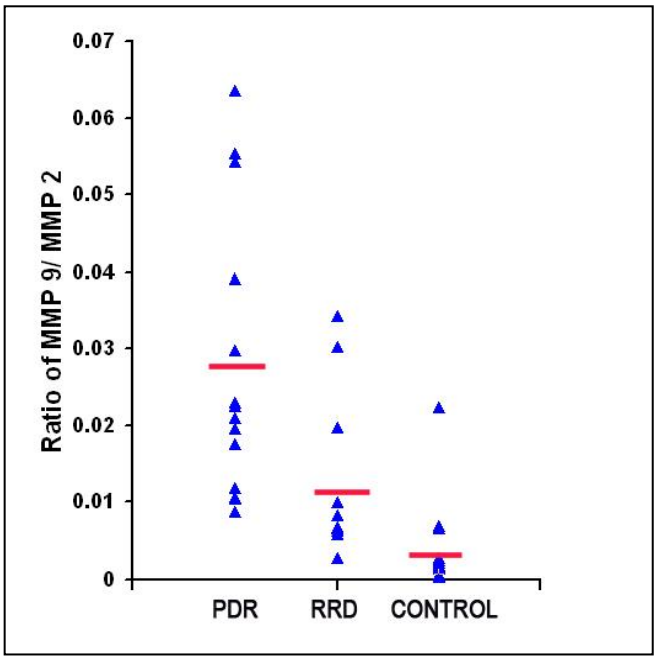

5.3.4 Hydroxyproline level in vitreous

Hydroxyproline levels which was measured to predict collagen turnover status was found to be significantly increased in PDR with a mean of 14.25 ± 4.40 μm/mg protein (p=0.040) as well as in RRD with a mean of 14.93 ± 3.23 μm/mg protein (p=0.024), compared to the control of 4.55±0.74μm/mg protein. **(Table 5.3)** The distribution profile of hydroxyproline in the vitreous was found to be in the range of 2.97 to 49.98 in PDR, 1.94 to 49.80 in RRD and 1.23 to 9.27 in control. The decrease in LOX is reflected as increased collagen turnover as measured by hydroxyproline content in PDR and RRD. (Figure 5.7)

Figure 5.7: Distribution profile of vitreous hydroxyproline in PDR, RRD and donor eyeball controls.

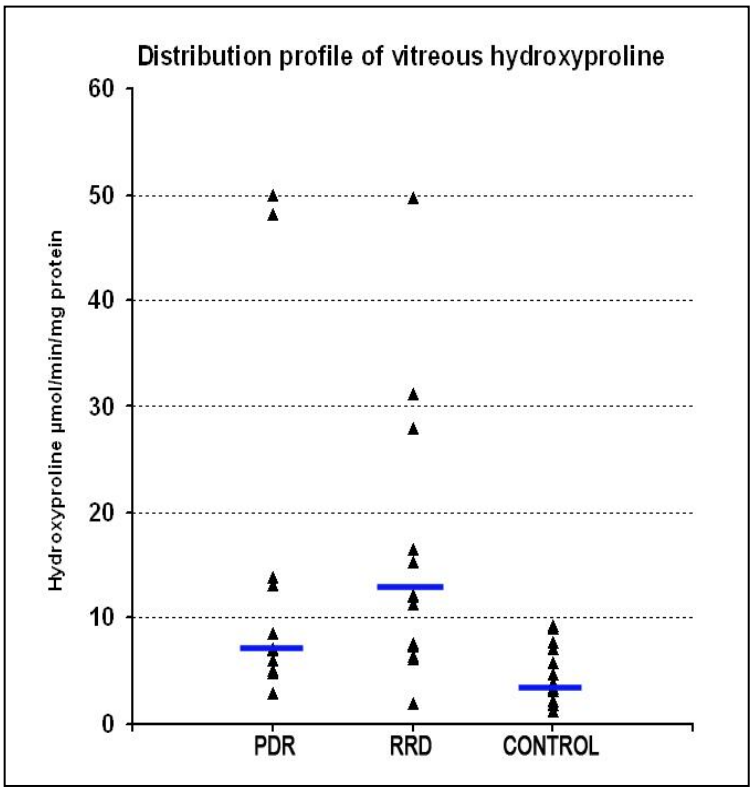

The median is indicated as solid lines. The median hydroxyproline level is 7.05 μmoles /mg protein in PDR, 12.0 μmoles /mg protein in RRD compared to 3.58 μmoles /mg protein in controls.

Figure 5.8: LOX immunolocalisation in epiretinal membranes from PDR and PVR

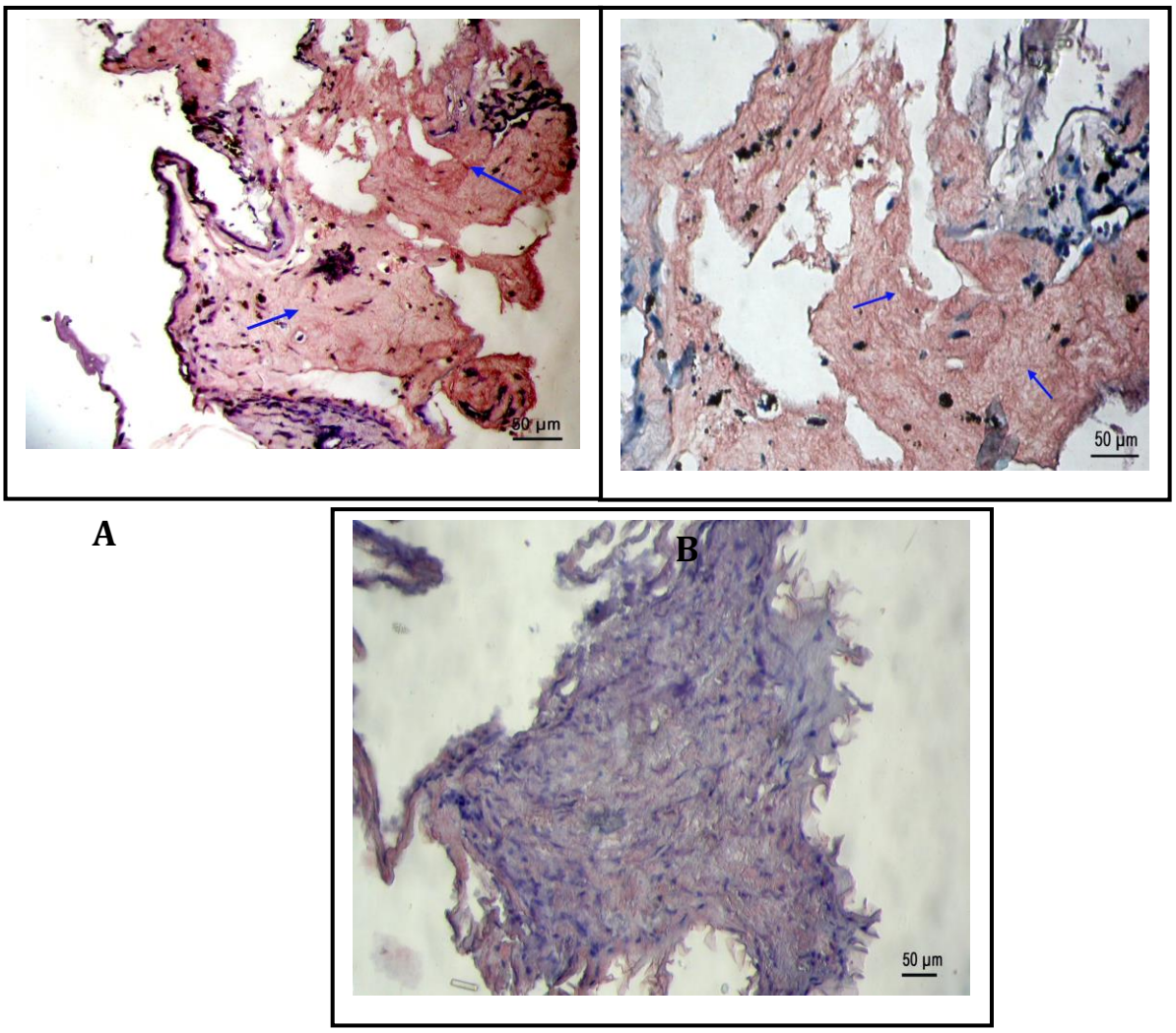

Figure 5.8 shows the immunolocalisation of LOX in the epiretinal membranes from PDR (A)and PVR(B) showing positivity in stroma, negative control(C).

5.4 CONCLUSION

This is the first report of vitreous levels of LOX in PDR and RRD. The observed decrease in LOX activity may contribute to inadequate collagen cross-linking and with improperly crosslinked collagen, there could be a net vitreous degradation leading to liquefaction. The increase in the vitreous protein level is indicative of the high ECM activity associated with the pathology. To gain a deeper understanding of the role of LOX, factors that can have a regulatory role have to be looked into in the vitreoretinal diseases such as PDR and RRD.

CHAPTER 6 - ESTABLISHMENT OF RETINAL PIGMENT EPITHELIAL CULTURE

6.1. INTRODUCTION:

Cell culture models of retinal pigment epithelium provide powerful systems in biological research for the scientist to investigate the architecture, barrier function and regulation of the ocular barriers *in vitro*. Cell culture models can be used for studying numerous other features such as

- Passive and active transport of drugs and endogenous substances.
- Cell physiology and metabolism.
- Protein expression and signal transduction.
- Development of delivery systems for genes and antisense oligonucleotides.
- *In vitro* toxicity tests and
- Transplantation studies

These models can also be used to identify compounds and formulations with favourable pharmacokinetic properties and to evaluate structure–absorption and structure–metabolism relationships. Cell culture models offer the advantage of a highly defined system, in which parameters and conditions can be easily changed. The results are often more reproducible in comparison to *in vitro* studies with excised animal tissue. Numerous cell culture models have been established as models of the inner and outer blood–retinal barrier (Table 6.1). Any disruption of either the inner or the outer blood–retinal barrier results in the development of retinal edema and can lead to a loss of vision (Cunha-Vaz et al., 1997). Investigation of the mechanisms of blood–retinal barrier breakdown, which occurs in diseases such as diabetic retinopathy, retinitis pigmentosa, uveitis, and age-related macular degeneration, warrants such cell culture models. In addition, these cell culture models can be used for the development of drug delivery systems targeted to the posterior segment of the eye.

Table 6.1: Different cell culture models of the retinal pigment epithelium (RPE) showing variation in transepithelial resistance (TER)

Species	Cell culture	TER	Characterizati	Application	References

	conditions	(Ωcm^2)	on		
Primary cell culture					
Xenopusiaevis (African clawed frog)	Matrigel coated filters; serum free defined medium; culture time 5-7 days	~ 400	Morphology, electrophysiological characterization, distribution of Na^+, K^+ - ATPase	Membrane polarity of Na^+, K^+ Pump, retina epithelium interactions	Defoe et al., 1994 b
Rat	Laminin-coated filters; serum-free medium; culture time 5-7 days	~200	Morphology, bioelectric parameters, permeability	Influence of serum on tight junction formation	Chang et al., 2000
PVG rat	Uncoated filters; medium contains 2% serum; culture time 3 days	~70	Permeability, bioelectric parameters; tight junction morphology	Effect of cytokines and NO on permeability	Zech et al, 1998
Chick embryo	Laminin-coated filters; serum free medium; retinal-conditioned medium; culture time 9 days	40-140*	Morphology, bioelectric parameters; permeability, distribution of ZO-I, actin	Development and regulation of tight junctions; influence of medium composition.	Ban , et al 1997., 2000
Cow	Uncoated filters, co-culture with endothelial cells; culture time 14 days	~200	Permeability, bioelectric parameters, expression of VEGF	Effect of endothelial cells on barrier function of RPE	Hartnett et al., 2003
Human	Matrigel coated filters; medium contains 1% serum; assays performed after 90 days in culture	~30	Morphology, bioelectric parameters; permeability, secretion of cytokines after stimulation	Polarized secretion of cytokines; comparison between ARPE-19 cell line and human RPE cells	Holtkamp et al., 1998
Human fetal	Millicell PCF, Chesse essential medium, Culture time- one month	~530	Permeability, bioelectric parameters, expression of tight junction proteins	Influence of Na^+, K^+ ATPase on tight junction function.	Hu et al., 2001

Immortalized cells					
Human ARPE-19 cells	Laminin-coated filters; medium contains1% serum, culture time 4 weeks	~100	Morphology, bioelectric parameters; permeability, expression of marker proteins	Characteri-zation of monolayer formed by ARPE-19 cell line	Dunn et al., 1996

The transepithelial electrical resistances (TER) are used as parameters to characterize the tightness of the *in vitro* epithelium. A mean TER value of 148 Ω cm^2 is reported for human RPE explants.

6.1.1 Retinal pigment epithelium culture:

Due to the many specialized features of RPE, the establishment of a cell culture system that is an appropriate *in vitro* model for the barrier function of the RPE remains still a scientific challenge. Cell culture conditions can alter the morphological and functional appearance of the cultured cells (Engelmann et al, 2004). Unless the appropriate cell culture conditions are used, the cells lose their polarized features.

As RPE cells proliferate only in pathologic conditions *in vivo*. For *in vitro* cell culture the induction of proliferation in RPE cells depends on various factors, such as the species, donor age, isolation, process time, and the culture conditions. Primary cell culture models of the RPE utilizing frog (Defoe et al, 1994), rat (Chang et al., 2000; Zech et al., 1998), chick (Ban et al, 1997; Ban et al, 2000;), bovine (Hartnett et al., 2003) and human RPE cells have been established in the literature. Although retinal pigment epithelium cultures have been successfully propagated for many years, the phenotype of cultured cells is less uniform than that of epithelial cells within the tissue. The *in vitro* heterogeneity of cells is usually attributed to the artificial environment of culture systems which are presumed to lack the complement of signals required for the cells to achieve a high degree of epithelial organization. Alterations in media components or substrate coatings can modulate cell shape, often reversibly, resulting in a shift in the overall appearance of cell cultures to more or less epithelioid. Many studies conducted earlier have had successful attempts for RPE isolation and culture establishment carried out on both human and animal eyecups using 0.25%

Trypsin solution with an incubation at 37° C for 1 hour (Tezel et al.,1998). Other enzymes that could be used for dislodging the cells are 0.03% Papain, (Eva et al., 1996), 2.4% Pronase and 2.0 %(Dispase (Defoe et al., 1994b) and 150 U /ml Collagenase (Seko et al., 1999) along with Hyaluronidase.

Most researchers focus on the use of human RPE cells to avoid species related applicability problems. Primary cell culture models of human RPE are used for studies of uptake and transport (Hamann et al., 2000; Huang et al., 1997; Kennedy, 2002; Lu et al., 1995), protein expression (Ishida et al., 2004; Kennedy, 2002), for evaluation of delivery systems for genes and antisense oligonucleotides (Abul-Hassan et al., 2000; Detrick et al., 2001), and for cytotoxicity studies (Kon et al., 1998).

Immortalized human cell lines derived from corneal epithelial (Kahn et al., 1993) conjunctival epithelial and retinal pigment epithelial cells (Davis et al., 1995; Dunn et al., 1996), are currently available commercially. Immortalized cell lines have some advantages over primary cells. The isolation from tissues, followed by harvesting and purification of cells, is not required. In addition, the characteristics of the cultures remain stable for a large number of passages, and cell cultures can be rapidly expanded if a large number of cells are needed for experiments (Daniele et al., 2002). On the other hand, after immortalization these cell lines may have abnormal characteristics compared to primary cells, and their gene expression profile might be significantly different from the normal, native cells (Tian et al., 2004). If adequate conditions are used, the cells in primary culture are likely to reflect *in vivo* cell morphology and function more accurately. These cells, however, stop growing after a few passages in culture and they revive after storage in liquid nitrogen weakly or not at all. Therefore, new cells have to be isolated frequently, and taking the limited availability of human donor eyes into account, it has become clear that the primary cell culture methods are not optimal for larger scale screening of pharmaceutical compounds and formulations.

Different continuous cell lines (rat and human) have been established of retinal pigment epithelial cells (Davis et al., 1995; Dunn et al., 1996). These cell lines

differ from each other in various properties and an adequate *in vitro* model of the barrier function of the RPE is yet to be established.

The rat RPE-J cell line produced by infection of rat RPE cells with a temperature sensitive SV40 virus and subsequent isolation of epithelial clones were demonstrated (Nabi et al., 1993). These cells exhibited a highly differentiated phenotype in culture, and the polarity of Na^+, K^+-ATPase and the neural cell adhesion molecule N-CAM differs from the *in vivo* localization.

Davis et al. cloned a spontaneously arising cell line (D407) from a primary culture of human retinal pigment epithelium (Davis et al., 1995). The cells were shown to possess most of the metabolic and morphologic characteristics of RPE cells *in vivo*, such as epithelial cobblestone morphology, expression of typical keratins, and synthesis of retina specific CRALBP protein. However, there was loss of some enzymatic activities and cytoskeletal polarization. Consequently, the cell line is mainly used for cytotoxicity studies, as model for retinal metabolism, and for retinal gene delivery (Mannerstrom et al., 2001; Mannerstrom et al., 2002), and not as model for barrier and transport function.

The second human RPE cell line (ARPE-19) was established and characterised by Dunn et al. (Dunn et al., 1996). This cell line, which arose spontaneously, was purified until a highly epithelial culture of RPE cells with a strong growth potential was obtained and is commercially sold by American type cell culture (ATCC) company. The cells were characterized with regard to their morphology such as defined cell borders, a ‘cobblestone’ appearance and pigmentation, the expression of retina specific markers (CRALBP and RPE65), and their barrier properties. This cell line provides a suitable model for polarity studies in RPE cells. Moreover, monolayers of ARPE-19 cells were used by researchers for a variety of other *in vitro* experiments, including studies of the regulation of gene expression, polarized distribution and secretion of proteins (Philp et al., 2003), delivery of genes and antisense oligonucleotides, for toxicity studies, and as models of retinal diseases (Amin et al., 2004).

A third immortalized cell line of human RPE (hTERT-RPE) was established by transfecting RPE cells with vectors encoding the human telomerase catalytic subunit With this method the cellular life span, which in absence of telomerase is limited due to telomer loss, can be extended while the cells maintain the diploid status, growth characteristics and gene expression pattern of normal cells (Bodnar et al., 1998). Rambhatla et al. investigated the cell culture conditions necessary for the differentiation of TERT-RPE cells and found that they formed a monolayer of homogenous and melanin containing cells expressing RPE-associated proteins (Rambhatla et al., 2002).

The disadvantages of the so far described cell culture models of human RPE are the long culture duration of up to 2 months described by some authors (Hartnett et al., 2003), during which the cells might lose their tissue specific features, and also their barrier functions as indicated by TER values of only 30–50 U cm^2 (Dunn et al., 1996). In comparison, mean TER values of 206 and 148 Ω cm^2 were reported for RPE explants of human fetal and human adult eyes (Quinn et al, 1992).

The limited availability of human donor eyes is another drawback in the development of *in vitro* models of the blood–retinal barriers. In comparison to human donor eyes, continuous supply of animal tissue for cell isolation can be more easily arranged and so primary cell culture models from animal sources are valuable for comparison in the characterization of immortalized RPE cell lines.

6.2 MATERIALS & METHODS

6.2.1 Eye ball procurement

Bovine eyeballs were got from the local slaughter house following aseptic conditions, within 2 hours of the death of the animal. The enucleated eyes were placed in ice cold PBS which was filled to ¼ of a sterile steel container with antibiotics and placed on ice pack. Precautions were taken to maintain sterility while the eyeball was being cut and transported and processing was completed within an hour of receiving the eye ball in the laboratory.

6.2.2 Eye ball processing

Eyeball was taken out of the container and rinsed well in three changes of PBS with antibiotics 5 minutes each. The anterior segment was removed by a circumferential incision using blade about 5 mm posterior to the limbus. Vitreous was aspirated out using sterile syringe. The neurosensory retina was peeled out carefully using forceps and cut free at the end of the optic nerve.

The eyecup was filled with 4 ml of medium. To dislodge the RPE cells from the Bruch's membrane a sterile cotton tipped swab, was used. The RPE cells which appeared heavily pigmented due to melanin pigments were swabbed out from the peripheral and posterior region of eyecup and suspended in the medium in the eye cup. The medium was aspirated out into sterile centrifuge tube and the cells were washed twice in the medium. The cell pellet was then seeded into 25 cm^2 tissue culture flasks containing M199 medium and incubated at 37° C in 5 % CO_2 atmosphere.

6.2.3 Maintenance of flask: The flasks were observed every 2 days under phase contrast microscope for morphological changes. Change of medium was given for every 2 days. The RPE cultures grown were trypsinised, subcultured and passaged for 5 generations.

6.2.4 Subculture: The cells when reached a monolayer in the tissue culture flask were sub cultured into another flask. The cells were trypisined using 0.1 % trypsin EDTA for 2 – 3 minutes. The wall of the flask to which the cells were adhered was rinsed well with the medium and half of this medium in which the dislodged cells are present were transferred to a new flask with a split ratio of 1:3. The cells were plated on different dishes or on coverslips if marker studies are to be performed.

6.2.5 Cell count:

Initial harvest of RPE cells is heavily pigmented and hence the staining of the vital dye is not well seen. 100 µl of cell pellet that is used for seeding into flask was taken. 1:5 dilutions were done in 0.9% saline. 10 µl of diluted cell

suspension was charged on to an improved neubauer chamber. The four 1mm sized squares were counted for the pigmented cells. Calculation was done and cell count expressed as the number of cells per mm^3. This was the yield of the cells.

6.2.6 Viability count:

The trypan blue dye exclusion test was carried out to find the number of viable cells in culture. A mixture of 1 volume of dye and 9 volumes of cell suspension was made. This was charged on to an improved neubauer chamber, the four corners 1mm sized squares were counted as mentioned in methodology chapter and calculated. Cell count was carried out thrice to confirm results.

6.2.7 Immunoflourescence for cytokeartin, actin and vimentin.

Microfilaments and microtubules occur in most cell types and are therefore of little potential use as cell markers, but they can be informative with regard to cellular activities such as locomotion and phagocytosis. Intermediate filaments, five types of which have been identified, are tissue specific . In general vimentin occurs in mesenchymal cells, desmin in cells of myogenic origin, neurofilament proteins in neurones, glial fibrillary acid protein (GFAP) in glia of the central nervous system and the cytokeratins in epithelial cells. The cytokeratins, a related family of about 19 polypeptides identified by two-dimensional gel electrophoresis, occur in varying combination in different epithelia . Therefore epithelia can be characterized by the cytokeratins they express. Because of their usefulness in tumour identification, antisera and monoclonal antibodies to intermediate filaments are readily available from commercial sources.

Cultured bRPE cells were grown on coverslips or in chambered slides. The entire staining procedure was done in moist chamber. Briefly the cells were fixed in ice cold ethanol and proceeded for staining with primary antibody (Pan cytokeratin, cytokeratin 8.13, Vimentin -1:100 dilution) and followed by secondary antibody as mentioned in methodology chapter.

6.2.8 Proliferation Assay: RPE cells from passage one were seeded onto 6 well plates containing 3000 Cells/well. After overnight incubation the cells

were washed with fresh M199 medium and pulsed with 30nCi of ^{3}H thymidine (As given in methodology chapter) to each well and incubated at 37°C. 100µl of the medium was taken after 1st, 3rd, 5th and 7th days of culture growth. The amount of ^{3}H thymidine in the medium was counted using liquid scintillation system.

In a duplicate 6 well plate, cultured cells were scraped after 2nd, 4th, 6th and 8th days of culture and were washed with warm maintenance medium, fixed in 0.5 ml of ice cold 10% TCA at 4°C for 30 minutes. 10 % TCA was removed and 0.5 ml of 0.1 % SDS in 0.2M NaOH was added to each cell pellet and was then incubated for 2 hours at 60°C. 100µl of solubilized DNA was added to scintillation cock tail and the amount of incorporated radioactivity was counted using liquid scintillation system in order to determine the ^{3}H uptake by the RPE cells.

Calculation:

$$\% \text{ Reference} = \frac{\text{Sample DPM} - \text{Blank DPM}}{\text{Ref DPM} - \text{Blank DPM}} \times 100 \times \text{Factor for } {}^{3}H$$

Reference DPM (Standard): 1.0 μCi ^{3}H thymidine gave 49665 DPM counts.

6.2.9 Western blotting for cytokeartin:

RPE cells cultured in T25 flask for 7 days were gently washed three times with PBS, trypsinised and the cell pellet was sonicated and lysate was prepared as given in methodology chapter. Briefly 50 μg of protein was subjected to 12.0 % SDS-polyacrylamide gel electrophoresis (PAGE) and transferred to Nitrocellulose membranes using the transblot apparatus with 100 volts for 1 hour. The membrane was blocked and incubated overnight at 4ºC with anti-cytokeratin 8.13 antibody (Sigma) diluted 1:2000 with TBS followed by secondary antibody and immunodetection using ECL detection reagents as given in methodology chapter.

6.3 RESULTS:

6.3.1 Establishment of RPE cultures:

After initiation of primary culture, BRPE cell adhesion occurred during the first 24 hours. More than 60% of the cells adhere and the remaining unattached cells were removed during subsequent medium change. The isolated cells were dark, heavily pigmented hexagonal in shape (when viewed enface). Cells were spread irregularly through out the culture flask as single cells or in clusters (Figure 6.1).

Figure 6.1: Phase contrast micrograph of primary BRPE cells

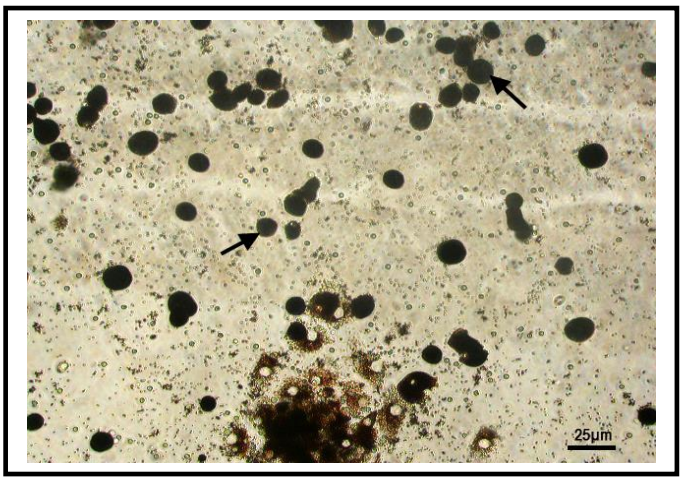

Figure 6.1 shows isolated BRPE cells in singles or in clusters which are heavily pigmented (indicated in arrow).

By day 4 to 6 small foci of aggregated cells start to divide. They become large flattened and polygonal. The melanin pigments of the cells moved to the periphery with a prominent (Figure 6.2). The cells varied in size and in the amount of pigment granules.

Figure 6.2: Phase contrast micrograph of primary BRPE showing foci of cell growth.

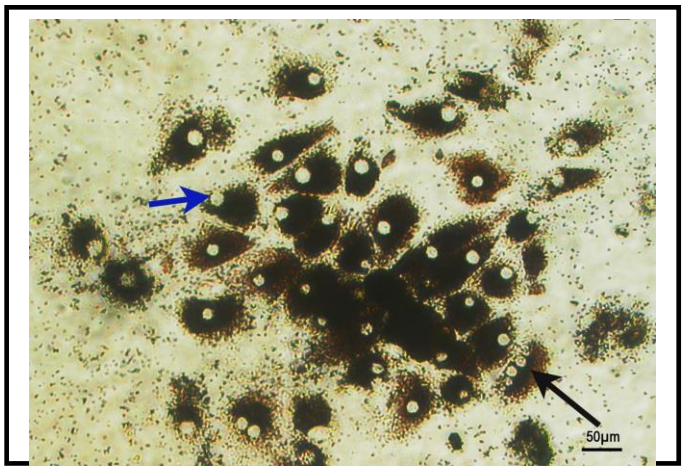

The Figure 6.2 shows BRPE cells dividing; the melanin pigments of the cells are moved to the periphery with prominent nucleus. Some cells are binucleate (indicated by arrow), the shed pigments are seen.

In successful cultures dense colonies expand and fill the culture flask by 50-60 % in 10 to 12 days with pigments being shed in the medium, a process called depigmentation (Figure 6.3).

Figure 6.3: Phase contrast micrograph showing dividing epitheloid cells in 10 to 12 days culture

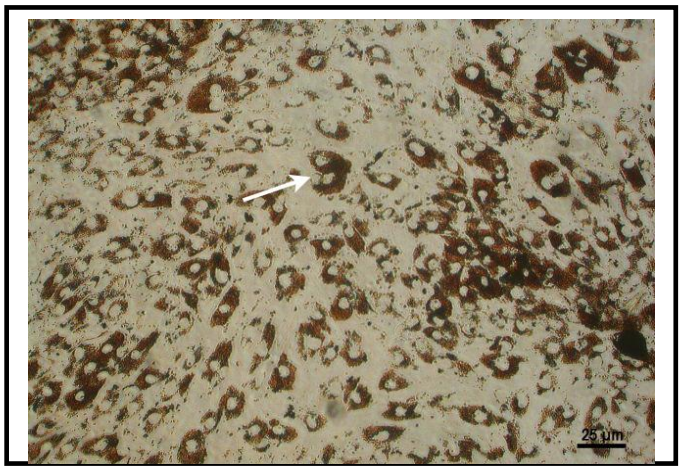

The Figure 6.3 shows proliferating BRPE cells depigmenting and forming a monolayer. Cells with binucleate forms are also seen.

By day 14-16 the RPE colonies proliferate and reach confluence with more than 50% of the cells depigmented. The peripheral cytoplasm is thin and relatively transparent with prominent or often retractile cell/cell boundaries (Figure 6.4). During the process of cell growth change of medium was given for every two or three days.

Figure 6.4: Phase contrast micrograph showing confluent BRPE cells in 14-16 days culture.

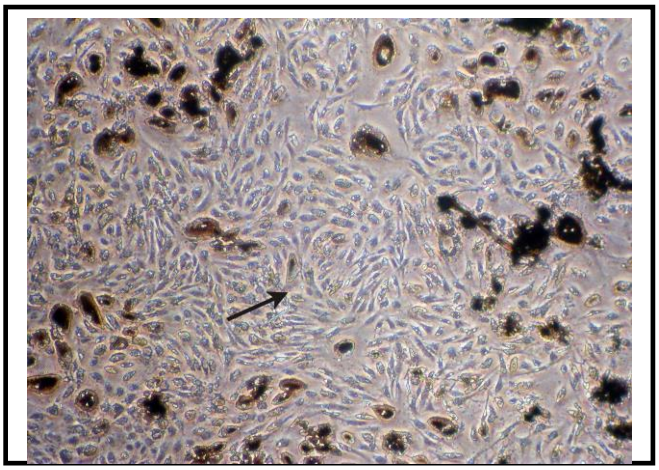

The Figure 6.4 shows confluent BRPE cultures with more than 50% of the cells showing loss of pigments and transparent peripheral cytoplasm

The confluent cultures were trypsinised with 0.1 % Trypsin EDTA and reseeded onto new culture dishes in 1: 4 split ratio. These cells grew to confluency in 5-7 days depending upon the seeding density. Subsequent passaging of RPE cells was characterized by gradual loss of pigmentation (Figure 6.5A,B).

Figure 6.5 A: Phase contrast micrograph of BRPE cells after 1st passage.

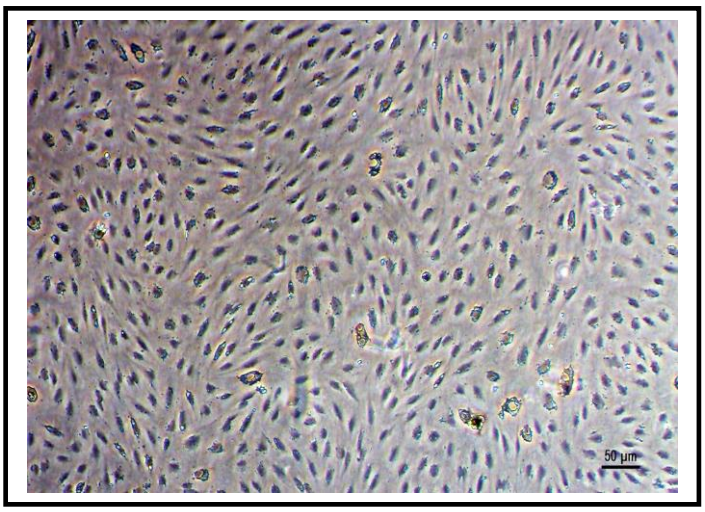

The Figure 6.5A shows1st passage BRPE cells with epitheloid morphology.

Figure 6.5 B: Phase contrast micrograph of BRPE cells after 1st passage.

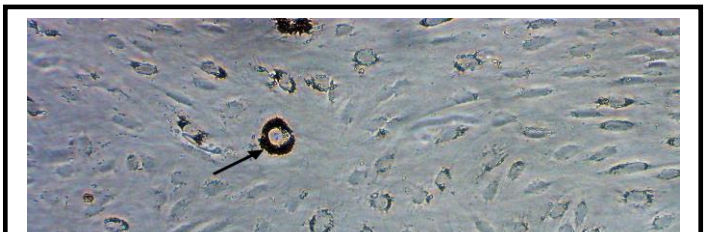

The Figure 6.5B shows1st passage BRPE cells with epitheloid morphology

There was an increasingly disordered growth in passages more than 5 and hence only passages 1-4 were used for the experiments. Some cultures had variable morphology which was looking fibroblastic or they were mixed cultures. Only cultures that were >95% pure and having epitheloid morphology were used in experiments.

Commercially available human RPE cell line (ARPE-19) was procured from ATCC and cultured. This cell line is a spontaneously transformed cell line which was purified until a highly epithelial culture of RPE cells with a strong growth potential was obtained. The ARPE-19 cells retained characteristic morphological features such as defined cell borders, a 'cobblestone' appearance (Figure 6.6).

Figure 6.6: Phase contrast micrograph of ARPE-19 culture

The Figure 6.5 [illegible] E cells procured from ATCC.

Human RPE cells were grown with limited success rate. The growth period for HRPE was long; it took more than 28 days to reach confluence. The confluent

cultures were looking epitheloid but slightly elongated (Figure 6.7). The relative growth rates of the three sources of cell types varied and are shown in table 6.2.

Figure 6.7: Phase contrast micrograph of HRPE culture.

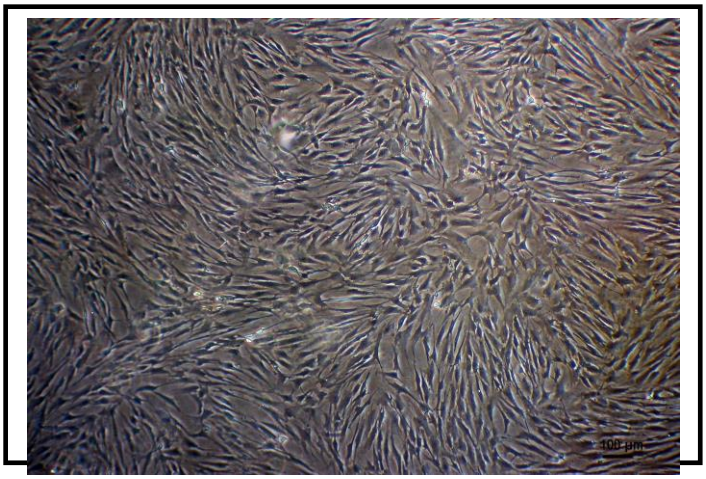

The Figure 6.7 shows the slightly elongated epitheloid morphology of human RPE cells

Table 6.2: Relative growth rate of the three RPE cells.

No	Cell type	Relative growth rate
1	HumanRPE(ARPE-19)	Fast 4days
2	Bovine RPE	Medium 14 days
3	Human RPE	Slow > 28 days

6.3.2 Retinalpigment epithelial cell characterization:

Immunoflourescence: The grown RPE cells were characterized with regard to their morphology, the expression of specific markers cytokeratin, actin and vimentin. Immunoflourescence for cytokeratin 8.13 showed positive fluoresce of keratins in the cytoplasm (Figure 6.8).

Figure 6.8: Immunofluorescence for cytokeratin 8.13 in BRPE cells

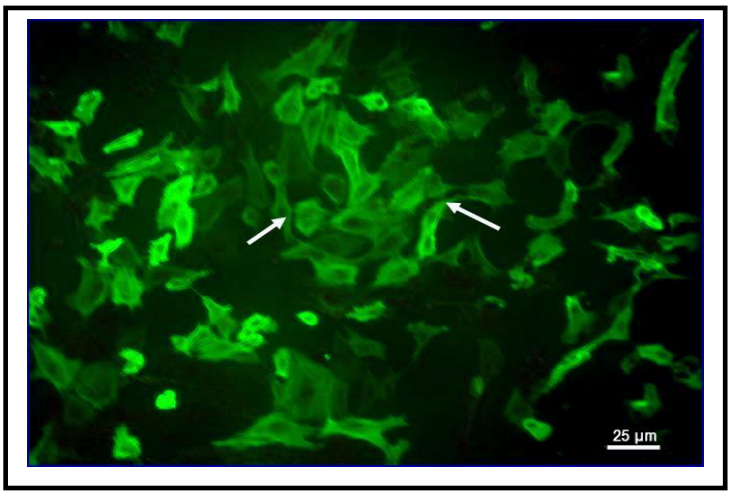

The figure 6.8 shows cultured BRPE cells immunostained for cytokeratin 8.13 conjugated to FITC. The green fluorescence indicated by arrows shows cytoplasm positive for cytokeratin.

Cytokeratin was found to be positive upto 5 passages. ARPE – 19 cells were also stained for cytokeratin as a comparison. Actin cytoskeleton was stained and vimentin was also positive for BRPE (Figure 6.9 and 6.10).

Figure 6.9: Immunofluorescence for actin in BRPE cells

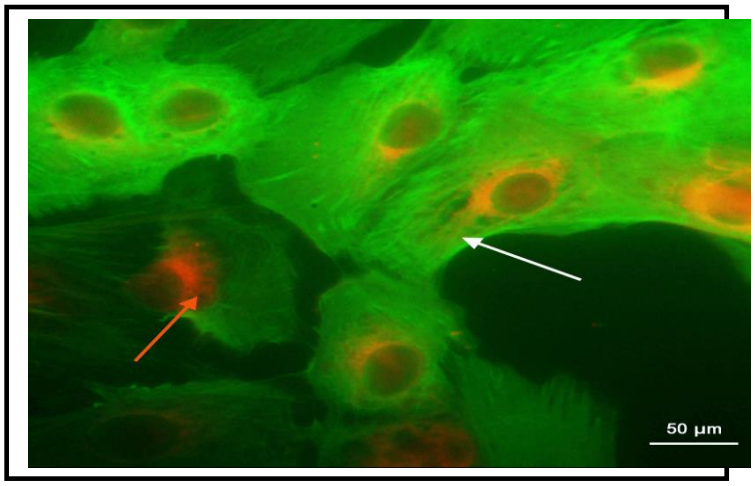

The Figure 6.9 shows cultured BRPE cells immunostained for actin conjugated with FITC. The green fluorescence indicated by arrows show cytoplasm positive for actin fibres. Nucleus is counterstained with Evans blue (red in colour).

Figure 6.10 : Immunofluorescence for vimentin in BRPE cells.

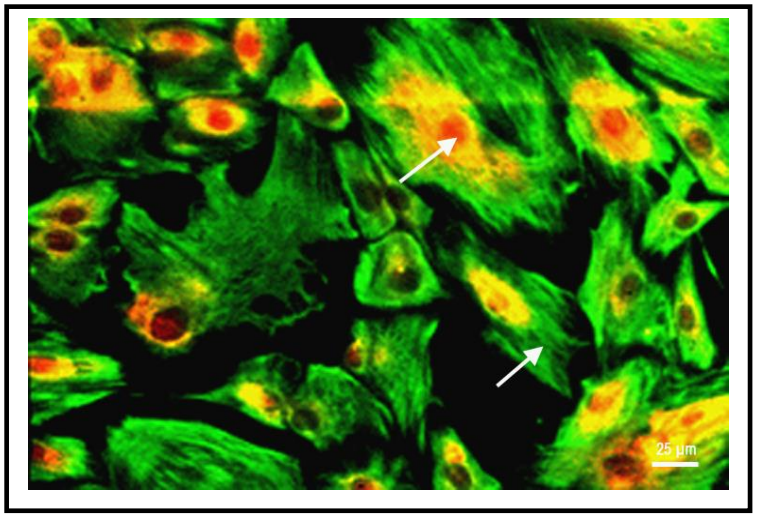

The Figure 6.10 shows cultured BRPE cells immunostained for vimentin conjugated with FITC. The green fluorescence indicated by arrows show cytoplasm positive for vimentin. Nucleus is counterstained with Evans blue (red in colour). HRPE cells were not stained for any of the markers since the success rate was low and hence was not used in experiments.

6.3.3 Western Blot:

By western blotting an immunoreactive band at 46 kDa was seen for cytokeratin (Figure 6.11). This was seen in all the 4 passages of BRPE. For subsequent experiments the BRPE cultures were used upto 4 passages since the cytokeratin expression was reduced to about 50 % in 5th passage of many BRPE cultures.

Figure 6.11: Western blot for cytokeratin 8.13 in BRPE cell lysates.

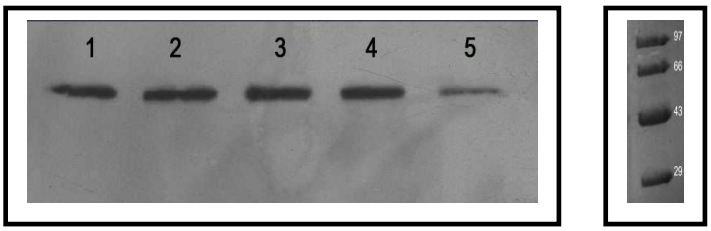

Western blotting of cytokeratin showing a 46 Kda band at passages 1-5 as indiacted by the lanes 1-5. BRPE cell lysates 50 µg each was resolved in 10 % SDS PAGE. Molecular weight markers are indicated.

6.3.4 Proliferation Assay: Tritiated thymidine was added to cultures and was measured in both medium and cell lysate to assess the rate of BRPE proliferation. The 1st passage BRPE of cells pulsed with 30 nCi ^{3}H showed a decline of tritiated ^{3}H in the medium. The levels of ^{3}H in the medium decline to 57.4 ± 2.8 % after 7 days in culture. (Figure 6.12)

Figure 6.12: **^{3}H Thymidine depletion from the medium by BRPE cultures**.

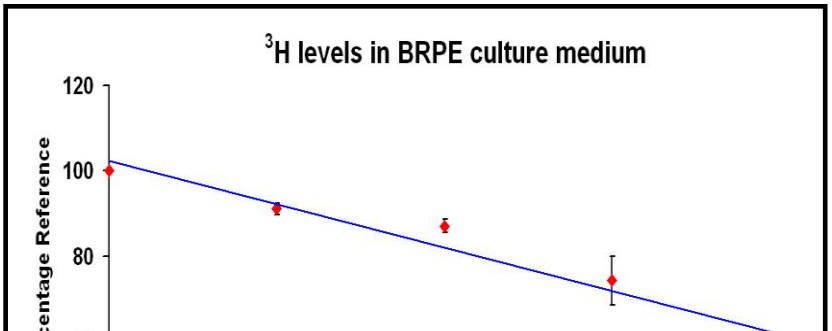

The Graph shows the ^{3}H Thymidine depletion in culture medium from 100 % in day 0 to less than 50% by day 5 indicating that as cells start proliferating as they utilize the ^{3}H Thymidine. Each point is mean ± SD value of triplicate experiments.

The 1st passage of RPE cells pulsed with 30 nCi ^{3}H showed a gradual increase in ^{3}H uptake by 8 days. (Figure 6.13)

Figure 6.13: ^{3}H Thymidine uptake by BRPE cultures

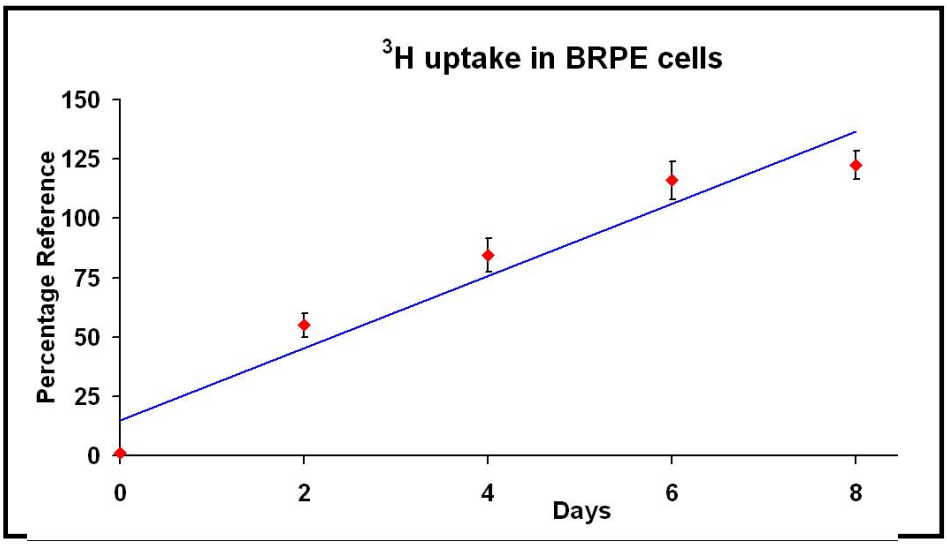

The Graph shows ^{3}H Thymidine uptake by proliferating BRPE cells from 1 % in day 0 to 120 % by day 8 showing the ^{3}H Thymidine incorporation in the cells. Each point is mean ± SD value of triplicate experiments.

6.4 CONCLUSION:

This study established methods for the isolation and phenotypic characterization of primary bovine retinal pigment epithelial cells in comparison with the commercially available human cell line ARPE-19. These two cultures provide the *in vitro* cell model for the experiments described in the later chapters.

CHAPTER 7- EFFECT OF OXIDATIVE STRESS ON LYSYL OXIDASE IN RETINAL PIGMENT EPITHELIAL CULTURES

7.1 INTRODUCTION:

Oxygen metabolism, although essential for life, imposes a potential threat to cells because of the formation of partially reduced oxygen species. Oxidative stress is the general term used to describe the steady state level of oxidative damage in a cell, tissue or organ, caused by the reactive oxygen species (ROS). This damage can affect a specific molecule or the entire organism. Free radicals such as the ROS are formed during a variety of biochemical reactions and cellular functions (such as mitochondrial metabolism). The steady state formation of pro-oxidants (free radicals) is normally balanced by a similar rate of consumption by antioxidants (Halliwell et al.,2000).

Various pathological processes disrupt this balance by increasing the formation of free radicals in proportion to the available antioxidants, thus leading to oxidative stress. Examples of increased free radical formation are immune cell activation, inflammation, ischemia, cancer, neurological diseases, chronic fatigue syndrome, and autoimmune disorders and so on. These highly reactive and unstable free radicals have an unpaired electron in their outer shell, which reacts with (oxidize) various cellular components including DNA, proteins, and lipids. The reactions between the cellular components and free radicals lead to DNA damage, structural and functional damage of proteins, cell membrane damage, mitochondrial malfunction, and eventually cell death or apoptosis (Halliwell et al., 1995).

Retinal pigment epithelial cells due to their anatomic location are exposed to high levels of oxygen radicals, produced by photo transduction. Therefore, the cells are a prime target of oxidative injury. Injury to the RPE cells in the degeneration of the sensory retina may contribute to the pathogenesis of age related macular degeneration (ARMD), which is the leading cause of blindness in elderly individuals. Epidemiological studies indicate that the incidence and severity of ARMD are negatively correlated with the plasma antioxidant levels and supplementation with antioxidants can delay the onset the disease.

The RPE cells may undergo apoptosis by cellular stress factors such as ROS, ischemia, blue light etc which are capable of triggering cell death. Various types of oxidative challenges to the retinal epithelium can result in sub RPE deposits or lipofuscin accumulation (Young RW.1987), It has been proved experimentally that oxidative stress mediates RPE cell death. Tetra Butyl hydroperoxide (tBH) a chemical oxidant, has been extensively used *in vitro*, to understand the mechanism of cell damage in these cells.

tBH is a relatively stable alkyl peroxide that readily penetrates the cell membranes, promotes cellular oxidation, depletes intracellular GSH, causes mitochondrial damage and eventually leads to cell death. Once inside the cell, it is reduced by glutathione peroxidase to t-butanol that promotes the reduction of intracellular GSH. Owing to its higher stability and the presence of hydrophobic butyl moiety, tBH can penetrate easily through the membrane to cause apoptosis by loss of mitochondrial membrane potential along with cytochrome c release. Cai *et al*, 2000 showed that, after exposure to the model oxidant tBH, cells undergo apoptosis with a sequence of processes involving the loss of mitochondrial membrane potential, release of cytochrome C and activation of caspase- 3 like activity. Anti oxidants that contain thiol groups can protect against tBH induced apoptosis by acting as a metal chelator and removing the potential for Fenton mediated production of reactive hydroxyl radicals from the hydroperoxide (Dunaief et al.,2002).

Factors such as exposure to sunlight, cigarette smoke, insufficient dietary intake of anti oxidants etc are the most important factor that predisposes the cells to the oxidative damage leading to various ocular diseases. The exact cause of RPE cell death is still unclear, since the degeneration of the cells may progress over years or decades in humans and it is difficult to model with animal studies.

ECM changes in ARMD :

Apart from apoptosis abnormalities of the RPE morphology are observed at the Bruch's membrane/RPE interface with pathological sub-RPE deposit formation, termed basal laminar deposits (Curcio and Millican, 1999). Histologically,

massive age-dependent accumulation of electron-dense deposits between the RPE and Bruch's membrane are seen. The deposits contain excess BM material and are similar to basal laminar deposits. They precede the atrophic as well as the exudative type of ARMD. The NVMs in ARMD are reported to contain large "feeder" vessels with many new capillaries in different stages of maturation. The majority of the nonvascular cells were either retinal pigment epithelial (RPE) cells or fibroblast-like cells. The RPE cells were formed as single or multiple layers on one side of the membranes. The stroma was composed mainly of collagen types I and IV and fibronectin (Das et al., 1999).

There are relatively few studies on the effect of oxidative stress on LOX . It is reported that LOX is up-regulated in the brain and spinal cord of late stage amyloid sclerosis of Cu, Zn-SOD mutant mice (mSOD1). Since RPE cell is prone to oxidative stress and it is one of the key factors in the degeneration of RPE. The effect of oxidative stress on the lysyl oxidase activity was studied in this chapter.

7.2 DESIGN OF EXPERIMENTS:

Human RPE cell line, ARPE-19 was cultured according to procedure mentioned in methodology and were used in these experiments. Cells were plated in 25cm^2 flasks or 96 well plates for experiments and subsequently changed to M199 medium. They were grown to 90% confluence. Before subjecting them to experimental condition they were downshifted from 10% FBS to 5% and then to 1 % FBS over a 24 hour time period and replaced in fresh 1 % FBS containing M199 medium (phenol red free) for 12 hours prior to experiments.

Oxidative stress was induced by exposing the cells to tBH to see the effect of reactive oxygen species mediated changes on LOX activity. The cells were exposed to tBH (0.2 mM, 0.4 mM, 0.6 mM, 0.8 mM and 1.0 mM) and incubated for 1, 3 and 6 hours.

7.2.1 Cytotoxicity assay

Cytotoxic effect of tBH, was assayed using a colorimetric 3-(4,5-dimethylthiazol-2-yl)-2,5-diphenyl tetrazolium bromide (MTT) assay. Briefly, the human RPE cells were plated at a density of 2500 cells per well in 96-well plates. Cells were then exposed to tBH (0.2 mM, 0.4 mM, 0.6 mM, 0.8mM and 1.0 mM) for 1, 3

and 6 hours. Cells without tBH treatment was used as control. After incubation MTT was added as given in methodology chapter and the solubilized crystals was read in a microtiter plate reader at a wavelength of 540 nm.

7.2.2 Assay for lysyl oxidase enzyme activity in conditioned media (For extracellular LOX activity):

Activity assays for detection of LOX and BAPN-inhibitable LOX was assayed as previously described in methodology chapter using concentrated conditioned medium. Activity assays were repeated three times and each experiment were performed at least in duplicates. Protein estimation was done by Lowry's method.

7.2.3 DQ Gelatinase assay:

Activity assay for the detection of gelatinase was assayed as described in methodology chapter using concentrated conditioned medium with and without inhibitor phenanthroline.. Protein estimation was performed by Lowry method. Results were normalized to protein content.

7.2.4 TUNNEL ASSAY:

For detection of cell death, a fluorescein (terminal deoxynucleotidyl transferase [TdT]-mediated dUTP [deoxyuridine triphosphate] nick-end labeling [TUNEL] assay) staining kit was used. RPE cultures after exposure to tBH (0.4, 0.6, 0.8 mM) after 6 hrs were fixed in 2% paraformaldehyde and permeabilised. Cells were incubated in TdT together with dUTP-FITC as given in methodology. To determine the percentage of apoptotic nuclei, TUNEL-FITC cells were visualized by fluorescence microscopy and counting was performed from digital images after contrast enhancement by using Image J software.RPE cells treated with 3000 units DNAse to induce DNA breakage followed by TUNNEL staining was used as the positive control.

7.2.5 Intracellular Reactive Oxygen Species Measurement

Cells were plated 24 hours before initiation of the experiment at a density of 5000 cells per well in 96-well plates. Cells were loaded with DH_2F_2DCA at a final

concentration of 50 μM for 45 minutes. After incubation with a bolus dose of tBH (0.2, 0.4, 0.8 mM) for 6 hours, the fluorescence was determined as given in methodology chapter.

7.2.6 Statistics : All results are expressed as mean ±SD. Results are expressed as percent of controls and normalized by protein content. Student *t* test was done to compare with controls. P value of <0.05 was considered significant.

7.3 RESULTS:

7.3.1 Cytotoxic effect of tBH:

ARPE cells exposed to different concentrations of tBH showed a dose and time dependent decrease in viability. After 3 hrs of incubation the viability was 80 % in 0.2 mM tBH which dropped to 63 % at 1.0 mM tBH. After 6 hrs of incubation the viability was 75 % in 0.2 mM tBH which dropped to 50 % at 1.0 mM tBH. The LD 50 for tBH was 1.0 mM at 48hrs. (Figure 7.1)

Figure 7.1: MTT assay in ARPE-19 cells exposed to tBH

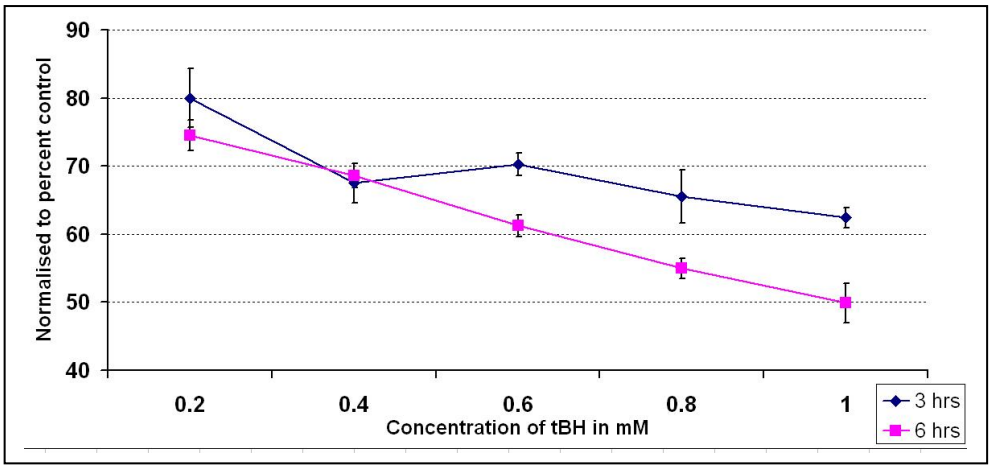

7.3.2 Morphology of the cells after treatment with tBH

There morphology of the cells was not altered in 0.4 mM. Few cells showed rounded morphology in 0.6 mM and 0.8 mM concentration. This was around 20 % in 0.8 mM after 6 hours. Although the viability of the cells as seen by MTT was decreased in 0.6 mM and 0.8 mM , the cell morphology was altered to that extent as this could be due to the density dependent protection of RPE cells in culture (Wada et al., 2001: Garg et al., 2003). (Figure 7.2 and Figure 7.3)

Figure 7.2: Phase contrast micrographs of RPE cells after 3 hour treatment with tBH

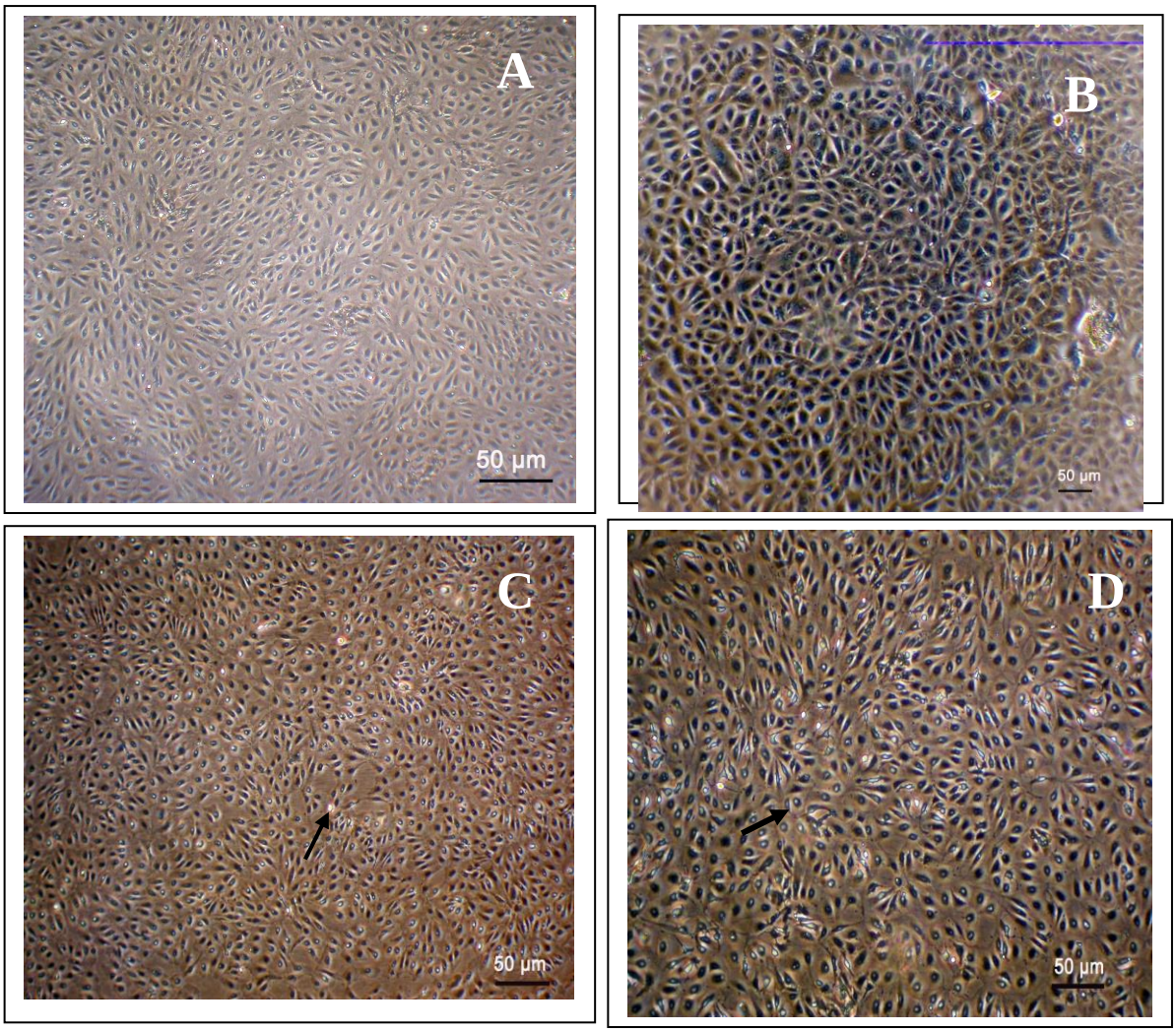

Figure 7.2 shows the phase contrast micrographs of RPE cells treated with tbH for 3 hours. A- Control, B- 0.4 mM tBH, C- 0.6 mM tBH, D-0.8 mM tBH. Compared to control few cells show round and shrinked morphology (Shown in arrow) in response to tBH

Figure 7.3 Phase contrast micrographs of RPE cells after 6 hour treatment with tBH

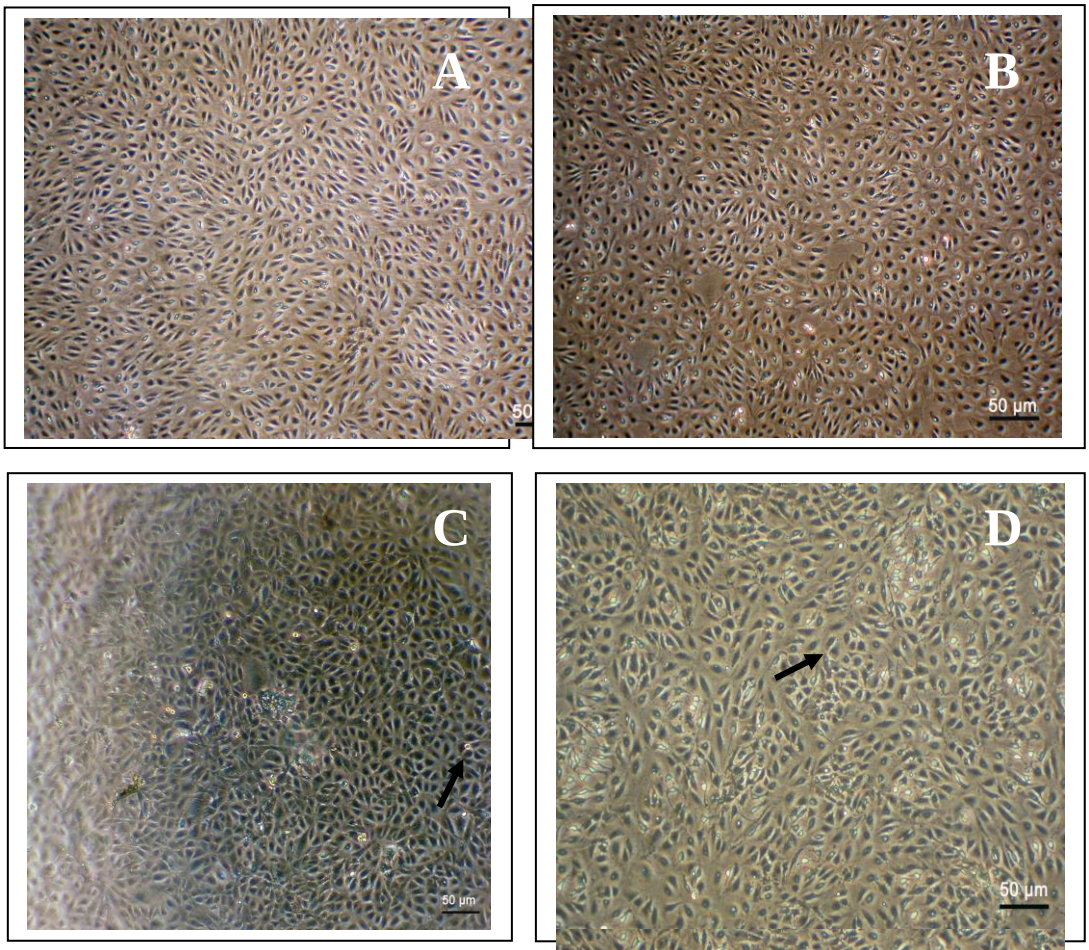

Figure 7.3 shows the phase contrast mic H for 6 hours. A- Control, B- 0.4 mM t l. Compared to control few cells show rou n arrow) in response to tBH

7.3.3 Specific activity of Lysyl oxidase

There was a dose dependent increase in t e exposed to 0.4, 0.6 and 0.8 mM concentration of tBH. When compared to controls there was a staistically significant increase in LOX activity at 0.4 mM (p value 0.012 – 3hrs, 0.002- 6 hrs), 0.6 mM (p value 0.013- 3 hrs, 0.001- 6 hrs) and 0.8 mM (p=0.001- 3 hrs, 0.001- 6 hrs). (Figure 7.4)

Figure 7.4: Specific activity of LOX in ARPE 19 cells exposed to tBH

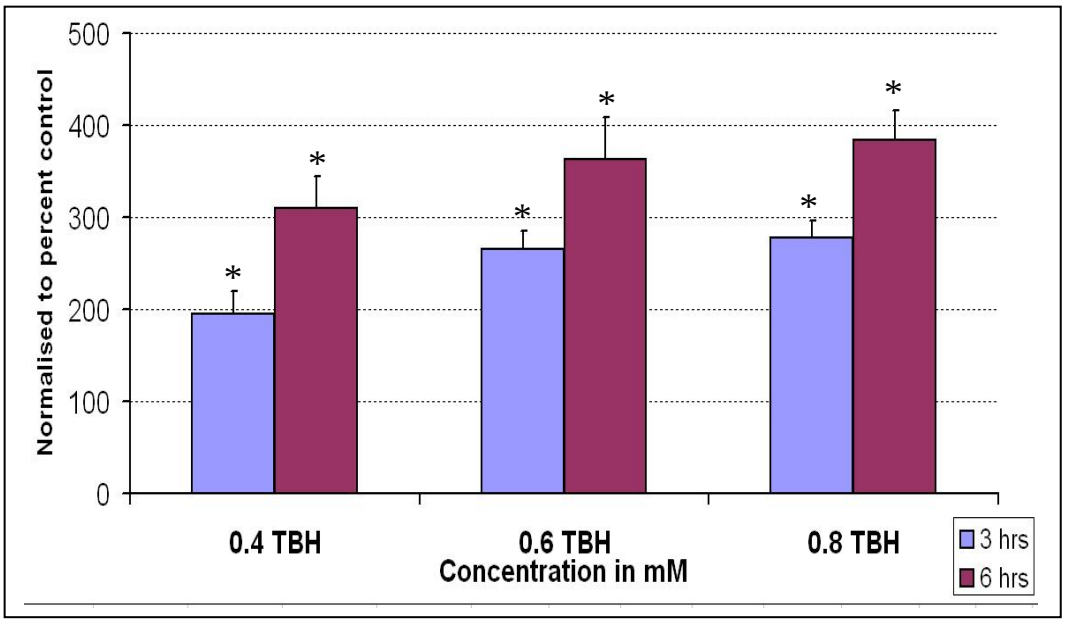

Figure 7.4 shows the LOX specific activity measured in culture media from RPE cells incubated for 3 and 6 hours with increasing concentrations of tBH (0.4 mM, 0.6 mM, 0.8 mM). *P < 0.05 is considered significant. The p value is a comparison 3 hours and 6 hours with control.

7.3.4 DQ gelatinase assay

Compared to the control, the MMP activity was found to be increasing with increase in tBH concentration (Figure 7.5). The increase was found to be significant at 0.6 mM and 0.8 mM compared to control at 3 hrs (p = 0.024, p = 0.021) and 6 hrs (p = 0.031, p = 0.028) .

Figure 7.5: DQ gelatinase assay in ARPE-19 cells exposed to tBH

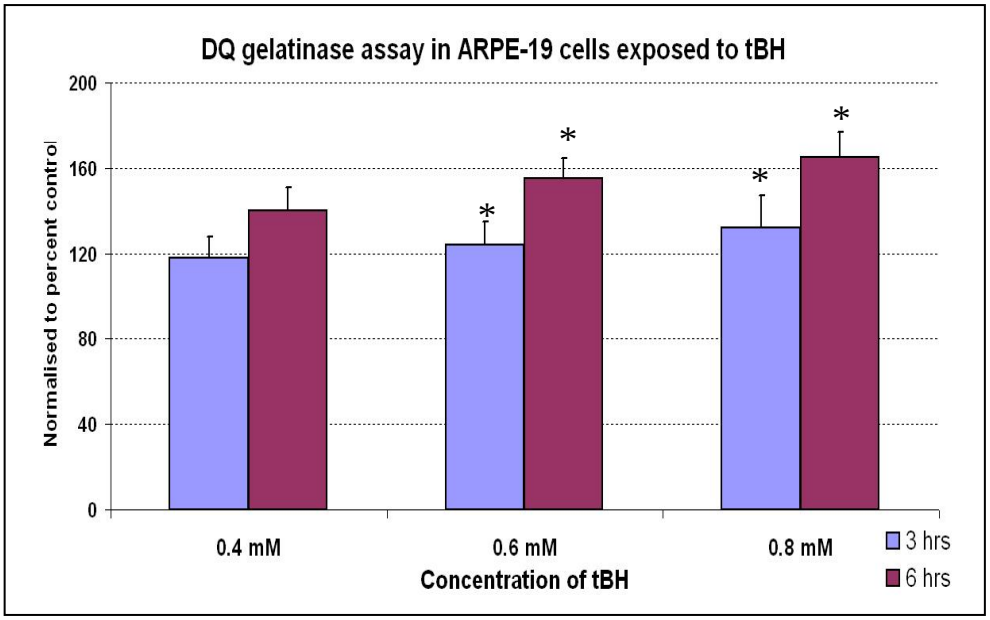

Figure 7.5 shows the activity of MMP normalized to percent control in culture media from RPE cells incubated for 3 and 6 hours with increasing concentrations of tBH (0.4 mM, 0.6 mM, 0.8 mM). *$P < 0.05$ is considered significant.

7.3.5 TUNEL STAINING:

To check the apoptotic cell death the ARPE-19 cells were assessed for TUNEL positive cells. The total number of cells which were positive was counted in different areas of the slide was quantified using Image J software. After 6 hrs of exposure the ARPE 19 cells showed 8 %, 14 % and 25 % tunel positive cells in 0. 4 mM, 0.6 mM and 0.8 mM tBH treatment. Figure.7.6

Figure 7.6: TUNEL staining in ARPE-19 cells exposed to tBH after 6 hours

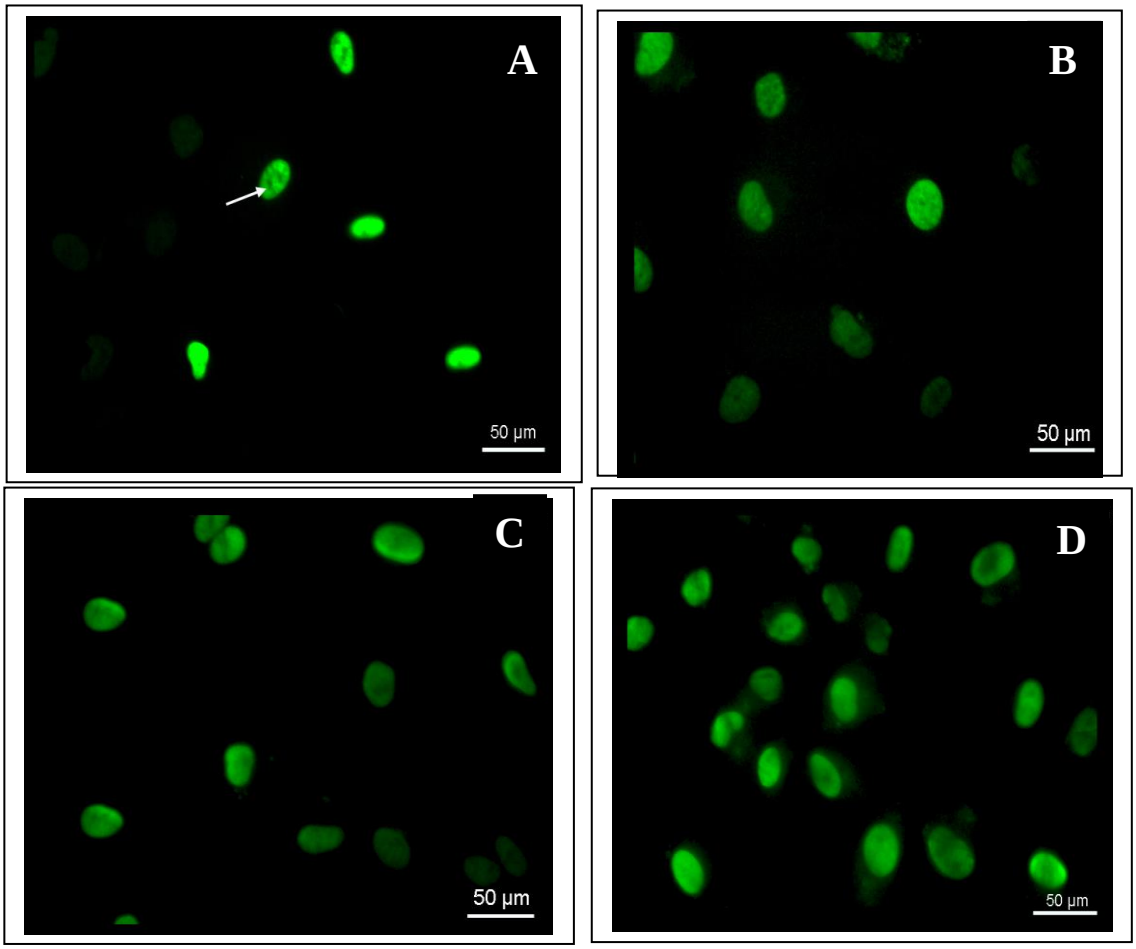

Figure 7.6 shows TUNEL positive cells which are stained using FITC labeled tU-TDP as shown in arrow. (A) cells exposed to 0.4 mM tBH, (B) cells exposed to 0.6 mM tBH and (C) cells exposed to 0.8 mM tBH (D) positive control cells treated with 3000 units of DNAase. Scale bar 50µm. It is a representation of 3 fields in each of the condition.

7.3.6 Intracellular reactive oxygen species (ROS)

Exposure to tBH caused an increase in intracellular ROS accumulation in the cultured RPE cells. By 6 hours there was a 2 fold increase in 0.2 and 0.4 mM and a 2.5 fold increase in 0.8 mM of tBH, which was statiscitally significant compared to control.

Figure 7.7: Intracelluar reactive oxygen species measurement in ARPE-19 cells exposed to tBH

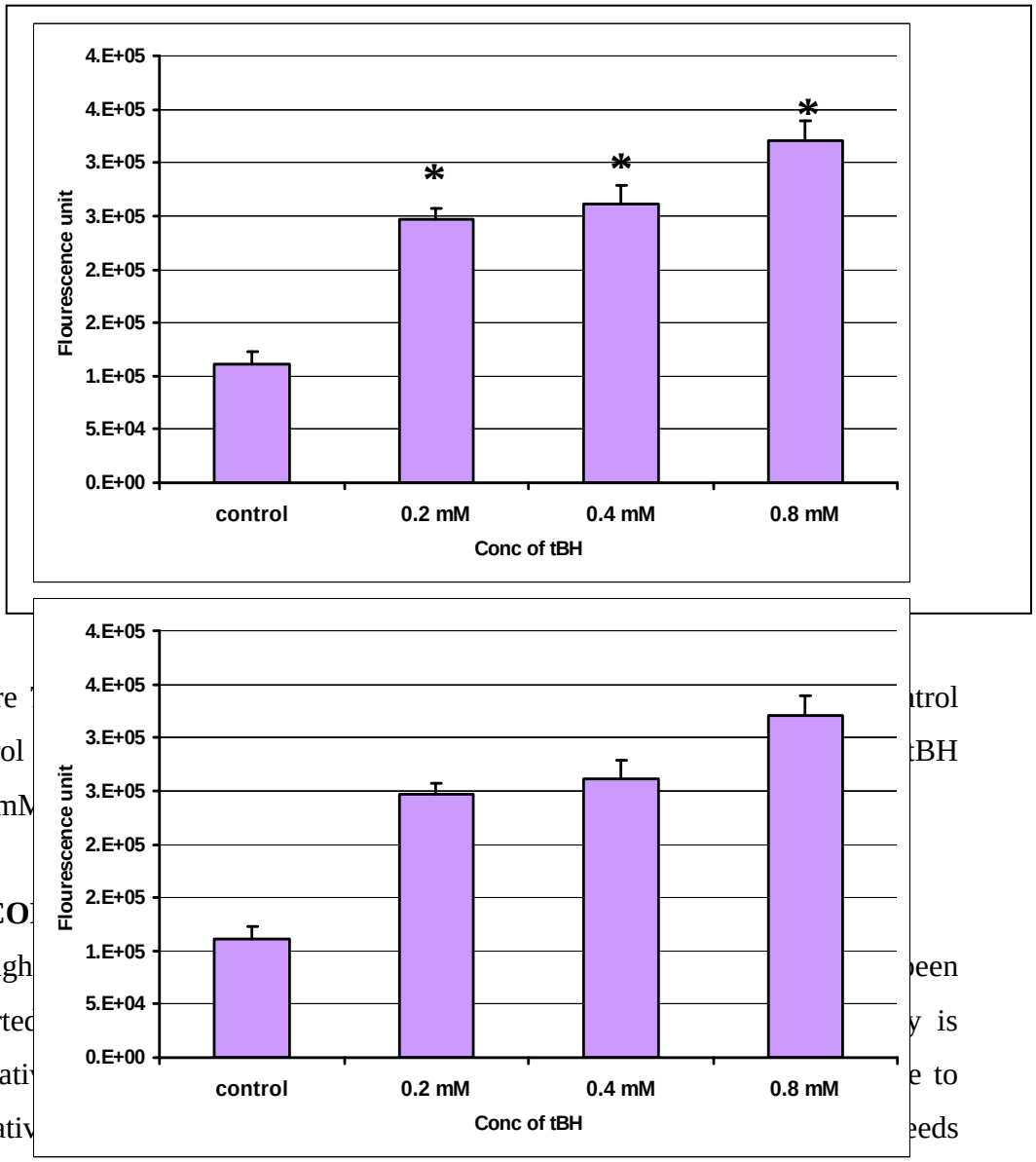

4.E+05
4.E+05
3.E+05
3.E+05
2.E+05
2.E+05
1.E+05
5.E+04
0.E+00
Flourescence unit
control
0.2 mM
0.4 mM
0.8 mM
Conc of tBH

Figure trol control tBH (0.2 mM

7.4 **CO**

Though been reported y is indicati e to oxidativ eeds to be further explored. But increased LOX can also give rise to increase hydrogen peroxide production, which at low levels are having proliferative activity on RPE cells and also can augment the oxidative stress condition further.

CHAPTER 8: EFFECT OF HYPEROSMOTIC STRESS ON LYSYL OXIDASE IN RETINAL PIGMENT EPITHELIAL CULTURES

8.1 INTRODUCTION:

Changes in RPE cell volume *in vivo* in response to a hyperosmotic stress may alter the composition of the extracellular (subretinal) space surrounding photoreceptors. In addition to the intra cellular changes and thus isosmotic volume regulation, RPE could play a key physiological role in maintaining the integrity and health of the neural retina in normal and pathophysiological conditions by compensatory volume regulation mediated by Na (K),Cl co-transport at the apical membrane. Efficient movement of solute and water define healthy RPE. (Adornae et al., 1990.). The intraocular pressure continually forces water into the retina, while choroidal osmotic pressure draws water across the RPE and toward the choroid. These two passive forces help maintain retinal attachment as well as remove water from the subretinal space. In conjunction with these passive forces, there is active transport of small solutes across the RPE. Studies report on the RPE cells exposed to hyperosmolar conditions leading to a marked stimulation of myo-inositol uptake (15-fold) and a twofold increase in the uptake of GABA. Thus, the net balance of solute flux across the RPE is in the apical (retinal) to basolateral (choroidal) direction and is a function of polarized expression and activity of an array of channels and transporters

Hyperosmolarity stimulates the intestinal epithelial cells to an inflammatory cascade involving the activation of MAP kinase and NF-κB (Li et al.,2006). The effect of hyperosmolarity studied in the ciliary epithelium of rabbits showed damage to the pigment epithelial cells and appearance of vacuoles in the non-pigmented epithelial cells (Marmor et al.,1980). Hyperosmolarity also induces the MMP-1,-9,-3 activities in corneal epithelial cells when exposed to 350-500mOsm NaCl via the activation of JNK pathway (Li et al., 2004). Studies with the human RPE cells reveal that these cells have regulatory systems that govern the intracellular osmolarity. The sodium-potassium ATPase activity was increased in response to hyperosmolarity, which is related to the accumulation of

organic osmolytes such as myoinositol and taurine. An *in vitro* study on the effect of sub retinal fluid from retinal detachment patients revealed low collagenase activity with increased synthesis of collagens in the RPE cells. Subretinal fluid absorption is accelerated by the systemic injection of hyperosmotic solution or acetazolamide (Marmor et al, 1986). RPE cells grown in microporous membranes when exposed to hyperosmotic conditions showed an increased LOX mRNA level which is believed to parallely influence the LO activity (Omori et al.,2002).

It is relevant to study the effect of hyperosmotic stress because fluctuations in cell volume have been associated with diseases such as ischemia and reperfusion during diabetic retinopathy, macular edema, apart from neurodegeneration and there are no detailed reports on the extra-cellular matrix activity Therefore the objective of this study was to see the effect of hyperosmotic stress on the LOX activity in RPE cultured *in vitro*.

8.2 DESIGN OF EXPERIMENTS:

Bovine RPE cultures were grown according to procedure mentioned in methodology chapter and passages 2-4 were used for these experiments. Human RPE cell line, ARPE-19 was cultured according to procedure mentioned in methodology and were used in these experiments. Cells were plated in 25cm^2 flask, 6 well or 24 well plates for experiments and subsequently in M199 medium. They were grown to 90% confluence. Before subjecting them to experimental condition they were downshifted from 10% FBS to 5% and then to 1 % FBS over a 24 hour time period and replaced in fresh 1 % FBS containing M199 medium (phenol red free) for 12 hours period of time prior to experiments. Cells were exposed to hyperosmotic mannitol (50 mM, 100 mM) and incubated for 1, 3, 6 and 12 hours and proceeded for the following assays.

8.2.1 Cell proliferation assay

The proliferation rate was determined by measurement of the DNA synthesis rate. Briefly, the human RPE cells were plated at a density of 2500 cells per well in 24-well plates. Cells were then exposed to 50, 100 mM mannitol for a time

point of 1, 3, 6, and 12 hours. Cells without added mannitol was used as controls. The incorporation of bromodeoxyuridine (BrdU) into the genomic DNA was determined with the use of the anti BrdU antibody followed by an enzyme substrate reaction as per BrdU Kit (Roche).

8.2.2 Cytotoxicity assay:

The metabolic activity in RPE after treatment with mannitol was done using a colorimetric 3-(4, 5-dimethylthiazol-2-yl)-2,5-diphenyl tetrazolium bromide (MTT) assay. Briefly, the Bovine RPE cells were plated at a density of 2500 cells per well in 24-well plates. Cells were then exposed to 50, 100 mM mannitol for a time point of 1, 3, 6, and 12 hours. Cells without mannitol were used as controls. After incubation MTT was added as given in methodology chapter and the solubilized crystals was read in a microtiter plate reader at a wavelength of 540 nm.

8.2.3 Assay for lysyl oxidase enzyme activity in conditioned media :

Activity assays for detection of LOX was assayed as previously described in methodology chapter using concentrated conditioned medium. Activity assays were repeated three times and each experiment were performed at least in duplicates. Protein estimation was done by Lowry's method.

8.2.4 Gelatin zymography: The activity of gelatinases, MMP 2 and MMP 9 was detected by gelatin zymography. Briefly the conditioned media collected after exposure to mannitol was electrophoresed into 10 % SDS-PAGE gels containing 0.1% gelatin as given in methodology chapter. Gels were stained with Coomassie blue stain for 1 hour and then distained to visualize the negative bands. MMP 2 and 9 standards were also loaded. MMP activity in the medium was analysed and expressed in terms of the band intensity using Image J software.

8.2.5 Statistics : All results are expressed as mean ±SD. Results are expressed as percent of controls and normalized by protein content. Student *t* test was done to compare with controls. P value of <0.05 is considered significant.

8.3 RESULTS :

8.3.1 Cell proliferation assay:

When RPE was exposed to increasing mannitol concentration, the BrdU assay showed a net proliferation effect at 6 hours in 50 mM and 100 mM mannitol which declines thereafter as observed at 12 hours. (Figure 8.1).

Figure 8.1: BrdU assay in BRPE cells exposed to mannitol

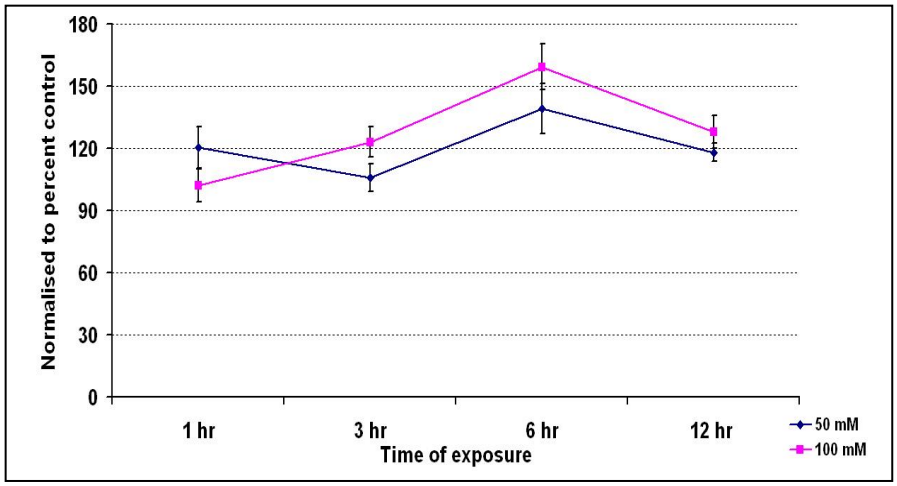

8.3.2 Cytotoxicity effect of mannitol : BRPE cells incubated with mannitol showed a initial fall in the metabolic activity by 20% which increased to a maximum of 20% over and above the control. Thereafter there was a decrease in the metabolic activity of the cell as observed at the end of 12 hours..(Figure 8.2). BRPE cells incubated with mannitol although showed an initial 15 % drop in viability then with increase in time the viability increased at 6 hours. The initial shock for the cell could have been managed by the cell with its regulatory volume capacity.

Figure 8.2 : MTT assay in BRPE cells exposed to mannitol

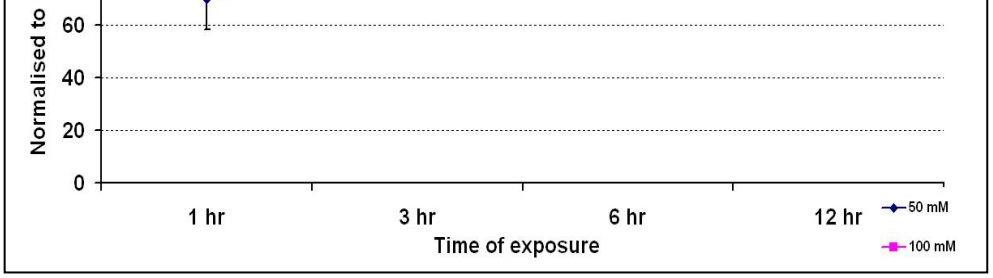

8.3.3. Morphology of the cells after treatment with mannitol

The cells as observed in the phase contrast microscope no significant change in the morphology upto 12 hrs in 50 mM and 100 mM mannitol. Only in 200 mM mannitol there was rounding of cells and this concentration is not used in the study.

Figure 8.3: Phase contrast images of RPE in culture after treatment with 50 mM mannitol

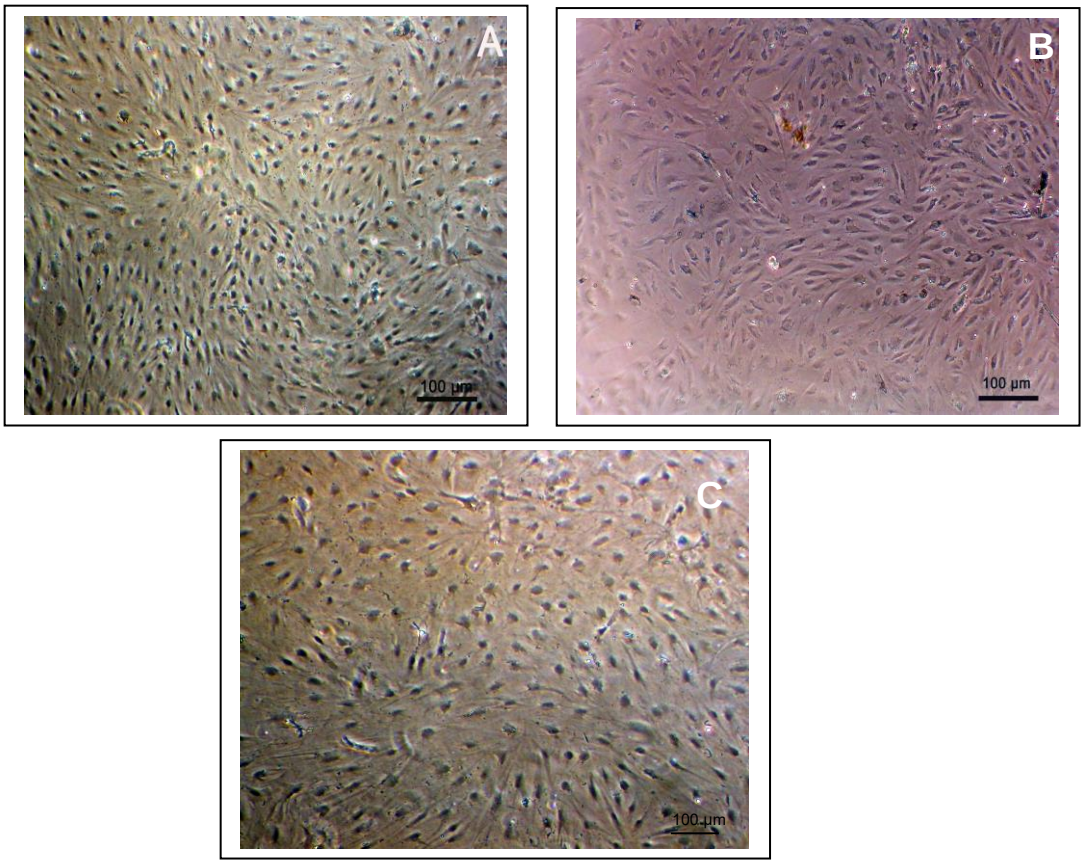

Figure 8.3 shows the phase contrast micrographs of RPE cells treated with mannitol at 50 mM concenatrion. A- 50 mM 6 hrs , B50 mM 12 hrs, C- control. Scale 100 µm bar

Figure 8.4: Phase contrast images of RPE in culture after treatment with 100 mM mannitol

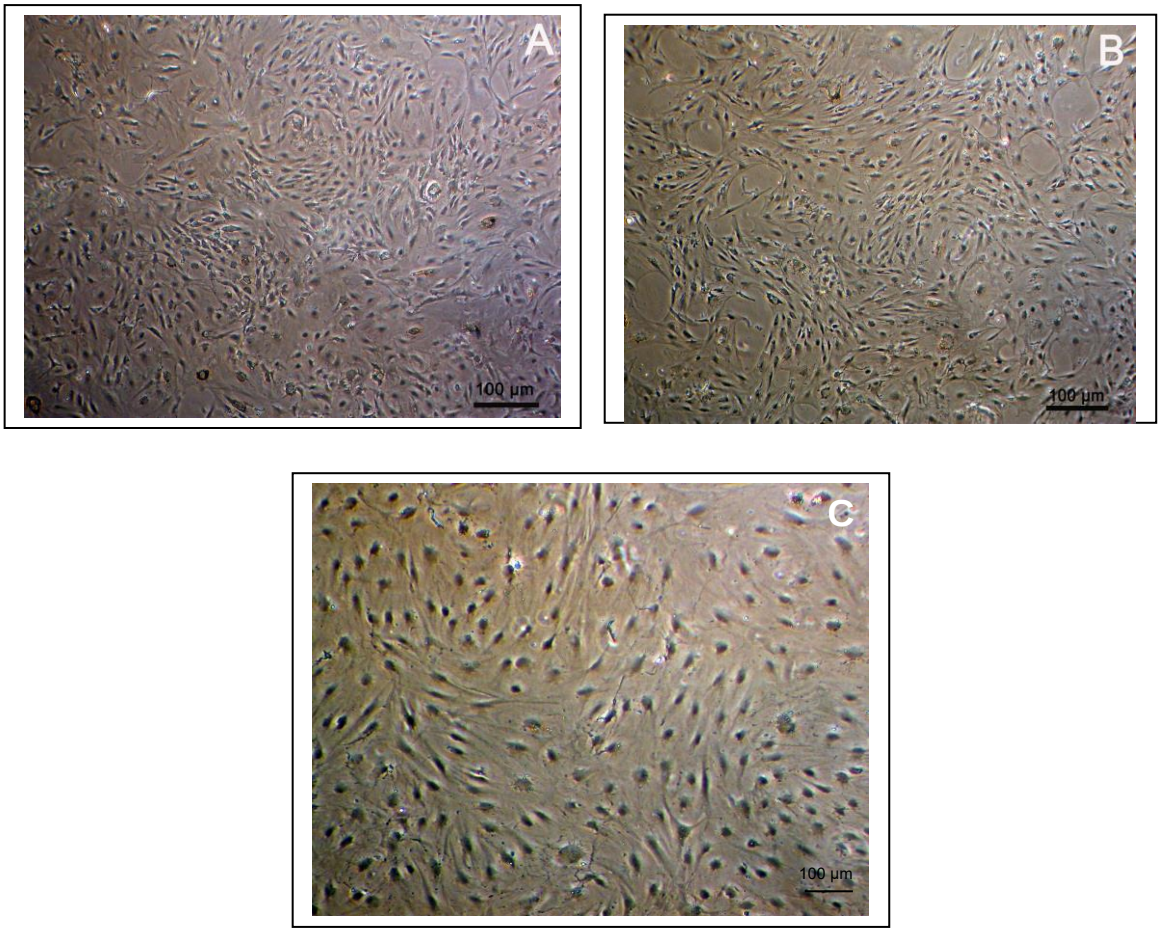

Figure 8.4 shows the phase contrast micrographs of RPE cells treated with mannitol at 100 mM concenatrion. A- 100 mM 6 hrs , B- 100 mM 12 hrs, C- control. Scale 100 µm bar

Figure 8.5: Phase contrast images of ARPE in culture in 50 mM and 100 mM mannitol after 12 hours

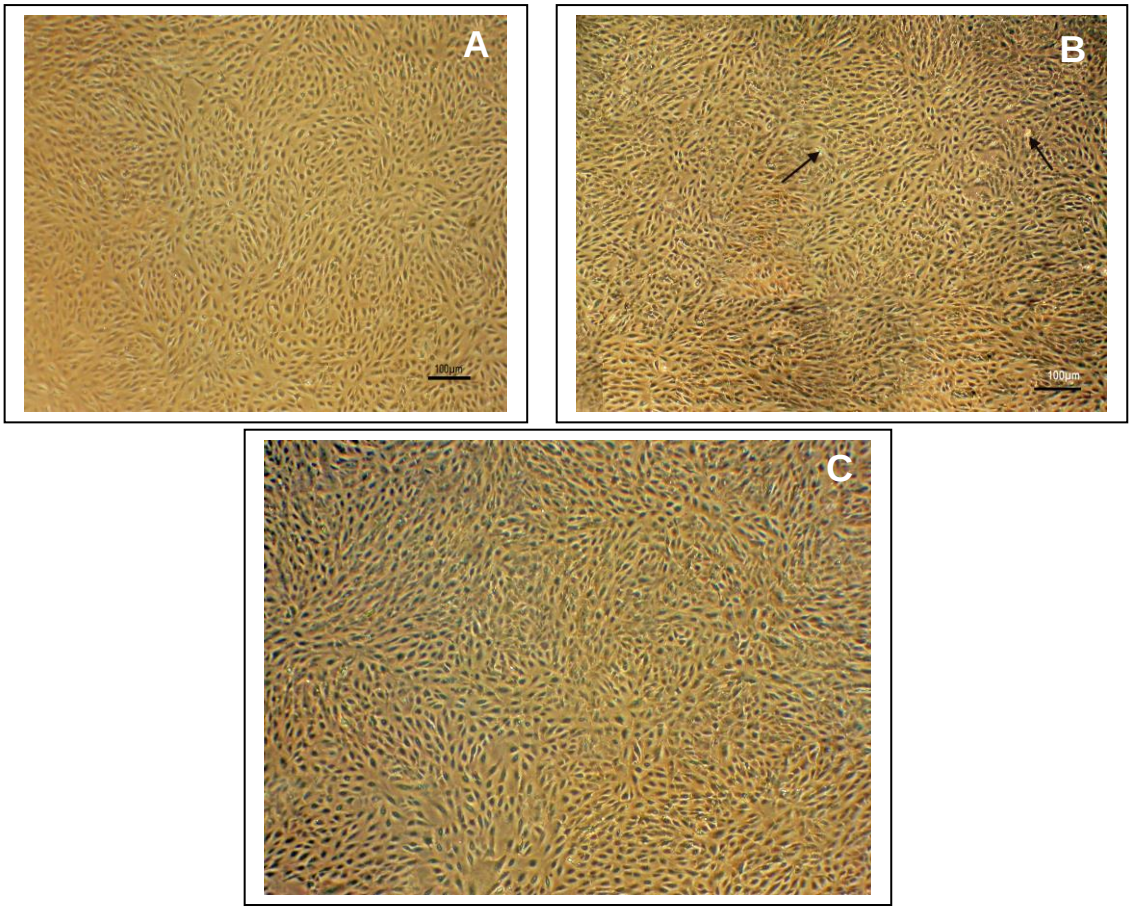

Figure 8.5 shows the phase contrast micrographs of RPE cells treated with mannitol after 12 hrs. A- 50 mM : 12 hrs, B- 100 mM : 12 hrs, C- control. Scale 100 µm bar

8.3.4 Specific activity of LOX in conditioned media after treatment with mannitol:

In the cells exposed to 50 mM and 100 mM mannitol stress there is an decrease in the specific activity of LOX up to 6 hrs. At the end of 12 hrs there is an increase in the LOX activity compared to control which was statistically significant ($p=0.02$) A similar picture is seen in 100mM with a fall in the activity with time until 3 hours with an increase at 6 hours and a significant increase at the end of 12 hours ($p=0.034$)

Figure 8.6: Specific activity of Lysyl oxidase in RPE cells exposed to mannitol

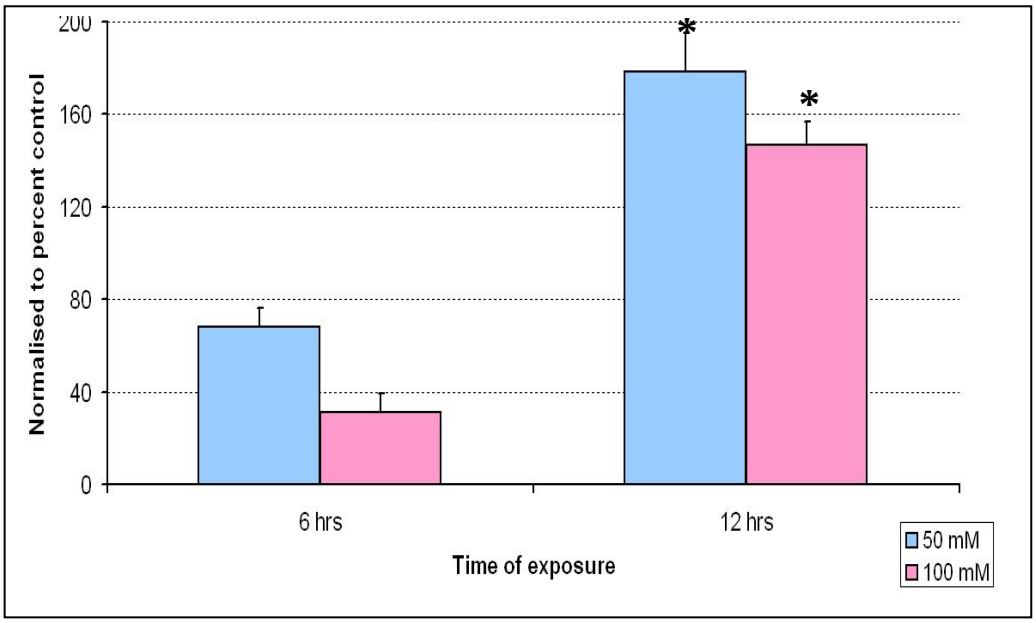

Figure 8.6 shows the LOX specific activity measured in culture media from RPE cells incubated for 6 and 12 hours with increasing concentrations of mannitol (50mM and 100 mM). p value >0.05 is significant.

8.3.5 Quantitative real-time RT-PCR : Since there was a significant change in the LOX activity at 6 hrs and 12 hrs real time PCR was done LOX gene expression in ARPE -19 cells. As seen by specific actoivity the LOX expression was decreaeed in 6 hrs and increased in 12 hrs in 50 mM and 100 mM mannitol . (Figure 8.7).

Figure 8.7: Real time gene expression of ARPE-19 cells exposed to mannitol

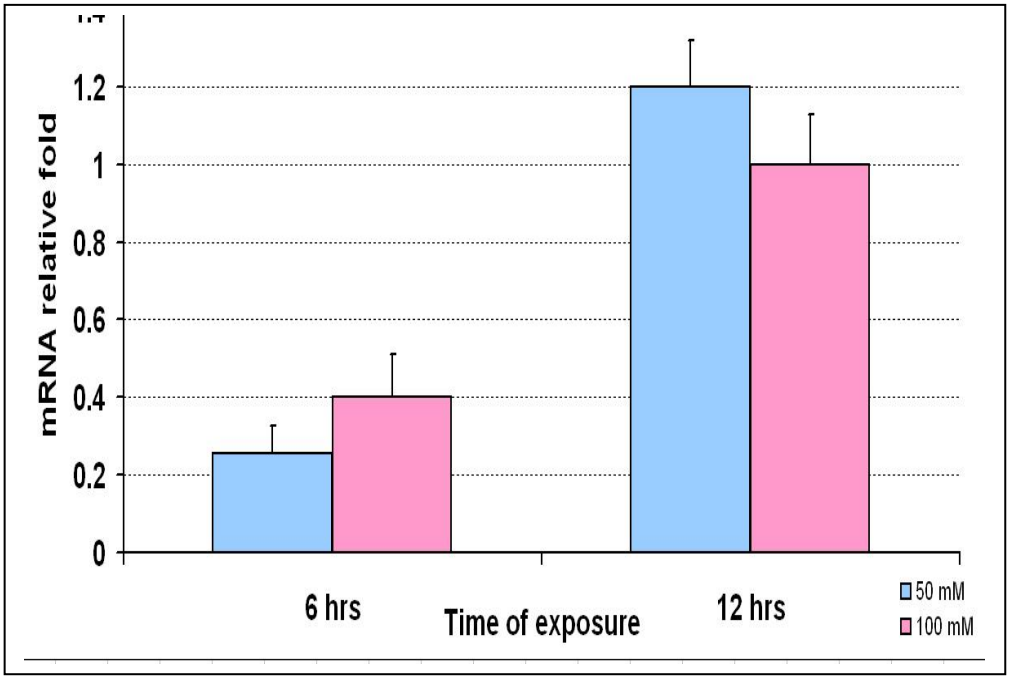

8.3.6 MMP activity by zymography:

The matrix-cleaving enzyme MMP activity increased with increasing concentration of mannitol with time. (Figure 8.8)

The percentage increase was 15.4 % in 50 mM concentration after 12 hrs and 25.3 % in 100 mM concentration after 12 hrs as analysed by image J analysis.

Figure 8.8: 10% SDS PAGE – gelatin zymography showing MMP

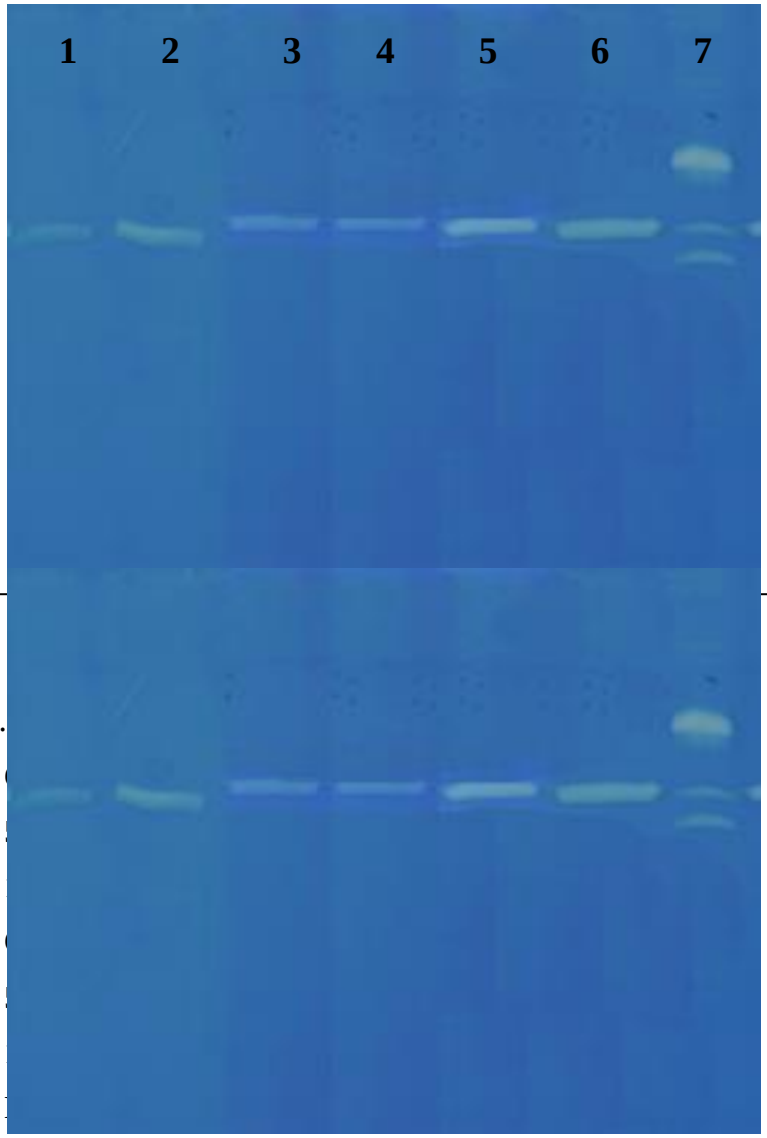

Figure 8.

Lane 1 :

Lane 2 :

Lane 3 :

Lane 4 :

Lane 5 :

Lane 6 :

Lane 7 :

pro MMP 9 (92 kDa)

Active MMP 9 (84 kDa)

Pro MMP 2 (68 kDa)

Active MMP 2 (62 kDa)

8.4 CONCLUSION

There was an increased expression of LOX activity at the end of 12 hours in response to osmotic stress. A similar increased LOX activity was also seen when cells were exposed to oxidative stress. As osmotic stress can lead to oxidative stress the increase could be due to the same mechanism too. Whether the increased LOX activity and expression is protective to RPE for increased cross linking of collagen in the basement membrane or the catalytic end product of LOX ie H_2O_2 further augments the oxidative stress condition needs to be explored.

CHAPTER 9: EFFECT OF GLUCOSE ON LYSYL OXIDASE IN RETINAL PIGMENT EPITHELIAL CULTURES

9.1 INTRODUCTION:

Diabetes mellitus (DM) is one of the major medical problem affecting millions of people all over the world. The two distinct forms of DM are type 1, juvenile or insulin-dependent diabetes mellitus (IDDM) and type 2, adult onset or non insulin-dependent diabetes mellitus (NIDDM). Type 1 patients run a higher risk of severe ocular complications. Approximately 25% of patients with type 1 DM have shown to be affected with retinopathy, with the incidence increasing to 60% after 5 years and 80% after 10 to 15 years of affliction. Breakdown of the blood–retinal barrier (BRB) is an early feature of diabetic retinopathy characterized by histopathological changes which include loss of pericytes in the retinal blood capillaries, haemodynamic alterations (changes in retinal blood flow and areas of capillary non-perfusion), vascular abnormalities (micro aneurysms, intraretinal microvascular abnormalities and venous bleeding), basement membrane thickening and reduced vascular integrity which results in vascular leakage and the development of retinal edema and finally proliferative diabetic retinopathy.(Sulochana et al., 2001)

In PDR newly developing vessels commonly arise from the retina and optic disc. These new vessels are fragile and prone to rupture, resulting in vitreous haemorrhage, and subsequent detachment of the retina. Vascular permeability in the retina is partially regulated by the structural components of the BRB, the integrity of which is essential in maintaining normal visual function. The BRB forms a selective partition between the circulatory system and the neuronal and glial components of the retina. This partition is not absolute and allows some normal level of exchange between the retinal tissue and the circulation. The BRB consists of two anatomical entities: the inner BRB, which is formed by junctions between endothelial cells of the retinal capillaries, and the outer BRB, which is composed of tight junctions between retinal pigment epithelial cells. (Bito et al.,

1980) RPE cells form the outer blood retina barrier and play a key role in the pathologic process of neovascularization that leads to loss of vision.

9.1.1 RPE in diabetic retinopathy:

The anatomical position of the RPE is a highly critical interface, interposed between the choriocapillaris, which is the source of glucose and oxygen, to the retinal neurons that utilize large amounts of glucose and oxygen. A number of studies demonstrate that the barrier function and transport properties of the RPE are crucial to the maintenance of the outer retina (Steinberg et al, 1979).

Glucose is the major source of energy for retinal metabolism (Berman et al.,1991). In a variety of vertebrate species, retinal glucose utilization is several-fold higher than in other body tissues. Studies of Badr *et al* in an experimental diabetes model has demonstrated that the fraction of glucose entering the retina in diabetes is likely to be greater across the RPE than across the retinal vasculature (Badr et al., 2000). Glucose transport into the retina is also a central component of the hypothesis of glucose toxicity in the pathogenesis of diabetic retinopathy (Diabetes Control and Complications Trial (DCCT) Research Group, 1993). Joe G. Hollyfield et al have shown that glucose is rapidly removed from the culture medium by both the apical and basal RPE cell surfaces. Further, at the time where extracellular glucose levels are high, a portion of the glucose recovered by the RPE cells is stored as glycogen with a portion of the glycogen depolymerized within lysosomes to maltodextrins such as maltose, maltotriose, maltotetraose, etc. As glucose in the culture medium is depleted, glycogen and maltodextrins also decrease (Badr et al., 2000).

In the eye the extra cellular matrix play a role in retinal adhesion, prevention of sub retinal choroidal neovascular membrane formation. As the RPE resides in-between the retina and the choroid its role in the production of extra cellular matrix may have relevance in these processes. RPE basement membrane has collagen types I, II, III, IV, fibronectin, laminin (Campochiaro et al; 1986). The RPE is partially responsible for the synthesis and maintenance of Bruch's membrane, found at its basal surface on the choroidal side, and the interphotoreceptor matrix, found at its apical surface on the photoreceptor side. Because of the pivotal role of the RPE and its ECM in supporting the visual process and maintaining the BRB integrity defects in RPE basement membrane

and tight junction integrity leads to various retinal pathologies (Campochiaro et al; 1986).

Two groups of extracellular proteinases, matrix metalloproteinases (MMPs) and the serine proteinase urokinase plasminogen activator (uPA) have been shown to play a role in the retinal neovascularization seen in the later stages of diabetic retinopathy. MMPs are a class of approximately 25 known proteinases that function to degrade at least one component of the extracellular matrix in addition to other substrates. Earlier studies have shown that the gelatinases, MMP-2, MMP-9 and uPA are increased in the epiretinal neovascular membranes of patients with proliferative diabetic retinopathy, (Das et al., 1999) as well as in the retina of animal model with retinal neovascularization.**7** MMP-2 and MMP-9 have also been shown to have significantly increased levels of activation in vitreous samples from individuals with proliferative diabetic retinopathy. (Noda et al., 2003) Although there are numerous studies on the alteration of ECM by MMPs, *in vitro* and *in vivo* there are no reports on the lysyl oxidase levels in relevance to glucose toxicity.

Anatomical and functional changes occur not only in the retina but also in retinal pigment epithelium (RPE) prior to clinical symptoms of the disease. However, the molecular mechanisms responsible for these early changes, particularly in the RPE, remain unclear. Defining the pre-retinopathic changes affecting the RPE could provide important insight into the molecular events that lead to this disease. (Decanini et al., 2008).

With new promising therapies directed at ameliorating the early and late stage of clinically significant retinopathy, it is of profound interest to examine whether intervention immediately at the time of diagnosis of diabetes, in addition to tight control, is feasible to prevent the complications of diabetes such as found in diabetic retinopathy. Investigations of how cells respond to acutely high levels of glucose may provide information about prevention of the cumulative effects of high glucose and thus the RPE culture serves as *in vitro* model to study the effect of high glucose in relevance to diabetic retinopathy.

Hence in this chapter, changes at the level of lysyl oxidase and MMPs were studied after exposing the RPE cells to different concentrations of glucose.

9.2 Design of experiments: Human RPE cell line, namely ARPE-19 was cultured according to procedure mentioned in methodology and were used in these experiments. Cells were plated in 25cm2 flask or 96 well plates for experiments and subsequently changed to M199 medium (because DMEM/F12 has 18.5 mM glucose whereas Medium 199 has 5.5 mM glucose). They were grown to 90% confluence. Before subjecting them to experimental condition they were downshifted from 10% FBS to 5% and then to 1 % FBS over a 24 hour time period and replaced in fresh 1 % FBS containing M199 medium (phenol red free) for 12 hours prior to experiments. Cells were then exposed to 10, 20,30 mM Glucose for a time point of 24, 48 and 72 hours.

9.2.1 Cytotoxicity assay: Cytotoxic effect of glucose was assayed using a colorimetric 3-(4,5-dimethylthiazol-2-yl)-2,5-diphenyl tetrazolium bromide (MTT) assay. Briefly, the human RPE cells were plated at a density of 2500 cells per well in 96-well plates. Cells without added glucose were used as controls. After incubation MTT was added as given in methodology chapter and the solubilized crystals was read in a microtiter plate reader at a wavelength of 540 nm.

9.2.2 Cell proliferation assay: The proliferation rate was determined by measurement of the DNA synthesis rate. Briefly, the human RPE cells were plated at a density of 2500 cells per well in 96-well plates. Cells were then exposed to 10, 20,30 mM Glucose along with BrdU labeling solution for a time point of 24, 48 and 72 hours. Cells without added glucose were used as controls. The incorporation of bromodeoxyuridine (BrdU) into the genomic DNA was determined with the using an anti Brdu antibody followed by an enzyme substrate reaction according to the kit protocol as given in methodology chapter.

9.2.3 Assay for lysyl oxidase enzyme activity in conditioned media (For extracellular LOX activity):

Activity assays for detection of BAPN-inhibitable LOX was assayed as previously described in methodology chapter using concentrated conditioned

medium. Activity assays were repeated three times and each experiment were performed at least in duplicates. Protein estimation was done by Lowry's method.

9.2.4 RNA extraction and Reverse transcription for LOX

Total RNA was extracted from the cell pellet by the guanidine isothiocyanate and chloroform method (TRI Reagent) as given in methodology chapter.

9.2.5 Real-time RT-PCR analyses

TaqMan gene expression assays for LOX (Hs00184706_m1) and two endogenous controls, GAPDH (Hs99999905_m1) and TBP (Hs99999910_m1), were obtained from Applied Biosystems. Quantification of gene expression was performed in a 20 μl volume in 96 well plates on an ABI prism 7300 real time PCR System, in triplicate. Each reaction included 1× TaqMan primer probe mix, 1× TaqMan Universal PCR Master Mix and 100ng of cDNA. Cycling conditions were as follows: 2 min at 50°C, 10 min at 95°C and 40 cycles of 15s at 95°C plus 1 min at 60°C. The normalized gene of interest expression levels was calculated by the following method. Ct values were transformed to quantities by using the comparative Ct method. The untreated control cells were set to 1 as calibrator. The normalization factor for each sample was calculated by taking the geometric mean of the two housekeeping genes (GAPDH and TBP) quantities of that sample using geNorm software. The normalized gene of interest (GOI) expression levels was calculated by dividing the raw GOI quantities for each sample by the appropriate normalization factor. (Bustin et al., 2005).

9.2.6 Semiquantitaive RT-PCR for Lysyl oxidase

PCR amplifications were performed in a 50μl cocktail with primers against LOX, amplifying a fragment of 156 bp and 498bp for GAPDH. The amplification was done for 45 cycles at 60 °C annealing temperature.

9.2.7 Immunostaining for LOX

The cells were grown in 8 well-chambered slides and after the experimental protocol they were fixed in 100 % methanol and subsequently immunostained for LOX using NovolinkTM Min polymer detection system as given in methodology chapter. (Wakasaki et al., 1990).

9.2.8 DQ gelatinase assay:

Activity assay for the detection of gelatinase was assayed as described in methodology chapter using concentrated conditioned medium with and without inhibitor phenanthroline. Protein estimation was performed by Lowry method. Results were normalized to protein content.

9.2.9 Statistics : All results are expressed as mean ±SD. Results are expressed as percent of controls and normalized by protein content, from three experiments performed in duplicate. Student *t* test was done to compare with controls. P value of <0.05 is considered significant.

9.3 RESULTS:

9.3.1 Cytotoxic effect of glucose: ARPE 19 cells incubated with 10, 20 and 30 mM glucose did not show any cytotoxic effect as observed by the morphology (Figure 8.3) and percentage viability estimated by MTT at the end of 3,6, 24, 48 and 72 hours (Figure 9.1).

Figure 9.1: MTT assay of RPE cells exposed to different concentrations of glucose

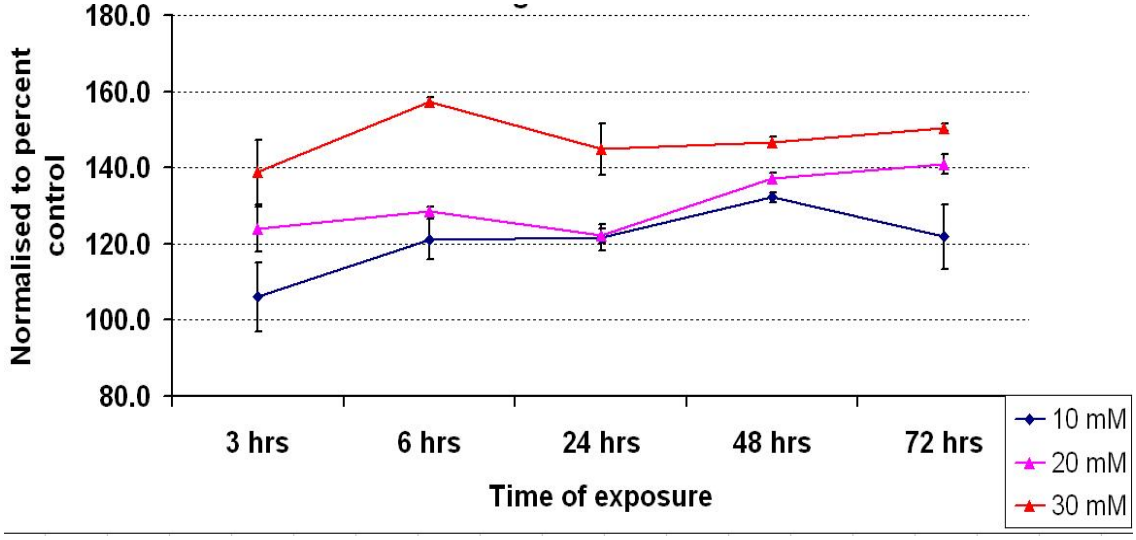

Figure 9.2 : Phase contrast micrograph of RPE cells exposed to glucose

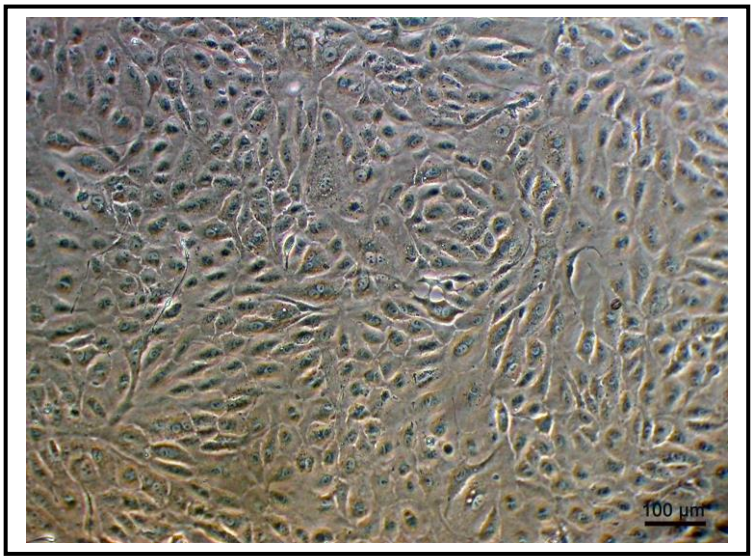

Figure 9.2 shows RPE cells treated with 30 mM glucose at the end of 72 hrs. The cells were confluent and the morphology was not altered.

9.3.2 Cell proliferation assay:

When RPE was exposed to increasing glucose concentration, the BrdU assay for cell proliferation showed a net increase in proliferation at 24 hours time in 10 mM (140%), 20 mM (130%) and 30 mM (122%). (Figure 9.3)

Figure 9.3:BrdU assay in RPE cells exposed to different concentration of glucose

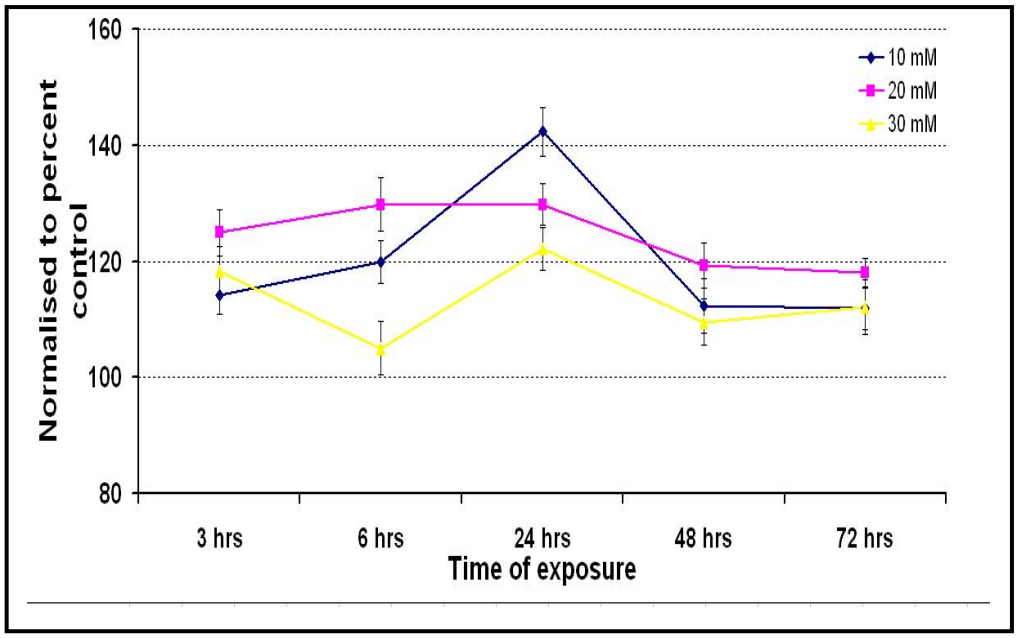

9.3.3 Specific activity of LOX in conditioned media after treatment with glucose: The conditioned media from RPE cultures exposed to 10, 20 and 30 mM glucose, were collected after 24, 48 and 72 hours and after concentrating the media with 10 kDa cutoff filter, the LOX specific activity was assayed with and without BAPN. (Figure 9.4)

Figure 9.4: Specific activity of LOX in conditioned media of ARPE-19 cells.

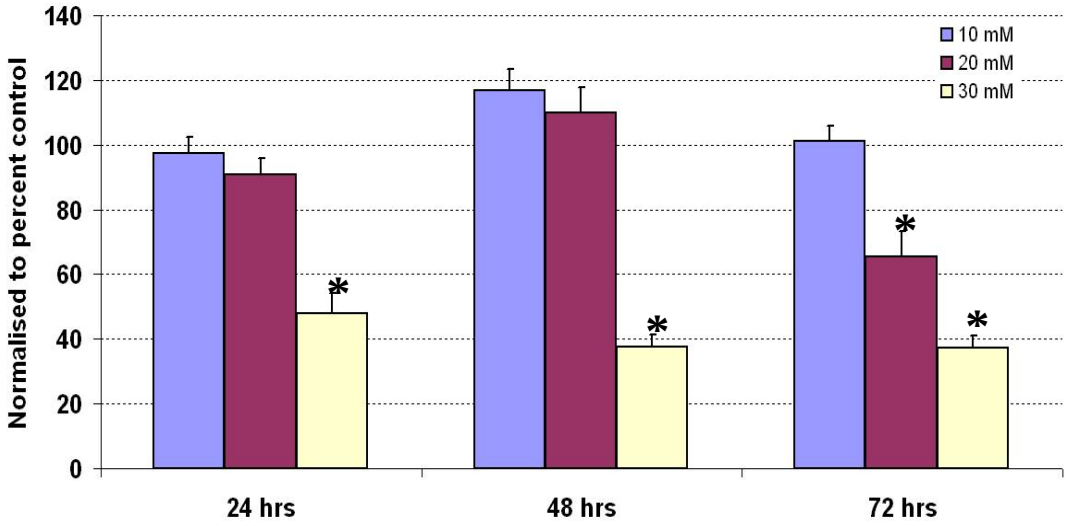

Figure 9.4 shows the LOX specific activity measured in culture media from RPE cells incubated for 24, 48 and 72 hours with increasing concentrations of glucose (10 mM, 20 mM, 30 mM). *$P < 0.05$ was considered significant. The *p* value is a comparison between controls.

There was no significant change in the LOX activity, when RPE cells were exposed to 10 mM glucose concentration, though a mild increase in specific activity of LOX was seen at the end of 48 hrs which subsequently reached to control levels by 72 hours. With increase in concentration of glucose to 20 mM, there was mild increase at 48 hrs with a significant fall in the activity at the end of 72 hrs. (p=0.001). A significant fall (60%) in the specific activity of LOX was seen when the cells were exposed to 30 mM glucose concentration as seen at the end of 24 hours (p=0.001), which continued to be low even at the end of 72 hours (p=0.001). (Figure 9.4).

9.3.4 mRNA expression of lysyl oxidase after treatment with glucsoe:

The levels of LOX messenger RNA (mRNA) was determined in the RPE cells exposed to glucose compared to controls by conventional semi quantitative RT-PCR. Quantification was done by analyzing the band area pixel intensity using Image J software. In 10 mM glucose there was no significant change in the LOX mRNA levels at 24hrs and 72 hrs. In 20 mM glucose there was a 60% decrease in mRNA expression at 72 hours when compared to controls. In 30 mM glucose

there was a 17 % decrease after 24 hrs and 40% decrease in mRNA expression after 72 hrs when compared to controls. (Figure 9.5) This correlated with the decreased specific activity of LOX. (Figure 9.4)

Figure 9.5 shows the RT-PCR results of LOX in ARPE cells after exposure to glucose

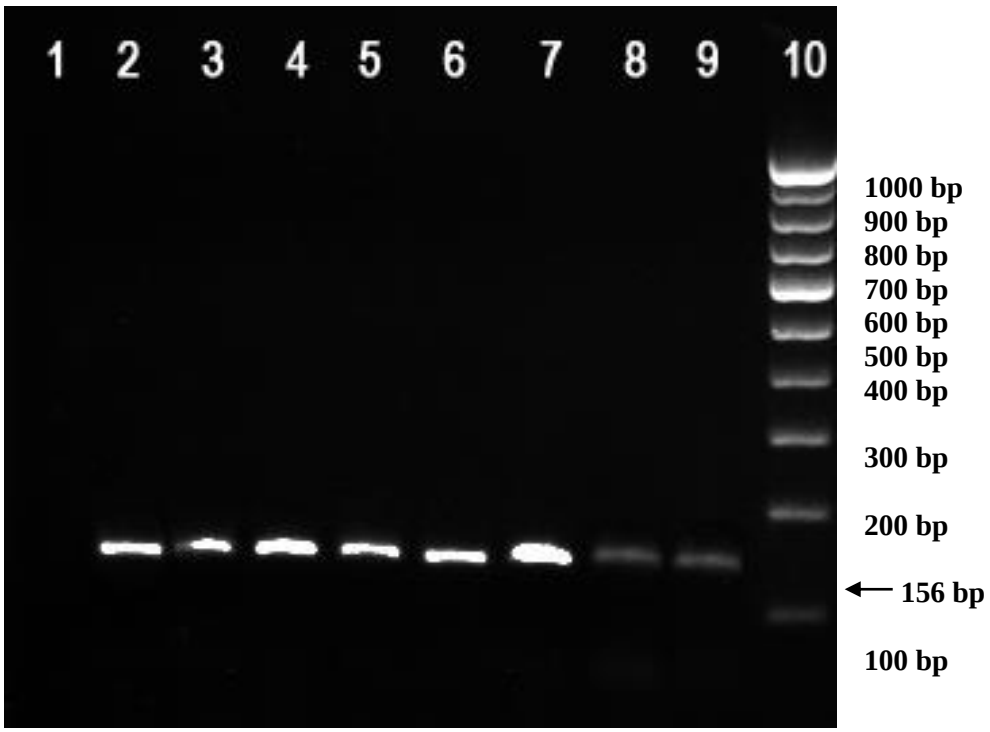

The gel photograph shows the expression of the LOX on the cells harvested after 24 hours and 72 hours. Bands resolved on 2% agarose gel with ethidium bromide. LOX mRNA expression (156bp)was seen in all conditions with a 60% and 40% lowered expression in 20 mM and 30 mM of 72 hours (Lane 8 and 9).

Lane 1 : Negative control
Lane 2 : 24 hrs –control (5.5 mM Glucose)
Lane 3 : 24 hrs – 10 mM Glucose
Lane 4 : 24 hrs - 20 mM Glucose
Lane 5 : 24 hrs - 30 mM Glucose
Lane 6 : 72 hrs –control (5.5mM Glucose)
Lane 7 : 72 hrs – 10 mM Glucose
Lane 8 : 72 hrs - 20 mM Glucose
Lane 9 : 72 hrs - 30 mM Glucose
Lane 10 : 100 bp ladder

Figure 9.6 shows the RT-PCR results of GAPDH in ARPE cells after exposure to glucose.

Lane 1 : 24 hrs –control (5.5 mM Glucose)
Lane 2 : 24 hrs – 10 mM Glucose
Lane 3 : 24 hrs - 20 mM Glucose
Lane 4 : 24 hrs - 30 mM Glucose
Lane 5 : 72 hrs –control (5.5mM Glucose)
Lane 6 : 72 hrs – 10 mM Glucose
Lane 7 : 72 hrs - 20 mM Glucose
Lane 8 : 72 hrs - 30 mM Glucose
Lane 9 : 100 bp ladder
Lane 10 : Negative control

9.3.5 Quantitative real-time RT-PCR: Real time PCR was done to confirm the changes seen by conventional RT-PCR. The LOX gene expression decreased with increasing time after glucose exposure and the decrease was maximal at the 30 mM glucose concentration. A 10 percent decrease was observed in 30 mM glucose at 48 hours, which decreased to 20 percent at the end of 72 hours. In 20 mM glucose there was a 10 percent decrease at the end of 72 hours. (Figure 9.7)

Figure 9.7: mRNA expression of LOX by quantitative real time PCR

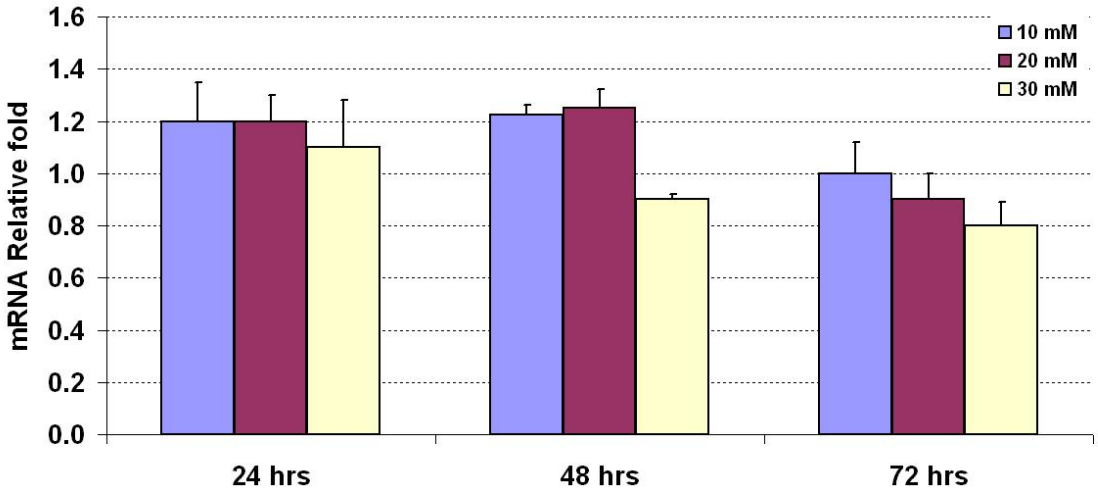

9.3.6 Immunohistochemistry for intracellular lysyl oxidase:

Intracellular LOX immunoreactivity was seen as a dot like positivity in the cytoplasm near the nucleus in ARPE cells. The total number of cells, which were positive, was counted in different areas of the slide and was quantified using Image J software. The control cells immunoreactivity was taken as 100% and the cells exposed to glucose were calculated with respect to control cells positivity. The cells which were exposed to 30 mM glucose there was a 60% decrease in LOX immunoreativity after 72 hours.

(Figure 9.8 -A, B, C, D, E).

Figure 9.8: Immunolocalisation of LOX in ARPE cells exposed to glucose

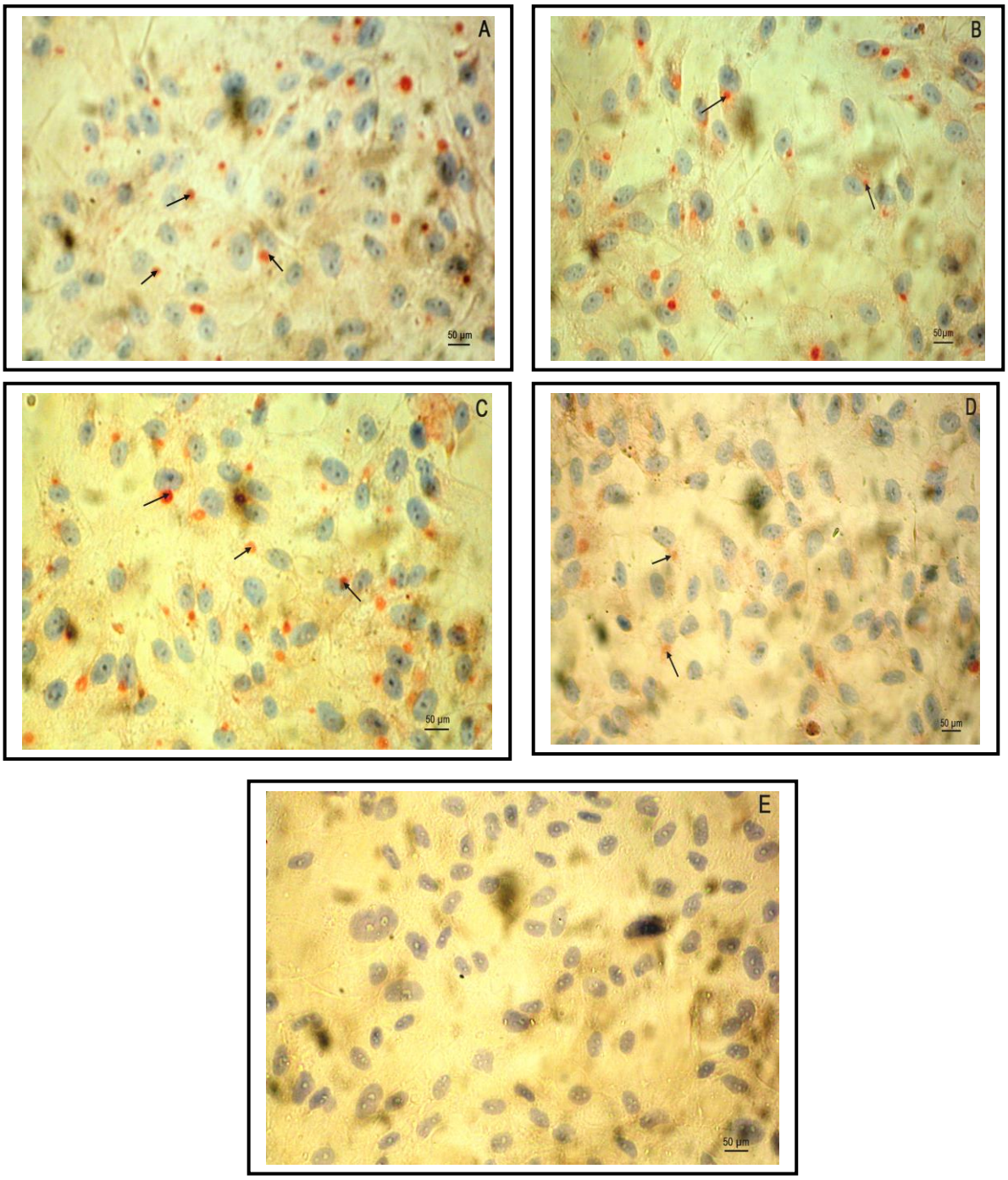

Figure 9.8 shows Immunolocalisation of LOX protein in ARPE cells exposed to glucose after 72 hours by labeled streptavidin biotin method. Positive labeling seen as (reddish brown staining) is shown as arrows in control (A), 10 mM glucose (B), 20mM Glucose (C), 30 mM Glucose (D) and negative control (E). Haematoxylin was used as counter stain. Scale bars 50 µm.

9.3.7 DQ gelatinase assay: The conditioned media from RPE cultures exposed to 10, 20 and 30 mM glucose, were collected after 24 hours and 72 hours and after concentrating the media with 10 kDa cutoff filter, the MMP activity was assayed with and without inhibitor phenanthroline. Compared to the control, the MMP activity was found to be increasing with increase in glucose concentration (Figure 9.9). The increase was found to be significant at 20 mM and 30 mM compared to control at 24 hrs (p = 0.038, p = 0.041) and 72 hrs (p = 0.041, p = 0.028) when compared to controls.

Figure 9.9: DQ gelatinase activity assay in ARPE-19 cells exposed to glucose

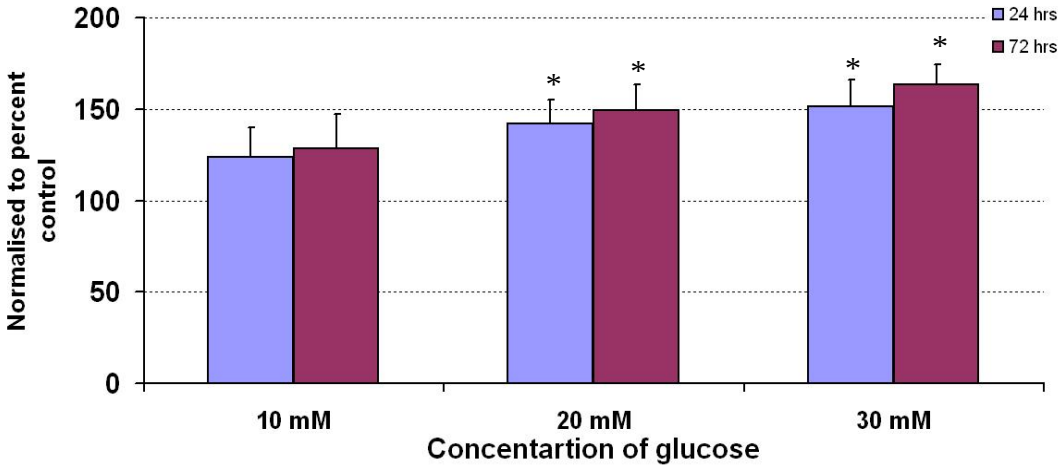

Figure 9.9 shows the unit activity of MMP measured in culture media from RPE cells incubated for 24 and 72 hours with increasing concentrations of glucose (10 mM, 20 mM, 30 mM). Results, expressed as percent of controls, from three experiments performed in duplicates. Students '*t*' test was done and $*P < 0.05$ is considered significant. There was a statistical significant increase in MMP at 20 mM and 30 mM concentration in 24 hrs (p = 0.038, p = 0.041) and 72 hrs (p = 0.041, p = 0.028) when compared to control.

9.4 CONCLUSIONS:

This was the first study to see the changes in LOX activity and expression in response to high glucose exposure in cultured ARPE-19 cells. The decreased LOX specific activity and mRNA expression was significant at 30 mM glucose concentration with time. Further studies are required to see the effect of glucose on LOX and MMPs in long-term glucose exposure. The LOX isoforms should also be explored for understanding the molecular events that leads to this disease by RPE cells.

CHAPTER 10: ROLE OF HOMOCYSTEINE ON THE ACTIVITY OF LYSYL OXIDASE ; *IN VIVO* AND *IN VITRO*

10.1 INTRODUCTION:

Homocysteine (Hcys) is a sulphur containing amino acid with a free thiol (sulphydryl –SH) group, formed from methionine through S–adenosyl methionine in blood. (Castro et al., 2006).

Methionine → S –adenosyl methionine → homocysteine

It is easily oxidized in the blood to Hcys and other disulphides with other amino acids like cysteine in which the thiol group is replaced by a disulphide (- S-S) group.

In humans, 15–20 μM of Hcys is synthesized each day, but most of them are converted to either cysteine or methionine. The three main metabolic fates of Hcys are: to be remethylated to methionine, or to enter the cysteine biosynthetic pathway, or to be released into the extracellular medium. Hyperhomocysteinemia is described; it is denoted as moderate (15–30 μ*M*), intermediate (30–100 μ*M*) or severe (100 μ*M*) (Brazioniset al., 2008). Hyperhomocysteinemia (HHcy) has been associated with both folate and cobalamine deficiencies, and also with pregnancy complications, neural tube defects, mental disorders, cognitive impairment in the elderly, psoriasis and some tumors (Refsum et al., 1998) New metabolic roles of Hcys is being described that could help to understand the pathological consequences of increased levels of homocysteine in the system. They include its interactions with key modulator molecules, its own ability to modulate certain enzyme activities, or its involvement in protein modification.

Elevated plasma Hcys has been associated with vascular remodeling in the context of both cardiovascular (Perla-Kajan et al., 2007) and cerebrovascular diseases (Lominadze et al., 2006). Although severe hyperhomocysteinemia (Hhcys) (>100μM) is a rare phenomenon affecting 1/200,000 births, mild Hhcys (30–100 μM) is present in ≈6% of the general population (Hankey et al., 1999) High levels of Hcys impair endothelial function and cause endothelial damage in humans as well as in animal models, indicating that the endothelial monolayer is

very sensitive to changes in plasma HC levels (Finkelstein et al.,1990). Hhcys is clinically related to high risk of thrombotic events mainly due to an enhancement in platelet aggregation and tissue factor generation, and an inhibitor of both thrombomodulin cell-surface expression and protein C activation (Selhub et al.,1992) Increase in Hcys at the level of plasma has been implied not only in cardiovascular disease but also in ocular diseases such as in ectopia lentis (Lieberman et al., 1966), secondary glaucoma (Roedl et al., 2007), optic atrophy (Stanger et al., 2005), ARMD (Coral et al., 2006), CRVO (Narayanasamy et al., 2007) and diabetic retinopathy (Brazionis et al., 2008).

10.1.1 Homocysteine in Diabetes:

Plasma total Hcys concentration may be a useful biomarker and a novel risk factor for increased risk of diabetic retinopathy in people with type II diabetes. A higher mean plasma total homocysteine concentration was observed in diabetic individuals with retinopathy than in those without retinopathy (11.5 µmol/l [95% CI 10.4 –12.5] vs. 9.6 µmol/l [9.1–10.2], p = 0.001). Furthermore, the relationship between homocysteine and diabetic retinopathy was not explained by renal dysfunction and was independent of the other major risk factors for diabetic retinopathy (duration of diabetes, A1C, and systolic blood pressure) and determinants of higher homocysteine concentrations (age, sex, and red cell folate) (odds ratio 1.20 [95% CI 1.023–1.41], p =0.024) (Bracionis et al.,2008).

Different molecular mechanisms have been proposed to explain the pathological alterations promoted by Hcys. One of them is that Hcys leads to an imbalance in the redox state (Hankey et al.,1999) Plasma Hcys is rapidly oxidized in a reaction that generates reactive oxygen species (ROS) such as superoxide anion ($O_2^{\cdot -}$) that decrease NO bioavailability (Hankey et al.,1999). Another mechanism that could explain the deleterious effects of Hcys is the increase of endoplasmic reticulum (ER) stress (Antonio et al., 1997; Jakubowski et al., 1999) that seems to be associated with the Hcys induced endothelial cell death (Zhang et al.,2001)

10.1.2 Lysyl oxidase and Homocysteine:

Hhcys is also associated with extracellular matrix (ECM) alterations including changes on the elastic properties of the vascular wall (Toohey et al.,2008). Lysyl

oxidase (LOX) is one of the enzymes involved in ECM maturation. Inhibition of LOX activity has been related with Hhcys and has been studied in terms of its molecular mechanisms in vascular diseases (Liu et al., 1997; Raposo et al., 2004). Hcys related compounds contain a thiol-group (cysteine) which inhibits LOX, while methionine and homocystine (non-thiol containing molecules) did not exert any effect. Thus the presence of the thiol-group is necessary to inhibit LOX. Exposure of aortic endothelial cells to high Hcys concentrations is reported to give a significant down regulation of LOX mRNA levels through a reduction of LOX promoter activity.

10.1.3 Homocysteine in vitreoretinal pathology

The role of Hcys has been hardly studied in vitreous during vitreoretinal pathology except for a recent report by Aydemir *et al* on the elevated levels of Hcys in the vitreous and plasma of patients with PDR (Aydemir et al., 2008). Where they have reported a mean vitreous and plasma Hcy concentrations for the diabetic group as 3.64 ± 0.65 µmol/L (range, 2.03–4.50 µmol/L) and 16.04 ± 2.75 µmol/L (range, 7.97–19.16 µmol/L), respectively. The mean vitreous and plasma Hcy concentrations ± SD for the control group were 1.08 ± 0.45 µmol/L (range, 0.08 –1.82µmol/L) and 9.18 ± 3.91 µmol/L (range, 3.77–16.76 µmol/L), respectively. Both plasma and vitreous Hcy concentrations for the diabetic group were significantly higher than those for the control group (P =0.001). Intravitreal Hcy concentrations for the diabetic patients appeared to correlate with plasma Hcy levels.

Therefore the aim of the present study was to estimate vitreous levels of Hcys in eyes with PDR and RRD and to see if there is any correlation with the specific activity of LOX. Along with this ARPE-19 cells were also exposed to homocysteine to see if there is any effect on LOX specific activity.

10.2 MATERIALS AND METHODS:

All experiments involving human subjects adhered to the tenets of Helsinki declaration. Undiluted vitreous samples from 25 patients (Age 54 ± 10: M =21 and F=4) with PDR and 18 patients (Age 48 ± 15: M =15 and F= 3) with RRD

were collected by the vitreoretinal surgeon at the time of vitreoretinal surgery. Clinical details of the patients are given Table 5.1 and 5.2 given in appendix I.

10.2.1 HPLC analysis of homocysteine

Hcys was analyzed using high-pressure liquid chromatography (HPLC) as described by Tcherkas *et al* with slight modification (Tcherkas et al., 2001). The HPLC system Agilent 1100 series model consisted of two pumps fitted with a 50 µl loop rheodyne injection valve and fluorescent detector. Separation was achieved on a phenomenex ODS column (150 X 4.6 mm, internal diameter 5 µm). The elution procedure was performed with 0.05M acetate buffer (pH 7.0) containing 75% methanol in isocratic mode, at 26°C with a flow rate of 0.7 ml/min. Fluorescent detector with excitation at 330nm and emission at 450 nm was used for detection. Prior to analysis the system was calibrated with authentic DL homocysteine standards in the range of 25-100 ng. Hcys was eluted at 2.9minute retention time. Inter assay coefficient variation (CV) was 2.8 %.

10.2.2 Processing of vitreous sample:

In brief, to 20µl of vitreous sample 2µl of 2-mercaptoethanol was added for reduction of disulphide bonds, followed by 40µl of 0.8 M iodoacetic acid and 120µl of 0.1 M borate buffer pH 11.5. After incubation for 30 sec at room temperature 20µl of OPA-2-ME reagent was added and 50µl was injected onto the HPLC system.

10.2.3 Statistics: With SPSS software, (version:14.0) the raw data was analyzed for statistical significance using independent sample *t* test and Pearson's correlation. *p* value of <0.05 is considered significant.

10.3 RESULTS *in vivo*

10.3.1 HPLC analysis of homocysteine in vitreous

Homocysteine was eluted at 2.8 minute retention time (Figure 10.1). The mean total Hcys level in PDR was found to be 2.76 ±0.28 µM (p=0.011) showing a 2 fold increase compared to controls. In RRD there was a 3.5 fold increase with a mean of 4.68±0.74µM (p=0.001) compared 1.28±0.31 µM in control. (Table

10.1) The distribution profile of Hcys in the vitreous was found to be in the range of 0.53 to 4.6 in PDR, 0.50 to 9.6 in RRD and 0.0 to 4.18 in control. There was an undetectable Hcys level in 7 out of 19 donor vitreous controls.. Within the two disease conditions Hcys was found to be significantly increased in RRD compared to PDR (p =0.019).

Table 10.1: Comparative levels of homocysteine, lysyl oxidase in control versus diseased vitreous

Conditions	Protein (mg/ml)	Homocysteine (μM)	LOX (nm/min/mg protein)
Control	1.12 ± 0.18	1.28 ± 0.31 (n=19)	534.8 ± 162.5 (n=34)
PDR	3.82 ± 0.80* (*p*=0.002)	2.76 ± 0.28 * (*p*=0.011) (n=18)	145.1 ± 52.3 * (*p*=0.028) (n=25)
RRD	8.82 ± 2.00 * (*p*=0.000)	4.68 ± 0.74** (*p*=0.001) (n=17)	59.1 ± 20.6 ** (*p*=0.006) (n=18)

Values are expressed as Mean □ SEM.

p value : Control with PDR and RRD, respectively

Figure 10.1 HPLC chromatogram of vitreous sample

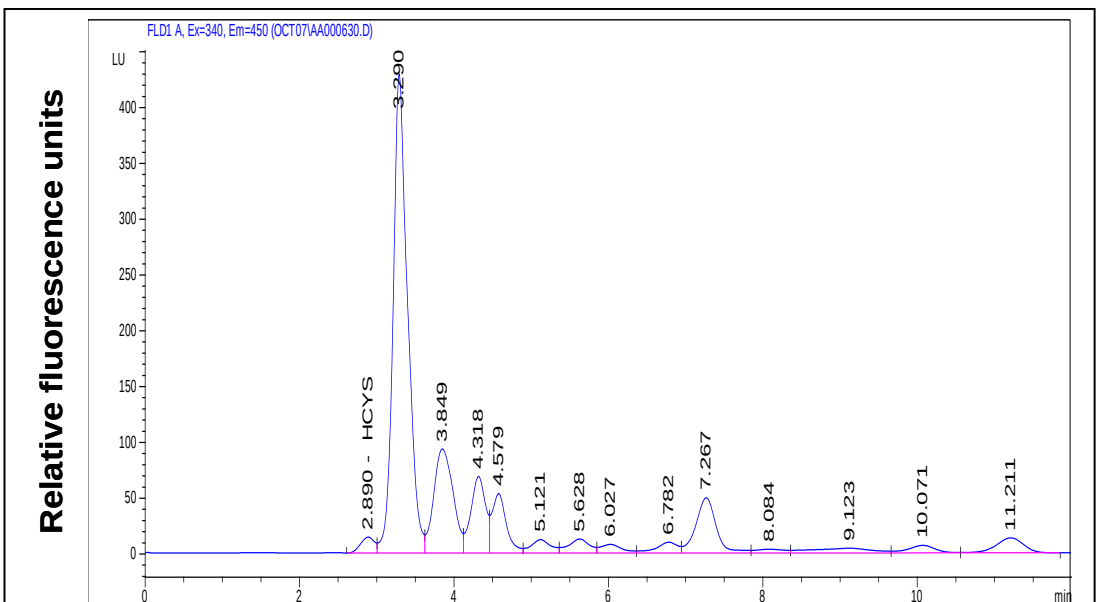

Figure 10.2: Distribution profile of vitreous homocysteine in eyes with PDR, RRD and the donor eyeball controls.

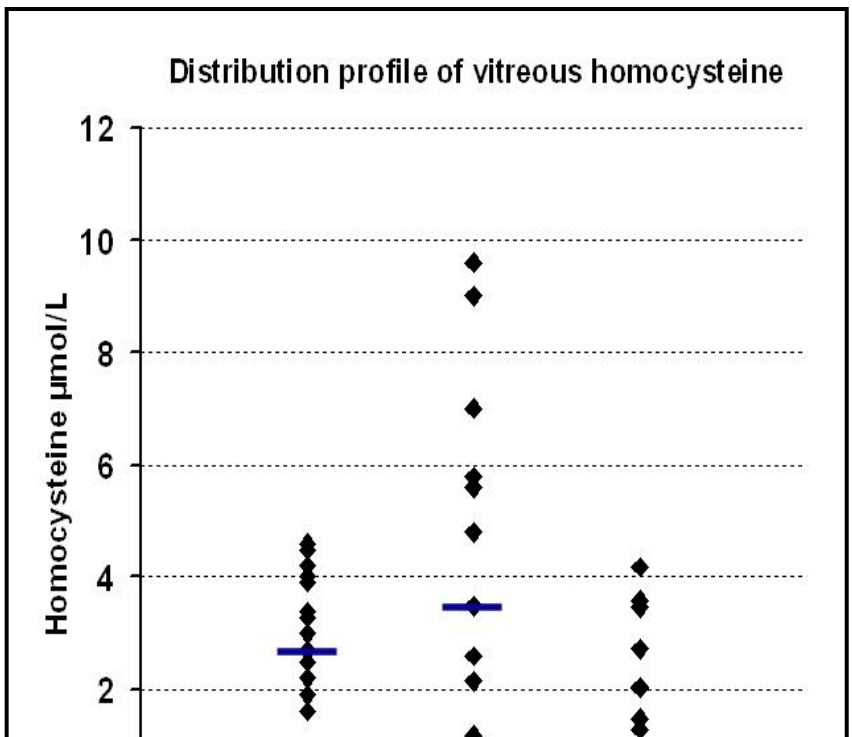

The median is indicated as solid lines. The median Hcys level in PDR is 2.6 μM, in RRD 3.5 μM compared to 0.78 μM in controls. (PDR n=18, RRD n=17, Control n=19)

Since plasma Hcys is a known risk factor in hypertension, clinically the PDR and RRD cases were analyzed as with and without hypertension. However there was no significant difference in the vitreous levels of Hcys in both the groups. However larger sample sizes have to be dealt with before any conclusions is drawn from this. Among the 17 RRD eyes, 3 of them showed anterior segment pathology associated with inflammation and all these cases had relatively higher Hcys level in the vitreous compared to other eyes.

10.3.2 Correlation between Lysyl oxidase and Homocysteine in Proliferative diabetic retinopathy and Rhegmatogenous retinal detachment:

In order to determine whether there is statistically significant inverse relationship between LOX and Hcys we analyzed the data by doing Pearson's correlation. We found that there was a statistically significant negative correlation between vitreous Hcys and LOX in PDR cases ($p=0.040$) and in RRD ($p = 0.029$). (Figure 10.3 and 10.4) Thus the detailed analysis of individual data show statistically significant correlation between decreased specific activity of LOX and increased Hcys in PDR and RRD.

Figure 10.3: Pearson's correlation between homocysteine and LOX specific activity in vitreous of eyes with PDR. (n=15)

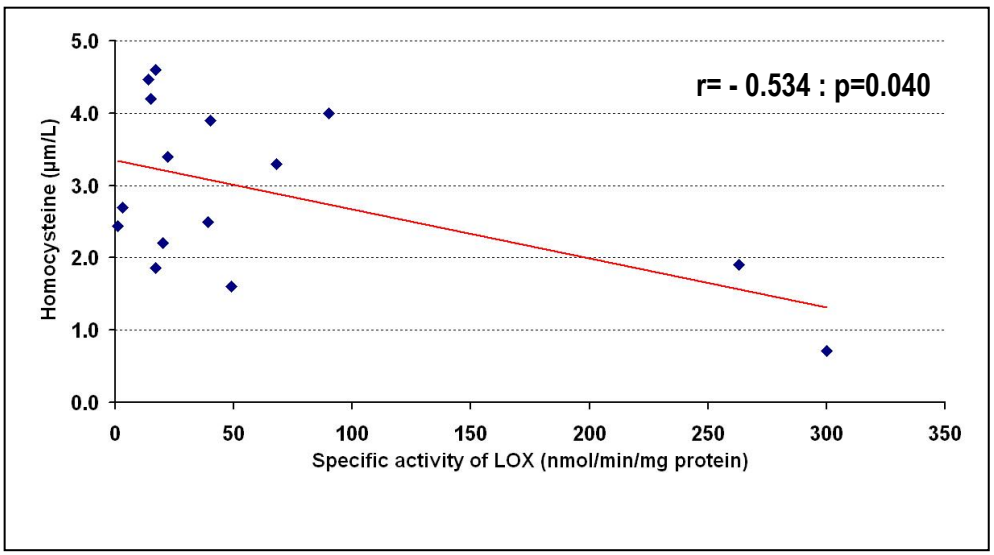

There is a statistically significant negative correlation with r= -0.534: p=0.040.

Figure 10.4: Pearson's correlation between homocysteine and LOX specific activity in vitreous of eyes with RRD.

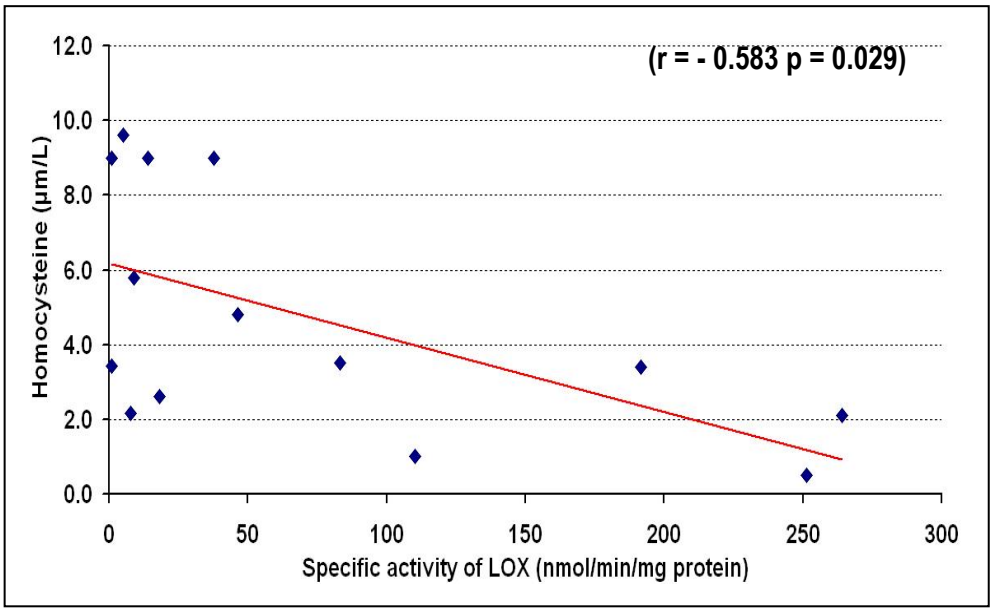

There is a statistically significant negative correlation with r = - 0.583 p = 0.029. (n=14)

10.4. Experimental condition for *in vitro* effect of homocysteine :

ARPE 19 cells were grown to confluence and exposed cells to DL-Homocysteine to see the thiol mediated effect on LOX activity

After a period of 12 hour exposure in 1 % FBS containing M199 medium the cells were exposed to DL-Homocysteine at concentrations of 5 µM, 15 µM, 30 µM, 60 µM and 100 µM) and incubated for 24 and 48 hours.

10.4.1 Cytotoxicity assay

Cytotoxic effect of tBH and DL-Homocysteine, was assayed using a colorimetric 3-(4,5-dimethylthiazol-2-yl)-2,5-diphenyl tetrazolium bromide (MTT) assay. Briefly, the human RPE cells were plated at a density of 2500 cells per well in 96-well plates. Cells were then exposed to DL-Homocysteine at concentrations of 5 µM, 15 µM, 30 µM, 60 µM and 100 µM and incubated for 24 and 48 hours. Cells without homocysteine were used as controls. After incubation MTT was added as given in methodology chapter and the solubilized crystals was read in a microtiter plate reader (Bio-Tek, USA) at a wavelength of 540 nm. The percentage viability was calculated using the formula: optical density of treated sample/optical density of untreated control ×100.

10.4.2 Assay for lysyl oxidase enzyme activity in conditioned media (For extracellular LOX activity):

Activity assays for detection of BAPN-inhibitable LOX was assayed as previously described in methodology chapter using conditioned medium concentrated using 10kDa cutoff Millipore filters. The fluorescent product was excited at 560 nm and the emission was read at 590 nm every 10 min for 2 hours using a Dynex TRIAD multimode plate reader (Palamakumbura et al., 2002). Activity assays were repeated three times and each experiment were performed at least in duplicates. Protein estimation was done by Lowry's method.

10.4.3 **Semiquantitaive RT-PCR for Lysyl oxidase**

Total RNA was extracted from the cell pellet by the guanidine isothiocyanate and chloroform method (TRI Reagent) as given in methodology chapter. PCR amplifications were performed in a 50µl cocktail with primers against LOX,

amplifying a fragment of 156 bp and 498bp for GAPDH. The amplification was done for 45 cycles at 60 °C annealing temperature.

10.4.3 Statistics: All results are expressed as mean ±SD. Results are expressed as percent of controls and normalized by protein content, from three experiments performed in duplicate. Student *t* test was done to compare with controls. P value of <0.05 is considered significant

10.5 Results *in vitro*:

10.5.1 Cytotoxic effect of homocysteine on ARPE-19 cells:

ARPE cells exposed to different concentrations of homocysteine showed a dose and time dependent decrease in metabolic activity from 10 µM concentration of homocysteine. After 24 hrs of incubation the metabolic activity was 85 % in 10 µM Hcys that dropped to 50 % at 100 µM Hcys concentration. Compared to 24 hours, at 48 hours the metabolic activity of the cell was found to be marginally higher. After 48 hrs of incubation the metabolic activity was near control level in 10 µM Hcys that dropped to 62 % at 100 µM Hcys concentration. There was no change observed in the morphology of the cells at all concentrations. The LD 50 for Hcy was 100 µM. **(Figure 10.5)**

Figure 10.5: MTT assay in ARPE-19 cells exposed to DL Homocysteine

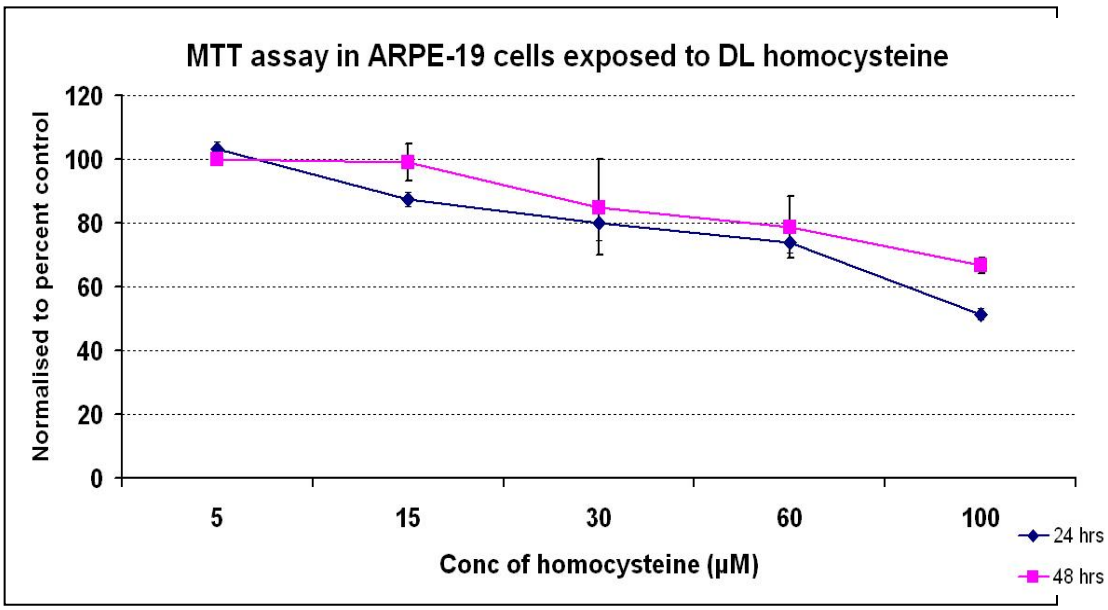

10.5.2 Specific activity of LOX in ARPE 19 cells exposed to homocysteine

There was a dose dependent decrease in the LOX activity, when ARPE cells were exposed to different concentration of homocysteine. The decrease was statistically significant when compared to the controls in 30, 60 and 100 µM concentrations after 24 and 48 hrs ($p=0.001$). At 48 hrs the LOX activity increased above the control levels at 5 and 15 µM concentrations and later decreased to 50% compared to controls at 100 µM concentrations. (Figure10.6)

Figure10.6: Specific activity of LOX in ARPE-19 cells exposed to DL-Homocysteine:

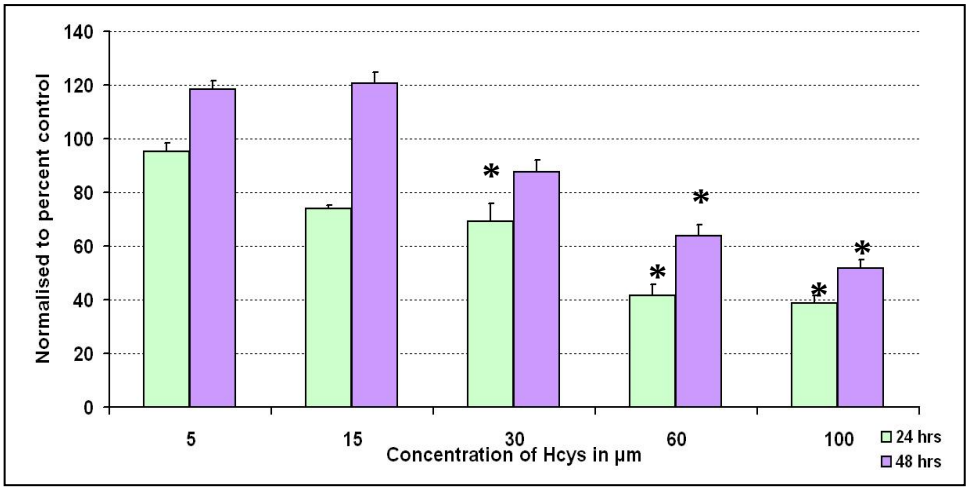

Figure 10.6 shows the LOX specific activity measured in culture media from RPE cells incubated for 24 and 48 hours with increasing concentrations of homocysteine (5 µM – 100 µM). Results, expressed as a percent of controls and normalized by protein content, from three experiments performed in duplicate. Students '*t*' test was done and $*P < 0.05$ is considered significant. The p value is a comparison between controls.

10.5.3 : **mRNA expression of lysyl oxidase after treatment with homocysteine:**

Figure 10.7 shows the mRNA of LOX in RPE cells exposed to DL-Homocysteine

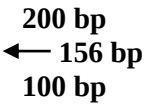

The gel photograph shows the expression of the LOX on the cells harvested after 24 hours and 48 hours after exposure to homocysteine. Bands resolved on 2% agarose gel with ethidium bromide.
LOX mRNA expression (156bp) was seen 30 μM and 50 μM (Lane 1, 2 and 5,6 in 24 and 48 hours).

Lane 1 : 30 μM – 24 hours
Lane 2 : 50 μM – 24 hours
Lane 3 : 100 μM – 24 hours
Lane 4 : control
Lane 5 : 30 μM – 48 hours
Lane 6 : 50 μM – 48 hours
Lane 7 : 100 μM – 48 hours
Lane 8 : Negative control
Lane 9 : 100 bp marker Negative control

10.6 CONCLUSION

This is the first study in measuring vitreous homocysteine levels in RRD. Based on this study it is hypothesized that that the increased levels of Hcys in the vitreous could down regulate LOX activity and/or up regulate the MMPs. LOX inhibition favours the presence of soluble forms of collagen that are highly susceptible to degradation by MMPs. This altered ECM is reflected as increased collagen turnover. The decreased LOX can probably lead to inadequate collagen cross linking, which may pave way for vitreous liquefaction. Growth factors such as tumor necrosis factor α (Rodriguez et al., 2008a) and CTGF can play a role in regulating the LOX and MMP activities needs to be further explored.

CHAPTER 11 : DISCUSSION

RPE lodged in the basement membrane is important for blood retinal barrier integrity. Any alterations at the level of basement membrane can lead to the dislodgment of RPE, leading to migration and proliferation as a pathological process. Proper anatomical apposition between the retina, the RPE, and BM is crucial for nutritional support of the photoreceptors, retinol metabolism, phagocytosis of the photoreceptors outer segments, and formation of the outer blood-retinal barrier, and thus for good visual function. The attachment of the RPE to basement membrane is possibly complemented through regions of hemidesmosomes containing fine filaments of laminin, proteoglycans and collagen types IV and V. (Campochiaro et al., 1986; Marshall et al., 1993;) The structural integrity of BM depends on the collagen cross-links. During the formation of intermolecular cross-links, collagen fibers become increasingly insoluble and refractory to the action of enzymes and show a progressive increase in tensile strength which is essential for normal connective tissue functioning (Vater et al., 1979).

Collagen as well as elastin the most abundant connective tissue protein are substrates for the enzyme Lysyl oxidase (LOX). The metabolic turnover of mature collagen and elastic fibers in adult animals is relatively slow (Shapiro et al., 1991). Snowden *et al.* found a relatively large number of immature cross-links in collagen from adult bovine vitreous, consistent with increased collagen production (Snowden et al., 1982).

LOX is reported to be increased in Hepatic fibrosis, Wilson's diseases, Liver granuloma, Lung fibrosis, Cardiovascular disease, metastatic breast cancer (Ciszar et al., 2002) plaque deposits in Alzheimer's disease (Gilad et al.,2005), hypertropic scarring, Keloids, scleorderma (Chanoki et al., 1995) and diabetic skin. It is reported to be decreased in Type IX Ehlers Danlos syndrome (Di Ferrante et al., 1975) and Menkes disease (Vulpe et al., 1993).

The level of LOX in ocular tissue has not been reported. Recently, Hewitt *et al* has reported mRNA expression of LOXL1 mRNA and protein, in human donor ocular tissues (Hewitt et al.,2007).

This study revealed the presence of LOX in the various ocular tissues in terms of specific activity, localization and mRNA expression. Vitreous showed the highest specific activity amongst the ocular tissues studied which was also confirmed by dot blot analysis. This distribution profile of LOX is found to be similar to the collagen content in the ocular tissue reported by Siddiqi *et al*. The variation in LOX distribution and activity could be reflective of the inherent differences in the collagen structure and composition in these tissues. Therefore this study helps in understanding the ocular tissues further with respect to the extent of collagen cross linking activity. Retina reportedly had the lowest content of soluble and insoluble collagen (Siddiqi et al., 2001) which was found to correlate with the lowest LOX expression.

This is the first report showing LOX distribution in terms of its specific activity and immunolocalization in ocular tissues. The variation in the specific activity of LOX in different ocular will be helpful in finding out the changes at the level of ECM in ocular pathology and therefore could be a target for intervention.

Lysyl oxidase activity in vitreoretinal pathology :

Despite progress in the treatment of vitreoretinal diseases such as PDR and PVR, they still continue to be major cause for visual impairment. Changes in the activity of MMP 2 and MMP 9 have already been documented in both PVR and PDR. While a low activity of MMP 2 is constitutively present in vitreous, the MMP 9 activity is reported to be increased in both PDR and PVR**.** The ratio of total MMP 9:2 as determined in this study shows that it is similar with the previous report by Abu El-Asrar *et al*, which was highest in PDR followed by RRD **(**Abu El-Asrar *et al*, 2007)

While the degredatory enzyme namely MMPs have been detected in the vitreous, fibrovascular and neovascular membranes, LOX may also play a crucial role in the ECM changes, which so far has not been looked into. This study shows that there is a significant decrease in the level of LOX specific activity that is possibly associated with the ECM remodeling. This is the first report showing a significant decrease in LOX specific activity in the vitreous of PDR and RRD.

In PDR, immature collagen cross linking is reported due to the non-enzymatic glycosylation of collagen as sugars can compete for the same lysine and hydroxylysine residues that serve as substrates for LOX and there could be substrate unavailability (Lien et al., 1984). It has also been reported that glucose inhibit collagen fibril formation *in vitro* (Buckingham et al., 1990). The degree of decreased collagen fibril formation has been shown to correlate with the loss of ability of collagen to serve as a substrate for LOX (Buckingham et al., 1990). In spite of the collagen turnover, the collagen fibrils may not be adequately cross linked owing to the decreased lysyl oxidase activity as observed in this study. However, additional work is needed to determine the relative roles of nonenzymatic glycosylation versus decreased LOX activity with respect to immature collagen cross linking in PDR.

Decreased LOX activity was also observed in the vitreous of patients with RRD, compared to controls. The decrease in LOX activity in RRD is intriguing as these patients were nondiabetic. LOX expression has been shown to be regulated by transforming growth factor β (Oleggini et al., 2007), tumor necrosis factor α (TNF α) (Alcudia et al., 2008). TNF α is produced locally as an inflammatory response and is reported to be increased in vitreous of PDR and RRD (Demircan et al., 2006; Limb et al., 2001). Although PVR and PDR have different causes and clinical characteristics, retinal membranes from both conditions share the features of fibroplasia, excessive matrix protein deposition, and cellular infiltration. The decrease in vitreous LOX could be due to the changes in the levels of growth factors, which is reported both PDR and RRD.

The only other report showing the relevance of LOX in ocular pathology comes from a recent study on LOXL1 knockout mouse model where in there is defective elastin fibre that has been associated with increased susceptibility to laser induced choroidal neovascularisation (Yu et al., 2008).

In this present study, we report that there is a decreased lysyl oxidase activity in the vitreous of PDR and RRD patients as part of the altered ECM activity. However the fact that there is a strong LOX positivity in the ERM is indicative of the pathogenic activity in RRD and PDR with respect to this membrane

formation (Figure 5.8). Increased MMP activity associated with increased turnover of collagen was also revealed by the increase in hydroxyproline content of the altered ECM.

This is the first report of vitreous levels of LOX in PDR and RRD. The observed decrease in LOX activity may contribute to inadequate collagen cross-linking and with improperly crosslinked collagen, there could be a net vitreous degradation leading to liquefaction. The increase in the vitreous protein level is indicative of the high ECM activity associated with the pathology. To gain a deeper understanding of the role of LOX, factors that can have a regulatory role on LOX have to be looked into in the vitreoretinal diseases such as PDR and RRD. One of the factors that can modulate LOX namely hcys was further studied both *in vitro* and *in vivo*.

Thus with the knowledge of LOX distribution in ocular tissues and vitreous showing the maximal activity, the cross-linking and the proteolytic activity in terms of LOX and MMPs were studied in established RPE cell cultures under *in vitro* stress conditions which mimic the ocular pathology namely ARMD, PDR and PVR.

Cell cultures can be established primarily from either human or animal origin with its own disadvantages and advantages. The advantage of using animal origin eyes over that of human eyeballs processed is that (i) the processing could be completed within 3 hours from the time of enucleation (ii) handling would be easier owing to the larger size of the globe (iii) and higher yield of RPE cells were obtained from bovine eye ball. Human eyes could be obtained only after 8 – 12 hours after the enucleation and the success rate was very less.

This study established methods for the isolation of primary bovine retinal pigment epithelial cells by mechanically removing the RPE using sterile swab. The time taken for the cells to reach confluence in the primary culture varied from 12- 16 days. Proliferation studies with 30nCi ^{3}H showed a proliferative log phase upto 8 days. We also found that the BRPE cells showed immunoreactivity to cytokeratin 8.13 from passages 1 to 5 by immunoflourescence and western blot. Thus the cells were characterized as RPE before the experiments and passages 1 to 5 were used for subsequent experiments. Human cell line ARPE-19

obtained commercially from ATCC was also used in experiments. These two cultures provide the *in vitro* cell model for the experiments done.

There are relatively few studies about the relevance of LOX in RPE cells. Omori *et al* have shown expression of LOX mRNA in rabbit RPE cells. (Omori et al., 2002). Wachi et al., reported that the ARPE-19 cells express fibrillin-containing microfibrils and lysyl oxidase. (Wachi et al., 2005). In addition LOX has also been studied extensively in normal and transformed cells like lung fibroblast (Boak et al., 1994), arotic smooth muscle cells (Bronson et al., 1987; Contente et al., 1993), gingival fibroblast, mesenchymal cells (Trackman et al., 1998), osetoblast (Pischon et al., 2004) and osteosarcoma cells), in response to various effectors of LOX (Csiszar et al., 2001). Jansen *et al*, demonstrated LOX activity and expression in two well-characterized epithelial cell lines MDCK II and MCF-10A which exhibit crucial features of polarized epithelia *in vivo*, and display the characteristic "cobblestone" morphology of epithelial cells in culture. (Jansen *et al*, 2007). The behavior of RPE cells in post confluent cultures, where intercellular adhesions are more mature, there is more close simulated RPE cells *in situ* than cells in early-confluence cultures. (Kaida M, et al 2000). On determining how confluence affects the properties of cultured human retinal pigment epithelium (RPE) cells, The mRNA expression of LOX was done in pre and post confluent cultures which showed increased LOX expression in post confluent ARPE cultures compared to preconfluene (figure11.1). Thus in the cell culture experiments we used 90 % confluent cultures while looking at the regulation of such enzymes which is relevant in ECM biology.

Figure 11.1: mRNA expression of LOX by real time PCR in ARPE-19 cultures

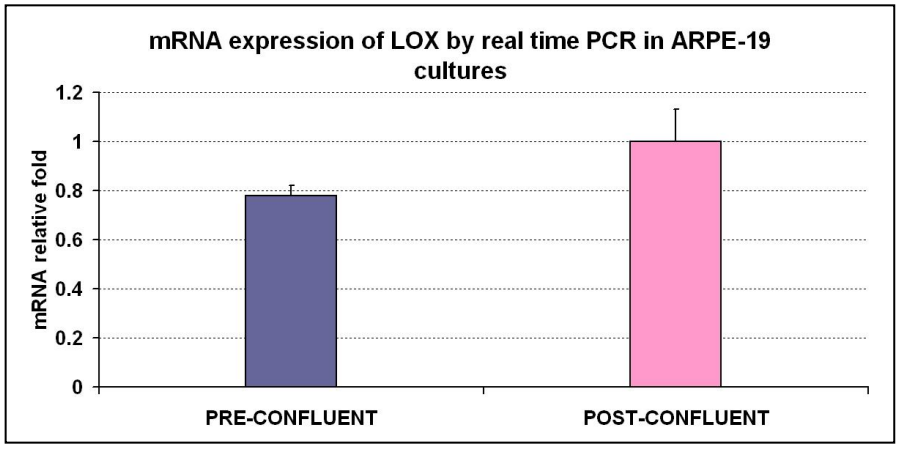

Effect of *in vitro* oxidative stress on lysyl oxidase

The chemical oxidant tBH is known to induce a high degree of oxidative stress to the RPE cells under *in vitro* conditions. When oxidative stress was induced by tBH the metabolic activity of the cell decreased with increase in oxidative stress, which is also found to be associated with increase in the number of apoptotic cells as stained by the TUNNEL staining. This study reveals that tBH, at 1.0 mM concentration decreases the viability of ARPE-19 cells to about 50% of the controls, after 6 hours exposure. Volobоueva et al had reported 50 % viability of RPE at 0.8 mM tBH in human fetal RPE cells (Volobоueva et al 2005).

There was a significant dose dependent increase in the LOX activity with increasing tBH concentration and with time of exposure. LOX is reported to be up-regulated in the brain and spinal cord of late stage Cu,Zn-SOD mutant mice (mSOD1). This increase has been attributed to the increased expression of LOX in response to enhanced oxidative stress induced by mSOD1. The presence of cAMP response element (CRE) in the LOX promoter and enhancer region has been shown to play a critical role in controlling cell survival signal cascades. Though elevated LOX in response to oxidative stress could be a part of protective mechanism, excessive activity of LOX can produce increased amount of H_2O_2 as a by-product during its catalytic reaction may exacerbate the oxidative stress. In the present study along with LOX the MMP activity was also found to be increasing with increase in tBH concentration. Therefore the net effect on the ECM changes will probably depend on the extent of the oxidative stress. A direct measure of intracellular ROS showed an increase in oxidative stress with increasing concentration of tBH.

Eyes with ARMD demonstrate accumulation of specific deposits and ECM molecules under the RPE (Kamei et al., 1999). Repetitive acute and transient oxidant-mediated injuries with hydroquinone-upregulated the collagen type IV accumulation in ARPE-19 cells. Active MMP-2 is the major RPE enzyme reported for the degradation of collagen I, collagen IV, and laminin, all important

components of Bruchs membrane (Strongin et al.,1995) Unfortunately, minimal information is available concerning turnover of BM in ARMD.

Marin Castano et al reported that nonlethal oxidant injury can induce RPE cell membrane blebbing and alter RPE expression of matrix metalloproteinase (MMP)-2 and type IV collagen (Marin Castano et al., 2005). Though studies relating to oxidative stress mediated change in MMP have been reported, there are no studies on the lysyl oxidase activity. This study is the first report indicative of the relatively increased LOX activity in RPE cells in response to oxidative stress.

Effect of *in vitro* osmotic stress on lysyl oxidase

Osmotic stress caused by altered extra cellular osmolarity is a challenge to a normal cell in a variety of tissues including RPE.

The osmotic induction by mannitol at 50 and 100 mM concentration showed a net proliferative activity in the BrdU assay with a corresponding increase in the metabolic activity as seen by the MTT. This proliferative activity was seen only at the end of 6 hours. Changes in the uptake of osmolyte namely taurine, and the protein taurine transporter localized in the plasma membrane have been reported in ARPE cells at the end of 6 hours exposed to 50mM and 100mM mannitol, *in vitro*. (Thomas et al., 1993)

At 6 hours the LOX specific activity dropped by nearly 30% at 50mM mannitol and this was further lowered by 70% at 100mM mannitol. Subsequently at the end of 12 hours there was a 2.5 fold increase in the activity of cells exposed to 50mM mannitol and a 2.0 fold increase in the cells exposed to 100mM mannitol. This was further confirmed with the mRNA expression that showed a similar significant increase at the end of 12 hours compared to 6 hours. This could probably be correlating with the osmoregulatory activity of the RPE by the altered inward flux of the osmolytes accompanied by the water regulation along with the active membrane pumps such as the Na^+K^+ ATPase. In retinal pigment epithelium Yokoyama *et al.* demonstrated that hypertonic stress increases Na^+ K^+

ATPase activity and leads to accumulation of taurine and myoinositol. The influx is by the upregulation of these transporters. The ability of the cells to resist osmotic shrinkage by cell volume regulation is reported to parallel their resistance to apoptosis after osmotic shock. Thus due to the volume regulation the RPE cells were able to with stand the 50 mM and 100 mM mannitol concentration.

These findings are important because there are significant changes in extracellular osmolarity in a broad range of RPE disorders, including retinitis pigmentosa, retinal detachment, and macular degeneration and in systemic disease such as diabetic retinopathy.

The cellular responses to this type of stress deal with the activity of water channels (aquaporins) and electrolyte transporters, and the accumulation of osmolytes as well as the protection of proteins and sub-cellular structures (Stammer et al., 2003). Zhang et al. reported the thought provoking observation that hyperosmolality increases reactive oxygen species (ROS) and protein carbonylation levels in renal inner medullary (IM) cells *in vitro* and *in vivo*. Increased LOX activity and expression seen at the end of 12 hours was similar as seen when cells were exposed to oxidative stress. As osmotic stress can lead to oxidative stress the increase could be due to the same mechanism too. Whether this is a direct effect of the osmotic stresss with changes in the osmolytes and the membrane transporters activity or due to oxidative stress needs to be explored. A recent study indicated that chronic taurine supplementation ameliorates oxidative stress in diabetic rat retina. (El-Sherbeny et al., 2004).

While oxidative stress can have a direct effect on RPE viability at the level of the mitochondrial dysfunction, the osmotic stress on the other hand can lead to auto regulation of the cell volume, characteristic of RPE. Thus in this *in vitro* study, at the end of 6 hours of oxidative stress by tBH, there is cell death, as against the osmotic stress where in at the end of 6 hours of mannitol exposure there is no cell death.

Effect of *in vitro* high glucose on lysyl oxidase

The cellular processes of RPE cells were found to be altered in a diabetic state and how they contribute to the progression of this disease has not yet been completely elucidated.

In the present study on the *in vitro* culture of RPE cells exposed to glucose, there was a decrease in the specific activity of lysyl oxidase as well as in the mRNA expression. This decrease was more pronounced in the high glucose (30 mM) and when exposed to longer duration up to 72 hours. At the same condition the intracellular LOX also showed a relative decrease as revealed by immunohistochemsitry. LOX expression has been shown to be regulated by transforming growth factor β (Oleggini et al., 2007), tumor necrosis factor α (TNFα) (Rodriguez et al., 2008a), platelet-derived growth factor, retinoic acid and fibroblast growth factor (Csiszar et al., 2001). Retinal microvascular cell cultures when exposed to glucose have been reported to increase the TGF β and TNF α levels. TGF β and fibrobnectin has been reported to be increased in RPE cells exposed to glucose. However the regulation of the LOX mediated by glucose and growth factors is yet to be looked in.

Endothelial dysfunction induced by TNF α has been shown to be associated with a decrease in LOX expression/activity as studied in human umbilical vein endothelial cells and porcine aortic endothelial cells (Rodríguez et al., 2008). Pischon e*t al* have also found that TNF α inhibits the expression and activity of lysyl oxidase in osteoblasts cultures but does not inhibit collagen synthesis, thereby contributing to perturbed collagen cross-linking and accumulation (Pischon et al., 2005). Apart from decreasing the LOX activity the ARPE-19 cells exposed to high glucose, showed a significant increase in the activity of gelatinase (MMP 2 and 9). Giebel *et al* have earlier reported that MMP 9 is significantly increased in ARPE 19 cells exposed to high glucose environment with in 24 hours (Giebel et al., 2005).

The lysyl oxidase activity in response to glucose has not been investigated yet and thus this is the first report showing decreased LOX activity and mRNA expression in response to glucose in RPE cells. Further studies are needed to investigate the mechanisms modulating the production of LOX by RPE cells.

These results suggest that the decreased LOX activity and mRNA activity by RPE cells in response to high glucose can augment the ECM instability and remodeling. Measurement of collagen synthesis and estimation of LOX in the ECM could pave way for better understanding.

Thus LOX activity seems to be modulated differentially depending upon the type of stress given to cultured RPE cells. The limitations are that these are *in vitro* cell culture models and the exposure of the stress conditions can be done as acute or chronic exposures for example the effect of glucose has been studied only up to 72 hours, which if extended in days can give greater insight on the modulation of LOX on ECM. But in this study along with the cell culture model vitreous samples and epiretinal membranes from vitreoretinal pathology was also studied.

Modulatory role of homocysteine on the activity of lysyl oxidase; *in vivo and in vitro*

Elevated plasma Hcys has been associated with vascular remodelling in the context of both cardiovascular (Perła-Kaján et al., 2007) and cerebrovascular diseases (Lominadze et al ., 2006) by activating MMPs. (Moshal KS et al., 2006) Ocular complications associated with Hcys include ectopia lentis (Lieberman et al., 1966) , secondary glaucoma(Roedl et al., 2007), optic atrophy(Stanger et al., 2005), ARMD (Coral et al., 2006), CRVO (Narayanasamy et al., 2007) and diabetic retinopathy (Brazionis et al., 2008). Hcys has also been shown to have implication in collagen synthesis and crosslinking (Toohey et al.,2008). Hydroxyproline levels are used to predict collagen turnover status and most of the endogenous hydroxyproline present in biologic fluids is derived from the degradation of various forms of collagen.(Ozyurt et al.,2003; Simsek et al.,2004). Collagen turnover in vitreous has been shown to be associated with ageing and vitreoretinal diseases, which predisposes to posterior vitreous detachment (Sivak et al., 2002). Vitreoretinal diseases such as proliferative diabetic retinopathy (PDR) and rhegmatogenous retinal detachment (RRD) have extensive ECM pathology as seen earlier in this work wherein there is decreased LOX activity associated with increased MMP 9 and MMP 2. In this study, vitreous Hcys levels was found to be significantly increased in eyes with PDR and RRD as compared to the donor vitreous used as controls. The mean total

Hcys level in PDR was found to be showing a 2 fold increase and in RRD there was a 3.5 fold increase compared to controls. This is the first report of Hcys levels in vitreous of eyes with RRD. Although the etiology of PDR and RRD is different, the increased level of Hcys in PDR may be due to Hcys mediated change in barrier permeability where as in RRD this could be due to the outer blood retinal barrier breakdown. Loss of blood retinal barrier permeability and blood retinal barrier breakdown (outer and inner) may augment the diffusion of Hcys into the vitreous. The fact that in RRD there is a significantly higher Hcys level compared to PDR indicates that the varying degree of outer blood retinal barrier breakdown can increase in vitreous Hcys levels. Sen *et al* suggested that increased Hcys accumulation is associated with matrix remodelling such as collagen type-1 synthesis and matrix metallo proteinases (MMP 9) activity (Sen et al., 2007). Studies have shown that Hcys increases MMP 2 and MMP 9 synthesis in endothelial cells and vascular smooth muscle cells (Doronzo et al., 2005; Moshal et al., 2006). Characteristic changes in the levels of MMP 2 and 9 activities attributing to ECM remodelling have been reported in both PDR (De La Paz et al., 1998; Jin M et al., 2001; Noda et al., 2003) and RRD (Abu El-Asrar et al., 1998; Kon et al., 1998). Hence the increased Hcys levels in vitreous could also be a causative factor for the observed increase in the activity of MMP 2 and MMP 9, thereby degrading the ECM. Hcys modulates ECM changes not only by activating MMPs (Noda et al., 2003) but also by down regulating LOX (Raposo et al., 2004). The present study shows a significant negative correlation between Hcys and LOX both in RRD ($p=0.029$) and PDR ($p=0.040$) which is substantiated by the higher mean Hcys level in the vitreous of eyes with RRD as compared to those with PDR. Rapso *et al*. have reported that pathophysiological concentrations of Hcys (35 µM) inhibited LOX activity and mRNA expression in cultured porcine aortic endothelial cells (Raposo et al., 2004) by a mechanism involving the thiol of hcys. Rodriguez *et al* have also reported that vascular LOX is down regulated in the early stages of atherosclerosis and increases in the advanced stage (Rodriguez et al., 2002).

The *in vitro* study on ARPE-19 cells exposed to homocysteine also showed a statistically significant decrease in the specific activity of LOX at 30µM, 60 µM and 100 µM, which was similar to the effect seen in vivo.

Rapso et al have hypothesized that the decrease of LOX in endothelial cells could be by these mechanisms

1. Thiol mediated
2. Through endoplasmic reticulum (ER) stress - LOX is also post-translationally modified in the ER and Golgi

Hcys has also been shown to increase the expression of connective tissue growth factor (CTGF) in vascular smooth muscle cells (VSMC) both in vivo and *in vitro* (Liu et al., 2008). CTGF expression in turn can down regulate LOX (Hong et al., 1999). However, in this study the role of growth factors has not been investigated in regulating the ECM changes in PDR as well as in RRD. This is the first study showing vitreous homocysteine levels in RRD. Based on this study it is hypothesized that that the increased levels of Hcys in the vitreous could down regulate LOX activity and/or up regulate the MMPs (Fig 11.2) . LOX inhibition favours the presence of soluble forms of collagen that are highly susceptible to degradation by MMPs (Woessner et al.,1991) This altered ECM is reflected as increased collagen turnover. The decreased LOX can probably lead to inadequate collagen cross linking, which may pave way for vitreous liquefaction. Growth factors such as tumor necrosis factor α (Rodriguez et al., 2008b) and CTGF can play a role in regulating the LOX and MMP activities which needs to be further explored.

Figure 11.2 : Role of vitreous Homocysteine in LOX and MMP mediated changes of the ECM

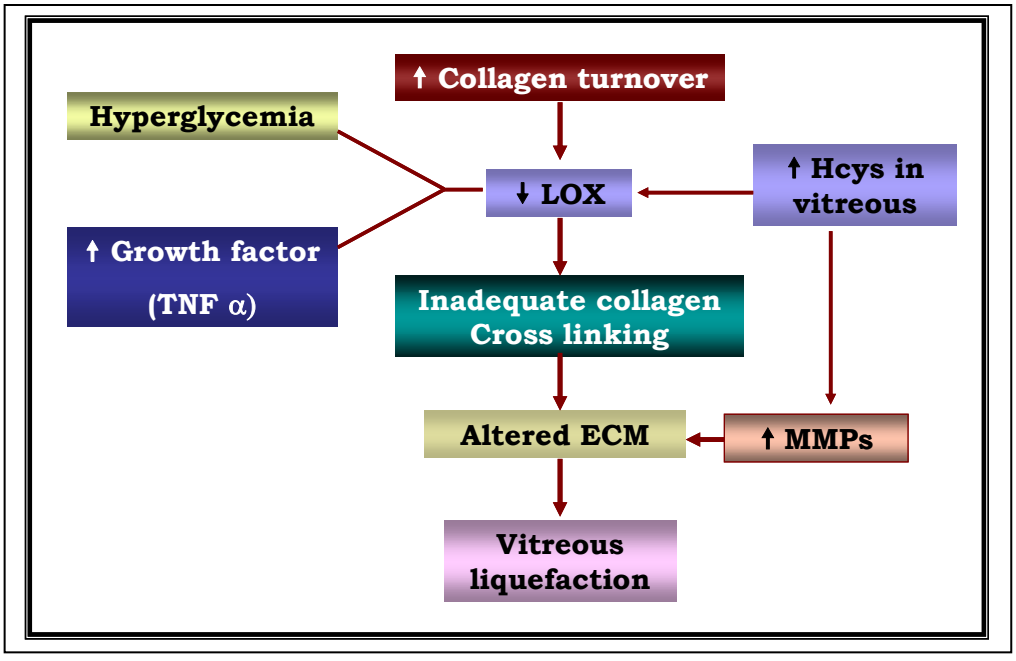

CHAPTER 12 SUMMARY AND CONCLUSION

- A detailed distribution profile of LOX activity in ocular tissues, revealed the presence of the enzyme Lysyl oxidase, (LOX) in the various ocular tissues in terms of specific activity, protein localization and mRNA expression and this is the first study on the ocular tissue distribution of LOX, which has been published. Vitreous showed the highest specific activity amongst the ocular tissues studied. This study helps in understanding the ocular tissues further with respect to the extent of collagen cross linking activity. The variation in the tissue level of LOX could be reflective of the changes in the ECM in ocular pathology and therefore could be a target for intervention.

- This was the first study to report LOX activity in vitreous samples from patients with PDR and RRD. There is decreased lysyl oxidase activity in the vitreous of PDR and RRD patients along with increased MMP activity, associated with increased turnover of collagen as revealed by the increase in hydroxy proline content. In addition the ERM are associated with increased LOX localization that obviously shows a role of LOX in these membranes.

- Established methods for the isolation and characterization of primary bovine retinal pigment epithelial cells in comparison with human cell line commercially available. These two cultures provide the *in vitro* cell model for the experiments.

- Increased LOX activity was seen in RPE cells in response to oxidative stress. There is an increased gelatinase activity seen associated with and therefore the net effect on the ECM changes will probably depend on the extent of the oxidative stress.
- Increased LOX activity and mRNA expression was seen at the end of 12 hrs in response to osmotic stress. A similar increased LOX activity was also seen when cells were exposed to oxidative stress. As osmotic stress

can lead to oxidative stress the increase could be due to the cell response similar to oxidative stress.

- This was the first study to see the changes in LOX activity and expression in response to high glucose insult to cultured ARPE-19 cells. The decreased LOX specific activity and mRNA expression was significant at high glucose concentration of 30mM glucose exposed for 72 hrs. There is also an increased gelatinase activity seen associated with the net effect on the ECM.

- Homocysteine mediated regulation of LOX *in vitro* and *in vivo* revelaed that the vitreous from eyes with PDR and RRD had increased homocysteine which showed a statistically significant negative correlation with LOX. When RPE cells were exposed to homocysteine *in vitro* the specific activity of LOX decreased significantly with increased homocysteine concentration. As LOX is regulated by various cytokines, growth factors and homocysteine. The vitreous LOX is probably down regulated by these regulatory factors.

- LOX inhibition favours the presence of soluble forms of collagen that are highly susceptible to degradation by MMPs. This altered ECM is reflected as increased collagen turnover. The decreased LOX can probably lead to inadequate collagen cross linking, which may pave way for vitreous liquefaction. Growth factors such as tumor necrosis factor α (Rodriguez et al., 2008b) and CTGF can play a role in regulating the LOX and MMP activities which needs to be further studied.

Future scope of work:

- The enzyme LOX apart from its crosslinking function has got novel roles in cell proliferation, migration in matrix biology and cancer biology. The identification of LOX and LOX like proteins is being studied as hot

molecules recently. The role of LOX isoforms in angiogenesis in relevance to ocular diseases can be studied further.

- The intracellular LOX and the extracellular LOX may have different mechanism of action. As the signal transduction pathways involved in LOX is not cleary understood this can be further studied in relevance to cell migration and adhesion.

- The increased localization and activity of LOX in the anteroir chamber and the numerous publications on LOXL1 gene in pseudoexfoliation can be explored and estimating the LOX enzyme activity in aqueous aspirate could be of diagnostic importance.

- LOX regulation on MMPs can be studied in hyalocytes cultures and also the regulation of LOX by growth factors can be studied.

- LOX relevance in ARMD can be studied as LOX null mice develop choroidal neovascularization when induced with laser. This could be further studied to understand the mechanism of LOX in choroidal neovascularization.

- Overall the LOX and its isoforms will be the future candidate molecules to be unraveled by research scientist for understanding ocular diseases and possibly for management of diseases as targets for drug discovery.

APPENDIX I

Materials for procurement and processing of bovine eye ball:

1. Sterile stainless steel containers.
2. Phosphate Buffered Saline (pH 7.4)

NaCl	8.0g
KH_2PO_4	0.2g
Na_2HPO_4	1.15g
KCl	0.2g
DH_2O	1000 ml

2. Antibiotics – Ciprofloxacin, Penicillin, Amphotericin B (Himedia)
3. Ice pack.
4. Sterile Dissection Set (Scissors and forceps)
5. Sterile Petri dishes

Materials for cell Isolation and culture:

1. Sterile cotton tipped swab
2. Sterile plastic centrifuge tube (Tarsons)
3. M199 Medium (GIBCO) commercially available with 1.2 % glutamine with phenol red

M199 Medium base	90 ml
10%FBS	10 ml

<u>Cell culture reagents and preparation of media</u>

DMEM/F12 Medium:

1 vial of DMEM/F12 powder dissolved in 900 ml of double sterilized milli Q water and filter sterilized under vacuum (sterility check-up – Incubation at room temperature, (overnight). After sterility check the growth media was prepared by mixing

DMEM/F12 Medium base	90 ml
10%FBS	10 ml

Gibco Trypsin: The trypsin was diluted to 0.1% with Dulbecos' Phosphate Buffered Saline (PBS) (Himedia)

M199 Medium (GIBCO) commercially available with 1.2 % glutamine without phenol red

The growth media was prepared by mixing,

M199 Medium base	90 ml
10%FBS	10 ml

Viability count:

0.4 % Trypan Blue (Sigma) dissolved in Phosphate buffered saline (pH 7.4)

Improved Neubaeur Chamber (haemocytometer)

Marker studies:

Immunoflourescence staining:

Pan cytokeratin antibody (1:400) (DAKO)

Cytokeratin 8.13 (sigma)

Vimentin (DAKO)

Anti mouse antibody FITC conjugated (1:15)

0.05% Evan's blue

Immunoperoxidase staining:

Tris buffered Saline (pH 7.6)

Tris: 1.2 g

NaCl: 1.6g

DH2O: 200ml

Protein estimation:

Reagents

Standard BSA	0.1g/dL
Na_2CO_3	2% in 0.2 N NaOH
$CuSO_4$	0.5% in 1% Trisodium citrate
Alkaline copper reagent	49 ml of (2) + 1 ml of (3)
Follin's Ciocalteau Reagent	1:1 dilution

Western blotting Reagents

1. Acrylamide (30%):

Acrylamide-14.6gm
Bis acrylamide-0.4gm
Dissolved in 30ml of water made up to 50ml.

2. Tris-HCl Buffer (PH 8.8):

Tris-9.0gm
Water-25ml
Adjust the PH to 8.8 with1N HCl and made up to 50ml with Distilled water.

3. Tris-HCl Buffer (PH6.8):

Tris-3.0gm
Water-25ml
Adjust the PH to 6.8 with 1N HCl and made up to 50ml with Distilled Water.

4. 10% APS:

Polymerization catalyst required for gel formation. 10% solution used – always prepared fresh.

Increasing APS concentration will make the gel set quicker.

Ammonium per sulphate-10gm
Distilled water-100ml.

5. TEMED (readily available):

Polymerization catalyst. Catalyses the formation of persulphate free radicals from the APS, which in turn initiates polymerization.Always the last reagent added to the gel.

6. 10% SDS: Binds proteins so they all become negatively charged, therefore separation is on the basis of size alone and not the intrinsic protein charges.

SDS-10gm
Distilled water-100ml
Stored at room temperature.

Separating gel preparation: Sieves and separates the proteins by size. Percentage gel depends upon the size of target proteins.

Acryl amide %	Range of separation (kDa)
15	12-43
10	16-68
7.5	36-94
5.0	57-212

10%gel:

30%Acrylamide- 4ml
TrisHCl PH 8.8-2.5ml
10%APS-50µl & TEMED-5µl
10%SDS-100µl
Distilled water-3.344ml

Stacking gel: Large pore size gel with little or no molecular sieving on the sample. Standard 4%

Acrylamide – large enough pore size for most samples.

30% Acrylamide-1.33ml
TrisHCl- (PH 6.8)-2.5ml
10%APS-50µl
TEMED-10µl
10%SDS-100µl
Distilled water-6.01ml.

Western blotting transfer buffer:

Tris-3.3gm
Glycine-14.4gm
SDS-1.0 gm

The contents were dissolved in 800ml of distilled water. The final volume was then made up to 1000ml with methanol.

Ponseau stain:

Ponseau S-0.5gm
Glacial acetic acid-1ml
Made up to 100ml with distilled water. Prepared just before use.

Electrophoretic buffer (5x):

Tris base-15.1gm
Glycine-72.0gm
SDS-5.0gm

Distilled water-made up to 1000ml.Donot adjust the PH of the stock, as the PH will be 8.3 when diluted. Stored at 4^0C until use (up to 1 month).

HEPES buffer (Lysis buffer)

10mMHEPES
1mMEDTA
10mMDTT
Dissolved in 10 ml dH_2O

Protease inhibitor cocktail (PIC)-1mg/ml
HEPES buffer and PIC solution –10ml HEPES+200µl PIC

Sample loading Buffer (3x):

1M Tris HCl (PH 6.8)-2.4ml
20%SDS-3ml
Glycerol-3ml
b-Mercaptoethanol-1.6ml
Bromophenol Blue-0.006gm

Tris buffered saline (pH:7.6) (TBS):

Sodium chloride-8gm
1M tris HCl-20ml
Diluted to 1000ml with distilled water.
Tween- 20-10ml.

5% Skimmed milk: 2.5g of skimmed milk powder was dissolved in 50ml of TBS

H_2O_2 standard for LOX assay

a) Make 20 mM stock - add 23µl of 3% stock H_2O_2 (Amplex Red kit) into 977 µl of dH_2O.

b) Make 100 µM stock - add 5 µl of above (20 mM) to 995 µl of dH_2O.

c) In 6 eppendorfs, mix the standards (this is enough to do each in triplicate):

d) Add 100 µl of each to triplicate wells in 96-well microplate. It is best to use the opaque white microplates to reduce background

#	DH_2O (µl)	100 µM H_2O_2 (µl)	*Final* Concentration (in 200 µl)
1	400	0	0 µM
2	396.8	3.2	0.4 µM
3	393.6	6.4	0.8 µM
4	390.4	9.6	1.2 µM
5	387.2	12.8	1.6 µM
6	384	16	2.0 µM

.

4X LOX Buffer

- 4.8 M Urea (57.6 g in 200 mL dH_2O)
- 200 mM Sodium Borate (15.25 g for 200 mL)
- pH to 8.2 w/HCl
- stored at RT

2M 1,5 diamniopentane (or Cadaverine)

- 0.35 g in 10 mL dH_2O
- stored at 4˚C

10 mM Amplex Red

- add 60 µl of DMSO to vial of Amplex Red, dissolve with vortexing
- make fresh from kit, or use previously dissolved (stored @ -20˚C)

200 U/mL HRP

- HRP from Sigma and aliquoted many tubes of 200 U/mL

500 µM BAPN

- 0.64 g in 50 mL dH_2O
- stored at 4˚C

Assay reaction mixture

50 mM NaBorate (pH 8.2)
1.2 M Urea
50 µM Amplex Red
0.1 U/ml HRP
10 mM 1,5-diaminopentane substrate

RNA extraction and Reverse transcription for LOX

RNA extraction:

Tri reagent (sigma)
Chloroform
Isopropanol
Ethanol
DEPC treated water
Cooling centrifuge
TURBO DNase
Thermoscript (Invitrogen)

PCR:

Gene specific primers: The stock was diluted in 100µl of TE buffer and heated at 65^0C for 5 min.

Taq buffer with $MgCl_2$
100mM DNTP mix (Banglore genei)
Taq DNA polymerase 3U/µl (Banglore genei)
Sterile water

Gel Electrophoresis

Electrophoresis is a method by which the amplification of the gene sequence is confirmed after PCR. DNA, negatively charged moves to the cathode on subjected to electric field and moves according to the olecular weight in a matrix like agarose or polyacrylamide gels. The gels are suitably stained to visualize the product (Fluorescent dyes for agarose gels and silver staining of poly acryl amide gels).

Agarose gel electrophoresis

Preparation of TBE buffer: 54.1 g of Tris, 27.8g of boric acid and 3.65 g EDTA were added in 500 ml water and pH adjusted to 8.0.The stock solution is diluted 1: 10 for further use.

Tracking dye- Bromophenol blue : 0.1gm BPB+100ml 1X TBE buffer in equal volumes of 40%sucrose solution.

Requirements

Molecular weight marker, Agarose, 10 X TBE buffer,Ethidium bromide (2mg/ml), BPB Preparation of agarose gel The gel trough was cleaned with ethanol and the ends were sealed with cellophane tape with the combs placed in the respective positions to form wells. Two percentage of agarose gel was prepared by dissolving agarose in 1X TBE buffer and 8µl of ethidium bromide being finally added and mixed thoroughly and poured on to the trough followed by electrophoresis of the amplified products at 100 V for 30 to 45 minutes. The gel was then captured and analysed using ImageJ software

Real time PCR components:

5X first- strand buffer

0.1M DTT

Ribonuclease Inhibitor (40 units/µl)

ELISA for vascular endothelial growth factor: ELISA assay kits, which measure total MMP2 and MMP were purchased from R&D Systems (Minneapolis,MN, USA)

APPENDIX II

S. No	CONSUMABLES	COMPANY
1	Ionised Calcium Electrode	KSK Diagnostics
2	Medium M 199 - Earles	Joyvel
3	MTT cell culture tested	Sigma -Aldrich

4	MMP 2 and MMP 9 – Zymography standard	Merck
5	Carboxy HDFCA	Molecular Probes
6	Fetal Bovine serum	Invitrogen
7	Amplex red monoamine oxidase Kit Amplex red reagent	Invitrogen
8	Tissue culture dish 60X15mm Tissue culture dish 100X20 mm	Greiner
9	Super signal west pico ECL substrate CL xposure X ray film	Pierce
10	Bench mark prestained protein ladder	Invitrogen
11	M199 medium	Invitrogen
12	TEMED Sample buffer for SDS PAGE Protein molecular weight medium range	Banglore genei
13	Snap pack	KSK Diagnaostics
14	Annexin V flous staining kit Cell proliferation BrdU Insitu cell death detection kit	Roche diagnostics Ind Pvt Ltd
15	Retinol all Trans	Sigma- Aldrich
16	M199 Earles without phenol red	Invitrogen
19	Antibiotic solution 100 X liquid PBS	Hi media
20	Sodium chloride cell culture tested Mannitol	Sigma- Aldrich
21	Standard Clear plate 24 well 96 well flat bottom with lid Tissue culture flask 25cmsq	Greiner
22	Polyclonal antibody to LOX	Imgenex , Biotech Pvt Ltd
23	Skimmed milk powder	5 stars Supreme

24	Novolink (mini polymer detection system)	Novocastra
25	Millicell, CM,0.4 micron	Millipore
26	Taqman R universal	Applied Biosystems
27	F bottom / Chimney well sterile- black	Greiner
28	Superscript II RNase H	Invitrogen
29	CRL 2302-ATCC cell line	ATCC
30	DMEM /F12	Invitrogen
31	Cell culture plates Freezer storage rack	Greiner
32	N acetyl cysteine Superoxide dismutase	Sigma
33	Sucrose	Merck
34	Trypsin	Invitrogen
35	LOX primers	Banglore Genei
36	Diethylpyrocabonate	Sigma
37	Assay on demand gene epression, human part	Applied Biosystems
39	Rabbit antigoat IgG FITC	Bangalore Genei